Stability analysis and control design for time-delay systems with applications to automotive steering systems

Ali Diab

université
PARIS-SACLAY

Stability analysis and control design for time-delay systems with applications to automotive steering systems

Analyse de stabilité et conception de lois de commande pour des systèmes à retards avec applications aux systèmes de direction automobiles

Thèse de doctorat de l'université Paris-Saclay

École doctorale n°580 : Sciences et technologies de l'information et de la communication (STIC)
Spécialité de doctorat : Automatique
Graduate School : Sciences de l'ingénierie et des systèmes
Référent : Faculté des sciences d'Orsay

Thèse préparée dans l'unité de recherche **Laboratoire des signaux et systèmes (Université Paris-Saclay, CNRS, CentraleSupélec)**, sous la direction de **William PASILLAS-LÉPINE**, Chargé de recherche, et le co-encadrement de **Giorgio VALMORBIDA**, Enseignant-Chercheur

Thèse soutenue à Paris-Saclay, le 18 avril 2023, par

Ali DIAB

Composition du jury

Membres du jury avec voix délibérative

Catherine BONNET Directrice de recherche, Inria, Université Paris-Saclay	Présidente
Michel DAMBRINE Professeur des universités, Université de Valenciennes et du Hainaut-Cambrésis	Rapporteur & Examinateur
Jean-Jacques LOISEAU Directeur de recherche, CNRS, Ecole Centrale de Nantes	Rapporteur & Examinateur
Frédéric GOUAISBAUT Maître de conférences, Université Paul Sabatier	Examinateur
Dalil ICHALAL Professeur des universités, Université d'Évry-Val-d'Essonne	Examinateur
Jean-François TRÉGOUËT Maître de conférences, INSA de Lyon	Examinateur

THESE DE DOCTORAT
NNT : 2023UPAST057

Acknowledgments

I would like to express my deepest gratitude to all the individuals who have played a crucial role in the completion of my thesis.

Firstly, I would like to acknowledge my thesis advisors, William PASILLAS-LÉPINE and Giorgio VALMORBIDA, for their continuous support, insightful feedback, and encouragement throughout the research process. Their expertise and precious advice have been crucial in shaping and refining my work, and I am truly grateful for their mentorship. The trust they have placed in me brought me to the necessary scientific rigor to be a researcher.

I would also like to thank the members of my thesis committee. I am grateful to Michel DAMBRINE and Jean-Jacques LOISEAU for accepting to review the following thesis report in detail. Thanks to Catherine BONNET, Frédéric GOUAISBAUT, Dalil ICHALAL, and Jean-François TRÉGOUËT for agreeing to be part of this thesis committee and for their valuable comments and discussions. I would also like to extend my sincere appreciation to the members of my midterm evaluation committee, Wim MICHIELS and Saïd MAMMAR, for their valuable input that helped me to improve the quality of my work.

I am also thankful to my beloved family for their endless love, encouragement, and understanding throughout my academic journey. Their unwavering commitment to my success has been inspirational. Their support and love have been my driving force and helped me overcome all the challenges I faced along the way.

I am grateful to my friends and colleagues, who have been a source of inspiration and motivation throughout this journey

Finally, I would like to express my gratitude to all those who directly or indirectly contributed to this work. Thank you all for your invaluable support and encouragement.

Contents

Résumé étendu de la thèse **1**

Introduction **9**
Background and motivation 9
Overview and contributions 11
Mitigate the impact of delays on EPS performance 11
A modified Smith predictor for SBW systems 12
Projection methods and Lyapunov-Krasovskii functionals 14
Related publications 16
Organization of the manuscript 17

I Steering systems **19**

1 Preliminaries on steering systems **21**
1.1 A model for steering systems 22
1.2 Control objectives and performance criteria 26
1.3 Literature review on steering systems 30

2 Increasing the delay margin of electric power steering systems **33**
2.1 EPS model and problem statement 34
2.2 Robustness with respect to delays 37
2.2.1 Delay margin without filter 37
2.2.2 Improving the delay margin with a lead filter 39
2.2.3 Analysis of a lead-lag filter 42
2.2.4 Filter-based dynamic compensation 44
2.2.5 Stability of the coupled system and disturbance rejection . . 45
2.3 Simulations 47
2.3.1 Maximum achievable delay margin with a lead filter 48
2.3.2 Analytical approximation of the delay margin for a lead filter 48
2.3.3 Comparison between the delay margins of the different filter structures 49
2.3.4 Comparison between different filter structures in term of the steering feel and road feel 50
2.3.5 Time-varying delay case 53
2.3.6 Controller sensitivity with respect to rejection of disturbances 54
2.3.7 Comparison with existing results 55

2.4 Conclusions 55

3 Increasing the delay margin of steer-by-wire systems 59
3.1 A modified Smith predictor 59
3.2 Stability analysis 62
3.3 Simulations 66
3.4 Conclusions 69

II LKF computation approaches 73

4 Preliminaries on time-domain stability analysis 75
4.1 Stability of time-delay systems 76
4.2 Construction of Lyapunov-Krasovskii functionals using the delay Lyapunov matrix 77
4.2.1 Computation of the delay Lyapunov matrix 78
4.2.2 Construction of the Lyapunov-Krasovskii functional 79
4.2.3 The parameter $\boldsymbol{T}$ is not separable 83
4.3 Literature review on LKF 85

5 Verification methods for the LKF inequalities 87
5.1 Delay systems with projections 89
5.2 SDP-based stability conditions using a separable parameter $\boldsymbol{T}$ . . . 92
5.2.1 General formulation 93
5.2.2 Formulation based on integral inequalities 98
5.2.3 Formulations based on polynomial SOS constraints 102
5.3 Numerical validation on academic examples 104
5.3.1 Example 1 105
5.3.2 Example 2 107
5.3.3 Example 3 107
5.3.4 Notes on the numerical implementation 114
5.4 Applications to steering systems 115
5.4.1 Applications to the EPS 115
5.4.2 Applications to the SBW 120
5.5 Conclusions 123

Conclusions and perspectives 125

A Technical proofs of Chapter 2 131

B Technical proofs of Chapter 5 145

C Adopted methods to reduce the conservatism of stability criteria 155

Bibliography

Résumé étendu de la thèse

Ce manuscrit porte sur les systèmes linéaires avec retards et étudie de façon plus détaillée deux applications aux systèmes de direction automobiles, à savoir la « *direction assistée électrique* » (EPS) et le « *steer-by-wire* » (SBW). L'analyse de stabilité, la conception de lois de commande et l'évaluation des performances sont abordées pour des systèmes interconnectés avec retards, en utilisant à la fois des approches dans le domaine fréquentiel et dans le domaine temporel. Dans le domaine fréquentiel, notre étude se concentre sur les systèmes de direction automobile mentionnés ci-dessus. En revanche, dans le domaine temporel, nous abordons l'analyse de la stabilité des systèmes linéaires à retard dans un cadre plus général et appliquons les conditions de stabilité obtenues aux systèmes de direction. Ce résumé étendu donne un aperçu de ces approches et propose une introduction aux systèmes de direction. Nous motivons d'abord les problèmes étudiés en décrivant les deux systèmes de direction considérés et en présentant les approches que nous avons développées pour contrer les problèmes de stabilité induits par les retards. Nous soulignons également la contribution de notre travail en comparant nos résultats avec ceux de la littérature.

Contexte et motivation

Dans les véhicules de conception standard, un couple d'auto-alignement est produit au niveau des roues de façon à les ramener naturellement en position centrale. Ce couple résulte des forces de réaction générées par le contact entre les pneus et la route. Au niveau du volant, le couple d'auto-alignement fournit au conducteur un retour sur les forces exercées sur les pneus, ce qui est essentiel pour éviter l'instabilité de la dynamique latérale du véhicule [39]. Malgré l'effet stabilisateur bénéfique du couple d'auto-alignement, celui-ci doit être contré par le conducteur pour guider le véhicule. L'effort du conducteur dépend de la vitesse, étant plus élevé pour les manoeuvres à faible vitesse, comme par exemple les manoeuvres de stationnement. Pour ces raisons, l'assistance de direction a été introduite pour réduire l'effort du conducteur lorsqu'il manoeuvre son véhicule [68].

Généralement, dans les systèmes de direction conventionnels, une colonne de direction relie le volant au pignon de la crémaillère et le système est équipé d'une pompe hydraulique ou d'un moteur électrique permettant de fournir un couple d'assistance [14]. Sur la plupart des véhicules, la direction assistée électrique a une efficacité supérieure à celle des systèmes hydrauliques en termes de

consommation d'énergie [47, 68]. Grâce aux technologies « *by-wire* », le lien mécanique entre l'interface de conduite et les roues du véhicule peut être remplacé par un système composé d'actionneurs, de capteurs, d'une unité de contrôle et d'un réseau de communication. Dans le cas du système « *steer-by-wire* », les capteurs sont des codeurs incrémentaux et les actionneurs sont des moteurs électriques. Ces éléments sont placés sur la crémaillère (pour déplacer les roues) et sur le volant (pour fournir un retour d'effort). L'unité de contrôle électronique (ECU) calcule les signaux de commande envoyés aux moteurs électriques et le réseau de communication relie tous les composants du système entre eux. Les deux principaux avantages de la suppression de la colonne de direction sont la réduction des risques en cas d'accident et une flexibilité accrue pour la conception de l'intérieur du véhicule. Ce système simplifie également la tâche d'intégration des demandes du conducteur et du pilote automatique (voir [5, 95] et [92]). Cependant, l'acquisition et le traitement des événements des codeurs incrémentaux et la communication entre l'ECU et les actionneurs introduisent des retards dans les boucles de rétroaction du système interconnecté.

Dans un système de direction classique, le couple associé au retour d'effort est fourni par la rigidité de la colonne de direction. Dans un système de direction assistée électrique, le couple d'assistance est calculé à partir d'une mesure de couple effectuée au niveau de la colonne de direction. Dans un système « *steer-by-wire* », en l'absence de liaison mécanique, le retour d'effort et le couple d'assistance sont calculés en introduisant une rigidité virtuelle dans le système [8], et en utilisant des mesures d'angle au niveau du volant et du pignon de la crémaillère [47]. À la fois pour les directions assistées électriques et pour le système « *steer-by-wire* », plus le niveau d'assistance est élevé, plus la marge de retard des boucles de rétroaction est faible. De plus, dans le cas du « *steer-by-wire* », de multiples retards apparaissent dans les boucles de rétroaction, ce qui rend l'analyse de la stabilité difficile [102].

La première partie de ce manuscrit vise à analyser l'effet des retards apparaissant dans les boucles de rétroaction sur la stabilité des systèmes de direction. Des lois de commande permettant d'augmenter la marge de retard du système (par rapport aux stratégies actuelles) sont proposées. Nous suivons l'approche utilisée pour les systèmes de direction électrique [52], où les contrôleurs considérés sont des lois de commande proportionnelles-dérivées [51], incluant une loi d'assistance (éventuellement non linéaire) et un filtre linéaire. L'objectif principal du filtre est de compenser la réduction de la marge de retard associée à l'injection d'énergie. Ensuite, nous proposons des filtres linéaires pour lesquels l'analyse dans le domaine fréquentiel nous permet de présenter les limitations imposées par les retards sur le système et les paramètres du filtre. L'objectif principal de la loi d'assistance est d'améliorer le confort du conducteur [55].

Puisque ces lois d'assistance sont, en général, non linéaires, nous avons également développé des techniques dans le domaine temporel avec l'objectif à long terme d'étudier le système global. À cette fin, nous considérons une fonctionnelle quadratique de Lyapunov-Krasovskii, qui fournit des conditions nécessaires et suffisantes pour la stabilité d'un système linéaire à retard [40, 45]. La principale difficulté de cette approche est de construire une fonctionnelle de Lyapunov-Kra-

sovskii et, en particulier, de fournir des conditions qui garantissent la positivité de cette fonctionnelle et la négativité de sa dérivée temporelle le long de la solution du système à retard [44]. Par conséquent, même dans le cas de systèmes linéaires à retard, des outils mathématiques sophistiqués sont nécessaires pour formuler des conditions constructives d'analyse de stabilité. À cette fin, les méthodes numériques basées sur la programmation semi-définie sont couramment utilisées, où les principales approches pour l'analyse de stabilité des systèmes à retard sont la méthode basée sur des inégalités intégrales exploitant les projections dans les polynômes de Legendre [100] et la méthode basée sur la programmation en sommes de carrés de polynômes [90].

La deuxième partie de ce manuscrit développe des méthodes dans le domaine temporel pour les systèmes avec retards. Nous proposons des méthodes de vérification des inégalités associées à des fonctionnelles de Lyapunov-Krasovskii pour l'analyse de stabilité avec des paramétrisations générales autres que les polynômes. Ensuite, nous mettons en relation deux approches numériques basées sur la programmation semi-définie utilisées dans la littérature [100, 90]. Enfin, nous appliquons ces méthodes du domaine temporel aux systèmes de direction.

Aperçu et contributions

Dans cette section, nous soulignons les principales contributions du manuscrit et discutons brièvement leur comparaison avec les approches disponibles dans la littérature. Une comparaison plus détaillée est fournie dans les Chapitres 1 et 4. Les contributions du manuscrit sont décrites dans les trois sous-sections suivantes. Les deux premières sous-sections concernent la première partie du manuscrit, où une approche dans le domaine fréquentiel est adoptée, et la dernière sous-section concerne la deuxième partie du manuscrit, où une approche dans le domaine temporel est adoptée.

Atténuer l'impact des retards sur les performances de l'EPS

Les retards dans les boucles de rétroaction des contrôleurs d'assistance sont négligés dans la plupart des études précédentes sur les systèmes de direction assistée [118, 119, 68, 52]. Pourtant, ces retards ont un impact significatif sur l'atténuation des vibrations et sur la stabilité. Ils peuvent conduire à une dégradation sévère des performances en raison de l'utilisation d'un gain élevé d'assistance dans les contrôleurs nominaux conçus en négligeant le retard. Comparativement à d'autres spécifications de conception, nous montrons que l'augmentation de la marge de retard est particulièrement importante dans les systèmes de direction puisque, pour ces systèmes, les retards dans la boucle de rétroaction apparaissent comme le principal terme déstabilisant [70]. Nous considérons la boucle de rétroaction principale du système de direction assisté électrique, qui se compose d'un système stable du second ordre, d'un filtre C, et d'un seul retard τ. Le système du second ordre représente la dynamique du sous-système du pignon, qui est le composant de la direction assistée électrique le plus sensible aux retards. Plus précisément, nous étudions la stabilité du système en boucle fermée

donné par la fonction de transfert

$$G(s) = \frac{1}{Kk_s}\left(\frac{\frac{Kk_s}{J_p s^2 + \sigma_p s + k_s}}{1 + \frac{Kk_s}{J_p s^2 + \sigma_p s + k_s} C(s) e^{-\tau s}}\right),$$

où C est la fonction de transfert du filtre, J_p, σ_p, et k_s sont les paramètres du système, et K est le gain d'assistance. La marge de retard $\Delta\bar{\tau}$ est définie par

$$\Delta\bar{\tau} = \sup\left\{\bar{\tau} \geq 0 : G(s) \text{ is stable } \forall \tau \leq \bar{\tau}\right\}.$$

Il est important de signaler que, pour une dynamique sans retard, un schéma d'assistance proportionnel résulte en une boucle fermée stable pour tout gain de commande positif. En revanche, un retard dans la boucle de rétroaction introduisant le terme $e^{-\tau s}$ dans $G(s)$ ci-dessus peut déstabiliser le système, en particulier pour de grandes valeurs du gain d'assistance, sauf si un terme de filtrage, $C(s)$ dans l'expression ci-dessus, est inclus pour augmenter la marge de retard.

Dans ce contexte, nous abordons le problème de l'augmentation de la marge de retard pour les boucles de contrôle du système de direction assistée électrique en choisissant le filtre C. Nous proposons une approche de conception simple basée sur l'introduction de différents filtres à structure fixe. Il est important de noter que nous nous concentrons sur les structures de filtre avec un ordre limité pour permettre un calcul analytique de la marge de retard ou une limite inférieure de celle-ci en fonction des paramètres du filtre. De plus, dans les applications, les filtres d'ordre faible sont souvent préférés en raison de leur simplicité de mise en oeuvre [14]. En conséquence, l'amélioration de la marge de retard est certifiée par les expressions analytiques obtenues qui dépendent à la fois du système et des paramètres du filtre. Aussi, nous proposons des lignes directrices pour la sélection du filtre et nous montrons une amélioration par rapport aux méthodes de l'état de l'art. Par conséquent, nous considérons que la simplicité des structures des filtres et des lois de commande développés sont solides et peuvent être utilisées dans la pratique. Enfin, l'approche proposée peut être étendue à des structures de rétroaction similaires, comme celles qui apparaissent dans d'autres systèmes pratiques, tels que les systèmes « *steer-by-wire* » et les contrôleurs de téléopération bilatérale.

Un prédicteur de Smith modifié pour les systèmes SBW

D'après les résultats résumés ci-dessus, les retards dans les boucles de rétroaction du système de direction apparaissent comme un terme déstabilisant [18]. De plus, ces retards détériorent les performances de la boucle fermée [112]. Pour surmonter ces difficultés, une solution possible est d'utiliser un prédicteur de Smith [4]. Pour supprimer le retard de la boucle de rétroaction, ce type de compensation utilise un modèle P de la dynamique du système et suppose connue la valeur du retard τ dans la boucle de rétroaction du contrôleur nominal C, comme illustré sur la Figure 1a. Le principal avantage de cette méthode est que le retard

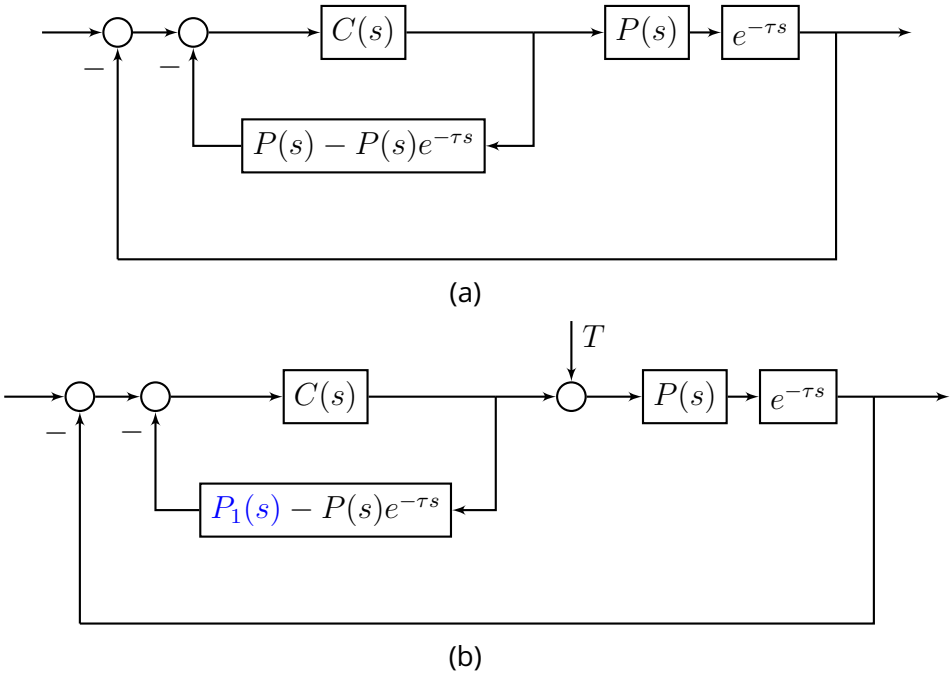

Figure 1 : (a) Système de commande du prédicteur de Smith. (b) Système de commande proposé dans [110].

est compensé à partir de l'équation caractéristique du système en boucle fermée. Par conséquent, le problème de la limitation des valeurs admissibles des retards peut être contourné, ce qui simplifie la conception d'une loi de commande.

Cependant, le prédicteur de Smith ne peut pas être appliqué à un système avec une *action intégrale* (un pôle à l'origine du plan complexe) puisque dans ce cas, un signal de perturbation produit une erreur stationnaire non-nulle. Par conséquent, un prédicteur de Smith modifié a été proposé dans [110] pour faire face au signal de perturbation et à l'action intégrale du système contrôlé. Le schéma modifié est illustré dans Figure 1b, avec P_1 sélectionné comme

$$P_1(s) = \frac{P(s)}{1+\tau s},$$

où $1/(1+\tau s)$ est l'approximation du premier ordre de la fonction de transfert $e^{-\tau s}$.

Inspiré par [110], nous proposons un prédicteur de Smith modifié pour l'application aux systèmes « *steer-by-wire* ». Pour ces systèmes, les signaux de perturbation sont les couples générés par le conducteur et par les efforts du pneumatique sur le pignon de la crémaillère. La difficulté réside donc dans le fait que ces perturbations dépendent largement de la position angulaire du système de direction. Plus précisément, ces perturbations introduisent des boucles de rétroaction dans le système interconnecté. Dans ce contexte, nous adaptons le prédicteur de Smith modifié proposé dans [110] aux systèmes « *steer-by-wire* » et, pour réduire le temps de réponse du système de direction, nous multiplions le contrôleur conventionnel $C(s)$ par $1+\tau s$, compensant ainsi le retard dans la fonction de transfert en boucle ouverte du système « *steer-by-wire* », ce qui peut également être utile pour analyser la stabilité du système.

De plus, nous associons l'architecture de commande proposée à une approche

simple d'analyse de stabilité donnant une approximation explicite de la marge de retard. Nous approximons la fonction de transfert en boucle ouverte du système de direction autour de la fréquence de croisement au gain unité du sous-système du volant en utilisant son approximation de Padé du premier ordre. Le lieu de Nyquist de cette approximation est un cercle tangent au lieu de Nyquist du système à la fréquence de croisement utilisée comme approximation. Elle fournit donc une expression analytique simple et facile à interpréter. Grâce à cette approximation, nous obtenons une expression explicite pour estimer la fréquence de croisement au gain unité, qui peut alors être utilisée pour estimer la marge de retard du système. Cette approche peut également être utile pour sélectionner les paramètres de la loi de commande.

De plus, nous proposons une méthode pour introduire une loi d'assistance non linéaire dans l'architecture de commande du système « *steer-by-wire* ». Cette méthode sépare le signal de commande en trois parties. La première partie est linéaire et fournit un modèle virtuel de la raideur de la valve de direction ou du capteur de couple. La seconde partie est le couple d'assistance, sur lequel nous appliquons une loi d'assistance non linéaire visant à améliorer le confort du conducteur. La troisième partie est un amortissement virtuel, utilisé pour augmenter les marges de stabilité du système. Par conséquent, le couple d'entrée résultant est

$$T_p(t) = k_w(\theta_w(t-\tau_w) - \theta_p(t-\tau_p)) + \frac{(k_p - k_w)}{k_w}\kappa(k_w(\theta_w(t-\tau_w) - \theta_p(t-\tau_p))) \\ + \rho_p(\dot{\theta}_w(t-\tau_w) - \dot{\theta}_p(t-\tau_p)),$$

où k_w est la rigidité de la colonne de direction virtuelle, k_p et ρ_p sont des paramètres de commande, κ est la loi d'assistance non linéaire, et θ_w et θ_p sont les positions angulaires mesurées, où τ_w et τ_p sont les retards. Contrairement à l'approche classique du « *steer-by-wire* », où le retour d'effort est basé sur un modèle [115], le principal intérêt de l'architecture proposée est de fournir au conducteur un retour d'information sur les forces de la route agissant sur les roues, comme cela peut se faire dans le domaine de la télémanipulation bilatérale [51].

Projections et fonctionnelles de Lyapunov-Krasovskii

Les fonctionnelles de Lyapunov-Krasovskii peuvent certifier la stabilité des systèmes à retard. Le calcul de ces fonctionnelles est une tâche difficile et la programmation semi-définie permet de résoudre les inégalités associées aux conditions de stabilité. Ces approches basées sur l'optimisation peuvent être d'une complexité croissante liée au nombre de paramètres définissant la fonctionnelle de Lyapunov-Krasovskii [104, 46, 83]. Pour présenter nos résultats sur la construction des fonctionnelles de Lyapunov-Krasovskii, nous considérons le cas d'un système linéaire à retard

$$\begin{aligned} \dot{x}(t) &= Ax(t) + A_d x(t-h), \qquad \forall t \geq 0, \\ x(t) &= \varphi_0(t), \qquad \forall t \in [-h, 0], \end{aligned}$$

où $A \in \mathbb{R}^{n\times n}$, $A_d \in \mathbb{R}^{n\times n}$, h est un scalaire positif, et $\varphi_0 \in PC([-h,0],\mathbb{R}^n)$ est la fonction initiale. La stratégie principale est d'étudier la fonctionnelle quadratique

de Lyapunov-Krasovskii, qui a la forme générale

$$V(\rho(0),\rho(\cdot)) = \int_{-h}^{0} \begin{bmatrix}\rho(0)\\ \rho(\theta)\end{bmatrix}^\top \begin{bmatrix}\dfrac{P}{h} & Q(\theta)\\ Q^\top(\theta) & R(\theta)\end{bmatrix} \begin{bmatrix}\rho(0)\\ \rho(\theta)\end{bmatrix} d\theta + \int_{-h}^{0}\int_{-h}^{0} \rho^\top(\theta) T(\theta,\eta)\rho(\eta) d\eta d\theta,$$

pour $\rho \in PC([-h,0],\mathbb{R}^n)$, où les matrices $P \in \mathbb{S}^n$, $R : [0,1] \to \mathbb{S}^n$, $Q : [-h,0] \to \mathbb{R}^{n\times n}$, et $T : [-h,0]\times[-h,0] \to \mathbb{R}^{n\times n}$. La fonction matricielle T vérifie également $T(\theta,\eta) = T^\top(\eta,\theta)$, pour tout $(\theta,\eta) \in [0,1]\times[0,1]$.

La dérivée temporelle de la fonctionnelle de Lyapunov-Krasovskii ci-dessus le long du trajet du système linéaire à retard est donnée par

$$\frac{d}{dt}V(x(t),x(t+\cdot)) = \int_{-h}^{0} \begin{bmatrix}x(t)\\ x(t-h)\\ x(t+\theta)\end{bmatrix}^\top \begin{bmatrix}\bar\Omega_{11} & PA_d - Q(-h) & \bar\Omega_{13}(\theta)\\ A_d^\top P - Q^\top(-h) & -R(-h) & \bar\Omega_{23}(\theta)\\ \bar\Omega_{13}^\top(\theta) & \bar\Omega_{23}^\top(\theta) & -R'(\theta)\end{bmatrix} \begin{bmatrix}x(t)\\ x(t-h)\\ x(t+\theta)\end{bmatrix} d\theta - \int_{-h}^{0}\int_{-h}^{0} x^\top(t+\theta)\left[\frac{\partial T(\theta,\eta)}{\partial\theta} + \frac{\partial T(\theta,\eta)}{\partial\eta}\right] x(t+\eta) d\eta d\theta,$$

où

$$\bar\Omega_{11} = PA + A^\top P + Q(0) + Q^\top(0) + R(0),$$
$$\bar\Omega_{13}(\theta) = A^\top Q(\theta) - Q'(\theta) + T(0,\theta),$$

et

$$\bar\Omega_{23}(\theta) = A_d^\top Q(\theta) - T(-h,\theta).$$

Pour les systèmes linéaires à retard, les paramètres P, Q, R, et T de la fonctionnelle quadratique de Lyapunov-Krasovskii peuvent être obtenus en identifiant sa dérivée temporelle avec une fonctionnelle quadratique prescrite [91]. Il est démontré que la fonctionnelle de Lyapunov-Krasovskii résultante est obtenue à partir de la « *delay Lyapunov matrice* », exprimée à l'aide de fonctions exponentielles [45, 11]. Cependant, pour conclure sur la stabilité en se basant sur ces résultats, la positivité de la fonctionnelle de Lyapunov-Krasovskii doit être vérifiée, ce qui peut être une tâche difficile [40, 111, 45].

Des approches numériques pour l'analyse de stabilité ont été adoptées comme une alternative permettant de contourner cette difficulté [100, 90, 24, 87, 34], où la fonctionnelle de Lyapunov-Krasovskii est définie en fonction d'un nombre fixe de paramètres. Les expressions de la fonctionnelle de Lyapunov-Krasovskii et de sa dérivée temporelle le long du trajet du système à retard sont réécrites dans des formes appropriées permettant de justifier les limites sur V et $\dot V$ numériquement en utilisant la programmation semi-définie.

Deux raisons principales empêchent la positivité de V obtenue à l'aide de la « *delay Lyapunov matrix* » d'être exprimée sous la forme de contraintes compatibles avec la programmation semi-définie. Premièrement, les termes intégraux

simples dans l'expression analytique de V et de $\dot{V}$ sont écrits en termes de fonctions exponentielles. Deuxièmement, la solution analytique pour le paramètre T dans le terme intégral double de V n'est pas séparable. En d'autres termes, le terme intégral double ne peut pas être écrit comme le produit de deux termes intégraux. Ce terme intégral double est souvent ignoré ou approché par un terme séparable [84, 90], et les inégalités intégrales sont utilisées pour fournir des limites sur la fonctionnelle de Lyapunov-Krasovskii et sa dérivée temporelle. Par conséquent, l'utilisation de telles inégalités intégrales introduit un conservatisme dans les limites fournies et donc dans les conditions de stabilité résultantes.

Dans ce contexte, dans ce manuscrit, nous soulignons d'abord les difficultés à évaluer la positivité de la fonctionnelle analytique de Lyapunov-Krasovskii obtenue à partir de la « *delay Lyapunov matrix* ». Nous développons une approche permettant de formuler les fonctionnelles de Lyapunov-Krasovskii avec des fonctions linéairement indépendantes arbitraires, pouvant inclure des fonctions exponentielles et trigonométriques. Notre approche projette d'abord l'état d'un système à retard sur l'ensemble de fonctions choisi et utilise ces fonctions pour paramétrer Q et T dans la structure ci-dessus pour V. Nous montrons également que cette méthode de projection fournit une formulation générale des inégalités intégrales couramment utilisées, en particulier l'inégalité de Jensen et l'inégalité intégrale de Bessel-Legendre.

Enfin, nous formulons les conditions de stabilité pour les systèmes linéaires à retard dérivés de la fonctionnelle de Lyapunov-Krasovskii en utilisant les deux principales approches de programmation semi-définie existantes : la programmation par somme de carrés [90] et les méthodes basées sur l'utilisation des inégalités intégrales [100]. Nous présentons explicitement les différences entre ces deux approches. Plus précisément, projeter le système dans un ensemble de fonctions polynomiales permet de manipuler une fonctionnelle de Lyapunov-Krasovskii paramétrée avec le même ensemble de polynômes en utilisant des méthodes de somme de carrés. Ensuite, en utilisant les inégalités intégrales, les conditions de stabilité peuvent être formulées comme des contraintes d'un problème d'optimisation basé sur des inégalités matricielles constantes, ce qui est numériquement plus efficace en termes de temps de calcul. De plus, cette approche basée sur les inégalités intégrales est généralisée à des fonctions autres que les polynômes. Une hypothèse limitative dans les deux approches est sur la séparabilité du terme intégral double dans l'expression de la fonctionnelle de Lyapunov-Krasovskii. De plus, pour l'approche basée sur les inégalités intégrales, nous montrons qu'il n'y a pas d'amélioration avec une paramétrisation du terme R autre qu'une fonction affine, ce qui n'est pas le cas en utilisant l'approche par somme de carrés.

En conclusion, la méthode de projection proposée nous permet d'établir des liens entre l'approche par somme de carrés et l'approche basée sur les inégalités intégrales.

Introduction

This manuscript studies linear time-delay systems, focusing on applications in two automotive steering systems, namely, Electric Power Steering (EPS) and Steer-by-Wire (SBW). The stability analysis, control law design, and performance assessment are addressed for interconnected systems with delays, using both frequency-domain and time-domain approaches. In the frequency domain, we treat the above automotive steering systems directly. In contrast, in the time domain, we address the stability analysis of general time-delay systems and apply the developed stability conditions to steering systems. This introduction gives an overview of these approaches and provides a background on steering systems. We first motivate the studied problems by introducing steering systems and presenting the approaches we adopted to counter the stability issues induced by delays. We also emphasize the contribution of our work by comparing the results with the literature. Finally, we present the structure of the manuscript.

Background and motivation

In standard vehicle designs, a self-aligning torque is produced at the wheels, aiming to return them to the center position. This torque results from the reaction forces generated by the contact between the tires and the road. At the steering wheel level, the self-aligning torque provides the driver feedback on the tire forces, which is essential to prevent the instability of the lateral dynamics [39]. Despite the beneficial role of the self-aligning torque and its stabilizing effect, it should be countered by the driver to steer the vehicle. The driver effort depends on the vehicle speed, being higher during parking maneuvers. For these reasons, steering assistance has been introduced to reduce driver effort in steering maneuvers [68].

Typically, in conventional steering systems, a steering column connects the steering wheel to the rack pinion (Figure 2a). Moreover, the system is equipped with a hydraulic pump or an electric motor that provides an assist torque [14]. Most often, the electric power steering has higher efficiency than the hydraulic power steering system in terms of energy consumption [47, 68]. With the help of “by-wire” technologies, the mechanical link between the driving interface and the wheels of the vehicle can be replaced by a system composed of actuators, sensors, a control unit, and a communication network. In the case of the steer-by-wire system (Figure 2b), the sensors are incremental encoders and the actuators are electric motors. These elements are placed on the rack (to move the

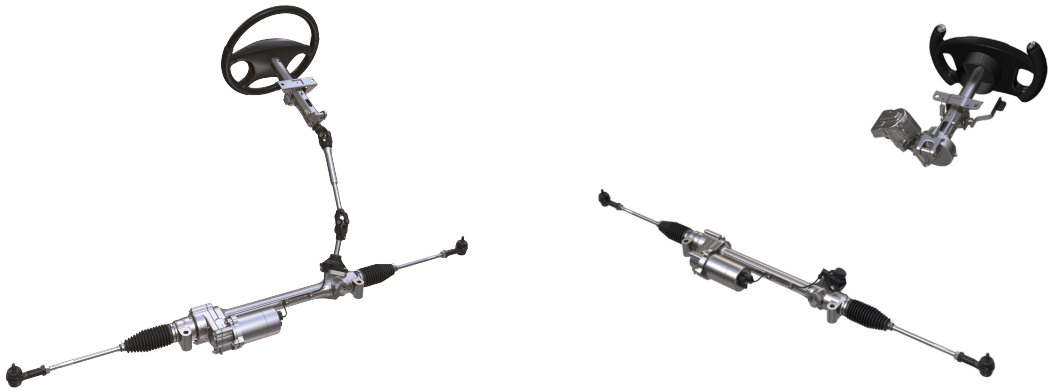

(a) (b)

Figure 2: (a) Rack-type electric power steering. (b) Steer-by-wire. Source: [41].

wheels) and on the steering wheel (to provide torque feedback). The Electronic Control Unit (ECU) computes the control signals that are sent to the electric motors and the communication network connects all the system components. The two main advantages of steering column removal are the reduced risk in the case of a car accident and the increased design flexibility for the interior of the vehicle. It also simplifies the task of integrating driver and autopilot demands (see [5, 95] and [92]). However, the acquisition and processing of encoder events and the communication between the ECU and the actuators introduce delays in the feedback loops of the interconnected system.

In a conventional steering system, the feedback torque is provided by the stiffness of the steering column. In an electric power steering system, the column stiffness yields the feedback torque and the assist torque is computed based on torque measurements at the steering column level. In a steer-by-wire system, since there is no mechanical link, both the feedback torque and the assist torque are computed based on a virtual stiffness [8] using both the steering wheel and the rack pinion angle measurements [47]. Broadly speaking, the larger the assistance level in both electric power steering and steer-by-wire, the smaller the delay margin on the feedback loops. Moreover, for steer-by-wire, multiple delays appear in the feedback loops, which makes the stability assessment a difficult task [102].

The first part of this manuscript aims to analyze the effect of feedback loop delays on the stability of steering systems. Control law designs to increase the delay margin (compared to current strategies) are proposed. We follow the approach used for electric power steering systems [52], where the considered controllers are proportional-derivative control laws [51], including a (possibly nonlinear) torque map and a linear filter. The main objective of the filter is to compensate for the delay margin reduction associated with energy injection. We proceed with linear filters where frequency-domain analysis allows us to present the limitations imposed by the delays on the system and filter parameters. The main objective of the torque map is to improve driver comfort [55].

Since these torque maps are, in general, nonlinear, we also developed time-domain techniques with the long-term goal of studying the global system. To

this end, we consider a quadratic Lyapunov-Krasovskii functional, which provides necessary and sufficient conditions for the stability of a linear time-delay system [40, 45]. The main difficulty of this approach is to construct a Lyapunov-Krasovskii functional and, in particular, to provide conditions that guarantee the positivity of this functional and the negativity of its time derivative along the solution of the time-delay system [44]. Therefore, even in the case of linear time-delay systems, sophisticated mathematical tools are required to formulate constructive stability analysis conditions. To that aim, numerical methods based on semidefinite programming are commonly used, where the main approaches for stability analysis of time-delay systems are the method based on integral inequalities exploiting projections into Legendre polynomials [100] and the method based on polynomials sum-of-square programming [90].

The second part of this manuscript develops time-domain methods for systems with delays. We propose methods for verifying Lyapunov-Krasovskii functional inequalities for stability analysis with general parameterizations than polynomials. Then, we relate two numerical approaches based on semidefinite programming used in the literature [100, 90]. Finally, we apply these time-domain methods for steering systems.

Overview and contributions

In this section, we highlight the main contributions provided in this manuscript and briefly discuss how they compare with the existing approaches in the literature. A more detailed comparison is provided in Chapters 1 and 4. The contributions of the manuscript are outlined in the three following subsections. The first two subsections concern the first part of the manuscript, where a frequency-domain approach is adopted, and the last subsection concerns the second part of the manuscript, where a time-domain approach is used.

Mitigate the impact of delays on EPS performance

The delays in the feedback loops of steering-assistance controllers are neglected in most previous studies on power steering systems [118, 119, 68, 52, 54]. Nevertheless, these delays significantly impact vibration attenuation and stability. They can lead to severe performance degradation because of the use of a large assistance gain in the nominal controllers designed neglecting the delay. Compared to other design specifications, we show that increasing the delay margin is particularly important in steering systems since, for these systems, feedback loop delays appear as the main destabilizing term [70]. We consider the main feedback loop of the electric power steering system, which consists of a stable second-order system, a filter C, and a single delay τ. The second-order system represents the pinion subsystem dynamics, which is the electric power steering component that is the most sensitive to delays. More precisely, we study the stability of the

closed-loop system given by the transfer function

$$G(s) = \frac{1}{Kk_s}\left(\frac{\dfrac{Kk_s}{J_p s^2 + \sigma_p s + k_s}}{1 + \dfrac{Kk_s}{J_p s^2 + \sigma_p s + k_s} C(s) e^{-\tau s}}\right),$$

where C is the transfer function of the filter, J_p, σ_p, and k_s are the system parameters, and K is the assist gain. The delay margin $\Delta\bar{\tau}$ is defined by

$$\Delta\bar{\tau} = \sup\left\{\bar{\tau} \geq 0 : G(s) \text{ is stable } \forall \tau \leq \bar{\tau}\right\}.$$

Note that, for a delay-free dynamics, a proportional assistance scheme results in a stable closed-loop for any positive control gain. In contrast, a delay in the feedback loop introducing the term $e^{-\tau s}$ in $G(s)$ above can destabilize the system, especially for large values of the assist gain, unless a filtering term, $C(s)$ in the above expression, is included to increase the delay margin.

In this context, we address the problem of delay margin augmentation for control loops of the electric power steering system by designing the filter C. We propose a simple design approach based on the introduction of different fixed-structure filters. Importantly, we focus on filter structures with a limited order to allow for an analytical computation of the delay margin or a lower bound of it as a function of the filter parameters. Moreover, in applications, low-order filters are often preferred because of their simplicity of implementation [14]. As a consequence, the delay margin improvement is certified by the obtained analytical expressions that depend both on the system and the filter parameters. In addition, we provide guidelines for the filter selection and we show an improvement over state-of-the-art methods. Therefore, we believe that the simplicity of the filter structures and the proposed control design are sound and can be used in practice. Finally, the proposed approach can be extended to similar feedback structures such as those appearing in other practical systems as steer-by-wire systems as well as in bilateral teleoperation controllers.

A modified Smith predictor for SBW systems

Based on the results summarized above, delays in the feedback loops of the steering system are the main destabilizing terms [18]. In addition, these delays worsen the closed-loop performance [112]. To overcome these difficulties, a possible solution is to use a Smith predictor [4]. To remove the delay from the feedback loop, this type of delay compensation uses a model of the plant dynamics P and the value of the delay τ in an inner feedback loop around the nominal controller C, as illustrated in Figure 3a. The main advantage of this method is that the delay is compensated from the characteristic equation of the closed-loop system. Therefore, the problem of limiting the admissible values of the delays can be circumvented, thus simplifying the design of a control law.

However, the Smith predictor cannot be applied to a system with an *integral action* (a pole at the origin of the complex plane) since in this case a disturbance

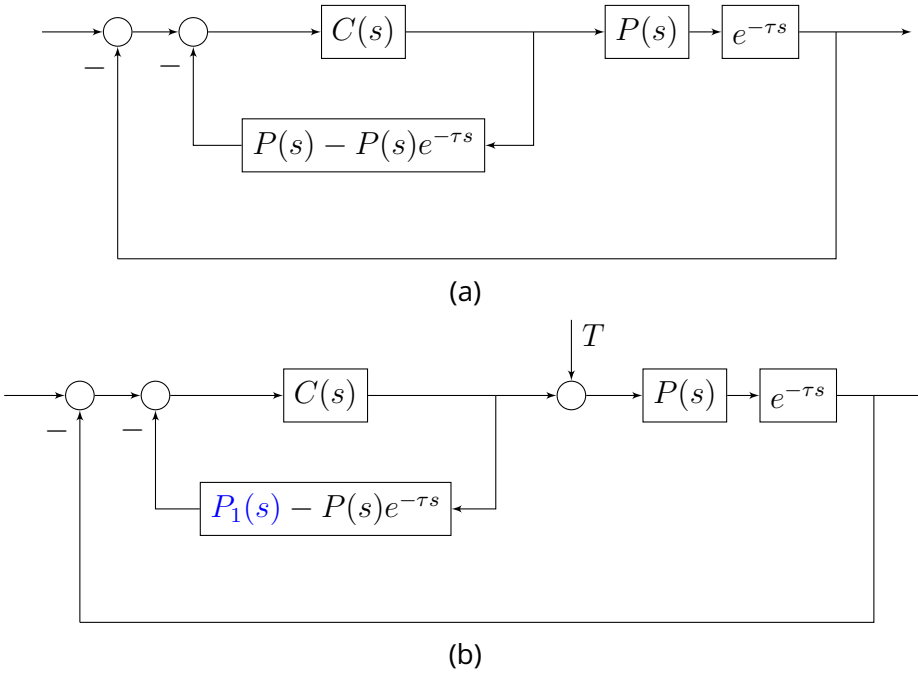

Figure 3: (a) Smith predictor control system. (b) Control system proposed in [110].

signal produces a non-zero steady-state error. As a result, a modified Smith predictor was proposed in [110] to cope with the disturbance signal and the integral action of the controlled system. The modified scheme is illustrated in Figure 3b, with P_1 selected as

$$P_1(s) = \frac{P(s)}{1+\tau s},$$

where $1/(1+\tau s)$ is the first-order approximation of the transfer function $e^{-\tau s}$ of a single delay τ.

Inspired by [110], we propose a modified Smith predictor for application to steer-by-wire systems. For these systems, the disturbance signals are the driver torque and road torque inputs. Thus, the difficulty lies in the fact that these disturbance inputs depend largely on the angular position of the steering system. More precisely, these disturbance inputs introduce feedback loops in the interconnected system. In this context, we adapt the modified Smith predictor proposed in [110] for steer-by-wire systems and, to reduce the steering system response time, we multiply the conventional controller $C(s)$ by $1+\tau s$, thereby compensating the delay in the open-loop transfer function of the steer-by-wire system, which can also be useful for analyzing the stability of the system.

In addition, we associate our proposed control architecture with a simple stability analysis approach yielding an explicit approximation of the delay margin. We approximate the open-loop transfer function of the steering system around the unity-gain crossover frequency of the steering wheel subsystem using its first-order Padé approximation. The Nyquist locus of this approximation is a circle in the complex plane, which is tangent to the Nyquist locus of the system at the approximated crossover frequency. Hence, it provides a simple analytical expression that is easy to interpret. Thanks to this approximation, we obtain an explicit expres-

sion to estimate the unity-gain crossover frequency, which can eventually be used to estimate the delay margin of the system. This approach can also be useful for selecting the control parameters.

Moreover, we propose a method to introduce a nonlinear torque map in the control architecture of the steer-by-wire system. This method separates the control signal into three parts. The first part is linear and provides a virtual steering column model. The second part is the net assist torque, on which we apply a nonlinear torque map aiming to improve driver comfort. The third part is a virtual damping, used to increase the stability of the system. Therefore, the resulting input torque is

$$T_p(t) = k_w(\theta_w(t-\tau_w) - \theta_p(t-\tau_p)) + \frac{(k_p - k_w)}{k_w}\kappa(k_w(\theta_w(t-\tau_w) - \theta_p(t-\tau_p))) + \rho_p(\dot{\theta}_w(t-\tau_w) - \dot{\theta}_p(t-\tau_p)),$$

where k_w is the stiffness of the virtual steering column, k_p and ρ_p are control parameters, κ is the nonlinear torque map, and θ_w, θ_p are the measured angular positions, where τ_w and τ_p are the delays. In contrast to the classical approach for steer-by-wire, where the force feedback is based on a model [115], the main interest of the proposed architecture is to provide the driver with feedback on the road forces acting on the wheels, as it is done for bilateral telemanipulation [51].

Projection methods and Lyapunov-Krasovskii functionals

Lyapunov-Krasovskii functionals can certify the stability of time-delay systems. Computing such functionals is a challenging task and semidefinite programming allows to solve the inequalities associated with the stability conditions. These optimization-based approaches can be of increasing complexity related to the number of parameters defining the Lyapunov-Krasovskii functional [104, 46, 83]—see also Appendix C. To present our results on the construction of Lyapunov-Krasovskii functionals, let us consider the case of a linear time-delay system

$$\begin{aligned} \dot{x}(t) &= Ax(t) + A_d x(t-h), \qquad \forall t \geq 0, \\ x(t) &= \varphi_0(t), \qquad \forall t \in [-h, 0], \end{aligned}$$

where $A \in \mathbb{R}^{n\times n}$, $A_d \in \mathbb{R}^{n\times n}$, h is a positive scalar, and $\varphi_0 \in PC([-h,0],\mathbb{R}^n)$ is the initial function. The main strategy is to study the quadratic Lyapunov-Krasovskii functional, which has the general form

$$V(\rho(0),\rho(\cdot)) = \int_{-h}^{0} \begin{bmatrix}\rho(0)\\ \rho(\theta)\end{bmatrix}^\top \begin{bmatrix}\dfrac{P}{h} & Q(\theta)\\ Q^\top(\theta) & R(\theta)\end{bmatrix} \begin{bmatrix}\rho(0)\\ \rho(\theta)\end{bmatrix} d\theta + \int_{-h}^{0}\int_{-h}^{0} \rho^\top(\theta) T(\theta,\eta)\rho(\eta)\, d\eta\, d\theta,$$

for $\rho \in PC([-h,0],\mathbb{R}^n)$, where the matrices $P \in \mathbb{S}^n$, $R : [0,1] \to \mathbb{S}^n$, $Q : [-h,0] \to \mathbb{R}^{n\times n}$, and $T : [-h,0]\times[-h,0] \to \mathbb{R}^{n\times n}$. The matrix function T also verifies $T(\theta,\eta) = T^\top(\eta,\theta)$, for all $(\theta,\eta) \in [0,1]\times[0,1]$.

The time derivative of the above Lyapunov-Krasovskii functional along the solution of the linear time-delay system is given by

$$\frac{d}{dt}V(x(t),x(t+\cdot)) = \int_{-h}^{0} \begin{bmatrix} x(t) \\ x(t-h) \\ x(t+\theta) \end{bmatrix}^\top \begin{bmatrix} \bar{\Omega}_{11} & PA_d - Q(-h) & \bar{\Omega}_{13}(\theta) \\ A_d^\top P - Q^\top(-h) & -R(-h) & \bar{\Omega}_{23}(\theta) \\ \bar{\Omega}_{13}^\top(\theta) & \bar{\Omega}_{23}^\top(\theta) & -R'(\theta) \end{bmatrix} \begin{bmatrix} x(t) \\ x(t-h) \\ x(t+\theta) \end{bmatrix} d\theta - \int_{-h}^{0}\int_{-h}^{0} x^\top(t+\theta)\left[\frac{\partial T(\theta,\eta)}{\partial\theta} + \frac{\partial T(\theta,\eta)}{\partial\eta}\right] x(t+\eta) d\eta d\theta,$$

where

$$\bar{\Omega}_{11} = PA + A^\top P + Q(0) + Q^\top(0) + R(0),$$
$$\bar{\Omega}_{13}(\theta) = A^\top Q(\theta) - Q'(\theta) + T(0,\theta),$$

and

$$\bar{\Omega}_{23}(\theta) = A_d^\top Q(\theta) - T(-h,\theta).$$

For linear time-delay systems, the parameters P, Q, R, and T in the quadratic Lyapunov-Krasovskii functional can be obtained by identifying its time derivative with a prescribed quadratic functional [91]. It is shown that the resulting Lyapunov-Krasovskii functional is obtained from the *delay Lyapunov matrix*, which is expressed using exponential functions [45, 11]. However, to conclude on stability based on these results, the positivity of the Lyapunov-Krasovskii functional must be verified, which can be a difficult task [40, 111, 45].

Numerical approaches for stability analysis were adopted instead [100, 90, 24, 87, 34], where the Lyapunov-Krasovskii functional is defined in terms of a fixed number of parameters. The expressions of the Lyapunov-Krasovskii functional and its time derivative along the solution of the time-delay system are rewritten in suitable forms allowing to justify bounds on V and $\dot{V}$ numerically using semidefinite programming.

Two main reasons prevent the positivity of V obtained using the delay Lyapunov matrix from being expressed as semidefinite program constraints. Firstly, the single integral terms in the analytical expression of V and $\dot{V}$ are written in terms of exponential functions. Secondly, the analytical solution for the parameter T in the double integral term of V is not separable. Namely, the double integral term cannot be written as the product of two integral terms. This double integral term is often ignored or approximated by a separable one [84, 90], and integral inequalities are used to provide bounds on the Lyapunov-Krasovskii functional and its time derivative. Therefore, using such integral inequalities introduces conservatism in the provided bounds and hence into the resulting stability conditions.

In this context, in this manuscript we first highlight the difficulties in assessing the positivity of the analytical Lyapunov-Krasovskii functional obtained from the delay Lyapunov matrix. We develop an approach allowing us to formulate Lyapunov-Krasovskii functionals with any set of linearly independent functions, which may include exponential and trigonometric functions. Our approach projects the

state of a time-delay system into the selected set of functions and uses these functions to parameterize Q and T in the above structure for V. We also show that this projection method provides a general formulation of the commonly used integral inequalities, in particular the Jensen inequality and the Bessel-Legendre integral inequality.

Finally, we formulate the stability conditions for linear time-delay systems derived from the Lyapunov-Krasovskii functional using the two main existing semi-definite programming approaches: the sum-of-squares programming [90] and the methods based on the use of integral inequalities [100]. We explicitly present the differences between these two approaches. More precisely, projecting the system into a set of polynomial functions allows a Lyapunov-Krasovskii functional parameterized with the same polynomials set to be manipulated using sum-of-squares methods. Then, using integral inequalities, stability conditions can be formulated as constraints of an optimization problem based on constant matrix inequalities, which is numerically more efficient in terms of computation time. Moreover, this approach based on integral inequalities is generalized to functions other than polynomials. A limiting assumption in both approaches is on the separability of the double integral term in the expression of the Lyapunov-Krasovskii functional. In addition, for the approach based on integral inequalities, we show that the parameter R in the Lyapunov-Krasovskii functional can be affine, which is not the case using the sum-of-squares approach.

In conclusion, the proposed projection method allows us to connect the sum-of-squares approach and the approach based on integral inequalities.

Related publications

This section lists the publications written in the framework of this dissertation.

Journal papers

[J.1] A. Diab, G. Valmorbida, and W. Pasillas-Lépine. Linear Assistance Filter Design for Electric Power Steering Systems with Improved Delay Margin. Accepted for publication in the *International Journal of Control*, 2023. DOI: 10.1080/00207179.2023.2201648.

[J.2] A. Diab, G. Valmorbida, and W. Pasillas-Lépine. Verification Methods for the Lyapunov-Krasovskii Functional Inequalities. Submitted to *SIAM Journal on Control and Optimization*.

Conference papers

[C.1] A. Diab, W. Pasillas-Lépine, and G. Valmorbida. A Steer-by-Wire Control Architecture Robust to High Assistance Gains and Large Transmission Delays. Proceedings of the *International Symposium on Advanced Vehicle Control* (Kanagawa), 2022.

Organization of the manuscript

Our study considers a generic model for steering systems encompassing the electric power steering and the steer-by-wire systems. We focus on linear systems with constant delays, where the frequency-domain approach can be employed. We begin with the example of electric power steering systems consisting of a feedback loop with a single delay. To mitigate the impact of delay, fixed-structure filters that increase the delay margin are proposed. Next, we study the example of steer-by-wire systems with multiple delays. A modified Smith predictor is adapted for steering systems to remove the delays from feedback loops and simplify the analysis process for steering systems. Finally, we complete the study by developing stability analysis methods for time-delay systems using Lyapunov-Krasovskii functionals, and we apply the obtained results to steering systems.

The manuscript is organized into two parts.

Part I

Chapter 1 presents steering systems with delays and describes the control signals that generate the assist torque. In addition, a generic model for steering systems, encompassing several configurations, is provided to point out the links between the electric power steering and the steer-by-wire systems. In addition, scenarios to evaluate the performance of steering systems are defined with several objective metrics, for control law comparison. Finally, a literature review on steering systems is proposed.

Chapter 2 focuses on the main destabilizing feedback loop in the system, where a single delay is considered. It addresses the analysis of the delay margin of electric power steering systems using several filter structures, where the delay margin is approximated as an explicit function of the filter parameters. We give guidelines on parameter tuning of the proposed filter structures to ensure system stability. Finally, the performance of the closed-loop is assessed based on scenarios described in Section 1.2 of Chapter 1. The material presented in this chapter is associated with [J.1].

Chapter 3 proposes a modified Smith predictor to compensate for the computational processing and measurement delays. Moreover, the delay margin is estimated using the Padé approximation of the open-loop transfer function. The proposed modified Smith predictor is compared to the conventional proportional-derivative controller in terms of the delay margin and the performance measures described in Chapter 1, Section 1.2. The material presented in this chapter is based on [C.1].

Part II

Chapter 4 recalls an existing analytical method to construct quadratic Lyapunov-Krasovskii functionals by prescribing its time derivatives. We point out the difficulties in verifying the positivity of this functional obtained from the solution of the delay Lyapunov matrix.

Chapter 5 introduces a projection method to provide general parameterizations of the Lyapunov-Krasovskii functionals. The inequalities stemming from the Lyapunov stability conditions for a time-delay system are formulated as linear matrix inequalities constraints. We highlight the contrasts and advantages of the two main trends in semidefinite programming approaches that have emerged in the last decade for the analysis of time-delay systems, namely the sum-of-square programming and the method based on the use of integral inequalities. The material presented in this chapter is based on [J.2]. The results presented in this chapter are applied, in Section 5.4, to steering systems. More precisely, the Lyapunov-Krasovskii functional and the projection method are adopted to analyze stability and compute the decay rate of steering systems.

Part I

Steering systems

Chapter 1

Preliminaries on steering systems

Thanks to technological advances, in the last twenty years Electric Power Steering (EPS) has almost completely replaced Hydraulic Power Steering (HPS) in passenger cars [47, 68]. Among the advantages of EPS, we can list: variable assistance gains, engine independence, and fuel economy [58]. In the future, by-wire technologies will offer more flexible architectures for automotive systems. Among the features of Steer-by-Wire (SBW) systems, we may cite the steering column removal [106] and the possibility of teleoperation [51]. They also allow more flexibility to accommodate performance requirements, in terms of driving characteristics, than the conventional automotive steering architectures [115]. However, the design of control laws for EPS/SBW still requires further robustness, in particular, to cope with computational and measurement delays [51, 48]. It is therefore crucial to study the stability margins of the resulting interconnected systems, where the communication between the steering wheel and the pinion subsystems is subject to *transmission delays*. Moreover, both subsystems are subject to *internal delays*, induced by the acquisition and processing of encoder events.

In the case of steer-by-wire systems, the study of this problem is similar to the questions addressed in Robotics in the context of bilateral teleoperation [51]. A human operator controls the position of a remote robot by acting on a local robot, which provides feedback on the environmental forces acting on the remote robot [79]. In this scenario, the force feedback problem is more complex [51] than the position tracking problem since adding a force sensor is not always desirable due to cost, reliability, or design constraints [68]. Moreover, even with a force sensor, information transmission delays (between sensors, processors, and actuators) can destabilize the feedback loop encompassing position and effort control, more significantly when the forces transmitted between the two robots are amplified.

In this context, control laws were proposed to increase robustness and improve performance. For the high feedback-loop gains required to reduce steering effort, a significant challenge is to preserve stability in the presence of delays. Indeed, these delays negatively impact the system performance and degrade the force feedback between the teleoperated systems. As performance indicators in steering systems, we can consider the driver *steering feel* and *road feel* [68]. Steering feel is related to how the steering torque is transmitted to the driver and

how the vehicle responds to steering wheel maneuvers—see, *e.g.*, [119] and [58]. Moreover, to achieve a satisfactory road feel, the driver must receive appropriate feedback from the forces generated by the contact between the tire and the road—see, *e.g.*, [103] and [68].

In this chapter, we introduce steering systems and present a generic model used in this manuscript to describe the steering dynamics. In Section 1.2, we introduce performance criteria for steering systems and define metrics that allow us to assess performance based on the system and control parameters. These performance assessment tests will be used later in the following chapters, particularly in the simulation sections to evaluate the proposed control laws. Finally, we present a literature review on the topics addressed in the first part of this manuscript, that is, the impact of delays on steering systems and the control schemes to deal with the delays.

1.1 A model for steering systems

The steering system builds a link between the driver torque T_d, applied on the steering wheel, and the road torque T_r, acting on the pinion and generated by the tire contact forces. The steering wheel angle will be denoted by θ_w and the pinion angle by θ_p. For HPS and EPS, the steering wheel and the pinion are connected mechanically by the steering column. In addition, a hydraulic pump or an electrical motor is integrated to generate an assist torque that reduces driver effort during steering maneuvers. Furthermore, the mechanical link between the steering column and the pinion can be suppressed in steer-by-wire systems, with the help of two electric motors: the first on the pinion, which steers the wheels of the vehicle, and the second on the steering wheel that provides feedback to the driver on the forces acting on the wheels.

The existence of a mechanical connection between the steering wheel and the pinion subsystems in HPS/EPS systems allows the use of a torque sensor. The stiffness of the torque sensor k_s is exploited to provide a measure of the steering column deformation, proportional to the difference between the wheel angular position θ_w and the pinion angular position θ_p,

$$T_s(t) = k_s(\theta_w(t) - \theta_p(t)). \tag{1.1}$$

For EPS and SBW, Figure 1.1, electric motors are used to provide *steering wheel assistance torque* $T_{a,w}$ and *pinion assistance torque* $T_{a,p}$ that may act on one or both subsystems—further details on the desired levels of the torques $T_{a,w}$ and $T_{a,p}$ are given below. Therefore, by selecting the value of the stiffness parameter k_s of the mechanical connection (for EPS) or of the virtual connection (for SBW), and by designing the control laws that generate the torques $T_{a,w}$ and $T_{a,p}$ of the electrical connection, we obtain the control signals T_w and T_p, given by

$$\begin{aligned} T_w(t) &= -T_s(t) + T_{a,w}(t), \\ T_p(t) &= T_s(t) + T_{a,p}(t). \end{aligned} \tag{1.2}$$

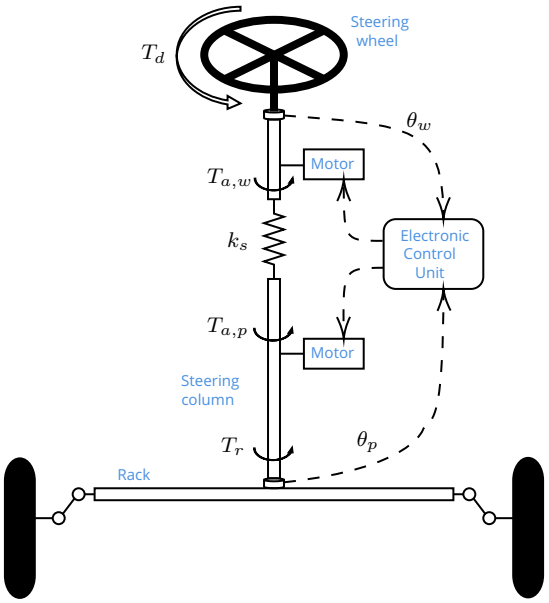

Figure 1.1: Scheme of the generic EPS/SBW system.

According to Newton's second law of motion, the *generic model* of the steering system is given by

$$\begin{aligned} J_w\ddot{\theta}_w(t) + \sigma_w\dot{\theta}_w(t) &= T_w(t) + T_d(t), \\ J_p\ddot{\theta}_p(t) + \sigma_p\dot{\theta}_p(t) &= T_p(t) + T_r(t), \end{aligned} \tag{1.3}$$

where J_w, J_p are the moments of inertia and σ_w, σ_p are the damping coefficients. The driver torque T_d and the road torque T_r are inputs of the system. T_w and T_p are the control signals interconnecting the two subsystems. The main objectives of the control signals T_w and T_p are to ensure the angular position tracking between θ_w and θ_p and to provide the driver with suitable feedback on the forces acting on the wheels. Moreover, the ratio between T_w and T_p indicates the assistance provided to the driver.

The role of the motor torques $T_{a,w}$ and $T_{a,p}$ is better understood in steady state, where the steering angles θ_w and θ_p are constant. In this case, from (1.3), we obtain $T_d = -T_w$ and $T_r = -T_p$. Therefore, the control T_w determines the torque level T_d that the driver must apply, and T_p compensates for the road torque T_r and steers the wheels of the vehicle. Indeed, the steering system receives the driver torque T_d and delivers the torque T_p, which can be larger thanks to the energy injected by the electric motors. We thus define the *assist torque*

$$T_a(t) = T_p(t) - T_d(t),$$

namely, as the difference between the control signal T_p and the driver torque T_d. Nevertheless, since measuring the driver torque applied to the steering wheel is difficult [13], we replace T_d by $-T_w$, which provides an estimate of the driver torque. Therefore, the assist torque is given by

$$T_a(t) = T_p(t) + T_w(t).$$

From (1.2), the above expression can be rewritten as

$$T_a(t) = T_{a,p}(t) + T_{a,w}(t).$$

Without power steering, $T_{a,w} = T_{a,p} = 0$ and the assist torque is null. For electric power steering systems, the assist torque is equal to the torque T_m generated by the electric motor (either $T_{a,w} = 0$ and $T_{a,p} = T_m$, in a rack-type EPS, or $T_{a,w} = T_m$ and $T_{a,p} = 0$, in a column-type system). For steer-by-wire systems, the torque $T_{a,w}$ and $T_{a,p}$ must have opposite signs to provide feedback forces.

The control signals T_w and T_p (equivalently, $T_{a,w}$ and $T_{a,p}$) are designed to allow the assist torque to follow a reference signal T_a^{ref}, given by

$$T_a^{ref}(t) = \kappa(\theta_w(t) - \theta_p(t))T_s(t), \tag{1.4}$$

where, in a general form, the *assist torque map* is a function $\kappa : \mathbb{R} \to \mathbb{R}$. Whenever the assist torque map κ is constant, that is $\kappa(\theta_w - \theta_p) = K$, we say $K > 0$ is the *assist gain*. The parameter K is determined by a steady-state analysis of system (1.3)-(1.4). In steady state, K is proportional to the ratio between the road torque and the driver torque. For a given road condition, if the value of K is small, the force applied by the driver should be higher to compensate for the road reaction forces. Therefore, the value of K is chosen to limit the forces the driver must apply, which guarantees a certain level of comfort from the assisted system.

However, the desired levels of the torques $T_{a,w}$ and $T_{a,p}$ are computed by an electronic control unit using measurements of the angular positions of the steering wheel and the pinion. Hence, internal delays τ_w and τ_p are introduced due to the time required for sensor processing. In the case of the electric power steering system, if the control laws are linear, the control signals T_w and T_p can be expressed in the Laplace domain as

$$\begin{aligned} T_w(s) &= k_s(\theta_p(s) - \theta_w(s)) + C_w(s)(e^{-\tau_p s}\theta_p(s) - e^{-\tau_w s}\theta_w(s)), \\ T_p(s) &= k_s(\theta_w(s) - \theta_p(s)) + C_p(s)(e^{-\tau_w s}\theta_w(s) - e^{-\tau_p s}\theta_p(s)), \end{aligned} \tag{1.5}$$

where C_w, C_p are the transfer functions of the controllers and τ_w, τ_p are the internal delays.

In the case of the steer-by-wire system, the steering column is removed, *i.e.*, there is no mechanical connection between the steering wheel subsystem and the pinion subsystem. Then, we must take $k_s = 0$ in the equations of the generic model of the steering system. In addition, for this system, the control signals for the steering wheel T_w and the pinion subsystems T_p can be processed by algorithms distributed on each motor control unit. Furthermore, in some cases, the two subsystems can be teleoperated. For this reason, we introduce transmission delays τ_1 and τ_2, which correspond respectively to the time required by a signal transmitted from the steering wheel subsystem to arrive at the pinion subsystem and vice versa. Hence, if the control laws are linear, the control signal T_w and T_p can be expressed in the Laplace domain as

$$\begin{aligned} T_w(s) &= C_w(s)(e^{-(\tau_p+\tau_2)s}\theta_p(s) - e^{-\tau_w s}\theta_w(s)), \\ T_p(s) &= C_p(s)(e^{-(\tau_w+\tau_1)s}\theta_w(s) - e^{-\tau_p s}\theta_p(s)), \end{aligned}$$

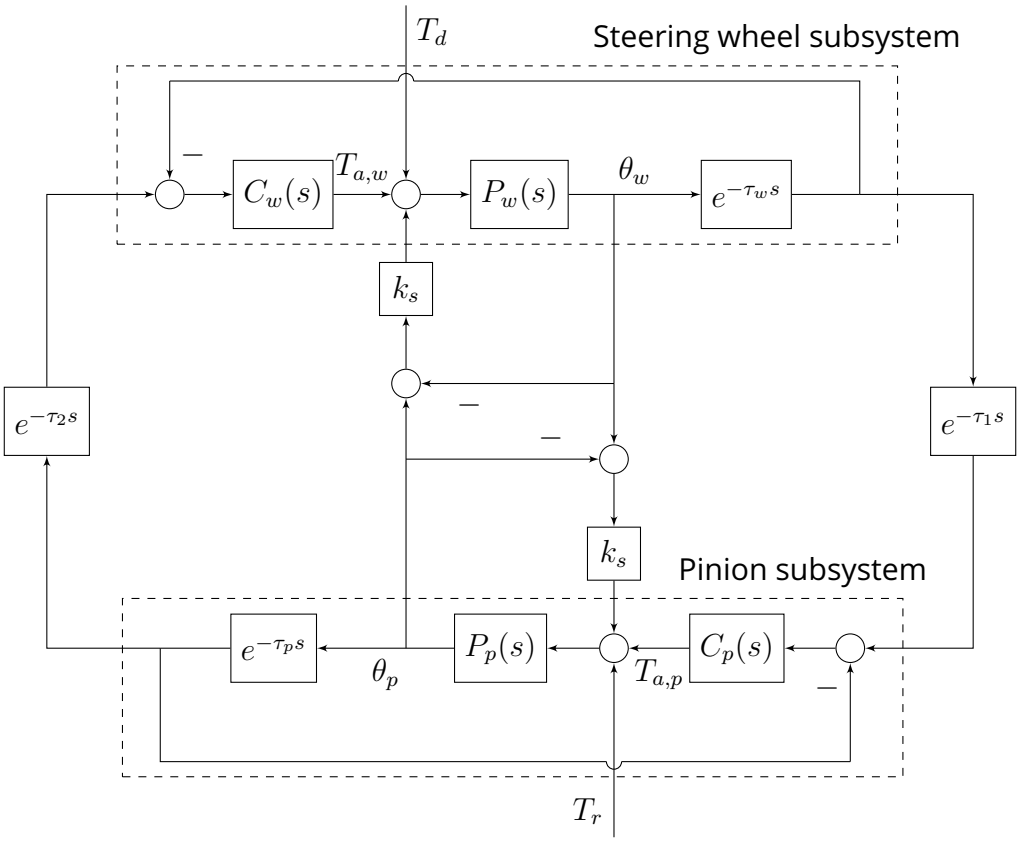

Figure 1.2: Block diagram of the EPS/SBW system.

where C_w, C_p are the transfer functions of the controllers, τ_w, τ_p are the internal delays, and τ_1, τ_2 are the transmission delays.

Therefore, for linear control laws, a generic representation of the control signals T_w and T_p is

$$\begin{aligned} T_w(s) &= k_s(\theta_p(s) - \theta_w(s)) + C_w(s)(e^{-(\tau_p+\tau_2)s}\theta_p(s) - e^{-\tau_w s}\theta_w(s)), \\ T_p(s) &= k_s(\theta_w(s) - \theta_p(s)) + C_p(s)(e^{-(\tau_w+\tau_1)s}\theta_w(s) - e^{-\tau_p s}\theta_p(s)). \end{aligned} \tag{1.6}$$

As an example of control design, let us consider the ideal proportional-derivative control laws. Then the transfer functions of the controllers C_w and C_p are expressed as

$$C_w(s) = k_w + \rho_w s$$

and

$$C_p(s) = k_p + \rho_p s,$$

where the control parameters k_w, k_p, ρ_w, and ρ_p are strictly positive.

Now we illustrate the generic model of steering systems in a block diagram, as shown in Figure 1.2 for the interconnected linear system (1.3)-(1.6) in the Laplace domain, where the transfer functions P_i, for $i \in \{w, p\}$, given as

$$P_i(s) = \frac{1}{J_i s^2 + \sigma_i s}.$$

Remark 1.1. The transfer functions P_w and P_p are defined as the transfer functions from the net torques acting on the steering wheel subsystem $T_w^* = T_w + T_d$ and the pinion subsystem $T_p^* = T_p + T_r$, respectively, to the steering wheel angle θ_w and the pinion angle θ_p, that is, for $i \in \{w, p\}$,

$$P_i(s) = \frac{\theta_i(s)}{T_i^*(s)} = \frac{1}{J_i s^2 + \sigma_i s}.$$

Finally, from (1.3)-(1.6), the closed loop system is given by

$$\begin{bmatrix} \theta_w(s) \\ \theta_p(s) \end{bmatrix} = \begin{bmatrix} \dfrac{P_w(s)\varphi_p(s)}{\varphi_w(s)\varphi_p(s) - \varphi_1(s)\varphi_2(s)} & \dfrac{P_p(s)\varphi_2(s)}{\varphi_w(s)\varphi_p(s) - \varphi_1(s)\varphi_2(s)} \\ \dfrac{P_w(s)\varphi_1(s)}{\varphi_w(s)\varphi_p(s) - \varphi_1(s)\varphi_2(s)} & \dfrac{P_p(s)\varphi_w(s)}{\varphi_w(s)\varphi_p(s) - \varphi_1(s)\varphi_2(s)} \end{bmatrix} \begin{bmatrix} T_d(s) \\ T_r(s) \end{bmatrix}, \quad (1.7)$$

where

$$\begin{aligned} \varphi_1(s) &= P_p(s)k_s + P_p(s)C_p(s)e^{-(\tau_1+\tau_w)s}, \\ \varphi_2(s) &= P_w(s)k_s + P_w(s)C_w(s)e^{-(\tau_2+\tau_p)s}, \\ \varphi_w(s) &= 1 + P_w(s)k_s + P_w(s)C_w(s)e^{-\tau_w s}, \\ \varphi_p(s) &= 1 + P_p(s)k_s + P_p(s)C_p(s)e^{-\tau_p s}. \end{aligned}$$

System (1.7) encompasses all the transfer functions appearing in the stability analysis of electric power steering and steer-by-wire systems studied, respectively, in Chapters 2 and 3 of this manuscript.

1.2 Control objectives and performance criteria

The goals of a controller in a steering system are to generate assist torque, attenuate vibrations, satisfy requirements on the steering feel, and provide informative road feedback. Several performance criteria [103, 68, 58] can be defined to validate the functionality of such controllers. In this section, we define the following criteria, which will be adopted in the simulation sections of Chapters 2 and 3 to assess performance and validate the controllers:

1. *Driver torque amplification*,
2. *Steering response*,
3. *Steering feel*,
4. *Road feel*.

Below, we provide a detailed description of each of these items, for the generic model of steering systems (1.3)-(1.6), and we identify different factors affecting driver comfort. To evaluate our results, to each criterion we associate one or more metrics that allow us to measure the controller performance, either in terms of its parameters or the pattern of its response to specific input signals. The application of these criteria in the case of electric power steering systems is developed in Chapter 2 and, in the case of steer-by-wire systems, in Chapter 3.

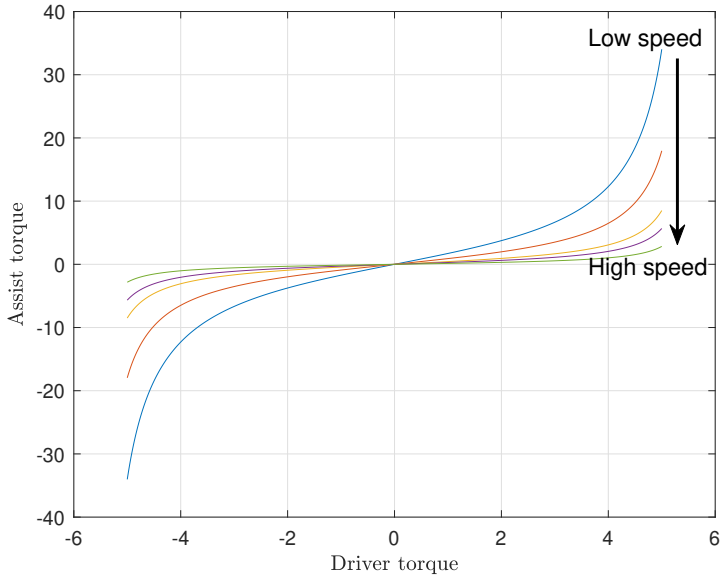

Figure 1.3: Boost curve characteristics.

Driver torque amplification

The primary objective of the controller in a steering system is to reduce the driver steering effort by providing an assist torque. This torque is computed using a *torque map* (see, *e.g.*, [55]) based on the driving conditions, namely the vehicle speed and the steering wheel angle. Usually, a *boost curve* is adopted as the torque map [1]. That is, the assist torque is a function of the driver torque and of the vehicle speed, as for example in (1.4). Figure 1.3 shows an example of boost curve characteristics for a steering system [68]. The assist torque required by the driver varies with the vehicle speed. As the vehicle speed increases, the assist torque decreases, increasing the centering torque on the steering wheel. In a small steering range, the torque map can be considered linear, that is $\kappa(\theta_w - \theta_p) = K$ is constant. To ensure the generation of the desired assist torque, the controller must guarantee the stability of the closed-loop system and provide a large assist gain K. Typically, car manufacturers will impose a lower bound on K, as $K \geq K_0$, for some $K_0 > 0$. As an example, in the steering system of Chapter 2, we use $K_0 = 35$.

Steering response

The steering response refers to the vehicle yaw rate and the vehicle lateral acceleration response to the steering input. The steering system can improve the steering response performance. While the steering wheel is turned and then released during cornering, it returns to the center position by the so-called *self-aligning torque* applied by the road on the tires. At low vehicle speeds, the friction between the tire and the road prevents the steering wheel from returning to the center position. At high vehicle speeds, the self-aligning torque increases and makes the steering wheel return to the center with excessive overshooting and oscillations [68]. This phenomenon can generate an unexpected yaw motion of the vehicle.

In a hydraulic power steering system, these oscillations are naturally damped by the inertia and high friction of the steering system [62]. In contrast, for steering systems equipped with electric motors, previous studies counter these oscillations by adding specific features to the steering system. A *return control* and an *active damping control* are combined to the controller of the steering system [47, 53]. The return control brings the steering wheel back to the center position quickly and accurately [113]. The active damping control prevents the oscillations usually present at high vehicle speeds [7]. Even if these features improve the returnability of the wheel to its center position, they often reduce the driver perception of the actual contact force between the road and the tires.

In order to provide the driver with a more direct feeling of road forces, we consider in this manuscript proportional-derivative control schemes for the controllers C_w and C_p described above. In this case, the steering response is improved since the proportional gain generates a high assist torque for a large steering wheel angle (corresponding to a return control), and the derivative gain provides active damping that increases with the angular velocity of a steering wheel.

Steering feel

The steering feel is defined as the torque that the driver feels during steering maneuvers. It is quantified by the shape of the parameterized curve obtained for the driver torque T_d as a function of a sinusoidal steering wheel angle θ_w, typically of frequency $2\,\mathrm{Hz}$. Objective metrics to compare and assess the steering feel can be obtained from this curve. Figure 1.4 shows a typical steering feel curve obtained using for θ_w a sinusoidal input. It should be stressed that a model of the road reaction torque generated by the forces applied by the road on the tire is required to carry out simulations that generate these curves.

Some characteristic points of this curve are selected as objective metrics for evaluating steering feel. They are reported to be closely related to the driver subjective perception of steering feel [80]. For example, the torque differences T_0 and T_1 are the torque hysteresis at zero and 70% maximum steering wheel angle, respectively. These metrics respectively represent the hysteresis during on-center and cornering maneuvers. This hysteresis is associated with an additional force that the driver must provide during maneuvers. When this hysteresis is large, it degrades the performance of the steering system. The torque T_2 is the maximum torque over the whole steering range, its preferred value is around $4\,\mathrm{Nm}$. A high value of T_2 will result in a heavy steering feel for the driver. The angle differences θ_0 and θ_1 are the angle hysteresis at 0 and $1.3\,\mathrm{Nm}$. These metrics quantify the backlash of the steering system since a high-angle hysteresis affects the driver feeling of the center position of the steering wheel [58].

The steering feel criterion is essential to assess the performance of a steering system. It overlaps partially other criteria presented in this section, namely the driver torque amplification and the steering response. For example, the metrics k_0 and k_1 can be considered to ensure driver torque amplification and to evaluate the stiffness of the steering system. These metrics represent the torque gradient to steering angle during on-center and cornering maneuvers. The steering stiffness

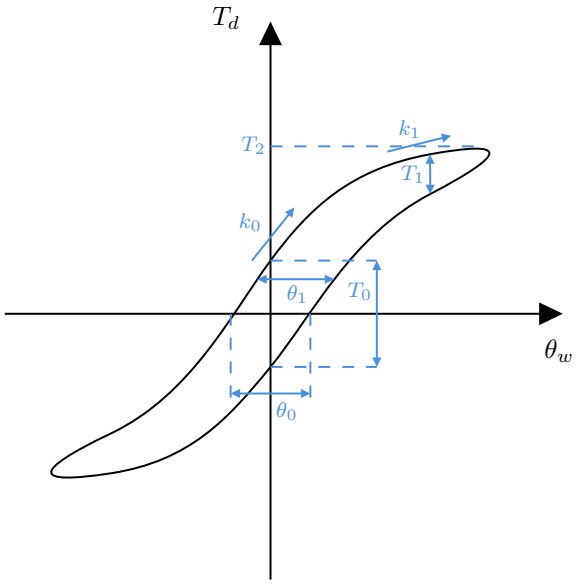

Figure 1.4: Steering torque versus steering wheel angle curve. The torque differences T_0 and T_1 are the torque hysteresis at zero and 70% maximum steering wheel angle, respectively. The torque T_2 is the maximum torque over the whole steering range. The angle differences θ_0 and θ_1 are the angle hysteresis at 0 and $1.3\,\mathrm{Nm}$. The metrics k_0 and k_1 represent the torque gradient to steering angle during on-center and cornering maneuvers.

is related to the feeling of rigidity to the reaction torque. The higher it is, the heavier the feeling of reaction torque rigidity that will be produced. Note that, for a slow steering maneuver, this curve can be deduced from the torque map of the steering system.

For proportional-derivative control schemes, even though the derivative gain parameter increases the stability robustness and the delay margin (see Chapter 2), it also increases the hysteresis of the steering system (the torque differences T_0 and T_1), which degrades the steering feel.

Road feel

The vehicle dynamics generates a contact force between the tires and the road. In the opposite direction, the driver must "feel the road" by receiving appropriate feedback on this contact force. In this way, the driver has a good road feel, which helps him to identify the stability limits of the vehicle.

The road feel is assessed by the torque that would be required from the driver to keep the steering wheel at $\theta_w = 0$, namely the torque T_d^* satisfying $T_d^* = -T_w$. In this situation, according to the expression of T_w^* in Remark 1.1, the net input to the steering wheel dynamics T_w^* is equal to zero. This torque from the driver then eliminates the effect of road reaction torque on the steering wheel.

Suppose that $\theta_w = 0$, then from (1.3) and (1.6), we obtain

$$T_d^*(s) = -(k_s + C_w(s)e^{-(\tau_2+\tau_p)s})\theta_p(s)$$

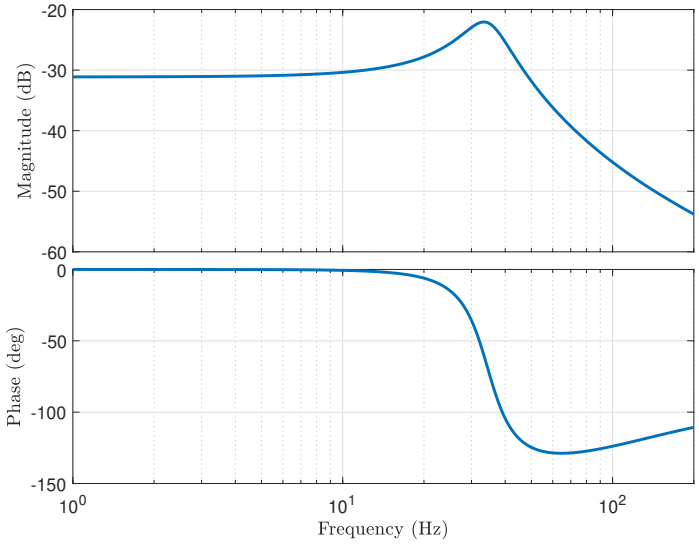

Figure 1.5: Closed-loop frequency response of the driver torque (required to keep $\theta_w = 0$) for road torque input, T_d^*/T_r.

and

$$\theta_p(s) = -(P_p(s)k_s + P_p(s)C_p(s)e^{-\tau_p s})\theta_p(s) + P_p(s)T_r(s).$$

Therefore,

$$\frac{T_d^*(s)}{T_r(s)} = -\frac{P_p(s)(k_s + C_w(s)e^{-(\tau_2+\tau_p)s})}{\varphi_p(s)},$$

with the same φ_p as in (1.7).

An illustrative frequency response of the above transfer function is represented in Figure 1.5, for the same parameter values as in [52]. Steering systems must have sufficient bandwidth to respond seamlessly to the driver fastest inputs while at the same time preserving the feel of the road through the mechanical steering mechanism [118]. Moreover, the resonance peak must be limited to prevent vibrations in the steering wheel that can worsen the driver feeling of the road forces.

1.3 Literature review on steering systems

Several research works have been conducted to improve the robustness and performance of steering systems. Two main phases can be outlined in the control law design process. The first phase defines the boost curve based on the ratio between the driver and road torques at equilibrium. In [16], an optimization procedure is applied to reproduce the shape of the boost curves. In [55], a torque map based on a third-order polynomial was proposed to improve the steering stiffness and return-to-center performance of the steering system. In [10], a torque assistance function and an active damping are developed based on nonlinear functions of the measured torque and electric motor velocity. In [60], the boost curve is designed based on the vehicle inherent road feel. The second phase introduces filters on the assistance designed in the first phase, to improve the performance of the steering system and increase its robustness against disturbances and delays.

In [47], a proportional-integral-derivative controller is developed for controlling the steering system motor torque. Experimental studies show that the proposed control law can improve return-to-center performance of the steering wheel by control of the assist motor. In [52], the robustness of a linearized system is studied by bounding the gain and phase margins, and an optimization-based computation of poles and zeros of a lead-lag compensator is proposed. In [118], the bandwidth is considered in an optimization-based control law design to balance useful signals transmitted to the driver and disturbances. In [119], an objective function allows to adjust the information transmitted from the road to the driver. In [68] the steering system is controlled using a sliding mode controller, where the motor angle is controlled to track a reference angle. In [114], an admittance control strategy is adopted. Some advantages of adopting a proportional-derivative control law to achieve the desired steering system performance are discussed in the *Steering response* paragraph above. However, the delays introduced in the feedback loop of the assistance controller are not considered in most of the previous studies. On the other hand, in [3], delays are introduced in the control law design to obtain a given closed-loop convergence rate despite disturbances and unmodeled dynamics.

Moreover, for steer-by-wire systems, the magnitude of delays is even larger than for electric power steering [35]. The study for these systems is similar to that of telemanipulation systems with haptic force feedback [19, 79]. In [15], a Smith predictor control scheme is considered to compensate for the delays in the system, where force sensors were used to provide feedback force between the two teleoperated systems. However, in such a scheme, a bias error in the force sensor or a disturbance signal produces a non-zero steady-state error because of the integral actions of the plants. In [107], modifications on the control scheme of the Smith predictor were proposed to cope with the integral action of the plant. Recently, more studies on this context were developed [2, 69, 112]. The control scheme proposed by [2] provides a fast time response. In [112], a modified Smith predictor was proposed for the application of an adaptive cruise control.

In the approaches we present in the next chapters, we provide answers to the problem of increasing the delay margin of the steering systems feedback loops pointing out the fact that the proposed frequency-domain techniques lead to filter design guidelines that are based on analytical bounds, which are difficult to obtain with the numerical methods often associated with the time representation.

Finally, it should be noted that almost all the studies on steering systems mentioned above have adopted frequency-domain approaches for the analysis and control law design for steering systems. Nevertheless, time-domain studies have also been conducted for applications on steering systems [94, 117, 59, 108, 109]. The stability of a steering system is certified by the existence of a Lyapunov function and stabilization conditions are formulated as a convex optimization problem in terms of linear matrix inequalities. Note also that the delay in steering systems is also not considered in the studies presented in these references. We may cite [57], in which a fuzzy state feedback controller is proposed for nonlinear time-delay systems. These studies motivated us to develop time-domain stability conditions for time-delay systems and apply them to steering systems with delays.

Chapter 2

Increasing the delay margin of electric power steering systems

This chapter studies the delay margin of the main feedback loop associated with the Electric Power Steering (EPS) system. For this system, the delays are *internal* since they are generated by the processing of local measurements and by the time required to compute the control input in real time. In contrast to the *communication and network transmission delays*, the internal delays are generally small. Moreover, even when they are time-varying, these delays remain *bounded* [57]. As a consequence, the apparent delays can still be made constant by buffering data up to a certain (known) worst-case maximum delay, using a timestamp—see, *e.g.*, [51].

Compared to other design specifications, the delay margin is particularly important for EPS since, for these systems, feedback loop delays appear as the main destabilizing term. Indeed, for the delay-free dynamics, a proportional assistance scheme results in a stable closed-loop for any control gain. In contrast, a delay in the feedback loop can destabilize the system unless a filtering term is included to increase the delay margin of the EPS system. For this reason, the feedback loop analyzed in this chapter consists of a stable second-order system in feedback with different filter structures and is subject to delays. The considered second-order system represents the pinion subsystem dynamics, which is the EPS subset that is most sensitive to delays. There exists already a large literature on filter design for EPS systems, where optimal filter parameters are proposed for a fixed filter structure. However, this is usually done without accounting for the delays in the feedback loop—see, *e.g.*, [119] and [52]. In addition, most existing results in this area aim to design filters by minimizing an objective function. To achieve the performance requirements of the steering system, they impose constraints on the filter gain, such as the phase margin and the location of poles and zeros, in general leading to high-order filters. Such high-order filters are prone to undesirable effects on the system. Moreover, the controller synthesis accounting for these constraints imposes the resolution of a complex nonlinear optimization problem. In contrast, our results aim to maximize the delay margin using low-order filters, which lead to analytical bounds for the delay margin and preserve the steering system performance.

In this chapter, for several of the previously considered filter structures, we carry out the stability analysis, which provides delay margin approximations in an explicit form as a function of the filter parameters. Importantly, we have focused on filter structures for which an analytical bound for the delay margin, or the delay margin itself, is explicitly obtained. For the Proportional-Derivative (PD) filter, a lower bound of the derivative gain parameter is obtained, providing explicit lower bounds of the achievable delay margin and an asymptotic value of the optimal filter parameter. The main benefit of the presented results is that these explicit forms provide guidance for the design of filters that take into account delay margin requirements. In the case of the proportional-derivative filter, the obtained bounds are related to the results in [66], where the derivative gain maximizing the delay margin has been analyzed for unstable systems.

The chapter is organized as follows: Section 2.1 presents the EPS system model and introduces the considered filter structures. In Section 2.2, explicit equations of the delay margin are presented with the different filter structures and present the main result at Theorem 2.4 and Theorem 2.5. The simulation section compares the performance of the filters for selected filter parameters; a comparison with a state-of-the-art controller is also included. The mathematical proofs of the proposed results are given in Appendix A.

2.1 EPS model and problem statement

We consider the following model for the EPS dynamics

$$\begin{aligned} J_w\ddot{\theta}_w(t) + \sigma_w\dot{\theta}_w(t) &= k_s(\theta_p(t) - \theta_w(t)) + T_d(t), \\ J_p\ddot{\theta}_p(t) + \sigma_p\dot{\theta}_p(t) &= k_s(\theta_w(t) - \theta_p(t)) + T_a(t) + T_r(t), \end{aligned} \tag{2.1}$$

where θ_w and θ_p are, respectively, the steering wheel angle and the pinion angular position. The road reaction torque T_r and the driver steering torque T_d are inputs of the system. The stiffness k_s of the torque sensor provides

$$T_s = k_s(\theta_w - \theta_p),$$

the torque that appears in (2.1). Figure 2.1 shows the mechanical model of an EPS system. The remaining model parameters and their numerical values are reported in Table 2.2, in Section 2.3.

In a general form, we use the assist torque map $\kappa : \mathbb{R} \to \mathbb{R}$, and functions $f : \mathbb{R}^n \times \mathbb{R} \to \mathbb{R}^n$, $g : \mathbb{R}^n \times \mathbb{R} \to \mathbb{R}$ to design the assist torque $\bar{T}_a$ as follows

$$\begin{aligned} T_a^{ref}(t) &= \kappa(\theta_w(t) - \theta_p(t))T_s(t), \\ \dot{x}(t) &= f(x(t), T_a^{ref}(t)), \\ \bar{T}_a(t) &= g(x(t), T_a^{ref}(t)), \\ T_a(t) &= \bar{T}_a(t - \tau), \end{aligned} \tag{2.2}$$

where x is the state variable of a filter and T_a^{ref} is a signal defining a reference for the assist torque [53]. The actual assist torque T_a corresponds to the output of the filter $\bar{T}_a$ delayed by τ seconds.

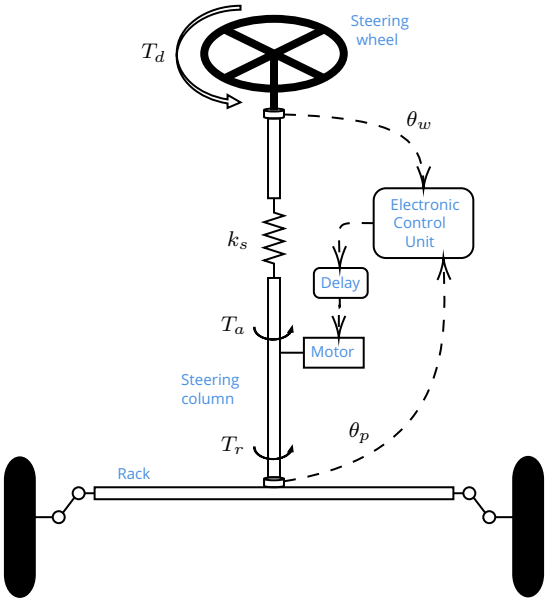

Figure 2.1: Scheme of the EPS system.

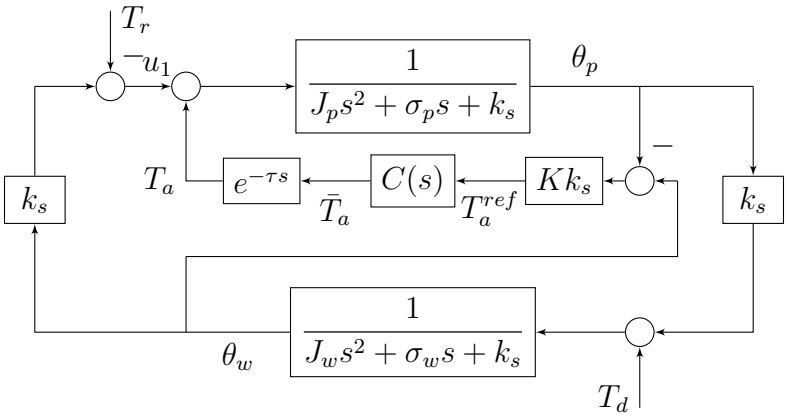

Figure 2.2: Block diagram of the EPS system.

Whenever the assist torque map κ is constant, that is $\kappa(\theta_w - \theta_p) = K$, we say $K > 0$ is the *assist gain*. If, moreover, f and g are linear mappings, system (2.2) is a linear system and it can be expressed in the Laplace domain as

$$T_a(s) = Kk_s e^{-\tau s} C(s)(\theta_w(s) - \theta_p(s)), \tag{2.3}$$

with C the Laplace transform of a linear filter.

The resulting linear system (2.1)-(2.3) is represented in Figure 2.2 with its intermediate signals as in (2.2). In this chapter, we study the feedback loop introduced by the delayed control law in the pinion subsystem. Namely, we focus on the subsystem depicted in Figure 2.3. More precisely, we study the stability of the transfer

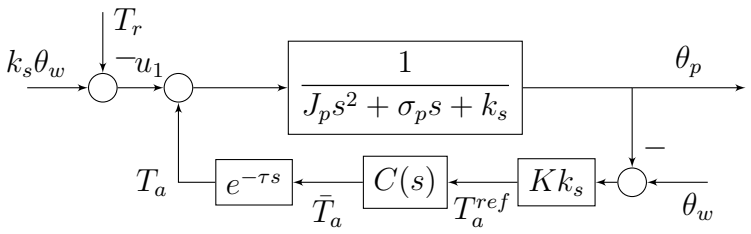

Figure 2.3: Block diagram of the pinion subsystem.

function between u_1 and θ_p given by

$$G(s) = \frac{1}{Kk_s}\left(\frac{\dfrac{Kk_s}{J_p s^2 + \sigma_p s + k_s}}{1 + \dfrac{Kk_s}{J_p s^2 + \sigma_p s + k_s} C(s) e^{-\tau s}}\right).$$

Defining $\omega_0 = \sqrt{\dfrac{k_s}{J_p}}$ and $\zeta = \dfrac{\sigma_p}{2\sqrt{k_s J_p}}$, and introducing $\bar{s} = \dfrac{s}{\omega_0}$ and $\bar{\tau} = \tau\omega_0$, we have that the above transfer function is expressed as

$$G(\bar{s}) = \frac{1}{Kk_s}\left(\frac{P(\bar{s})}{1 + P(\bar{s})C(\bar{s})e^{-\bar{\tau}\bar{s}}}\right), \tag{2.4}$$

with

$$P(\bar{s}) = \frac{K}{\bar{s}^2 + 2\zeta\bar{s} + 1}. \tag{2.5}$$

For a given control law $C(\bar{s})$, the *delay margin* [70] of the pinion subsystem (2.4) is defined by

$$\Delta\bar{\tau} = \sup\left\{\bar{\tau} \geq 0 : G(\bar{s}) \text{ is stable } \forall \tau \leq \bar{\tau}\right\}.$$

Remark 2.1. Since the actual $\bar{s}$ is a scaling of s, the delay margin is given by $\Delta\tau = \Delta\bar{\tau}/\omega_0$ in the above expressions. To keep the notation simple, we will use s instead of $\bar{s}$ in the rest of the chapter. Thus, when using $G(s)$ and $P(s)$, we refer to (2.4) and (2.5), respectively.

The goal of this chapter is to compute delay margin estimates of the feedback loop for five different structures of the linear filter C. These structures are partially inspired by approaches from the literature, for instance those in [118] and [52], where fixed-structure compensators have been proposed to stabilize the system and minimize torque vibrations. The suggested structures combine traditional lead-lag compensators. In particular, we will study the structures of C presented in Table 2.1: C_1 is the filter without any compensation, C_2 is an ideal PD filter where ω_a is the inverse of the derivative coefficient, while C_3 adds extra dynamics to the PD filter to make it proper and to reduce the high-frequency gain [52]. The filter C_4 is defined to compensate for the dynamics of the second-order system and impose a second-order behavior with two real poles [118] to provide an improved delay margin. Finally, to prevent the performance degradation of C_4,

Table 2.1: Filter structures.

$C_1(s)$	$C_2(s)$	$C_3(s)$	$C_4(s)$	$C_5(s)$
1	$\frac{s}{\omega_a}+1$	$\frac{\frac{s}{\omega_a}+1}{\frac{s}{\omega_b}+1}$	$\frac{s^2+2\zeta_f s+1}{\left(\frac{s}{\omega_p}+1\right)\left(\frac{s}{\omega_q}+1\right)}$	$\frac{(s^2+2\zeta_f s+1)\left(\frac{s}{\omega_a}+1\right)}{\left(\frac{s}{\omega_p}+1\right)\left(\frac{s}{\omega_q}+1\right)}$

the filter C_5 combines C_4 and C_2. For an EPS system without delay, when the system disturbances are not considered, the stability of the feedback loop can be achieved without using a filter, taking $C_1(s) = 1$. However, when time delays are included in the feedback loop, we propose to introduce a cascade of N lead-lag filters, where N is determined by the desired robustness level of the system. In this chapter, we focus on filters with a limited order to allow an analytical computation of the delay margin or a lower bound of it as a function of the filter parameters. Moreover, in applications, low-order filters are often preferred because of their simplicity of implementation [14]. Note that the filter parameters are usually chosen based on the parameters of the EPS system, namely the assist gain K and the damping coefficient ζ. Below, we will omit the dependence of the filter parameters on the EPS system parameters, hence, when there is no ambiguity, we will write ω_i instead of $\omega_i(K,\zeta)$, for $i \in \{a,b,p,q\}$.

2.2 Robustness with respect to delays

In this section, we study the effect of the filter parameters on the delay margin of the EPS system for the different filter structures considered in Table 2.1. A separate study of each filter is detailed below.

2.2.1 Delay margin without filter

We start analyzing the robustness of the system without any compensation filter, that is for $C(s) = 1$. The following result is well known. Its proof can be found in [78, Proposition 4.20 and Proposition 4.22].

Proposition 2.1. *Let G be given by* (2.4)*, with P given by* (2.5)*, where $K > 0$ and $\zeta > 0$.*

(i) The delay margin of G with $C = C_1$ is infinite if and only if

$$K \leq 1 \qquad \textit{and} \qquad \zeta^2 > \frac{1-\sqrt{1-K^2}}{2}; \tag{2.6}$$

(ii) If (2.6) *does not hold, then the delay margin* $\Delta\bar{\tau}$ *is given by*

$$\Delta\bar{\tau} = \begin{cases} \dfrac{\tan^{-1}\dfrac{2\zeta\hat{\omega}_c}{\hat{\omega}_c^2-1}}{\hat{\omega}_c}, & \text{if } \hat{\omega}_c > 1, \\ \dfrac{\pi}{2}, & \text{if } \hat{\omega}_c = 1, \\ \dfrac{-\tan^{-1}\dfrac{2\zeta\hat{\omega}_c}{1-\hat{\omega}_c^2}+\pi}{\hat{\omega}_c}, & \text{if } \hat{\omega}_c < 1, \end{cases}$$

where

$$\hat{\omega}_c = \sqrt{\frac{2-4\zeta^2+\sqrt{(2-4\zeta^2)^2-4+4K^2}}{2}}. \tag{2.7}$$

The following corollary gives an explicit upper bound for the delay margin in the case of Item (ii) of Proposition 2.1. This upper bound explicitly shows the dependence of the delay margin in terms of the assist gain K, which is the main parameter that limits the delay margin.

Corollary 2.2. *If* (2.6) *does not hold, the delay margin is a strictly decreasing function of* K *and is upper-bounded by*

$$\Delta\bar{\tau} \leq \begin{cases} \dfrac{4\zeta}{-4\zeta^2+\sqrt{(2-4\zeta^2)^2-4+4K^2}}, & \text{if } \hat{\omega}_c > 1, \\ \dfrac{\pi}{2}, & \text{if } \hat{\omega}_c = 1, \\ \dfrac{\sqrt{2}\pi}{\sqrt{2-4\zeta^2+\sqrt{(2-4\zeta^2)^2-4+4K^2}}}, & \text{if } \hat{\omega}_c < 1. \end{cases} \tag{2.8}$$

The proof of the above corollary relies on Lemma A.1 in Appendix A.

Remark 2.2. From the expressions (2.7) and (2.8), for a fixed ζ, there exist $K_0(\zeta)$ and $\alpha(\zeta)$ such that, for all $K \geq K_0$, we have $\Delta\bar{\tau} \leq \alpha/K$. From this upper bound we can thus observe that a large value of the assist gain K results in a small delay margin. Moreover, from (2.6), for $K \leq 1$ there always exist a value of ζ such that the delay margin is infinite. Since ζ depends only on the system parameters σ_p, k_s, and J_p, and since K is a design parameter, using (2.6) we can always obtain an infinite delay margin with

$$0 < K < \begin{cases} 2\zeta\sqrt{1-\zeta^2}, & \text{if } 0 < \zeta \leq \sqrt{\dfrac{1}{2}}, \\ 1, & \text{otherwise.} \end{cases}$$

One should stress that, even if theoretically the delay margin can be increased by decreasing the value of K, in practice this cannot be done since the parameter K describes the amount of assistance provided to the driver.

2.2.2 Improving the delay margin with a lead filter

In this section, we consider the second-order stable system in (2.5) in feedback with the filter

$$C_2(s) = \frac{s}{\omega_a} + 1. \tag{2.9}$$

The proposition below characterizes the delay margin for system (2.4) with $C = C_2$ in terms of the parameter ω_a.

Proposition 2.3. *Let G be given by* (2.4)*, with P given by* (2.5)*, where $K > 0$ and $\zeta > 0$.*

(i) The delay margin of G with $C = C_2$ is infinite if and only if

$$K \leq 1 \qquad \textit{and} \qquad \frac{1}{\omega_a^2} < \frac{2\sqrt{1-K^2} + 4\zeta^2 - 2}{K^2}. \tag{2.10}$$

Moreover, there exists a value of ω_a such that (2.10) *holds if and only if* (2.6) *holds;*

(ii) If (2.10) *does not hold, then the delay margin $\Delta\bar{\tau}(\omega_a)$ as a function of ω_a is given by*

$$\Delta\bar{\tau}(\omega_a) = \begin{cases} \dfrac{\tan^{-1}\dfrac{\tilde{\omega}_c(\omega_a)}{\omega_a} + \tan^{-1}\dfrac{2\zeta\tilde{\omega}_c(\omega_a)}{\tilde{\omega}_c^2(\omega_a) - 1}}{\tilde{\omega}_c(\omega_a)}, & \textit{if } \tilde{\omega}_c(\omega_a) > 1, \\ \dfrac{\pi}{2} + \tan^{-1}\dfrac{1}{\omega_a}, & \textit{if } \tilde{\omega}_c(\omega_a) = 1, \\ \dfrac{\tan^{-1}\dfrac{\tilde{\omega}_c(\omega_a)}{\omega_a} - \tan^{-1}\dfrac{2\zeta\tilde{\omega}_c(\omega_a)}{1 - \tilde{\omega}_c^2(\omega_a)} + \pi}{\tilde{\omega}_c(\omega_a)}, & \textit{if } \tilde{\omega}_c(\omega_a) < 1, \end{cases} \tag{2.11}$$

where

$$\tilde{\omega}_c(\omega_a) = \sqrt{\frac{\dfrac{K^2}{\omega_a^2} + 2 - 4\zeta^2 + \sqrt{\left(\dfrac{K^2}{\omega_a^2} + 2 - 4\zeta^2\right)^2 - 4 + 4K^2}}{2}}. \tag{2.12}$$

The proof of the above proposition is given in Appendix A. Note that when (2.6) is satisfied the delay margin of G with C_1 is infinite, it is therefore useless to add a lead filter C_2 in this case to increase the delay margin. Moreover, when (2.6) is satisfied, condition (2.10) can also be satisfied provided a large value of the parameter ω_a is used, and thus an infinite delay margin can be achieved. For this reason, the next theorem is restricted to the case where (2.6) is not satisfied. In this case, we also have that (2.12) is strictly positive.

Determining from (2.11) an explicit expression for the value of the parameter ω_a that maximizes the delay margin can be difficult. Nevertheless, we can obtain upper bounds for the values of ω_a that maximize the delay margin as in the following theorem.

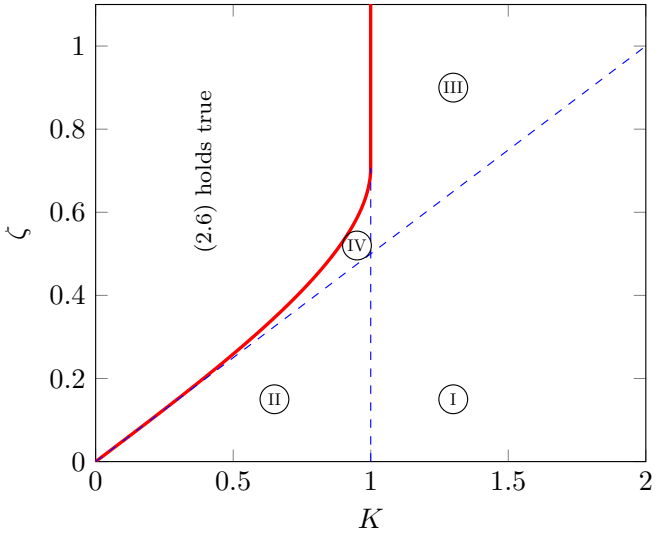

Figure 2.4: The four different cases where (2.6) does not hold true.

Theorem 2.4. *If* (2.6) *does not hold true, the maximum delay margin of* G *with* $K > 0$, $\zeta > 0$, *and* $C = C_2$, *is attained at* $\omega_a = \omega_a^*$ *satisfying*

$$\omega_a^*(\zeta, K) < \bar{\omega}_a^*(\zeta, K),$$

where the upper bound $\bar{\omega}_a^*(\zeta, K)$ *is expressed as*

(I) $\sqrt[4]{\frac{1}{5}(4 + 8K^2 + 4c_1^2 + 64c_2^4)}$, *if* $K > 1$ *and* $K \geq 2\zeta$,

(II) $\sqrt[4]{\frac{1}{5}(4 + 8K^2 c_0 + 4c_1^2 c_0^2 + 64c_2^4 c_0^4)}$, *if* $K \leq 1$ *and* $K \geq 2\zeta$,

(III) $\sqrt[4]{4 + 4K^2 + 2(c_1^2 + c_3^2) + 32(c_2^4 + c_4^4)}$, *if* $K > 1$ *and* $K < 2\zeta$,

(IV) $\sqrt[4]{4 + 4K^2 c_0 + 2(c_1^2 + c_3^2)c_0^2 + 32(c_2^4 + c_4^4)c_0^4}$, *if* $K \leq 1$ *and* $2\zeta\sqrt{1 - \zeta^2} < K < 2\zeta$,

where $c_0 = \dfrac{2 - 4\zeta^2}{\sqrt{(2 - 4\zeta^2)^2 - 4 + 4K^2}}$, $c_1 = \dfrac{4\zeta K^2 \hat{\omega}_c^2}{(\hat{\omega}_c^2 - 1)^2}$, $c_2 = \dfrac{4\zeta K^2}{(\hat{\omega}_c^2 - 1)^2}$, $c_3 = \dfrac{K^2\pi}{\hat{\omega}_c}$, *and* $c_4 = \dfrac{K^2\pi}{\hat{\omega}_c^3}$, *with* $\hat{\omega}_c$ *as in* (2.7).

First note that the four cases of Theorem 2.4, depicted in Figure 2.4, correspond to the set of values for K and ζ that do not satisfy (2.6). The proof of the above theorem is detailed in Appendix A. It is divided into three steps. The first step concerns the four cases and shows that there exists a maximum value for the delay margin as a function of the parameter ω_a. The second step details how the bounds are obtained for cases I and II, while the final step shows how to obtain the bounds for cases III and IV.

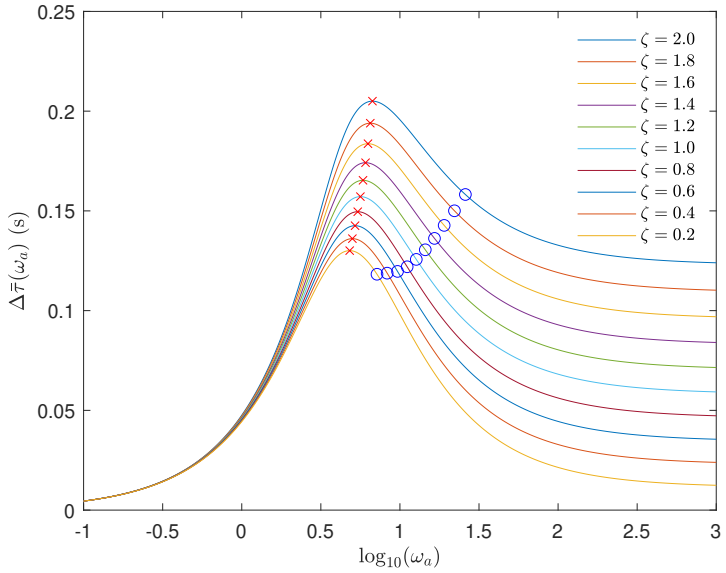

Figure 2.5: Delay margin as a function of ω_a as in (2.11)-(2.12), for $K = 35$ and for different values of ζ: The crosses in red correspond to the optimal delay margin for each value of ω_a^*, while the blue circles provide the upper bound $\bar{\omega}_a^*$ and the corresponding delay margin using (2.11)-(2.12) and the bounds of ω_a^*, given by Theorem 2.4.

For a fixed value of K and for several values of ζ, the upper bounds $\bar{\omega}_a^*$ (given by Theorem 2.4) are compared in Figure 2.5 to the filter parameters ω_a^* that maximize the delay margin (obtained by computing the optimal value of the delay margin with a line search). The curves for the delay margin as a function of ω_a were plotted from relations (2.11)-(2.12). One can observe from this figure that the sharpness of the obtained bound depends on the value of ζ.

Using Proposition 2.3, we can compute the delay margin for each fixed value of ω_a. The value of ω_a that provides the maximal delay margin is denoted $\omega_a^*(K, \zeta)$. The uniqueness of this optimum, for large values of K, is proven in Theorem 2.5 below. Moreover, even if an analytical expression of ω_a^* is not available, the following result shows that the value of ω_a^* does not depend on ζ, and it gives an asymptotic estimation of its value, for large values of K.

Theorem 2.5. *For any fixed value of $\zeta > 0$, we have*

$$\lim_{K \to +\infty} \frac{\omega_a^*(K, \zeta)}{\alpha\sqrt{K}} = 1,$$

where $\alpha > 0$ is the unique solution of the implicit equation

$$\frac{\beta(\alpha)}{\alpha\gamma(\alpha)} \tan^{-1} \frac{\beta(\alpha)}{\alpha} - \frac{\beta^2(\alpha) + \dfrac{\beta^2(\alpha)}{\alpha^2\gamma(\alpha)}}{1 + \dfrac{\beta^2(\alpha)}{\alpha^2}} = 0, \tag{2.13}$$

with $\beta(\alpha) = \sqrt{\dfrac{\frac{1}{\alpha^2} + \sqrt{\frac{1}{\alpha^4} + 4}}{2}}$ *and* $\gamma(\alpha) = \sqrt{\frac{1}{\alpha^4} + 4}$.

The proof of the above theorem is detailed in Appendix A.

Remark 2.3. The nonlinear equation (2.13) can be solved numerically, and it gives an approximate value $\alpha \approx 0.7820$.

Using Item (ii) of Proposition 2.3 and the lower bounds for $\tan^{-1}$ from [74, Equation (1)], the delay margin $\Delta\bar{\tau}(\omega_a)$ of (2.4) satisfies

$$\Delta\bar{\tau}(\omega_a) \geq \frac{\tan^{-1}\dfrac{\tilde{\omega}_c(\omega_a)}{\omega_a}}{\tilde{\omega}_c(\omega_a)} > \bar{h}(\omega_a), \qquad \forall \omega_a,$$

where

$$\bar{h}(\omega_a) = \frac{3}{\omega_a + 2\sqrt{\omega_a^2 + \tilde{\omega}_c^2(\omega_a)}}.$$

With the above lower bound for $\Delta\bar{\tau}$ given by $\bar{h}(\omega_a)$ and the asymptotic behavior given by Theorem 2.5 we can state:

Corollary 2.6. *The optimal value of the delay margin of* (2.4) *with* $C = C_2$ *is lower bounded as*

$$\Delta\bar{\tau}(\omega_a^*(K,\zeta)) > \frac{3}{\alpha\sqrt{K} + 2\sqrt{\alpha^2 K + \tilde{\omega}_c^2(\alpha\sqrt{K})}},$$

where α *is the solution to* (2.13) *and* $\tilde{\omega}_c$ *is defined as in* (2.12)*.*

2.2.3 Analysis of a lead-lag filter

A lead compensator increases the system crossover frequency and makes the plant very sensitive to high-frequency noise. To mitigate the high-frequency noise amplification while making the filter proper, we can replace $C_2(s)$ by a lead-lag filter as

$$C_3(s) = \frac{\frac{s}{\omega_a} + 1}{\frac{s}{\omega_b} + 1}, \qquad \omega_a, \omega_b > 0.$$

The frequency ω_b should be selected to prevent delay margin deterioration. The goal of this section is to obtain the achievable delay margin with a lead-lag structure. Namely, to study the effect of parameters ω_a and ω_b on the delay margin of system (2.4) controlled by C_3.

Proposition 2.7. *Let* G *be given by* (2.4)*, with* P *given by* (2.5)*, where* $K > 0$ *and* $\zeta > 0$*.*

(i) The delay margin of G with $C = C_3$ is infinite if and only if

$$\begin{cases} K \leq 1, \\ \omega_b^2 \geq 2 - 4\zeta^2, \\ \dfrac{1}{\omega_b^2} - \dfrac{K^2}{\omega_a^2} \geq 2 - 4\zeta^2, \end{cases} \qquad \textit{or} \qquad \begin{cases} K \leq 1, \\ -4p^3 - 27q^2 < 0, \end{cases} \tag{2.14}$$

where

$$p = 1 - \frac{(2-4\zeta^2)^2}{3} - \left(\frac{2-4\zeta^2}{3} + \frac{K^2}{\omega_a^2}\right)\omega_b^2 - \frac{\omega_b^4}{3}$$

and

$$q = \frac{2-4\zeta^2}{3} - \frac{2(2-4\zeta^2)^3}{27} + \left(\frac{2}{3} - K^2 - \frac{(2-4\zeta^2)^2}{9} - \frac{(2-4\zeta^2)K^2}{3\omega_a^2}\right)\omega_b^2 + \left(\frac{2-4\zeta^2}{9} + \frac{K^2}{3\omega_a^2}\right)\omega_b^4 + \frac{2\omega_b^6}{27};$$

(ii) If (2.14) *does not hold, and $\omega_b \geq \omega_a$, then, the delay margin $\Delta\bar{\tau}(\omega_a, \omega_b)$ is given by*

$$\Delta\bar{\tau}(\omega_a, \omega_b) = \begin{cases} \dfrac{\tan^{-1}\dfrac{(\omega_b - \omega_a)\omega_c}{\omega_b\omega_a + \omega_c^2} + \tan^{-1}\dfrac{2\zeta\omega_c}{\omega_c^2 - 1}}{\omega_c}, & \textit{if } \omega_c > 1, \\ \dfrac{\pi}{2} + \tan^{-1}\dfrac{\omega_b - \omega_a}{\omega_b\omega_a + 1}, & \textit{if } \omega_c = 1, \\ \dfrac{\tan^{-1}\dfrac{(\omega_b - \omega_a)\omega_c}{\omega_b\omega_a + \omega_c^2} - \tan^{-1}\dfrac{2\zeta\omega_c}{1 - \omega_c^2} + \pi}{\omega_c}, & \textit{if } \omega_c < 1, \end{cases}$$

where ω_c is a function of ω_a and ω_b, given by the maximum real positive root of the polynomial equation

$$\frac{\omega_c^6}{\omega_b^2} + \left(1 - \frac{2-4\zeta^2}{\omega_b^2}\right)\omega_c^4 - \left(\frac{K^2}{\omega_a^2} + 2 - 4\zeta^2 - \frac{1}{\omega_b^2}\right)\omega_c^2 + 1 - K^2 = 0.$$

Proof. Similar to the proof of Proposition 2.3. □

Proposition 2.8. *Given the system in* (2.5) *without delay, the system is unstable with filter C_3 if and only if*

$$\frac{\omega_b}{\omega_a} < \frac{\dfrac{\omega_b + K\omega_b}{\omega_b + 2\zeta} - 1 - 2\zeta\omega_b}{K}.$$

Proof. The claim is an immediate consequence of the Routh stability criterion in dimension 3, as detailed in [116, Theorem 2.4]. □

In Figure 2.6, for the pair of parameters $K = 35$ and $\zeta = 0.17$, we depict the delay margin contours as a function of the parameters ω_a and ω_b of the filter C_3. To simplify the illustration of these curves we use $\omega_a = \rho\omega_b$, with positive values

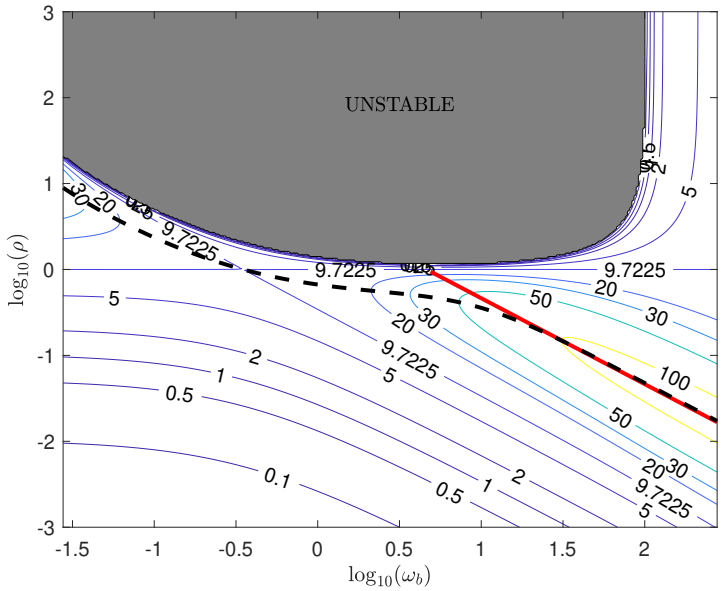

Figure 2.6: Delay margin contours, in ms, for $K = 35$ and $\zeta = 0.17$.

of ρ. The dashed black curve gives the value of ρ that maximizes the delay margin, as a function of ω_b, defined by

$$\rho^*(\omega_b) = \underset{\rho}{\operatorname{argmax}} \{\Delta\bar{\tau}(\rho\omega_b, \omega_b)\},$$

which is obtained with a line search; at every point ω_b, we obtain the value of ρ that maximizes the delay margin.

As indicated by Theorem 2.5, for large values of K, the asymptotic behavior of the optimal values of parameter ω_a, using C_2, is $\omega_a^*(K, \zeta) \approx \alpha\sqrt{K}$. In Figure 2.6, the solid red line corresponds to $\omega_a = \alpha\sqrt{K}$, thus to the points verifying $\rho = \alpha\sqrt{K}/\omega_b$. For large values of ω_b, filter C_3 is equivalent to filter C_2. Hence, following Theorem 2.5, with a large value of K (which is the case in the example since $K = 35$), we should retrieve the maximal values of the delay margins achievable with C_2 taking $\omega_a^*(K, \zeta) = \alpha\sqrt{K}$, for large values of ω_b. We observe this asymptotic behavior when the optimal delay margin curve approaches the predicted curve for C_2, for large values of ω_b.

2.2.4 Filter-based dynamic compensation

Finally, we consider the filter

$$C_4(s) = \frac{s^2 + 2\zeta_f s + 1}{\left(\frac{s}{\omega_p} + 1\right)\left(\frac{s}{\omega_q} + 1\right)}, \tag{2.15}$$

already studied in [118]. Imposing $\zeta_f = \zeta$ in this filter introduces a compensation of the stable dynamics of $P(s)$ and transforms it into

$$\begin{aligned} L(s) &= P(s)C_4(s) \\ &= \frac{K}{s^2+2\zeta s+1}\frac{s^2+2\zeta s+1}{\left(\frac{s}{\omega_p}+1\right)\left(\frac{s}{\omega_q}+1\right)} \\ &= \frac{K}{\frac{s^2}{\omega_p\omega_q}+2\left(\frac{1}{2\omega_p}+\frac{1}{2\omega_q}\right)s+1}. \end{aligned}$$

From this expression, the analysis of filter C_4 can be derived from Proposition 2.1, since it is the same transfer function for the feedback loop of the system, with

$$\zeta = \left(\frac{1}{2}\sqrt{\frac{\omega_q}{\omega_p}}+\frac{1}{2}\sqrt{\frac{\omega_p}{\omega_q}}\right) \quad \text{and} \quad \omega_0 = \sqrt{\omega_p\omega_q}.$$

Moreover, to further increase the delay margin, the filter (2.15) could also be combined with a lead compensator (2.9), thus resulting in the filter

$$C_5(s) = \frac{(s^2+2\zeta_f s+1)\left(\frac{s}{\omega_a}+1\right)}{\left(\frac{s}{\omega_p}+1\right)\left(\frac{s}{\omega_q}+1\right)}.$$

In this case, the analysis is equivalent to that of Section 2.2.2 since

$$\begin{aligned} L(s) &= P(s)C_5(s) \\ &= \frac{K\left(\frac{s}{\omega_a}+1\right)}{\frac{s^2}{\omega_p\omega_q}+2\left(\frac{1}{2\omega_p}+\frac{1}{2\omega_q}\right)s+1}. \end{aligned}$$

Unlike the lead and lead-lag filters, where the maximum achievable delay margin with fixed values of K and ζ is limited when (2.6) does not hold, the filters C_4 and C_5 can arbitrarily increase the delay margin of a stable system by compensating system poles and introducing well-damped ones. However, even if the filter zeros exactly compensate the system poles, a well-damped system dynamics can decrease the performance of the system in terms of the performance criteria described in Section 1.2 of Chapter 1.

2.2.5 Stability of the coupled system and disturbance rejection

In contrast with the previous sections, where the coupling between the two subsystems was not taken into account, here we analyze the stability of the electric power steering system considering the coupling between the steering wheel and the pinion subsystems. Moreover, the sensitivity of the proposed controller with respect to input disturbances is also considered.

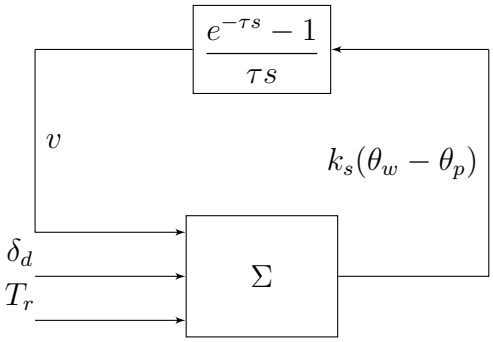

Figure 2.7: LFT representation of the EPS system.

Usually, in an electric power steering system, the driver torque is estimated using the torque sensor. In fact, the driver torque can be written as $T_d = T_s + \delta_d = k_s(\theta_w - \theta_p) + \delta_d$, where δ_d is the error between the driver torque input T_d and the measured signal T_s. Introducing this last expression in (2.1), the electric power steering system can be represented in the Linear Fractional Transformation (LFT) form as shown in Figure 2.7, where v is defined as

$$v(s) = \frac{(e^{-\tau s}-1)k_s(\theta_w(s) - \theta_p(s))}{\tau s}$$

and the system Σ is defined by

$$k_s(\theta_w(s) - \theta_p(s)) = G_v(s)v(s) + G_d(s)\delta_d(s) + G_r(s)T_r(s), \tag{2.16}$$

where

$$G_v(s) = -\frac{\tau s K k_s C(s)}{J_p s^2 + \sigma_p s + k_s + K k_s C(s)},$$

$$G_d(s) = \frac{(J_p s^2 + \sigma_p s)k_s}{(J_p s^2 + \sigma_p s + k_s + K k_s C(s))(J_w s^2 + \sigma_w s)},$$

and

$$G_r(s) = \frac{k_s}{J_p s^2 + \sigma_p s + k_s + K k_s C(s)}.$$

Note that

$$\left|\frac{e^{-\tau s}-1}{\tau s}\right| \leq 1.$$

From the above feedback loop, we can analyze the stability with respect to the delay by applying the small gain theorem [65], therefore yielding the stability of the feedback loop if

$$|G_v(s)| \leq 1.$$

Moreover, to guarantee disturbance rejection with respect to road torque noise, the filter must ensure a small magnitude for the transfer function G_r in the high-frequency range. At steady state, the magnitude of the transfer function G_r is equal to $1/(1+K)$, for all structures of filters C. This transfer function must also have a sufficient bandwidth to provide the driver a feedback torque of the forces

Table 2.2: EPS parameters–see [52].

Symbol	Description	Value
k_s	torque sensor stiffness	$143.24\,\mathrm{Nm/rad}$
J_w	steering wheel moment of inertia	$0.044\,\mathrm{Kg.m^2}$
σ_w	steering wheel viscous damping	$0.25\,\mathrm{Nm.s/rad}$
J_p	pinion moment of inertia	$0.11\,\mathrm{Kg.m^2}$
σ_p	pinion viscous damping	$1.35\,\mathrm{Nm.s/rad}$
K	assist gain	35

acting on the wheels [67]. In addition, to guarantee disturbance rejection with respect to driver torque estimation error, the filter must ensure a small magnitude for the product $G_d(s)\delta_d(s)$ over the whole frequency range. At steady state, from (2.1), we have $T_d(0) = k_s(\theta_w(0) - \theta_p(0))$, hence $\delta_d(0) = 0$ and therefore $|G_d(0)\delta_d(0)| = 0$. In the high-frequency range, the magnitude of the transfer function G_d must be small. In Section 2.3.6, these criteria on the transfer functions G_d and G_r are checked over the whole frequency-domain range to assess disturbance rejection for the considered set of system and control parameters.

Remark 2.4. In standard vehicle designs, a self-alignment torque is produced at the wheels, aiming to return them to the center position. This torque results from the reaction forces generated by the contact between the tires and the road. Even if this torque stabilizes the steering system and increases its robustness, in the stability analysis of the coupled system, we considered the worst-case scenario, in which $T_r = 0$. Therefore the above analysis is pessimistic since it neglects an additional stabilizing torque.

2.3 Simulations

To illustrate the theoretical results of Section 2.2, we simulate the EPS system using the parameter values detailed in Table 2.2. These values are taken from [52], in which a standard column-type EPS system is considered (corresponding to a Hyundai Motors i30 vehicle). In Sections 2.3.1 and 2.3.2, we illustrate numerically the results of Theorem 2.4 and Theorem 2.5, obtained for the lead filter C_2. These simulations give an insight of the delay margin achievable using C_2. Then, in Section 2.3.3, we compare the delay margins obtained using the filter structures described in Table 2.3. Afterwards, in Section 2.3.4, we compare these filters considering the steering and road feel performances of the EPS system. In Section 2.3.5, we test the robustness of our filter face to a time-varying delay. Finally, in Section 2.3.7, we provide a comparison with a recent controller in the literature [52], where the controller design is based on the solution to an optimization problem without taking into account the delay margin of the system. To present realistic values for parameters ω_a, ω_b, ω_p, and ω_q, we use their actual (non-normalized) values (see Remark 2.1).

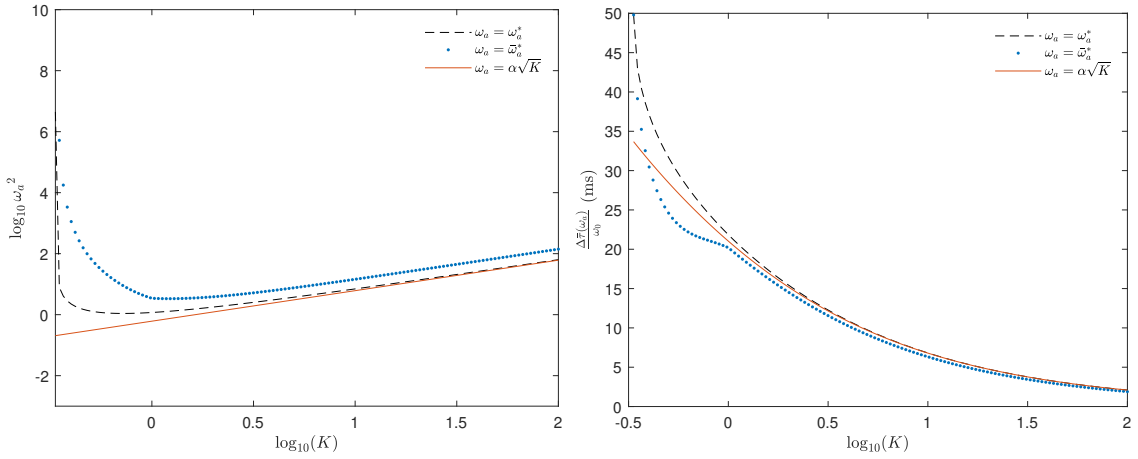

(a) (b)

Figure 2.8: (a) Upper bound and asymptotic value of ω_a^* as a function of K. (b) Comparison between the different delay margin bounds (for filter C_2) with the choice of ω_a resulting from Theorems 2.4 and 2.5.

2.3.1 Maximum achievable delay margin with a lead filter

In Figure 2.8a, we consider the plant (2.5) with the filter C_2, in which we allow the assist gain K to vary in the interval $[1, 100]$, fixing $\zeta = 0.17$, see Table 2.2. For each value of K, we compare the value of $\omega_a^*(K, \zeta)$ with its upper bound and its asymptote $\alpha\sqrt{K}$ using the results of Theorem 2.4 and Theorem 2.5, respectively. For a large value of the assist gain K, Figure 2.8a illustrates the asymptotic behavior outlined in Theorem 2.5. Figure 2.8b shows the delay margin obtained using the three values presented in Figure 2.8a, namely, the optimal value $\omega_a^*(K, \zeta)$, its upper bound, and its asymptotic value. Note that the delay margin curve computed with $\omega_a = \omega_a^*$ is an upper bound for the other two curves and converges asymptotically to the red curve, for large values of K. Since our filters were designed for a normalized frequency, the delay margins for the actual system are recovered by dividing the result by ω_0 (which is dimensionless). Figure 2.8b shows that, for $K > 1$, the maximum achievable delay margin with filter C_2 is limited.

2.3.2 Analytical approximation of the delay margin for a lead filter

In the remainder of this section, we fix $K = 35$ and $\zeta = 0.17$, as in [52]. Following Proposition 2.3, we compute the maximal achievable delay margin for $K = 35$, which is equal to $\Delta\bar{\tau}(\omega_a^*(35, 0.17)) = 3.58\,\mathrm{ms}$. In Theorem 2.4, we showed that for a given value of the assist gain K and a given value of the damping coefficient ζ of the EPS system, the value of the lead filter parameter that maximizes the delay margin of the EPS system is upper-bounded by $\bar{\omega}_a^*$. Then, to estimate the delay margin achievable with a lead filter, we approximate the parameter of the lead filter by the explicit value of its upper bound $\omega_a = \bar{\omega}_a^*$, given in Theorem 2.4. For $\omega_a = \bar{\omega}_a^* = 40.39\,\mathrm{Hz}$, the delay margin is $3.27\,\mathrm{ms}$ compared to the maximum

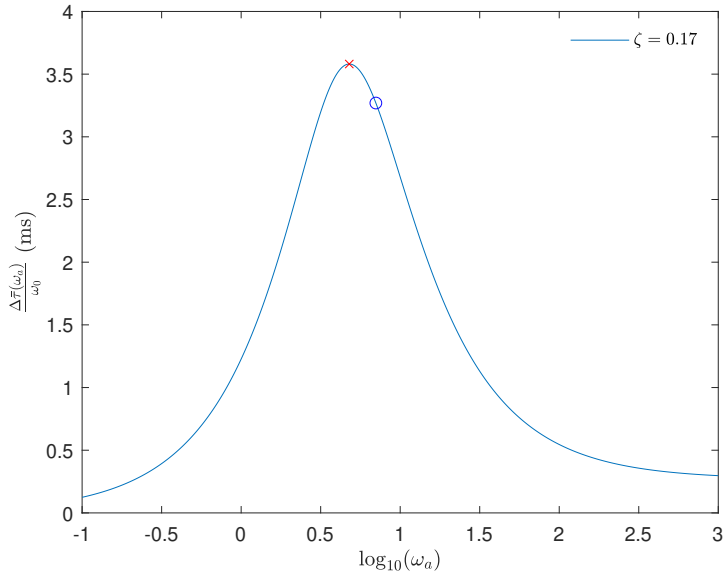

Figure 2.9: Delay margin as a function of ω_a, for $K = 35$ and $\zeta = 0.17$: The red cross correspond to the optimal delay margin for the optimal value ω_a^*, while the blue circle provides the upper bound $\bar{\omega}_a^*$ and the corresponding delay margin, given by Theorem 2.4.

achievable value of the delay margin $3.58\,\mathrm{ms}$ obtained at $\omega_a = \omega_a^* = 27.48\,\mathrm{Hz}$. The value ω_a^* giving the maximum delay margin is obtained by solving the implicit equation corresponding to (A.9) in Appendix A, with its left hand side set to zero. Figure 2.9 shows the achievable delay margin of the EPS system with a lead filter in function of the filter parameter. The figure illustrates that Theorem 2.4 gives a close approximation of the achievable delay margin.

2.3.3 Comparison between the delay margins of the different filter structures

Recall that $C_1(s) = 1$. For the lead filter C_2, we set the parameter of this filter at the value $\omega_a = \omega_a^*$ that achieves the maximum delay margin. For the lead-lag filter C_3, we chose $\omega_a = \omega_a^*$ in the same way as for the lead filter and we add a lag that corresponds to a more realistic implementation of this filter, fixing the parameter ω_b to the highest possible value allowed by the sensor noise level. Following [52], we set ω_b to $159.15\,\mathrm{Hz}$.

EPS systems must have sufficient bandwidth to respond seamlessly to the fastest driver inputs while maintaining road feel through the mechanical steering mechanism [68]. In [52], a nonlinear optimization problem is solved to maximize the phase margin and the gain margin of the controlled system. In [119], the bandwidth is considered in the optimal synthesis procedure of the controller to balance between useful information transmitted from the road to the driver and the unwanted disturbance and noise. In our approach, we select C_4 to satisfy the following items:

(i) Compensate the dynamics of the EPS system, that is $\zeta_f = \zeta$;

(ii) Preserve the bandwidth for the initial EPS system, that is $\omega_p\omega_q = \omega_0^2$;

(iii) Set the delay margin to $5.00\,\mathrm{ms}$.

Finally, the parameters of the filter C_5 are selected to satisfy to satisfy the following items:

(i) Compensate the dynamics of the EPS system, that is $\zeta_f = \zeta$;

(ii) Preserve the same bandwidth for the initial EPS system, that is $\omega_p\omega_q = \omega_0^2$;

(iii) Set the delay margin to $5.00\,\mathrm{ms}$ with $\omega_a = \omega_a^*$.

Table 2.3 summarizes the values of the filter parameters and the corresponding delay margin for the system parameters of Table 2.2, and three values for parameter σ_p: $\sigma_p = 1.35\,\mathrm{Nm.s/rad}$, $\sigma_p = 12.18\,\mathrm{Nm.s/rad}$, and $\sigma_p = 16.79\,\mathrm{Nm.s/rad}$.

A higher delay margin can be achieved with the filters C_4 and C_5 following the discussion in Section 2.2.4. However, this degrades the performance of the system, evaluated in terms of steering and road feel. The differences on the performance between two filters giving the same delay margin are discussed below.

2.3.4 Comparison between different filter structures in term of the steering feel and road feel

We now set the value of the delay in the feedback loop to $\tau = 4\,\mathrm{ms}$. We will study three different cases corresponding to the three different values of parameter σ_p detailed in Table 2.3.

To illustrate the behavior of the obtained filters, we consider two criteria. The first criterion (the "road feel"), is assessed by the driver torque T_d that would be required to keep the steering wheel at $\theta_w = 0\,\mathrm{deg}$. Namely, the torque T_d^* satisfying $T_d^* = -k_s\theta_p$. In this situation, the input to the steering wheel dynamics (in the bottom of Figure 2.2) is equal to zero. This torque from the driver then eliminates the effect of the road reaction torque on the steering wheel. From the system equations, we obtain the following transfer function

$$\frac{T_d^*(s)}{T_r(s)} = \frac{k_s}{J_p s^2 + \sigma_p s + k_s + K k_s C(s) e^{-\tau s}}.$$

For the second criterion (the "steering feel"), the EPS system is simulated under a steering input signal given by a sinusoid of amplitude $30\,\mathrm{deg}$ and of frequency $0.2\,\mathrm{Hz}$, applied during a single period. Differently from the "road feel" assessment test, a nonlinear torque map, the function κ in (2.2), has been included to provide a more realistic representation of the steering feel [58, Figure 6]. The considered torque map is represented in Figure 2.10. For the obtained trajectory, we plot the driver steering torque T_d as a function of the steering wheel angle θ_w. The steering feel is quantified from the "hysteresis" curves of driver steering torque versus steering wheel angle given by sinusoidal input. The amplitude of the steering wheel angle for the zero steering wheel torque is used to quantify the hysteresis. The higher

Table 2.3: Delay margin of the pinion subsystem, obtained with the different filter structures analyzed in this paper. The default system parameters are reported in Table 2.2. Additional settings of pinion damping σ_p were considered to increase the value of the delay margin.

Filter	$C_1(s)$	$C_2(s)$	$C_3(s)$	$C_4(s)$	$C_5(s)$
Structure	1	$\dfrac{s}{\omega_a}+1$	$\dfrac{\dfrac{s}{\omega_a}+1}{\dfrac{s}{\omega_b}+1}$	$\dfrac{\dfrac{s^2}{\omega_0^2}+\dfrac{2\zeta}{\omega_0}s+1}{\left(\dfrac{s}{\omega_p}+1\right)\left(\dfrac{s}{\omega_q}+1\right)}$	$\dfrac{\left(\dfrac{s^2}{\omega_0^2}+\dfrac{2\zeta}{\omega_0}s+1\right)\left(\dfrac{s}{\omega_a}+1\right)}{\left(\dfrac{s}{\omega_p}+1\right)\left(\dfrac{s}{\omega_q}+1\right)}$
Filter parameters (Hz) $\sigma_p = 1.35\,\mathrm{Nm.s/rad}$		$\omega_a = 27.48$	$\omega_a = 27.48$ $\omega_b = 159.15$	$\omega_p = 1.07$ $\omega_q = 30.75$	$\omega_p = 2.13$ $\omega_q = 15.50$ $\omega_a = 35.67$
Delay margin (ms)	0.27	3.58	2.69	5.00	5.00
Filter parameters (Hz) $\sigma_p = 12.18\,\mathrm{Nm.s/rad}$		$\omega_a = 35.67$	$\omega_a = 35.67$ $\omega_b = 159.15$	$\omega_p = 1.07$ $\omega_q = 30.75$	$\omega_p = 2.13$ $\omega_q = 15.50$ $\omega_a = 35.67$
Delay margin (ms)	2.54	5.00	4.13	5.00	5.00
Filter parameters (Hz) $\sigma_p = 16.79\,\mathrm{Nm.s/rad}$		$\omega_a = 39.15$	$\omega_a = 39.15$ $\omega_b = 159.15$	$\omega_p = 1.07$ $\omega_q = 30.75$	$\omega_p = 2.13$ $\omega_q = 15.50$ $\omega_a = 35.67$
Delay margin (ms)	3.64	5.87	5.00	5.00	5.00

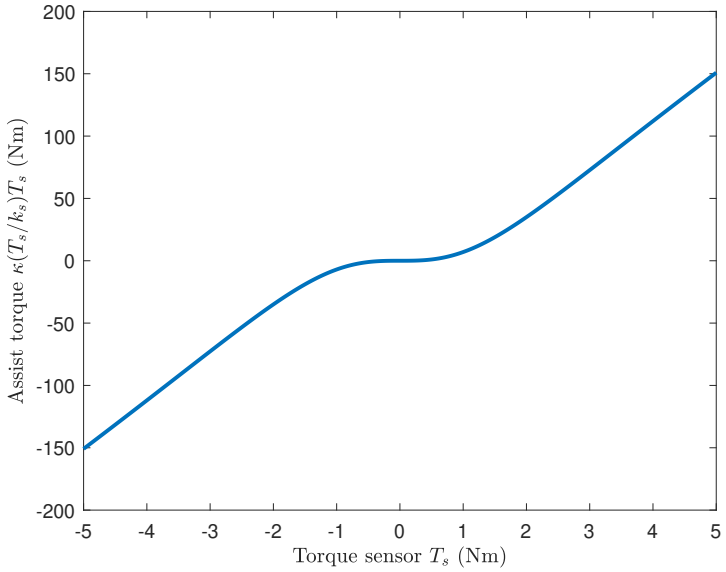

Figure 2.10: Torque map of the EPS.

the hysteresis is, the worse the steering feel is for the driver. An illustration of the hysteresis curve is provided in Figure 2.11d.

First case ($\sigma_p = 1.35\,\mathrm{Nm.s/rad}$). In this case, for filters C_1, C_2, and C_3, the feedback loop is unstable, since the Nyquist plots of C_1, C_2, and C_3 encircle the critical point (Figure 2.11a). Indeed, the delay margins in Table 2.3 are smaller than $4\,\mathrm{ms}$ for C_1, C_2, and C_3, when $\sigma_p = 1.35\,\mathrm{Nm.s/rad}$. In Figure 2.11b, for C_4 and C_5, the closed-loop transfer function of the road reaction torque to the driver torque T_d^* exhibits two resonant frequencies. These resonances may produce vibrations that are transmitted to the steering wheel and degrade the road feel. Figure 2.11c shows the time response of the torque required by the driver to lock the steering wheel in the center position for an input road torque signal given by a sequence of constant values. The figure shows that the response with filter C_5 presents a slightly faster response and smaller overshoot. For the same delay margin, the filter C_4 has a poorer performance than C_5. As shown in Figure 2.11d, the filter C_4 presents a larger hysteresis, associated to an increased damping of the steering system. This sightly reduces the steering feel. Moreover, the filters C_4 and C_5 allow for arbitrarily high delay margins, a property that cannot be obtained using C_2 (see Proposition 2.3). However, the filters C_2 and C_5 are not realistic. For this reason, we must consider the second and third cases described below, where we increase the value of the pinion damping to make filter C_3 stable in the presence of the prescribed delay.

Second case ($\sigma_p = 12.18\,\mathrm{Nm.s/rad}$). In this case, except for C_1, all filters considered in Table 2.1 ensure a stable feedback loop–see Table 2.3. With filter C_2, the feedback loop can achieve a delay margin of $5.00\,\mathrm{ms}$. But, since this is an ideal filter, the value of the pinion damping must be further increased to achieve a delay margin of $5.00\,\mathrm{ms}$ with filter C_3, which can be implemented physically.

Third case ($\sigma_p = 16.79\,\mathrm{Nm.s/rad}$). As in the previous case, except for C_1, all filters considered in Table 2.1 ensure a stable feedback loop with the delay $\tau = 4\,\mathrm{ms}$,

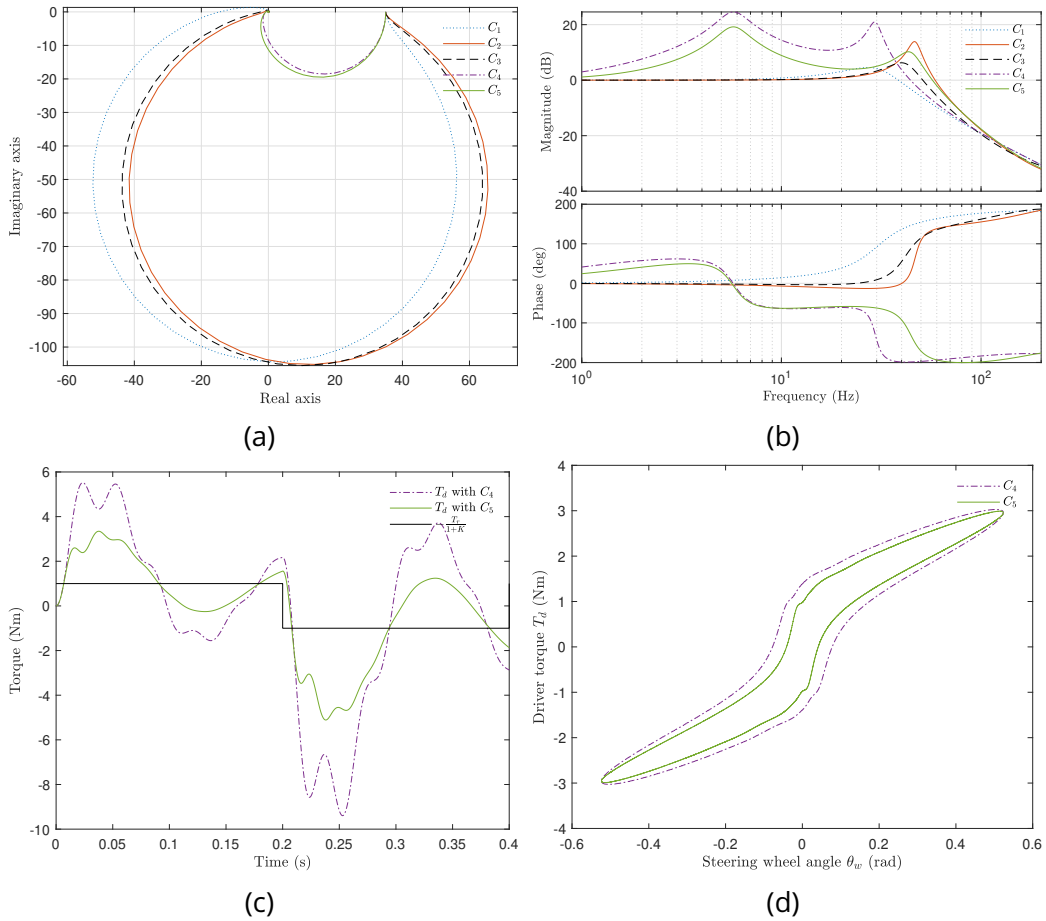

Figure 2.11: *First case* ($\sigma_p = 1.35\,\mathrm{Nm.s/rad}$). Top: (a) Nyquist plot of $L(s) = P(s)C(s)e^{-\tau s}$. (b) Frequency responses of the road reaction torque to the driver torque. Bottom: Driver comfort assessment tests. (c) Driver torque for a square road torque input. (d) Hysteresis curve to assess the steering feel.

as it can be observed in Figure 2.12a. In Figure 2.12b, we show that filter C_3 can improve the bandwidth of the closed-loop transfer function of the road reaction torque to the driver torque T_d^* and reduce the resonant frequency. Figure 2.12c shows that the response with the filter C_3 presents a slightly smaller time constant but also reduced overshoot. The filter C_4 has a poorer performance than C_3 for the same delay margin. As shown in Figure 2.12d, filter C_4 presents a larger hysteresis, associated with an increased damping of the steering system. This hysteresis generates an additional force that the driver must provide during maneuvers.

2.3.5 Time-varying delay case

In this section, we consider filter C_3 with $\sigma_p = 16.79\,\mathrm{Nm.s/rad}$, which is the one that provided the best performance in Section 2.3.4. For this filter, we simulate a time-varying delayed signal to test its robustness to a time-varying delay. The tests were carried out considering time-varying delays within the delay range for

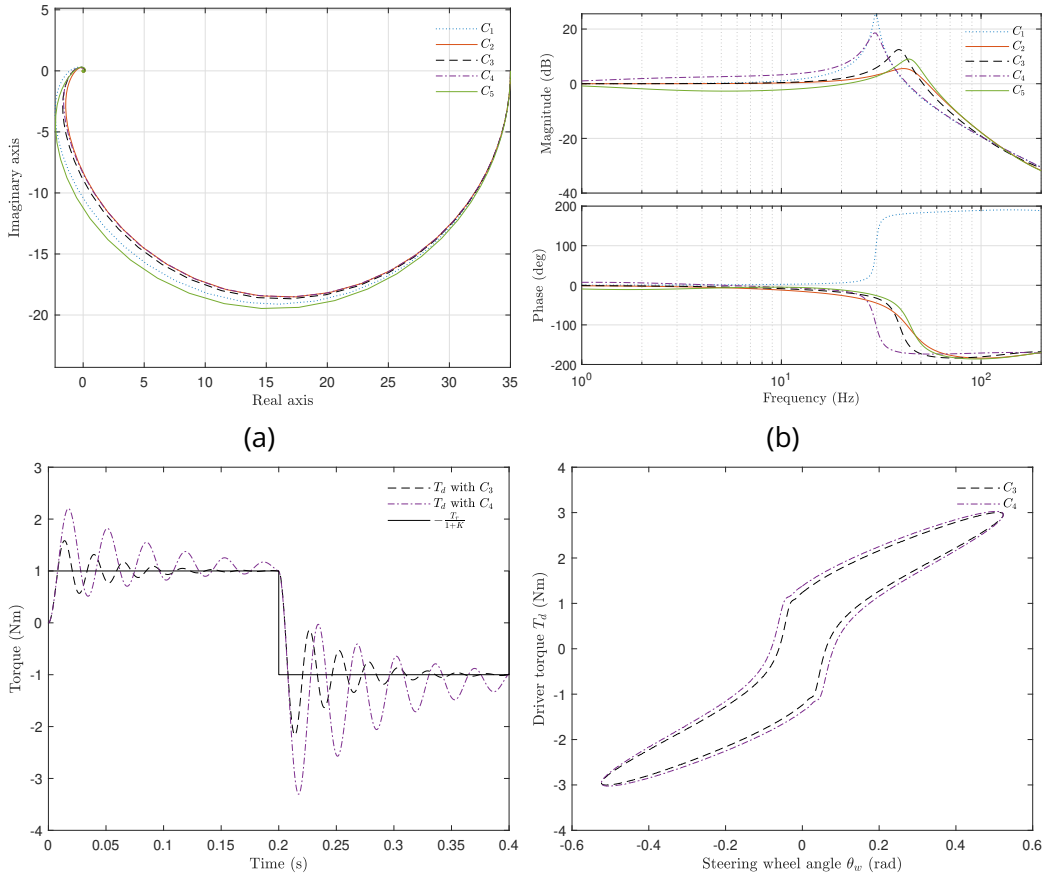

Figure 2.12: *Third case* ($\sigma_p = 16.79\,\mathrm{Nm.s/rad}$). Top: (a) Nyquist plot of $L(s) = P(s)C(s)e^{-\tau s}$. (b) Frequency responses of the road reaction torque to the driver torque. Bottom: Driver comfort assessment tests. (c) Driver torque for a square road torque input. (d) Hysteresis curve to assess the steering feel.

which the stability is guaranteed for fixed delays. We considered a time-varying delay (in ms) of the form

$$\tau(t) = \tau_0 + \epsilon \sin(\omega t),$$

where $\tau_0 = 4\,\mathrm{ms}$. Simulations are illustrated in Figures 2.13a and 2.13b, where the considered values of parameters ω and ϵ are provided in the legend of each plot. It is shown that the variations of the delay around a constant average value, as in the above expression, do not have a significant effect on the performance of the filter.

2.3.6 Controller sensitivity with respect to rejection of disturbances

In this section, we also consider filter C_3 with $\sigma_p = 16.79\,\mathrm{Nm.s/rad}$. For this filter, we plot in Figure 2.14 the Bode diagrams of the transfer functions G_d and $(1 + K)G_r$. We considered a constant delay $\tau = 4\,\mathrm{ms}$. It is shown that the magnitudes of the transfer functions G_d and G_r are small in the high-frequency range. More-

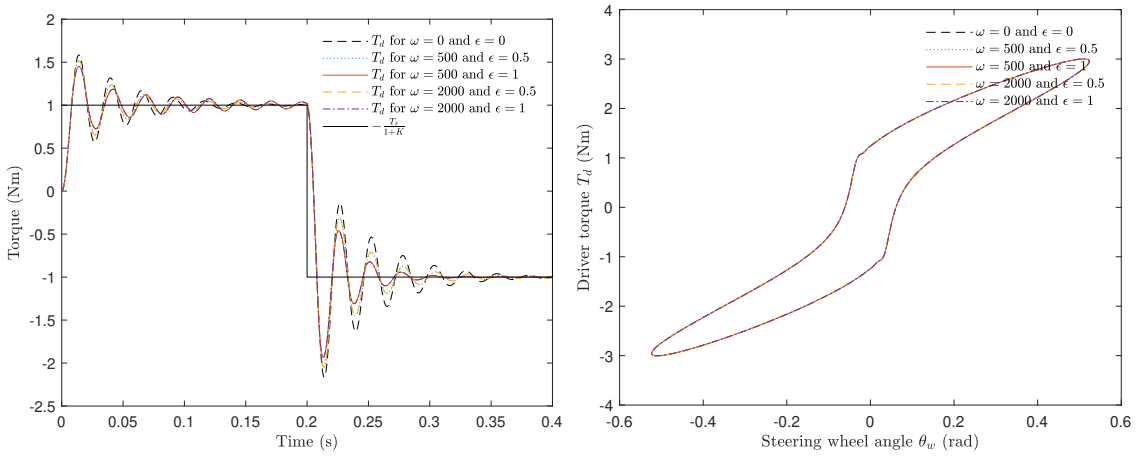

(a) (b)

Figure 2.13: Driver comfort assessment tests for $\sigma_p = 16.79\,\mathrm{Nm.s/rad}$, with a time-varying delay. (a) Driver torque for a square road torque input. (b) Hysteresis curve to assess the steering feel.

over, the transfer function G_r has a sufficiently large bandwidth that provides the driver feedback on the force acting on the wheels.

2.3.7 Comparison with existing results

In this section, a comparison with a recent state-of-the-art controller is carried out. For the parameters values given in Table 2.2 with $\sigma_p = 1.35\,\mathrm{Nm.s/rad}$, the selected optimal controller proposed in [52] is a cascade of three lead-lag filters, given by

$$C_6(s) = \frac{\left(\frac{s}{55.3}+1\right)\left(\frac{s}{32.7}+1\right)\left(\frac{s}{80.2}+1\right)}{\left(\frac{s}{1000}+1\right)\left(\frac{s}{6}+1\right)\left(\frac{s}{713}+1\right)}.$$

The design of the above control does not take into account delays in the loop. We measured the delay margin of the above controller to be $1.8\,\mathrm{ms}$, which is significantly smaller in comparison to the delay margin of $2.69\,\mathrm{ms}$ of C_3. Moreover, for a delay of $1.5\,\mathrm{ms}$, we apply the road feel and steering feel tests and, for both tests a worse performance is obtained for C_6 as illustrated in Figure 2.15.

2.4 Conclusions

Motivated by its applications to the analysis of EPS systems stability, we studied a feedback loop consisting of a second-order system in feedback with a control filter and delays. Since the analytic expression of exact delay margins is difficult to obtain, explicit formulas to lower bound them were proposed. For different filter configurations, we showed that improved delay margins can be obtained by reducing the assist gain or by increasing the damping of the system. However, in addition to the robustness with respect to delays, the simulation results indicate

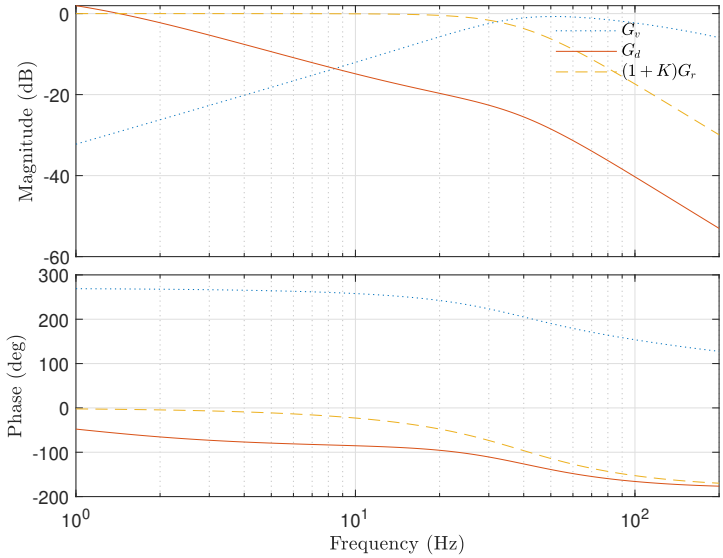

Figure 2.14: Frequency responses of the transfer function G_d, G_r, and G_v for $\sigma_p = 16.79\,\mathrm{Nm.s/rad}$, with a constant delay $\tau = 4\,\mathrm{ms}$.

that an increased damping can have a negative impact on the subjective steering feel and road feel performances. Future work will propose a trade-off between performance measures (in terms of steering feel and road feel) and delay margins.

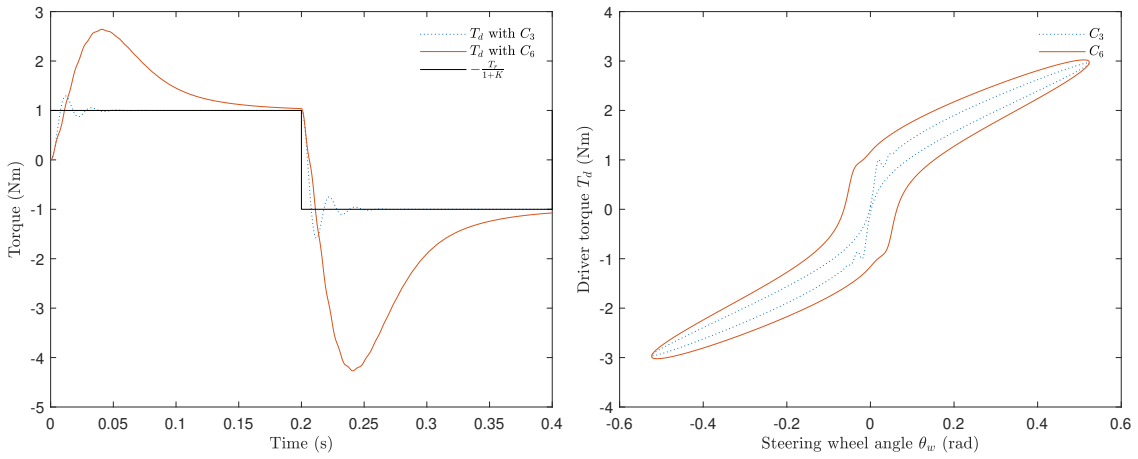

(a) (b)

Figure 2.15: Driver comfort assessment tests for $\sigma_p = 1.35\,\mathrm{Nm.s/rad}$, with a constant delay $\tau = 1.5\,\mathrm{ms}$. (a) Driver torque for a square road torque input. (b) Hysteresis curve to assess the steering feel.

Chapter 3

Increasing the delay margin of steer-by-wire systems

In this chapter, we propose a robust Steer-by-Wire (SBW) control architecture to provide high assistance gains in the presence of internal and transmission delays. The proposed controller is inspired by [110] and [2], where a modified Smith predictor [4] is proposed to compensate for the internal delays in the presence of disturbance signals. These internal delays are usually smaller than transmission delays and are assumed to be known and constant. Hence, their compensation allows to remove them from both local feedback loops, and the stability margin of the interconnected system is reduced to a robustness analysis with respect to the communication delays only. Our methodology is based on frequency-domain techniques for stability analysis of time-delay systems, which provide the allowable bound on the communication delay for the system. To that aim, a Padé approximation is used to compute an analytical expression of the delay margin of the SBW feedback loop. Finally, the delay robustness analysis presented also applies to remote vehicle operation, where the delays can be even larger than in the local vehicle network.

The chapter is organized as follows: The proposed modified Smith predictor is presented in Section 3.1. The controlled system is compared to the conventional Proportional-Derivative (PD) telemanipulation controller. In Section 3.2, a method for estimating the delay margin is proposed. Simulations that compare the proposed controller to a conventional PD controller are also included.

3.1 A modified Smith predictor

Consider the dynamics of the SBW system

$$\begin{aligned} J_w\ddot{\theta}_w(t) + \sigma_w\dot{\theta}_w(t) &= T_w(t) + T_d(t), \\ J_p\ddot{\theta}_p(t) + \sigma_p\dot{\theta}_p(t) &= T_p(t) + T_r(t), \end{aligned} \tag{3.1}$$

where θ_w, θ_p are the angular positions, J_w, J_p, the moments of inertia, σ_w, σ_p, the damping coefficients, and T_d, T_r, the torques generated by the driver and the road. For the PD controller, the control inputs T_w and T_p interconnect the system with

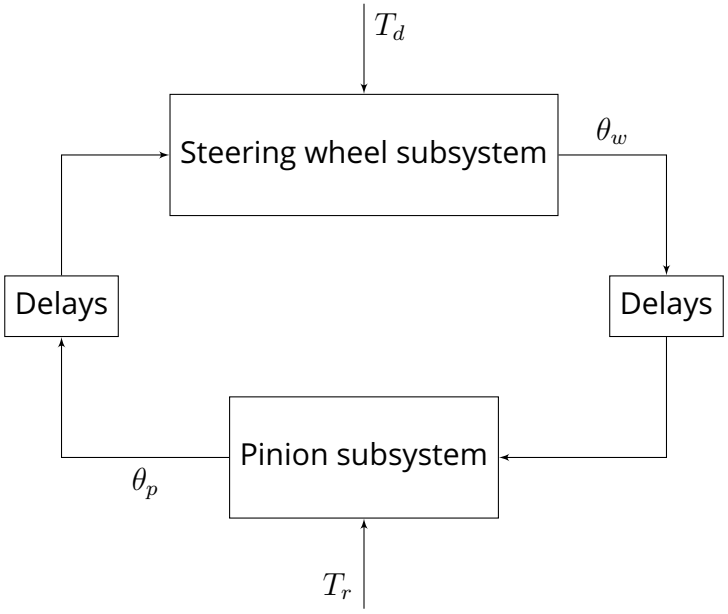

Figure 3.1: SBW block diagram.

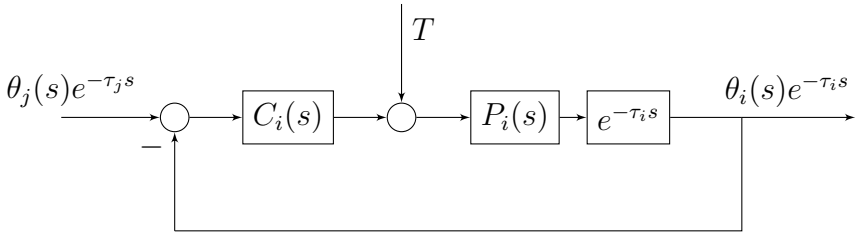

Figure 3.2: Steering wheel/Pinion subsystems block diagram with PD controller.

the control law

$$\begin{aligned} T_w(t) &= k_w(\theta_p(t-\tau_2-\tau_p)-\theta_w(t-\tau_w))+\rho_w(\dot{\theta}_p(t-\tau_2-\tau_p)-\dot{\theta}_w(t-\tau_w)),\\ T_p(t) &= k_p(\theta_w(t-\tau_1-\tau_w)-\theta_p(t-\tau_p))+\rho_p(\dot{\theta}_w(t-\tau_1-\tau_w)-\dot{\theta}_p(t-\tau_p)), \end{aligned} \tag{3.2}$$

where k_w, k_p, ρ_w, and ρ_p are positive control law parameters, τ_w, τ_p are the internal delays, and τ_1, τ_2 are the transmission delays (see, *e.g.*, [51]). This interconnected system (3.1)-(3.2) is represented in Figure 3.1, with the steering wheel and the pinion subsystems as shown in Figure 3.2, $(i,j,T)\in\{(w,p,T_d),(p,w,T_r)\}$, where the transfer functions P_i and C_i, for $i\in\{w,p\}$, are expressed in the Laplace domain as

$$P_i(s)=\frac{1}{J_i s^2+\sigma_i s}$$

and

$$C_i(s)=k_i+\rho_i s.$$

Inspired by [110] and [2], to eliminate the internal delays from the feedback loop of the closed-loop subsystems, we replace the PD control law (3.2) by the

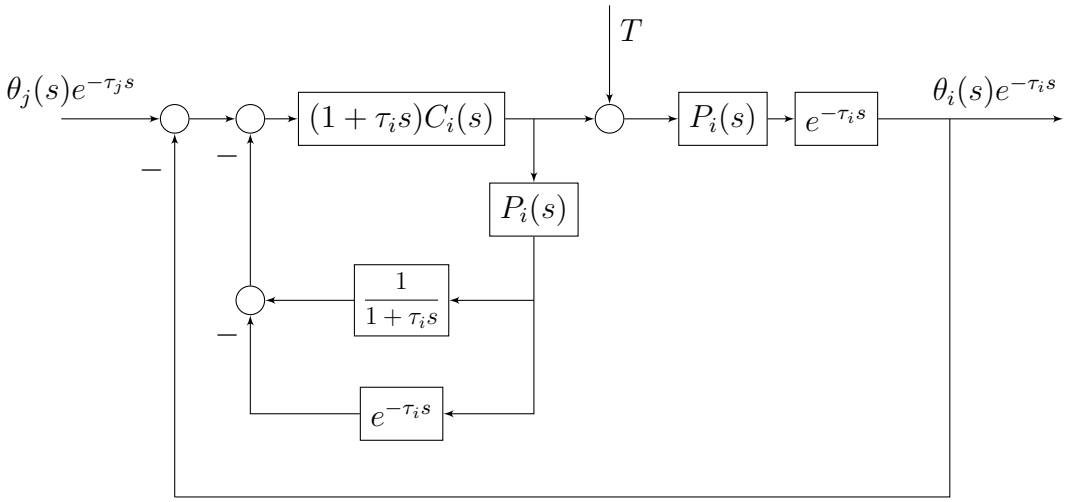

Figure 3.3: Steering wheel/Pinion subsystems block diagram with modified Smith predictor.

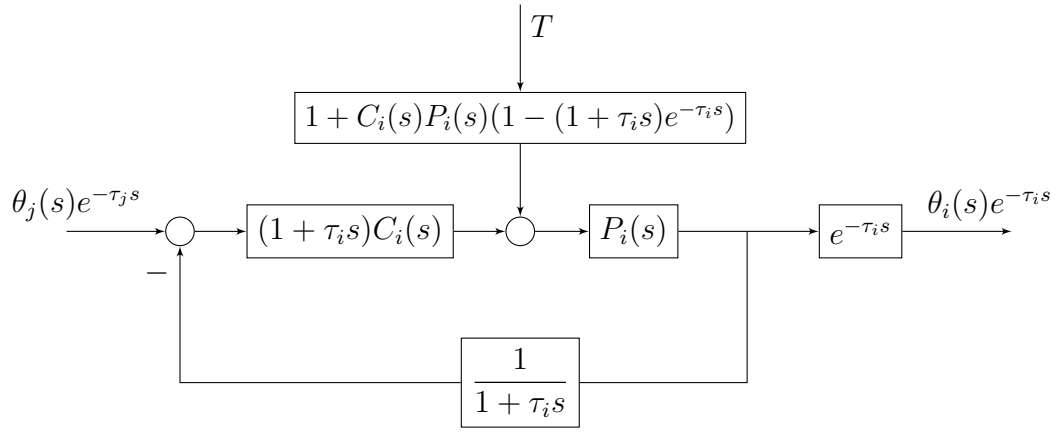

Figure 3.4: Steering wheel/Pinion subsystems block diagram with modified Smith predictor.

modified Smith predictor control architecture depicted in Figure 3.3, where the internal delays τ_w and τ_p, and the system parameters are assumed known. To improve the control architecture proposed in [110], we add to the PD controllers C_w and C_p two lead filters given, respectively, by $1+\tau_w s$ and $1+\tau_p s$.

Using the proposed control architecture, the transfer function from $\theta_j(s)e^{-\tau_j s}$ to $\theta_i(s)e^{-\tau_i s}$ is given by

$$\frac{\theta_i(s)e^{-\tau_i s}}{\theta_j(s)e^{-\tau_j s}} = \frac{(1+\tau_i s)C_i(s)P_i(s)e^{-\tau_i s}}{1+C_i(s)P_i(s)}, \tag{3.3}$$

and the transfer function from $T(s)$ to $\theta_i(s)$ is given by

$$\frac{\theta_i(s)}{T(s)} = \frac{P_i(s)(1+C_i(s)P_i(s)(1-(1+\tau_i s)e^{-\tau_i s}))}{1+C_i(s)P_i(s)}. \tag{3.4}$$

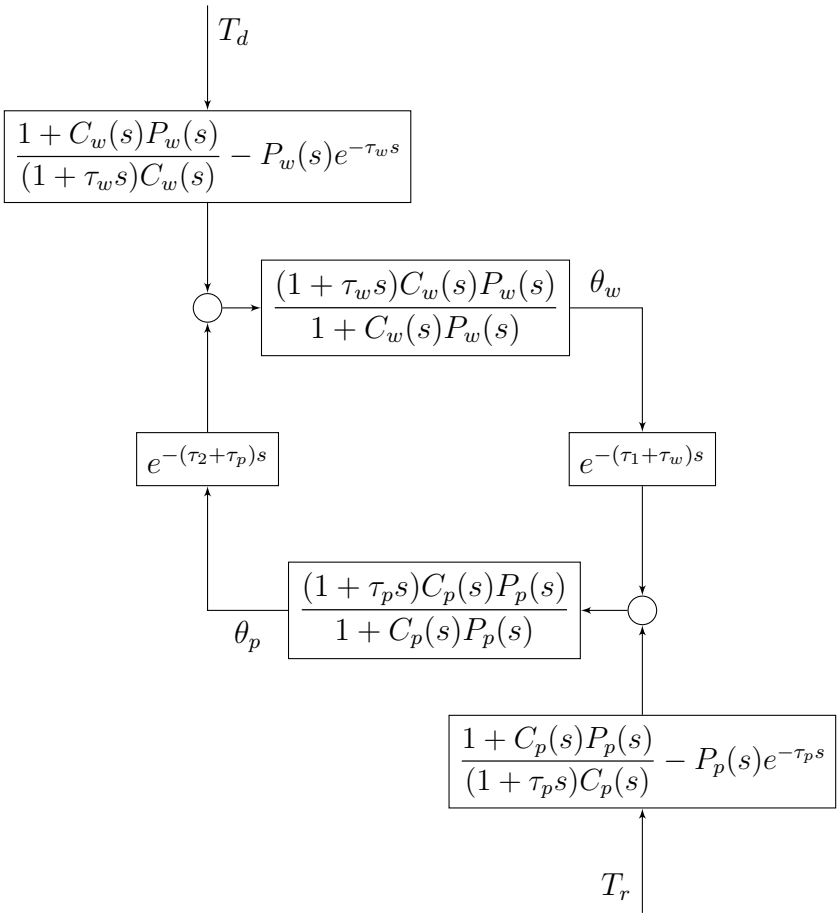

Figure 3.5: SBW block diagram with modified Smith predictor controllers.

Therefore, (3.3) and (3.4) imply that the block diagrams of Figure 3.3 and Figure 3.4 are equivalent. Moreover, without delays (*i.e.*, $\tau_1 = \tau_2 = \tau_w = \tau_p = 0$), the proposed control structure is equivalent to the conventional PD control law in (3.2). The main advantage of the proposed control structure is that the internal delays are removed from the feedback loop of the closed-loop subsystems. Therefore, the SBW system (3.1) with the control architecture of Figure 3.3 is represented by the interconnected system in Figure 3.5. In the sequel, we will consider the open-loop transfer function L defined as

$$L(s) = -\frac{(1+\tau_w s)C_w(s)P_w(s)}{1+C_w(s)P_w(s)} \times \frac{(1+\tau_p s)C_p(s)P_p(s)}{1+C_p(s)P_p(s)}. \tag{3.5}$$

3.2 Stability analysis

To check the stability of the interconnected system, we use the Nyquist criterion [107], which provides a convenient way to examine stability for linear time-delay systems.

Proposition 3.1. *Given the system in* (3.1)-(3.2) *without delays (*i.e., $\tau_1 = \tau_2 = \tau_w = \tau_p = 0$*), the closed-loop system is stable for any positive values of the control parameters* k_w, k_p, ρ_w, *and* ρ_p.

Proof. The claim is an immediate consequence of the Routh stability criterion in dimension 3, as detailed in [116, Theorem 2.4]. □

The *delay margin* [70] of a feedback loop with a single delay is the bound $\Delta\tau$ such that the closed-loop system is stable for any delay in the interval $[0, \Delta\tau)$. From Proposition 3.1, the system (3.1)-(3.2) is stable for any values of the control parameters k_w, k_p, ρ_w, and ρ_p if $\tau_1 = \tau_2 = \tau_w = \tau_p = 0$. We will study below the stability of the system, to obtain the largest value of the *round trip delay* $\bar{\tau}_R$ such that the feedback loop in Figure 3.5 is stable for all delay values in the set $\{(\tau_1, \tau_2, \tau_w, \tau_p) \mid \tau_1 + \tau_2 + \tau_w + \tau_p < \bar{\tau}_R\}$.

From the open-loop transfer function in (3.5), the unity-gain crossover frequencies ω_c are the real positive solutions of the equation $|L(j\omega_c)| = 1$. Finding the explicit expression for the solutions ω_c of this equation is difficult since the characteristic equation is a polynomial of degree 4. Nevertheless, we can determine conditions under which the unity-gain crossover frequency ω_c of L exists and is unique as detailed in the following proposition.

Proposition 3.2. *If the control parameters* k_w, ρ_w, k_p, ρ_w *verify*

$$\begin{cases} a > 0, \\ d < 0, \\ b^2c^2 + 18abcd < 27a^2d^2 + 4ac^3 + 4b^3d, \end{cases}$$

where

$$\begin{aligned}
a &= J_w^2 J_p^2 - \tau_w^2\tau_p^2\rho_w^2\rho_p^2, \\
b &= J_w^2(\rho_p + \sigma_p)^2 + J_p^2(\rho_w + \sigma_w)^2 - 2k_w J_w J_p^2 - 2k_p J_p J_w^2 \\
&\qquad - \tau_w^2\rho_w^2(\tau_p^2 k_p^2 + \rho_p^2) - \tau_p^2\rho_p^2(\tau_w^2 k_w^2 + \rho_w^2), \\
c &= 4k_w k_p J_w J_p + k_w^2 J_p^2 + k_p^2 J_w^2 - 2k_w J_w(\rho_p + \sigma_p)^2 \\
&\qquad - 2k_p J_p(\rho_w + \sigma_w)^2 + (\rho_w + \sigma_w)^2(\rho_p + \sigma_p)^2 \\
&\qquad - \tau_w^2 k_p^2\rho_w^2 - \tau_p^2 k_w^2\rho_p^2 - (\tau_w^2 k_w^2 + \rho_w^2)(\tau_p^2 k_p^2 + \rho_p^2), \\
d &= k_w^2(\rho_p + \sigma_p)^2 + k_p^2(\rho_w + \sigma_w)^2 - 2k_w J_w k_p^2 - 2k_p J_p k_w^2 \\
&\qquad - k_w^2\rho_p^2 - k_p^2\rho_w^2 - \tau_w^2 k_w^2 k_p^2 - \tau_p^2 k_w^2 k_p^2,
\end{aligned}$$

then, the unity-gain crossover frequency ω_c *of* L *exists and is unique.*

Proof. The unity-gain crossover frequency ω_c is the real positive solution of the equation $|L(j\omega_c)| = 1$, which is equivalent to

$$a\omega_c^6 + b\omega_c^4 + c\omega_c^2 + d = 0.$$

The discriminant of the above third-order polynomial is given by

$$\Delta = 18abcd - 4b^3d + b^2c^2 - 4ac^3 - 27a^2d^2.$$

Therefore, since $\Delta < 0$, the third-order polynomial has a unique real root and, since $a > 0$ and $d < 0$, the unity-gain crossover frequency ω_c is positive. □

Below, we assume that the conditions on the control parameters given in Proposition 3.2 hold. This is a realistic assumption since it is usually verified in conventional SBW systems. These conditions give an upper bound on the admissible round trip delay $\bar{\tau}_R$ as shown in the following theorem. However, it is also possible to find conditions on the control parameters to ensure stability independently of the delays.

Theorem 3.3. *Assume that the unity-gain crossover frequency ω_c of L exists and is unique. For the interconnected system given by Figure 3.1 and Figure 3.3, there exists a constant $\bar{\tau}_R$ such that the closed-loop system is stable for all the delay values in the set $\{(\tau_1, \tau_2, \tau_w, \tau_p) \mid \tau_1 + \tau_2 + \tau_w + \tau_p < \bar{\tau}_R\}$.*

Proof. Since the unity-gain crossover frequency ω_c of L exists and is unique, then, from [107], $\bar{\tau}_R$ correspond to the lower bound of $\tau_R > 0$ that satisfies, for $0 \leq \omega_c\tau_R \leq 2\pi$,

$$L(j\omega_c)e^{-\omega_c\tau_R} = -1.$$

□

In this case, the delay margin is given by

$$\bar{\tau}_R = \frac{\arg(L(j\omega_c)) + \pi}{\omega_c}, \tag{3.6}$$

and the unity-gain crossover frequency ω_{cw} of the steering wheel subsystem, given by

$$\omega_{cw}^2 = \max\left(0, \frac{-(\rho_w + \sigma_w)^2 + \rho_w^2 + 2k_wJ_w}{J_w^2}\right),$$

provides a first estimate of the solution ω_c. Below, we propose an approach to obtain a tighter estimate of ω_c.

First, we approximate the transfer function L using a Padé approximation at ω_{cw}, defined by a first-order transfer function $\tilde{L}$ with complex coefficients. That is, based on the Taylor series, we approximate separately the numerator

$$N_L(s) = -(1 + \tau_w s)(1 + \tau_p s)(\rho_w s + k_w)(\rho_p s + k_p)$$

and the denominator

$$D_L(s) = (J_w s^2 + (\sigma_w + \rho_w)s + k_w)(J_p s^2 + (\sigma_p + \rho_p)s + k_p)$$

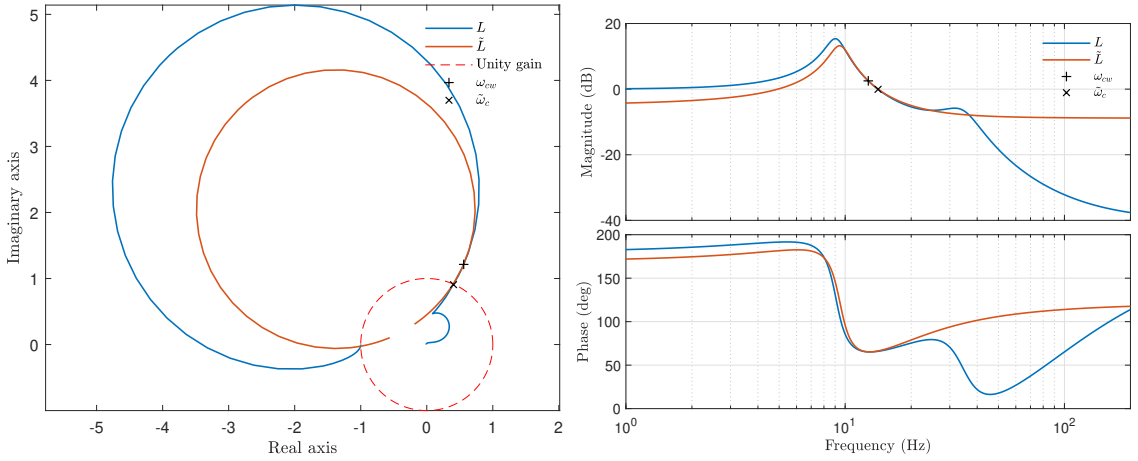

(a) (b)

Figure 3.6: Approximation at ω_{cw} of the open-loop transfer function L, for $\tau_w = \tau_p = 5\,\mathrm{ms}$: (a) Nyquist locus. (b) Bode diagram.

of L in the neighborhood of ω_{cw} to obtain

$$\begin{aligned}\tilde{L}(j\omega) &= \frac{N_L(j\omega_{cw}) + j(\omega-\omega_{cw})\dfrac{dN_L}{ds}(j\omega_{cw})}{D_L(j\omega_{cw}) + j(\omega-\omega_{cw})\dfrac{dD_L}{ds}(j\omega_{cw})} \\ &= \frac{aj\omega + b}{cj\omega + d},\end{aligned}$$

where a, b, c, and d are complex coefficients

$$\begin{aligned}a &= \frac{dN_L}{ds}(j\omega_{cw}), \\ b &= N_L(j\omega_{cw}) - j\omega_{cw}\frac{dN_L}{ds}(j\omega_{cw}), \\ c &= \frac{dD_L}{ds}(j\omega_{cw}), \\ d &= D_L(j\omega_{cw}) - j\omega_{cw}\frac{dD_L}{ds}(j\omega_{cw}).\end{aligned}$$

This approximation generates a circle tangent at ω_{cw} to the Nyquist locus (Figure 3.6). The unity-gain crossover frequency $\tilde{\omega}_c$ of $\tilde{L}$ can be calculated analytically since the characteristic equation is a polynomial of degree 2. It is given by

$$\tilde{\omega}_c = \frac{-(b_i a_r - b_r a_i - d_i c_r + d_r c_i) - \sqrt{\Delta}}{a_r^2 + a_i^2 - c_r^2 - c_i^2},$$

with

$$\Delta = (b_i a_r - b_r a_i - d_i c_r + d_r c_i)^2 - (a_r^2 + a_i^2 - c_r^2 - c_i^2)(b_r^2 + b_i^2 - d_r^2 - d_i^2),$$

where a_r, a_i, b_r, b_i, c_r, c_i, d_r, and d_i are, respectively, the real and imaginary parts of a, b, c, and d. Therefore, since $\tilde{L}$ is an approximation of L, $\tilde{\omega}_c$ approximates ω_c more precisely, which can be used to compute the delay margin $\bar{\tau}_R$ in (3.6).

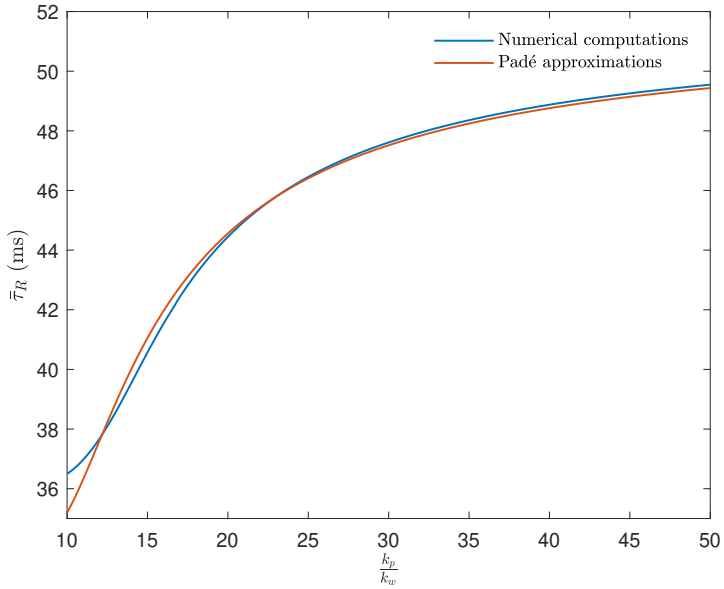

Figure 3.7: Comparison between the delay margins $\bar{\tau}_R = \tau_w + \tau_p + \tau_1 + \tau_2$ at several values of k_p/k_w, for $\tau_w = \tau_p = 5\,\mathrm{ms}$.

The approximate values of the delay margins obtained using $L(j\tilde{\omega}_c)$ and $\tilde{\omega}_c$ in (3.6) are illustrated in Figure 3.7. On the one hand, for small values of k_p/k_w, the unity-gain crossover frequencies of the steering wheel and pinion subsystems (ω_{cw} and ω_{cp}, respectively), are close to each other, which generates an abrupt change in the phase of the transfer function L. This change in phase introduces a significant error in the estimation of the delay margin. On the other hand, when the value of k_p/k_w is large, which is always the case in an assisted steering system, the frequency ω_{cw} is far apart from ω_{cp}. This prevents the abrupt change in the phase of the transfer function L and, in this case, the unity-gain crossover frequency ω_{cw} is close to ω_c, which provides a more accurate approximation of the delay-margin.

The assist gains k_w and k_p are fixed by the system requirements. The derivative gains ρ_w and ρ_p have a significant effect on the stability of the SBW system. However, determining an explicit expression for the values of the parameters ρ_w and ρ_p that maximize the delay margin is difficult [66, Theorem 3.1]. Figure 3.8 shows that the derivative gains ρ_w and ρ_p have a non-monotonic effect on the delay margin.

3.3 Simulations

In this section, we compare the performance of the proposed modified Smith predictor and the conventional PD controller, for the control parameter values reported in Table 3.1. We assume, moreover, that the road torque is given by

$$T_r(t) = -k_r\theta_p(t) - \rho_r\dot{\theta}_p(t), \tag{3.7}$$

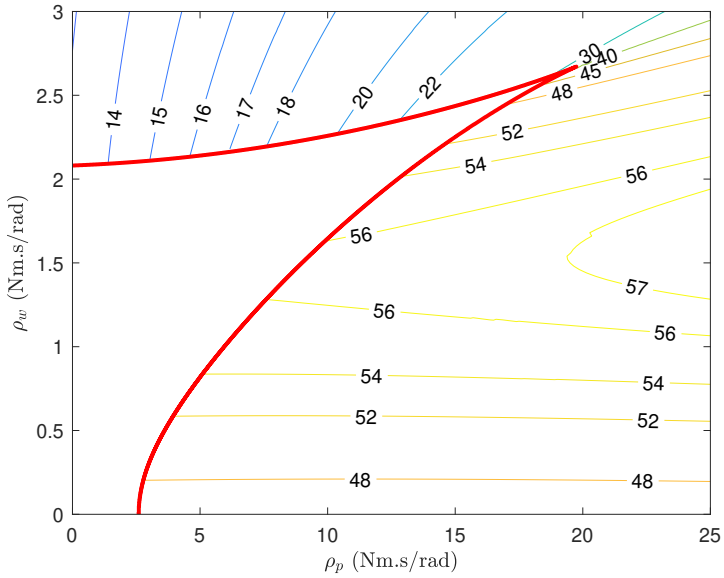

Figure 3.8: Delay margin $\bar{\tau}_R = \tau_w + \tau_p + \tau_1 + \tau_2$ contours, in ms, for $\tau_w = \tau_p = 5\,\mathrm{ms}$. The conditions of Proposition 3.2 do not hold inside the domain bounded by the red curve.

Table 3.1: SBW and controller parameters.

Parameter	Value
J_w	$0.044\,\mathrm{Kg.m}^2$
J_p	$0.11\,\mathrm{Kg.m}^2$
k_w	$143.24\,\mathrm{Nm/rad}$
k_p	$36k_w\,\mathrm{Nm/rad}$
ρ_w	$0.25\,\mathrm{Nm.s/rad}$
ρ_p	$7.75\,\mathrm{Nm.s/rad}$
σ_w	$0.25\,\mathrm{Nm.s/rad}$
σ_p	$1.34\,\mathrm{Nm.s/rad}$

where $k_r = 300\,\mathrm{Nm/rad}$ and $\rho_r = 25\,\mathrm{Nm.s/rad}$. To obtain a more realistic steering feel [58], we introduce a nonlinear torque map κ in the control law T_p,

$$\begin{aligned} T_p(t) = k_w(\theta_w(t-\tau_1-\tau_w) - \theta_p(t-\tau_p)) \\ + \frac{(k_p-k_w)}{k_w}\kappa(k_w(\theta_w(t-\tau_1-\tau_w) - \theta_p(t-\tau_p))) \\ + \rho_p(\dot{\theta}_w(t-\tau_1-\tau_w) - \dot{\theta}_p(t-\tau_p)), \end{aligned}$$

where κ is illustrated in Figure 3.9 and $k_p > k_w$.

We simulate the SBW system in three different cases, in which we change the values of the delays as depicted in Table 3.2. In each case, we consider two scenarios. In the first scenario, a square-like steering torque input is applied, and both the tracking performance and the control signals are examined. In the sec-

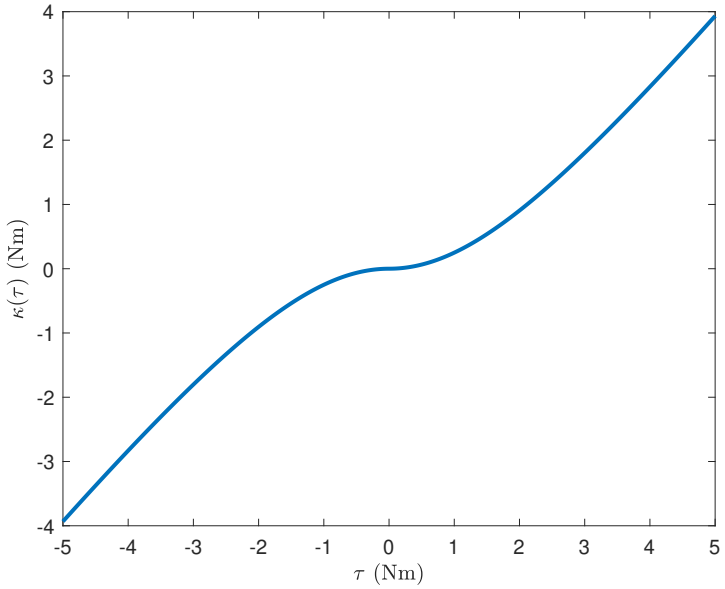

Figure 3.9: Normalized nonlinear torque map.

Table 3.2: Simulation cases.

Delay	Case 1	Case 2	Case 3
$\tau_w\,(\mathrm{ms})$	2.5	5	5
$\tau_p\,(\mathrm{ms})$	2.5	5	5
$\tau_1\,(\mathrm{ms})$	5	5	10
$\tau_2\,(\mathrm{ms})$	5	5	10
$\bar{\tau}_R\,(\mathrm{ms})$	46.04	48.47	48.47

ond scenario, a sinusoidal steering torque input of amplitude $5\,\mathrm{Nm}$ and frequency of $0.1\,\mathrm{Hz}$ is applied and the steering wheel angle is plotted with respect to the driver steering torque. The performance of the system is measured by the hysteresis of this curve. That is, by the distance between the two intersection points with the ordinary axis at $\theta_w = 0$.

For Case 1, since the values of the delays are small, the two controllers have approximately the same performance, as shown in Figures 3.10 and 3.11. For Case 2, as shown in Figures 3.12 and 3.13, the modified Smith predictor compensates for the internal delays and performs almost as in Case 1. However, the PD controller exhibits slight vibrations. These vibrations are a result of the fact that the internal delays are still present in the feedback loop of the steering wheel and pinion subsystems. For Case 3, where we consider larger communication delays $\tau_1 + \tau_2 + \tau_w + \tau_p = 30\,\mathrm{ms}$, as shown in Figures 3.14 and 3.15, the modified Smith predictor results in an oscillating behavior since it gets closer to the delay margin $\bar{\tau}_R = 48.47\,\mathrm{ms}$.

3.4 Conclusions

This chapter studied SBW control loops using PD control laws. To circumvent the lack of robustness with respect to internal and transmission delays of the PD laws with high gains, we introduce a modified Smith predictor. Thanks to the predictor, the closed-loop stability depends only on the round trip delays and not on each of the delays separately. Moreover, we provide an approximation to the delay margin based on a Padé approximation of the open-loop transfer function. Finally, to illustrate the superior performance of the closed-loop including the predictor, we consider a steering feel assessment based on the time response from driver inputs. For large values of the delays, we observe reduced oscillations during transients.

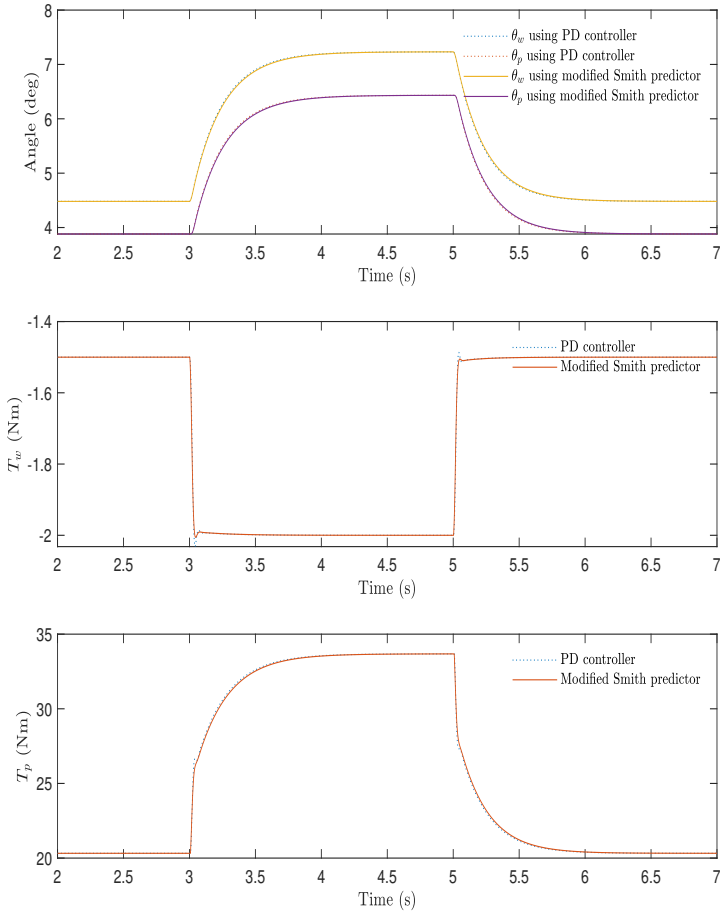

Figure 3.10: Case 1: Control signals for a square-like steering torque input.

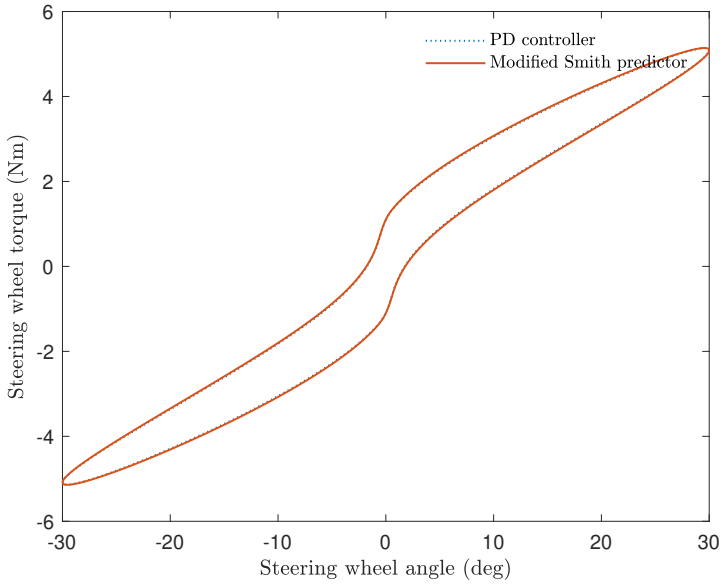

Figure 3.11: Case 1: SBW steering feel for a sinusoidal driver torque input.

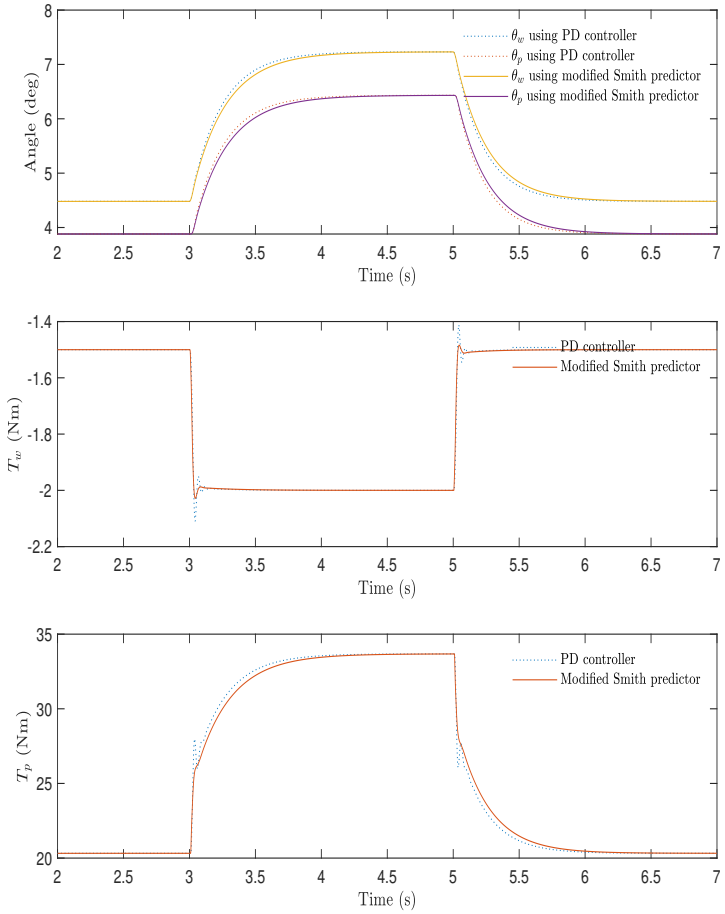

Figure 3.12: Case 2: Control signals for a square-like steering torque input.

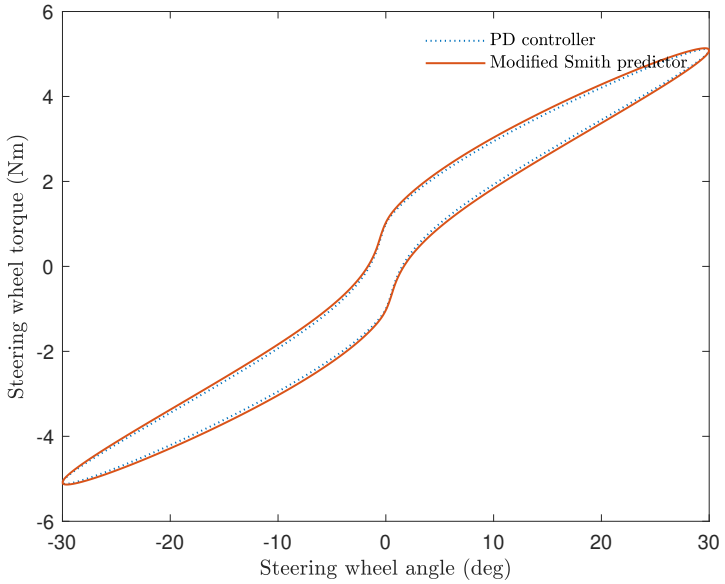

Figure 3.13: Case 2: SBW steering feel for a sinusoidal driver torque input.

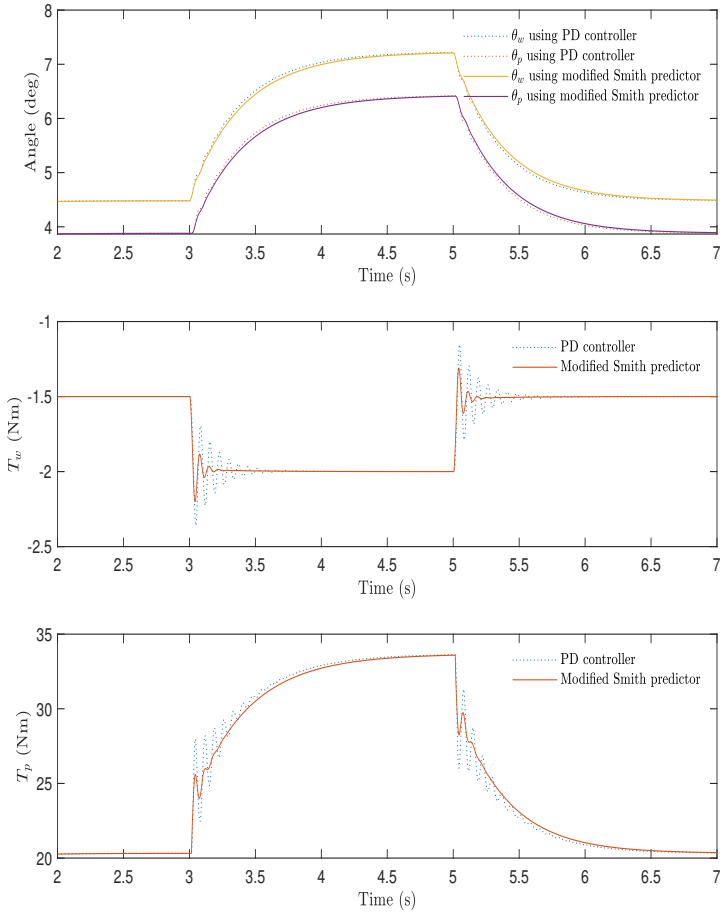

Figure 3.14: Case 3: Control signals for a square-like steering torque input.

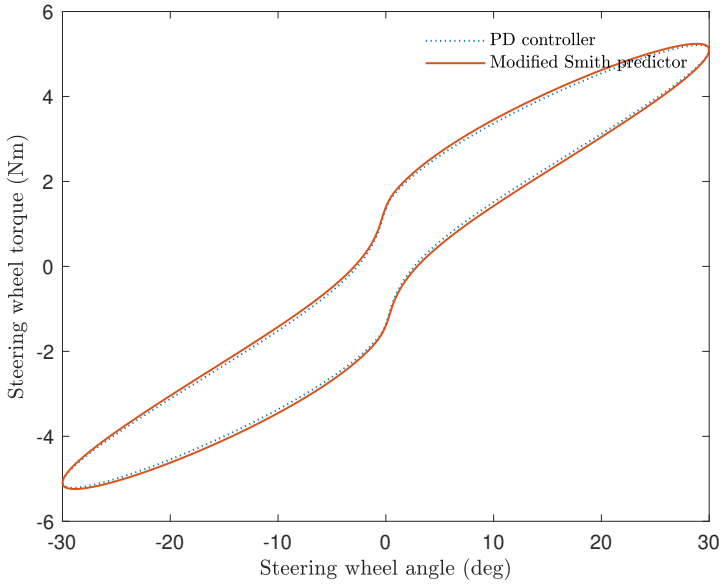

Figure 3.15: Case 3: SBW steering feel for a sinusoidal driver torque input.

Part II

Lyapunov-Krasovskii functional computation approaches

Chapter 4

Preliminaries on time-domain stability analysis

The use of Lyapunov's method for the stability analysis of difference-differential equations traces back to the work of Krasovskii [49]. For the particular case of linear time-delay systems, quadratic Lyapunov-Krasovskii Functionals (LKF) were studied in [91]. Importantly, the existence of a quadratic LKF is a necessary and sufficient condition for a linear time-delay system to be exponentially stable [21, Theorem 2.1].

For exponentially stable linear time-delay systems, a quadratic LKF can be constructed by identifying its time derivative with a prescribed quadratic functional [91, 20, 40, 111]. The LKF is then constructed from the delay Lyapunov matrix, the solution to a system of linear matrix differential equations associated with specific boundary conditions [43, Chapter 2]. Based on these results, to conclude on stability using the obtained LKF, its positivity must be verified, which can be a difficult task [43, pp. 73-74]. To check the positivity of the obtained LKF, necessary conditions based on its evaluation for particular functions are presented in [24]. In a different vein, the relation between the delay Lyapunov matrix and the eigenvalues of the time-delay system is presented in [63], where a numerical method for determining the stability exponent and the eigenvalue abscissas is provided.

In other numerical approaches for stability analysis, the LKF is defined in terms of a fixed number of parameters. Then the stability conditions impose constraints on the set of parameters that verify both upper and lower bounds on the LKF and the strict negativity of its time derivative along the trajectories of the system. These formulations are most often expressed as SemiDefinite Programs (SDP) [82], the solution of which yields the LKF parameters. The first numerical methods to compute LKF based on SDP imposed rather simple functional structures [104, 46, 83]. More complex structures, where the parameters are coefficients of polynomials, were introduced thanks to polynomial optimization or projection methods [88, 100]. To check the stability conditions associated with projection methods, some known inequalities such as the Wirtinger inequality are employed [97].

In this chapter, we present linear time-delay systems and recall the associated version of Krasovskii's theorem in Section 4.1. An overview of an analytical method for constructing a quadratic LKF with prescribed time derivatives is presented in

Section 4.2. Importantly, we prove that the kernel in a double integral term of the constructed LKF has a non-separable form. Finally, we present a literature review on the topics addressed in the second part of this manuscript, that is, existing methods to verify bounds on the Lyapunov-Krasovskii functionals.

4.1 Stability of time-delay systems

Consider a linear time-delay system of the form

$$\begin{aligned} &\frac{d}{d\bar{t}}x(\bar{t}) = Ax(\bar{t}) + A_d x(\bar{t}-h), \qquad \forall \bar{t} \geq 0, \\ &x(\bar{t}) = \varphi_0(\bar{t}), \qquad \forall \bar{t} \in [-h, 0], \end{aligned} \tag{4.1}$$

where $A \in \mathbb{R}^{n\times n}$, $A_d \in \mathbb{R}^{n\times n}$, h is a strictly positive scalar constant, and $\varphi_0 \in PC([-h,0],\mathbb{R}^n)$ is the initial function of (4.1), where $PC([a,b],\mathbb{R}^n)$ is the space of piecewise continuous functions mapping the interval $[a,b]$ into $\mathbb{R}^n$. To make the presentation of the results more compact and to simplify the system representation using projections into sets of functions defined on the interval $[0,1]$, for $h>0$, we recast (4.1) as the following interconnection of an ordinary differential equation and a transport equation [50, Chapter 2],

$$\begin{aligned} &\frac{d}{d\bar{t}}\phi(\bar{t},0) = A\phi(\bar{t},0) + A_d\phi(\bar{t},-h), \qquad \forall \bar{t} \geq 0, \\ &\partial_{\bar{t}}\phi(\bar{t},\bar{\theta}) = \partial_{\bar{\theta}}\phi(\bar{t},\bar{\theta}), \qquad \forall (\bar{t},\bar{\theta}) \in [0,+\infty)\times[-h,0]. \end{aligned}$$

Introducing $\theta = \frac{1}{h}\bar{\theta} + 1$, we obtain

$$\begin{aligned} \bar{\theta} = -h &\implies \theta = 0, \\ \bar{\theta} = 0 &\implies \theta = 1, \\ \frac{d\theta}{d\bar{\theta}} = \frac{1}{h} &\implies h d\theta = d\bar{\theta}, \end{aligned}$$

and the equation

$$\begin{aligned} &\frac{d}{d\bar{t}}\phi(\bar{t},1) = A\phi(\bar{t},1) + A_d\phi(\bar{t},0), \qquad \forall \bar{t} \geq 0, \\ &\partial_{\bar{t}}\phi(\bar{t},\theta) = \frac{1}{h}\partial_{\theta}\phi(\bar{t},\theta), \qquad \forall (\bar{t},\theta) \in [0,+\infty)\times[0,1]. \end{aligned}$$

Introducing $t = \frac{1}{h}\bar{t}$, we obtain

$$\begin{aligned} \bar{t} = 0 &\implies t = 0, \\ \bar{t} = +\infty &\implies t = +\infty, \\ h dt = d\bar{t} &\implies \frac{h}{d\bar{t}} = \frac{1}{dt}, \end{aligned}$$

and the equation

$$\frac{d}{dt}\phi(t,1) = hA\phi(t,1) + hA_d\phi(t,0), \qquad \forall t \geq 0,$$
$$\partial_t\phi(t,\theta) = \partial_\theta\phi(t,\theta), \qquad \forall (t,\theta) \in [0,+\infty) \times [0,1],$$

which is equivalent to

$$\frac{d}{dt}\phi(t,1) = A_1\phi(t,1) + A_0\phi(t,0), \qquad \forall t \geq 0, \tag{4.2a}$$
$$\partial_t\phi(t,\theta) = \partial_\theta\phi(t,\theta), \qquad \forall (t,\theta) \in [0,+\infty) \times [0,1], \tag{4.2b}$$

where $A_1 = hA$ and $A_0 = hA_d$, and the initial function

$$\phi(0,\theta) = \varphi_0(h\theta - h), \qquad \forall \theta \in [0,1].$$

Note that, in the above representation, the delay h appears as a parameter on the system matrices.

The goal of this part of the manuscript is to study the exponential stability of the origin of (4.2) by searching for a stability certificate, namely, the LKF satisfying the sufficient conditions of the Krasovskii theorem [49], stated below considering (4.2).

Theorem 4.1 ([49, 43]). *The origin of system* (4.2) *is Globally Exponentially Stable (GES) if there exists a functional* $V : PC([0,1],\mathbb{R}^n) \to \mathbb{R}$ *such that the following conditions hold*

1. *For some positive* α_1, α_2

$$\alpha_1\|\rho(1)\|^2 \leq V(\rho) \leq \alpha_2\|\rho\|^2_{[0,1]}, \qquad \forall \rho \in PC([0,1],\mathbb{R}^n). \tag{4.3}$$

2. *For some* $\beta > 0$ *the inequality*

$$\frac{d}{dt}V(\phi(t,1),\phi(t,\cdot)) \leq -\beta\|\phi(t,1)\|^2, \qquad \forall t \geq 0, \tag{4.4}$$

holds along the solutions of the system.

Note that the above theorem is not the only existing approach for stability analysis of time-delay systems using a Lyapunov-Krasovskii functional. Some alternative methods aim to derive stability conditions based on system transformations [28]—see Appendix C.

4.2 Construction of Lyapunov-Krasovskii functionals using the delay Lyapunov matrix

This section provides an overview of an analytical method to obtain quadratic LKFs, based on the delay Lyapunov matrix that results from prescribing time derivatives. The method parallels the computation of Lyapunov matrices for delay-free linear

systems obtained from the solution to the Lyapunov equation, where the positive definiteness of the Lyapunov matrix is a necessary and sufficient condition for stability. The contents of Section 4.2.1 and Section 4.2.2 are well known and are presented here to highlight the main differences with the approaches based on convex optimization for the computation of LKFs.

The construction of a quadratic LKF with a prescribed time derivative started in [91], where a system of matrix algebraic and partial differential equations was derived for computing the LKF. The set of matrix equations was further studied by [20, 21], and it is now well established [43] that the Lyapunov-Krasovskii functional associated with the prescribed time derivative can be constructed from the delay Lyapunov matrix [40]. The *delay Lyapunov matrix* is a matrix function $U : \mathbb{R} \to \mathbb{R}^{n\times n}$ obtained from the solution to the linear matrix differential equation and algebraic constraints [44, 40] given by

$$\frac{d}{d\theta}U(\theta) = U(\theta)A_1 + U(\theta-1)A_0, \qquad \forall\theta \geq 0, \tag{4.5}$$

$$U(-\theta) = U^\top(\theta), \qquad \forall\theta \geq 0, \tag{4.6}$$

and

$$U(0)A_1 + U(-1)A_0 + A_1^\top U(0) + A_0^\top U(1) = -W. \tag{4.7}$$

The three previous relations are known as the dynamic, symmetric, and algebraic properties, respectively.

4.2.1 Computation of the delay Lyapunov matrix

The solution of the delay Lyapunov matrix $U(\theta)$, for $\theta \in [-1, 1]$, associated with a symmetric matrix W is determined by two auxiliary matrices $Y(\theta)$ and $Z(\theta)$, for $\theta \in [0, 1]$, which are solutions of the following boundary value problem [44] of linear matrices ordinary differential equations

$$\begin{aligned}\frac{d}{d\theta}Y(\theta) &= Y(\theta)A_1 + Z(\theta)A_0,\\ \frac{d}{d\theta}Z(\theta) &= -A_0^\top Y(\theta) - A_1^\top Z(\theta),\end{aligned} \tag{4.8}$$

and the boundary conditions

$$\begin{aligned}&Y(0) = Z(1),\\ &A_1^\top Y(0) + Y(0)A_1 + A_0^\top Y(1) + Z(0)A_0 = -W.\end{aligned} \tag{4.9}$$

In [44], it is shown that if system (4.2) is exponentially stable, then it satisfies the Lyapunov condition [43, Definition 2.6]. In this case, we have $\det\left(M + Ne^L\right) \neq 0$, where

$$L = \begin{bmatrix} A_1 \otimes I_n & A_0 \otimes I_n \\ -I_n \otimes A_0^\top & -I_n \otimes A_1^\top \end{bmatrix}, \tag{4.10}$$

$$M = \begin{bmatrix} I_n \otimes I_n & 0_{n\times n} \otimes 0_{n\times n} \\ I_n \otimes A_1^\top + A_1 \otimes I_n & A_0 \otimes I_n \end{bmatrix},$$

and

$$N = \begin{bmatrix} 0_{n\times n} \otimes 0_{n\times n} & -I_n \otimes I_n \\ I_n \otimes A_0^\top & 0_{n\times n} \otimes 0_{n\times n} \end{bmatrix},$$

and (4.8)-(4.9) admits a unique solution, given by

$$\begin{bmatrix} \mathrm{vec}(Y(\theta)) \\ \mathrm{vec}(Z(\theta)) \end{bmatrix} = e^{L\theta}(M + Ne^L)^{-1} \begin{bmatrix} \mathrm{vec}(0_{n\times n}) \\ -\mathrm{vec}(W) \end{bmatrix}, \qquad \forall \theta \in [0,1], \tag{4.11}$$

where, for any matrix $X \in \mathbb{R}^{n\times n}$, we define the vector $\mathrm{vec}(X)$ by stacking up the columns of X. Moreover, [11] introduces the following lemma.

Lemma 4.2 ([11]). *The spectrum of system* (4.8) *is symmetric with respect to the origin of the complex plane.*

Denote by k the number of pairs of eigenvalues of L and by r_i, for $i = 1, \cdots, k$, the size of the largest Jordan block associated with one of its eigenvalues λ_i. From (4.11), using Lemma 4.2, the matrices $Y(\theta)$ and $Z(\theta)$ can be decomposed [11] as

$$\begin{aligned} Y(\theta) &= \tilde{Y}\tilde{F}^\top(\theta), \qquad \forall \theta \in [0,1], \\ Z(\theta) &= \tilde{Z}\tilde{F}^\top(\theta), \qquad \forall \theta \in [0,1], \end{aligned} \tag{4.12}$$

where $\tilde{Y}$ and $\tilde{Z}$ are constant matrices in $\mathbb{R}^{n\times np_u}$, with $p_u = \sum_{i=1}^{k}\sum_{j=1}^{r_i} 2$ and $\tilde{F}(\theta) = \begin{bmatrix} \tilde{f}_1(\theta) & \cdots & \tilde{f}_{p_u}(\theta) \end{bmatrix} \otimes I_n$, where, for all $i = 1, \cdots, p_u$,

$$\tilde{f}_i(\theta) \in \{e^{\pm\lambda_1\theta}, \cdots, \theta^{r_1-1}e^{\pm\lambda_1\theta}, \cdots, e^{\pm\lambda_k\theta}, \cdots, \theta^{r_k-1}e^{\pm\lambda_k\theta}\}, \tag{4.13}$$

with $\pm\lambda_i$, for $i = 1, \ldots, k$, the eigenvalues of matrix L.

From [44], the delay Lyapunov matrix $U : [-1, 1] \to \mathbb{R}^{n\times n}$ of the time-delay system (4.2), associated with a symmetric matrix W, is given by

$$U(\theta) = \begin{cases} \frac{1}{2}Y(\theta) + \frac{1}{2}Z^\top(1-\theta), & \forall \theta \in [0,1], \\ \frac{1}{2}Y^\top(-\theta) + \frac{1}{2}Z(1+\theta), & \forall \theta \in [-1,0), \end{cases} \tag{4.14}$$

with Y, Z solution of (4.8)-(4.9). Therefore, from (4.12)-(4.13), we have that the delay Lyapunov matrix is expressed in terms of the $2n^2$ exponential functions in (4.13).

Remark 4.1. In [64], a relation between the spectrum of a time-delay system and that of an auxiliary delay-free system of matrix equations is established. Namely, it is shown that any pure imaginary eigenvalue of the time-delay system (4.2) is also an eigenvalue of the auxiliary system (4.8)-(4.9).

4.2.2 Construction of the Lyapunov-Krasovskii functional

The steps to obtain V satisfying the conditions (4.3)-(4.4) are summarized as follows

Step 1. Assign the time derivative of $V(\rho)$ along the solution of (4.2) as

$$\frac{d}{dt}V(\phi(t,1),\phi(t,\cdot)) = -w(\phi), \tag{4.15}$$

where, for some $\beta > 0$, $w(\phi)$ satisfies $w(\phi) \geq \beta\|\phi(t,1)\|^2$, for all $t \geq 0$.

Step 2. Compute the delay Lyapunov matrix on the interval $[-1,1]$ by solving the differential equation (4.5) and algebraic constraints (4.6)-(4.7). The matrix W, in (4.7), depends on the parameters W_i included in w (see the paragraph below).

Step 3. Construct the corresponding functional V.

Step 4. Verify whether the bounds in (4.3) hold.

To illustrate these steps, let us consider two different choices for the functional w. First, consider

$$w(\phi) = \phi^\top(t,1)W_0\phi(t,1), \tag{4.16}$$

where W_0 is a positive definite matrix, and let us denote V_0, the solution to (4.15) (Step 1), which is obtained by first computing the delay Lyapunov matrix $U(\theta)$, $\theta \in [-1,1]$, associated with the matrix $W = W_0$ in (4.8)-(4.9) (Step 2). Then, from [45], the functional V_0 is expressed as (Step 3)

$$\begin{aligned} V_0(\rho(1),\rho(\cdot)) = \int_0^1 \begin{bmatrix}\rho^\top(1) & \rho^\top(\theta)\end{bmatrix} \begin{bmatrix} U(0) & U(-\theta)A_0 \\ A_0^\top U(\theta) & 0_{n\times n}\end{bmatrix} \begin{bmatrix}\rho(1)\\ \rho(\theta)\end{bmatrix} d\theta \\ + \int_0^1\int_0^1 \rho^\top(\theta)A_0^\top U(\theta-\eta)A_0\rho(\eta)d\eta d\theta. \end{aligned} \tag{4.17}$$

It has been shown in [40] that there exist exponentially stable systems for which the lower bound in (4.3) does not hold for V_0 in (4.17). Therefore, these instances of system (4.2) will not verify both conditions of Theorem 4.1 even if (4.15) holds with w as in (4.16). However, it is shown that, for an exponentially stable system (4.2), using w as

$$w(\phi) = \phi^\top(t,1)W_0\phi(t,1) + \phi^\top(t,0)W_1\phi(t,0) + \int_0^1 \phi^\top(t,\theta)W_2\phi(t,\theta)d\theta, \tag{4.18}$$

where W_0, W_1, and W_2 are positive definite matrices, we obtain a necessary and sufficient condition for the lower bound in (4.3) to hold for a solution to (4.15). And Steps 2 and 3 above give

$$\begin{aligned} V(\rho(1),\rho(\cdot)) &= V_0(\rho(1),\rho(\cdot)) + \int_0^1 \rho^\top(\theta)(W_1+\theta W_2)\rho(\theta)d\theta \\ &= \int_0^1 \begin{bmatrix}\rho^\top(1) & \rho^\top(\theta)\end{bmatrix} \begin{bmatrix} U(0) & U(-\theta)A_0 \\ A_0^\top U(\theta) & W_1+\theta W_2\end{bmatrix} \begin{bmatrix}\rho(1)\\ \rho(\theta)\end{bmatrix} d\theta \\ &\quad + \int_0^1\int_0^1 \rho^\top(\theta)A_0^\top U(\theta-\eta)A_0\rho(\eta)d\eta d\theta, \end{aligned} \tag{4.19}$$

where the delay Lyapunov matrix $U(\theta)$, $\theta \in [-1, 1]$, is associated with the matrix $W = W_0 + W_1 + W_2$ in (4.9). For an exponentially stable system, considering w as in (4.18) guarantees the lower bound in (4.3)—see [40, 45].

It remains to carry out Step 4 above. A necessary and sufficient condition for the system (4.2) to be exponentially stable is that the LKF in (4.19), associated with functional w given by (4.18), is positive. Hence, from $U(\theta)$, W_1, and W_2, the stability analysis is reduced to the verification of the positivity of $V(\rho)$. However, given a functional such as (4.17) or (4.19), it is generally difficult to check its positivity for any $\rho \in PC([0, 1], \mathbb{R}^n)$ using its analytical expression. Instead, in [24], a stability analysis tool for determining instability regions of linear time-delay systems is proposed. For a particular function, it provides necessary conditions in terms of the delay Lyapunov matrix to guarantee that a quadratic lower bound on the LKF is satisfied (see also [32] and [23]).

In the rest of the chapter, we will consider a general parameterization of LKFs as

$$V(\rho(1), \rho(\cdot)) = \int_0^1 \begin{bmatrix} \rho^\top(1) & \rho^\top(\theta) \end{bmatrix} \begin{bmatrix} P & Q(\theta) \\ Q^\top(\theta) & R(\theta) \end{bmatrix} \begin{bmatrix} \rho(1) \\ \rho(\theta) \end{bmatrix} d\theta + \int_0^1 \int_0^1 \rho^\top(\theta) T(\theta, \eta) \rho(\eta) d\eta d\theta, \quad (4.20)$$

with $P \in \mathbb{S}^n$, $Q : [0, 1] \to \mathbb{R}^{n \times n}$, $R : [0, 1] \to \mathbb{S}^n$, and $T : [0, 1] \times [0, 1] \to \mathbb{R}^{n \times n}$, where $\mathbb{S}^n$ is the set of $n \times n$ real symmetric matrices. Note that in this parameterization R is not necessarily affine. Note also that the functional (4.19) can be obtained when

$$P = U(0), \quad (4.21a)$$
$$Q(\theta) = U^\top(\theta) A_0, \qquad \forall \theta \in [0, 1], \quad (4.21b)$$
$$R(\theta) = W_1 + \theta W_2, \qquad \forall \theta \in [0, 1], \quad (4.21c)$$
$$T(\theta, \eta) = A_0^\top U(\theta - \eta) A_0, \qquad \forall (\theta, \eta) \in [0, 1] \times [0, 1]. \quad (4.21d)$$

As an example of LKF construction, consider the time-delay system given by

$$\dot{x}(t) = -\alpha x(t) - \beta x(t - h), \quad (4.22)$$

where α and β are scalars, with $\alpha < \beta$. It can be represented as in (4.2), where $A_0 = -h\beta$ and $A_1 = -h\alpha$. This example is regularly used in the literature to illustrate different approaches to construct Lyapunov-Krasovskii functionals—see, *e.g.*, [91] and [40]. The delay Lyapunov matrix $U(\theta)$, for $\theta \in [-1, 1]$, associated with a matrix W is given by (4.14), where

$$L = \begin{bmatrix} -h\alpha & -h\beta \\ h\beta & h\alpha \end{bmatrix},$$
$$M = \begin{bmatrix} 1 & 0 \\ -2h\alpha & -h\beta \end{bmatrix},$$
$$N = \begin{bmatrix} 0 & -1 \\ -h\beta & 0 \end{bmatrix},$$

and $\mathrm{vec}(W) = W$.

Let us define

$$k = \sqrt{\beta^2 - \alpha^2},$$

we have

$$e^{L\theta} = \begin{bmatrix} \dfrac{k\cos(kh\theta) - \alpha\sin(kh\theta)}{k} & -\dfrac{\beta\sin(kh\theta)}{k} \\ \dfrac{\beta\sin(kh\theta)}{k} & \dfrac{k\cos(kh\theta) + \alpha\sin(kh\theta)}{k} \end{bmatrix}$$

and

$$\begin{aligned} &(M+Ne^L)^{-1} \\ &\quad= \begin{bmatrix} \dfrac{-\beta\sin(kh)+k}{k} & \dfrac{-\alpha\sin(kh)-k\cos(kh)}{k} \\ \dfrac{h(\alpha\beta\sin(kh)-\beta k\cos(kh)-2\alpha k)}{k} & -\dfrac{\beta h(-\beta\sin(kh)+k)}{k} \end{bmatrix}^{-1} \\ &\quad= \frac{1}{2k}\begin{bmatrix} -\dfrac{\beta(-\beta\sin(kh)+k)}{k\sin(kh)-\cos(kh)\alpha-\beta} & \dfrac{\alpha\sin(kh)+k\cos(kh)}{h(k\sin(kh)-\cos(kh)\alpha-\beta)} \\ \dfrac{\alpha\beta\sin(kh)-\beta k\cos(kh)-2\alpha k}{k\sin(kh)-\cos(kh)\alpha-\beta} & \dfrac{-\beta\sin(kh)+k}{h(k\sin(kh)-\cos(kh)\alpha-\beta)} \end{bmatrix}. \end{aligned}$$

Then, from (4.11), we have, for all $\theta \in [0,1]$,

$$Y(\theta) = \left(-\frac{\sin(kh\theta)}{2kh} - \frac{\cos(kh\theta)(\alpha\sin(kh)+k\cos(kh))}{2kh(k\sin(kh)-\alpha\cos(kh)-\beta)}\right)W$$

and

$$Z(\theta) = \left(-\frac{\cos(kh\theta)(k-\beta\sin(kh))}{2kh(k\sin(kh)-\alpha\cos(kh)-\beta)} - \frac{\sin(kh\theta)(\alpha+\beta\cos(kh))}{2kh(k\sin(kh)-\alpha\cos(kh)-\beta)}\right)W.$$

Therefore, from (4.14), we have, for all $\theta \in [0,1]$,

$$\begin{aligned} 2U(\theta) &= Y(\theta) + Z^\top(1-\theta) \\ &= 2Y(\theta) \\ &= \left(-\frac{\sin(kh\theta)}{kh} - \frac{\cos(kh\theta)(\alpha\sin(kh)+k\cos(kh))}{kh(k\sin(kh)-\alpha\cos(kh)-\beta)}\right)W. \end{aligned}$$

Hence, we consider

$$\tilde{F}(\theta) = \begin{bmatrix}\cos(hk\theta) & \sin(hk\theta)\end{bmatrix}.$$

From (4.21b), the parameter $Q(\theta)$ can be written as $Q(\theta) = Y^\top(\theta)A_0 = \bar{Q}\tilde{F}^\top(\theta)$, where

$$\bar{Q} = \begin{bmatrix}\left(\dfrac{\beta(\alpha\sin(kh)+k\cos(kh))}{2k(k\sin(kh)-\alpha\cos(kh)-\beta)}\right)W & \left(\dfrac{\beta}{2k}\right)W\end{bmatrix}.$$

Also, from (4.21a), we have

$$P = Y(0) = \left(-\frac{\alpha\sin(kh)+k\cos(kh)}{2kh(k\sin(kh)-\alpha\cos(kh)-\beta)}\right). \tag{4.23}$$

4.2.3 The parameter T is not separable

Let us note that the parameter $T(\theta,\eta)$ in (4.20) is expressed as in (4.21d) in terms of the solution to (4.8)-(4.9) using $U(\theta)$ in (4.14). This section studies the *separability* of $T(\theta,\eta)$, namely we study whether T obtained from the construction of the LKF by assigning the time derivative, as discussed above, can be expressed as the product of functions as

$$T(\theta,\eta)=\tilde{F}(\theta)\bar{T}\tilde{F}^{\top}(\eta),\qquad \forall(\theta,\eta)\in[0,1]\times[0,1],$$

with $\bar{T}\in\mathbb{S}^{np_u}$. This is a relevant property since the use of a separable T is a key step in obtaining sufficient SDP-based stability conditions [90, 100]. Let us first observe that using (4.12), (4.14), and (4.21d), we obtain

$$T(\theta,\eta)=\begin{cases}\tilde{T}\tilde{F}^{\top}(\theta-\eta), & \forall\theta-\eta\in[0,1],\\ \tilde{F}(-\theta+\eta)\tilde{T}^{\top}, & \forall\theta-\eta\in[-1,0),\end{cases}\tag{4.24}$$

where $\tilde{T}\in\mathbb{R}^{n\times np_u}$ is a constant matrix.

Below, we show that T as in (4.21d) is not separable. Therefore, the same term in the LKF using the delay Lyapunov matrix will not possibly appear in SDP-based approaches that assume its separability. Let us first consider the following lemma [121]—see [96] for an alternative approach.

Lemma 4.3. *A function $\kappa:[0,1]\times[0,1]\to\mathbb{R}$ can be written as $\kappa(x,y)=\mu(x)\sigma(y)$ for some functions $\mu,\sigma:[0,1]\to\mathbb{R}$ if and only if, for every x, y, w, $z\in[0,1]$, it holds that*

$$\kappa(x,y)\kappa(w,z)=\kappa(x,z)\kappa(w,y).\tag{4.25}$$

Proof. The necessary condition follows directly from the commutativity of multiplication, since with $\kappa(x,y)=\mu(x)\sigma(y)$ we have

$$\kappa(x,y)\kappa(w,z)=\mu(x)\sigma(y)\mu(w)\sigma(z)=\kappa(x,z)\kappa(w,y).$$

To prove the sufficiency, we consider two cases. In the first case, we suppose that the function $\kappa(a,b)=0$, for all $(a,b)\in[0,1]\times[0,1]$. Then, in this case, we have $\mu(x)=0$ and $\sigma(y)=0$, for all $x,\,y\in[0,1]$. In the second case, we assume that $\exists(a,b)\in[0,1]\times[0,1]$ such that $\kappa(a,b)\neq 0$, then (4.25) gives

$$\kappa(x,y)\kappa(a,b)=\kappa(x,b)\kappa(a,y),$$

which implies that

$$\kappa(x,y)=\kappa(x,b)\frac{\kappa(a,y)}{\kappa(a,b)},$$

thus, for all $x,\,y\in[0,1]$, $\mu(x)=\kappa(x,b)$ and $\sigma(y)=\dfrac{\kappa(a,y)}{\kappa(a,b)}$. ∎

We now apply the necessary and sufficient condition in the above lemma to conclude that T in (4.21d) is not separable. Let a, b, c, and d be scalars satisfying $0\leq$

$d \leq c < b \leq a \leq 1$. Following (4.24), we have

$$\begin{aligned} T(a,b) &= \tilde{T}\tilde{F}^\top(a-b), \\ T(c,d) &= \tilde{T}\tilde{F}^\top(c-d), \\ T(a,d) &= \tilde{T}\tilde{F}^\top(a-d), \end{aligned}$$

and

$$T(c,b) = \tilde{F}(-c+b)\tilde{T}^\top.$$

Therefore, by selecting $a = b$, $c = d$, and $c < b$, we have

$$T(a,b)T(c,d) \neq T(a,d)T(c,b).$$

For example, in the scalar case $(n = 1)$, using (4.24), the parameter T can be written as

$$T(\theta,\eta) = \begin{cases} \alpha e^{\lambda(\theta-\eta)} + \gamma e^{-\lambda(\theta-\eta)}, & \forall \theta-\eta \in [0,1], \\ \alpha e^{\lambda(-\theta+\eta)} + \gamma e^{-\lambda(-\theta+\eta)}, & \forall \theta-\eta \in [-1,0), \end{cases}$$

for some values of $\alpha, \gamma, \lambda \neq 0$. In this case, we have

$$\begin{aligned} T(a,b)T(c,d) &= (\alpha e^{\lambda(a-b)} + \gamma e^{-\lambda(a-b)})(\alpha e^{\lambda(c-d)} + \gamma e^{-\lambda(c-d)}) \\ &= (\alpha+\gamma)^2 \end{aligned}$$

and

$$\begin{aligned} T(a,d)T(c,b) &= (\alpha e^{\lambda(a-d)} + \gamma e^{-\lambda(a-d)})(\alpha e^{\lambda(-c+b)} + \gamma e^{-\lambda(-c+b)}) \\ &= (\alpha e^{\lambda(-c+b)} + \gamma e^{-\lambda(-c+b)})^2. \end{aligned}$$

Therefore, since the last term varies with $-c+b$, we can find a pair (c,b) such that

$$T(a,b)T(c,d) \neq T(a,d)T(c,b).$$

Thus, from Lemma 4.3, we conclude that $T(\theta,\eta)$ in (4.21d) is not separable.

The above section presented the main properties of the analytical method to construct LKF from the delay Lyapunov matrix. We highlighted the main aspects that are in contrast with methods based on semidefinite programming for the computation of LKF, namely the presence of a finite number of exponential functions (4.13) in the definition of the LKF parameters and the fact that the resulting parameter $T(\theta,\eta)$ in (4.21d) appearing in the double integral in (4.20) is not separable.

Chapter 5 studies parameterized functions Q, R, and T in the LKF (4.20) considering a generic set of linearly independent functions, thus allowing to treat sets as (4.13) or polynomials. The goal is to propose tests based on semidefinite programming obtained by projecting the dynamics of a time-delay system into the same set of linearly independent functions that define the functions Q, R, and T.

4.3 Literature review on LKF

The analytical method for constructing a quadratic Lyapunov-Krasovskii functional with a prescribed time derivative was introduced in [91]. A system of matrix equations was derived by identifying the time derivative of a general form of quadratic functional along the solution of a linear time-delay system with a prescribed time derivative functional. This system of matrix equations includes a linear matrix partial differential equation, ordinary matrix differential equations, and matrix algebraic equations.

This approach for constructing Lyapunov-Krasovskii functionals was further studied in [20, 40, 21, 111, 64]. The steps to obtain a Lyapunov-Krasovskii functional, as presented in Section 4.2.2, was formulated in [20], in which stability and instability theorems for a linear time-delay system are represented using Hermitian forms. It is shown that if the time-delay system is exponentially stable, then there exists a solution to the system of matrix equations that is obtained by identifying the Lyapunov-Krasovskii functional.

In [40] and [111], systems composed of an ordinary matrix differential equation and matrix algebraic constraints, similar to that in (4.5)-(4.7), were adopted to construct Lyapunov-Krasovskii functionals. In [111], it is stated that a delay Lyapunov matrix is determined from these three properties, (4.5)-(4.7). It is also stated that if a time-delay system satisfies the Lyapunov condition [43, Definition 2.6], then, for any symmetric matrix W, there exists an associated delay Lyapunov matrix. In [40], it is shown that the unique solution of this system has an improper integral form that depends on the *fundamental matrix*. The explicit solution to a system of matrix equations as in (4.5)-(4.7) is studied in [11]. It is shown that, for any $W \in \mathbb{S}^n$, the solution of (4.5)-(4.7) belong to a finite space of n^2 exponential functions in the set (4.13).

In [111], the existence of the lower bounds for functionals of the form (4.17), associated with functional w given by (4.15), is studied. The paper shows that, for the case of exponentially stable systems, functionals of the form (4.17) admit a local cubic lower bound. In [40], the Lyapunov-Krasovskii functional presented there is equivalent to that in (4.19), associated with functional w given by (4.18). For this functional, quadratic lower and upper bounds of the form given in (4.3) were provided. The paper also mentions that, for the case of exponentially stable systems, functionals of the form (4.17) do not admit a quadratic lower bound. A brief account of the theory of Lyapunov matrices and functionals appears in [42].

Consequently, from the results presented in [40], a Lyapunov-Krasovskii functional that yields necessary and sufficient conditions for the stability of a linear time-delay system can be constructed using the approach in [91].

The relation between the delay Lyapunov matrix and the eigenvalues of the time-delay system is presented in [63], where a numerical method for determining the stability exponent and the eigenvalue abscissas is provided. This result highlights the relation between the delay Lyapunov matrix and the stability of a time-delay system. However, finding the stability conditions of a linear time-delay system in terms of the delay Lyapunov matrix $U(\theta)$ is a difficult problem. The first result in this direction was obtained in [71], where some necessary and sufficient

conditions are derived for the case of scalar equations. In [24], a stability analysis tool for determining instability regions of linear time-delay systems is provided. For a particular initial function, it provides necessary conditions in terms of the delay Lyapunov matrix to guarantee that a quadratic lower bound on the Lyapunov-Krasovskii functional is satisfied. They introduce properties on the delay Lyapunov matrix in terms of the fundamental matrix. In [25], it is shown that any continuously differentiable function can be approximated by a particular function that depends on the fundamental matrix of the time-delay system. Based on these results, in [23] and [32], it is proved that a finite number of mathematical operations is sufficient to verify the stability inequality.

In Section 4.2.3, we showed that the parameter T in the Lyapunov-Krasovskii functional obtained from the delay Lyapunov matrix is not separable. To provide bounds on the Lyapunov-Krasovskii functional, in the numerical methods [90, 100], the parameter T is replaced by a separable function. Further details on these numerical methods are presented in Chapter 5. Alternatively, a semi-separable kernel for the parameter T is studied in [89]. It is shown that semi-separable kernels, parameterized by positive semidefinite matrices, have advantages over separable kernels for the stability analysis of linear time-delay systems. However, to conclude on the positivity of the Lyapunov-Krasovskii functional, the positivity of the single integral term and the positivity of the double integral term in the expression of this functional are treated separately. Hence, sufficient conditions for the positivity of the proposed Lyapunov-Krasovskii functional are provided. The way to handle the positivity of the Lyapunov-Krasovskii functional with a separable kernel was later improved in [87], in which the Lyapunov-Krasovskii functional is constructed using a combined multiplier and integral operator parameterized using positive semidefinite matrices. Slack variables are also created to account for the limited equivalence between the multiplier and the integral operator. These results include positive operators defined by multipliers and semi-separable kernels are applied to the study of partial differential equations in [30] and [31].

Chapter 5

Verification methods for the Lyapunov-Krasovskii functional inequalities

In this chapter, we study projection-based parameterizations of Lyapunov-Krasovskii Functionals (LKF) to analyze the stability of linear time-delay systems. The set of functions considered in the projections can be an arbitrary set of linearly independent functions or include solutions of the delay Lyapunov matrix. From them we construct a Lyapunov-Krasovskii functional associated with a prescribed time derivative. We compare two approaches for the stability analysis of time-delay systems based on SemiDefinite Programming (SDP), namely the method based on integral inequalities and the method based on sum-of-squares programming, which have emerged as the main optimization-based methods to compute LKFs. We discuss the main assumptions and establish connections between both methods. Finally, we formulate a projection-based method allowing to use general sets of functions to parameterize LKFs, thus encompassing the sets of polynomial functions in the literature. The solutions of the proposed stability conditions and the construction of the corresponding LKFs as stability certificates are illustrated with numerical examples.

The LKF associated with the delay Lyapunov matrix, as shown in the previous chapter, can not be directly constructed using the polynomial-based SDP methods in the literature. We propose in this chapter a more general parameterization of LKFs than the existing polynomial parameterizations or piecewise linear parameterizations [34, 77], and we formulate the associated stability conditions as constraints of SDPs. The first step towards the general formulation is to represent the original time-delay system in projected coordinates related to a set of linearly independent functions, which can be for instance exponential functions or polynomials. Moreover, in the projected coordinates, it is possible to apply either Sum-of-Squares (SOS) methods [90] or methods using integral inequalities [100], both leading to SDP formulations to compute LKFs. We discuss the key difference between the two approaches, which is mainly in the way the constraints are enforced on the delay interval.

We point out the main assumptions leading to the approaches based on pro-

jections, requiring the use of sets of functions closed under differentiation and structured parameters in the LKF, in particular the separability of the kernel in a double integral term, a feature in contrast to the LKF obtained from the delay Lyapunov matrix. For the methods based on integral inequalities, we present a result allowing to retrieve integral inequalities used in the literature for the computation of LKFs, namely the Bessel-Legendre inequality and the Jensen inequality. We also show that methods based on integral inequalities impose one of the parameters of the LKF to be an affine function.

This chapter is organized as follows: The dynamics of the time-delay system are presented in Section 5.1, where the description of the system using projections is also introduced. Two approaches for stability analysis of linear time-delay systems are formulated in Proposition 5.5 and Proposition 5.8, in Section 5.2. The advantages of each method and a comparison between them are also provided. In Section 5.3, these approaches are applied to several time-delay systems in the literature. Then, in Section 5.4, we apply the obtained results to the electric power steering and steer-by-wire systems. We also show how the provided results can be extended to study the behavior of the steering systems, such as the decay rate. The mathematical proofs of the proposed results are given in Appendix B.

Notation

For $x \in \mathbb{R}^n$, we denote $\|x\| = \sqrt{\sum_{i=1}^n x_i^2}$ its Euclidean norm. We denote the inner product between f and g in $L_2([0,1],\mathbb{R})$ by

$$\langle f, g\rangle = \int_0^1 f(\theta)g(\theta)d\theta,$$

and $\|f\|_{[0,1]} = \sqrt{\langle f, f\rangle}$. For a set of linearly independent functions $\{f_1, \cdots, f_p\}$ verifying $f_i \in H^1([0,1],\mathbb{R})$—namely, for all $i = 1, \cdots, p$, $f_i, f_i' \in L_2([0,1],\mathbb{R})$, with $f_i'(\theta) = df_i(\theta)/d\theta$, for all $\theta \in [0,1]$—we define $f(\theta) = \begin{bmatrix} f_1(\theta) & \cdots & f_p(\theta)\end{bmatrix}$ and

$$F(\theta) = f(\theta) \otimes I_n, \tag{5.1}$$

where $\otimes$ stands for the Kronecker product and I_n is the identity matrix of dimension n. The notation $0_{n\times m}$ stands for the zero matrix of n rows and m columns. We denote

$$F'(\theta) = \frac{d}{d\theta}F(\theta). \tag{5.2}$$

Let us also define the matrix

$$\bar{F} = \begin{bmatrix} \langle f_1, f_1\rangle & 0 & \dots & 0 \\ \langle f_2, f_1\rangle & \langle f_2, f_2\rangle & \ddots & \vdots \\ \vdots & \ddots & \ddots & 0 \\ \langle f_p, f_1\rangle & \dots & \langle f_p, f_{p-1}\rangle & \langle f_p, f_p\rangle \end{bmatrix} \otimes I_n, \tag{5.3}$$

also written as $\bar{F} = \begin{bmatrix} \bar{F}_1 \\ \vdots \\ \bar{F}_p \end{bmatrix}$, with $\bar{F}_i = \begin{bmatrix} \langle f_i, f_1 \rangle I_n & \dots & \langle f_i, f_i \rangle I_n & 0_{n \times n(p-i)} \end{bmatrix}$.
The diagonal elements of $\bar{F}$ are the elements of the matrix

$$D_{\bar{F}} = \tilde{D}_{\bar{F}} \otimes I_n, \tag{5.4}$$

where $\tilde{D}_{\bar{F}} = \operatorname{diag}(\|f_1\|^2_{[0,1]}, \cdots, \|f_p\|^2_{[0,1]})$ and $\operatorname{diag}(v)$ is the diagonal matrix with the entries of vector v on its diagonal.

We also define the matrix

$$\bar{F}_\partial = \begin{bmatrix} \langle f_1, f_1' \rangle & \langle f_1, f_2' \rangle & \dots & \langle f_1, f_p' \rangle \\ \langle f_2, f_1' \rangle & \langle f_2, f_2' \rangle & \dots & \langle f_2, f_p' \rangle \\ \vdots & \vdots & & \vdots \\ \langle f_p, f_1' \rangle & \langle f_p, f_2' \rangle & \dots & \langle f_p, f_p' \rangle \end{bmatrix} \otimes I_n,$$

which can be rewritten as $\bar{F}_\partial = \begin{bmatrix} \bar{F}_{\partial 1} \\ \vdots \\ \bar{F}_{\partial p} \end{bmatrix}$, with $\bar{F}_{\partial i} = \begin{bmatrix} \langle f_i, f_1' \rangle I_n & \dots & \langle f_i, f_p' \rangle I_n \end{bmatrix}$.

We denote $PC([a,b], \mathbb{R}^n)$ the space of piecewise continuous functions mapping the interval $[a,b]$ into $\mathbb{R}^n$. The linear span of a set $\{f_1, \cdots, f_p\}$ of linearly independent functions, denoted $\operatorname{span}(f_1, \cdots, f_p)$, is the smallest linear subspace that contains all of functions in the set $\{f_1, \cdots, f_p\}$.

Let $\mathbb{S}^n$ be the set of $n \times n$ real symmetric matrices, $\mathbb{S}^n_{\geq 0}$ be the set of positive semidefinite matrices, and $\mathbb{S}^n_{>0}$ be the set of positive definite matrices. For the vector $Z_m(\theta) = \begin{bmatrix} 1 & \theta & \cdots & \theta^m \end{bmatrix}$ containing all monomials up to degree m in variable θ, denote $Z_{m,d} = Z_m(\theta) \otimes I_d$ and denote the set of sum-of-squares matrices of dimension $d \times d$ and degree m

$$\Sigma^{m,d}[\theta] = \left\{ Z^\top_{m,d}(\theta) M Z_{m,d}(\theta) \mid M \in \mathbb{S}^{md}_{\geq 0} \right\}.$$

5.1 Delay systems with projections

Consider a linear time-delay system of the form

$$\dot{\phi}(t,1) = A_1 \phi(t,1) + A_0 \phi(t,0), \qquad \forall t \geq 0, \tag{5.5a}$$
$$\partial_t \phi(t,\theta) = \partial_\theta \phi(t,\theta), \qquad \forall (t,\theta) \in [0,+\infty) \times [0,1], \tag{5.5b}$$

where $A_1 \in \mathbb{R}^{n \times n}$, $A_0 \in \mathbb{R}^{n \times n}$, and $\varphi_0 \in PC([-h,0], \mathbb{R}^n)$ is the initial function,

$$\phi(0,\theta) = \varphi_0(h\theta - h), \qquad \forall \theta \in [0,1].$$

The above interconnection of an ordinary differential equation and a transport equation was also adapted in Chapter 4 of this manuscript to model delay systems. We can alternatively write it in the following compact form

$$\begin{bmatrix} \dot{\phi}(t,1) \\ \partial_t \phi(t,\theta) \end{bmatrix} = \begin{bmatrix} A_1 & A_0 & 0_{n \times n} \\ 0_{n \times n} & 0_{n \times n} & I_n \end{bmatrix} \begin{bmatrix} \phi(t,1) \\ \phi(t,0) \\ \partial_\theta \phi(t,\theta) \end{bmatrix}, \qquad \forall (t,\theta) \in [0,+\infty) \times [0,1]. \tag{5.6}$$

Note that, in the above equation, the state $\phi(t,0)$ appears only in the term on the right hand side. Thus, the constant matrix that describes the dynamics of the above system is not a square matrix.

We rewrite the dynamics (5.5) by using projections of the state into an arbitrary set of linearly independent functions. Let $\{f_1, \cdots, f_p\}$ be a set of linearly independent functions, with $f_i \in H^1([0,1],\mathbb{R})$, for $i = 1, \cdots, p$, *not necessarily orthogonal*. For any piecewise continuous function $\rho : [0,1] \to \mathbb{R}^n$, let $\rho_{r0}(\theta) = \rho(\theta)$ and define recursively, for $i = 1, \cdots, p$,

$$\rho_{ri}(\theta) = \rho_{r(i-1)}(\theta) - \hat{\rho}_i f_i(\theta), \tag{5.7}$$

with $\hat{\rho}_i \in \mathbb{R}^n$, $\hat{\rho}_i = \left[\, \hat{\rho}_i^{(1)} \ \ldots \ \hat{\rho}_i^{(n)} \,\right]^\top$, where each component $\hat{\rho}_i^{(k)}$ is recursively defined, for $k = 1, \cdots, n$, as

$$\hat{\rho}_i^{(k)} = \frac{\langle \rho_{r(i-1)}^{(k)}, f_i \rangle}{\|f_i\|^2_{[0,1]}}. \tag{5.8}$$

We obtain from (5.7)

$$\rho(\theta) = \rho_{rp}(\theta) + \sum_{i=1}^{p} \hat{\rho}_i f_i(\theta). \tag{5.9}$$

To simplify the notation, we use below $\rho_r = \rho_{rp}$ as the *residual* term, we introduce the vector $\hat{\rho} : [0, +\infty) \to \mathbb{R}^{np}$,

$$\hat{\rho} = \begin{bmatrix} \hat{\rho}_1 \\ \hat{\rho}_2 \\ \vdots \\ \hat{\rho}_p \end{bmatrix}, \tag{5.10}$$

and we use (5.1) to write (5.9) as

$$\rho(\theta) = \begin{bmatrix} F(\theta) & I_n \end{bmatrix} \begin{bmatrix} \hat{\rho} \\ \rho_r(\theta) \end{bmatrix}. \tag{5.11}$$

Using the above decomposition of ρ, we obtain the following two lemmas.

Lemma 5.1. *Consider* (5.7)-(5.9)*, we have*

$$\int_0^1 F^\top(\theta)\rho_r(\theta)d\theta = (D_{\bar{F}} - \bar{F}^\top)\hat{\rho}, \tag{5.12}$$

with $D_{\bar{F}}$ as in (5.4)*.*

Lemma 5.2. *Consider* (5.7)-(5.9)*, we have*

$$\hat{\rho} = \bar{F}^{-1} \int_0^1 F^\top(\theta)\rho(\theta)d\theta. \tag{5.13}$$

The proofs of the above two lemmas are given in Appendix B.

Remark 5.1. The matrix $\bar{F}$ in (5.3) has a lower triangular structure with non-zero diagonal elements. For an orthogonal set of functions, that is, for a set of functions satisfying $\langle f_i, f_j \rangle = 0$, for all $i, j = 1, \cdots, p$ and $i \neq j$, (5.12) becomes

$$\int_0^1 F^\top(\theta)\rho_r(t,\theta)d\theta = 0_{np\times 1}.$$

In case the set $\{f_1, \cdots, f_p\}$ is not closed under differentiation, define a set of linearly independent functions $\{f_{p+1}, \cdots, f_{p+p_e}\}$ defined on the interval $[0, 1]$, with $0 \leq p_e \leq p$ such that, for all $i \in \{1, \cdots, p\}$,

$$f_i' \in \operatorname{span}(f_1, \cdots, f_p, f_{p+1}, \cdots, f_{p+p_e})$$

and

$$\operatorname{span}(f_1, \cdots, f_p) \cap \operatorname{span}(f_{p+1}, \cdots, f_{p+p_e}) = \{0\}.$$

In this case, we define $f_e(\theta) = \begin{bmatrix} f_{p+1}(\theta) & \cdots & f_{p+p_e}(\theta) \end{bmatrix}$ and $F_e(\theta) = f_e(\theta) \otimes I_n$. We can then express F' in (5.2) as

$$F'(\theta) = F(\theta)X + F_e(\theta)X_e. \tag{5.14}$$

with $X \in \mathbb{R}^{np\times np}$ and $X_e \in \mathbb{R}^{np_e\times np}$. Otherwise, in case the set $\{f_1, \cdots, f_p\}$ is closed under differentiation, namely if there exists a matrix X such that $F'(\theta) = F(\theta)X$, then, $F_e(\theta)$ and X_e are empty matrices. For example, let $n = 1$ and consider the set of shifted Legendre polynomial functions [93] up to degree two, that is $F(\theta) = \begin{bmatrix} 1 & 2\theta - 1 & \frac{3(2\theta-1)^2}{2} - \frac{1}{2} \end{bmatrix}$. Therefore, we have $p_e = 0$ and $\{f_{p+1}, \cdots, f_{p+p_e}\} = \emptyset$. We obtain

$$F'(\theta) = F(\theta) \begin{bmatrix} 0 & 2 & 0 \\ 0 & 0 & 6 \\ 0 & 0 & 0 \end{bmatrix}.$$

As a second example, let $n = 1$ and consider the set of trigonometric functions $F(\theta) = \begin{bmatrix} 1 & \sin(\theta) & \sin(2\theta) \end{bmatrix}$. Therefore, we have $p_e = 2$ and $F_e(\theta) = \begin{bmatrix} \cos(\theta) & \cos(2\theta) \end{bmatrix}$. We obtain

$$F'(\theta) = F(\theta)0_{3\times 3} + \begin{bmatrix} \cos(\theta) & \cos(2\theta) \end{bmatrix} \begin{bmatrix} 0 & 1 & 0 \\ 0 & 0 & 2 \end{bmatrix}.$$

System (5.5) can be expressed in terms of projections of the state ϕ into the set of functions $\{f_1, \cdots, f_p\}$ and the residuals ϕ_r as detailed in the proposition below, where we use $F_0 = F(0)$ and $F_1 = F(1)$.

Proposition 5.3. *Consider system* (5.5)*. The dynamics of* $\hat{\phi}(\cdot)$*,* $\phi_r(\cdot, 1)$*, and* $\phi_r(\cdot, \theta)$ *are governed by*

$$\begin{bmatrix} \dot{\hat{\phi}}(t) \\ \dot{\phi}_r(t,1) \\ \partial_t\phi_r(t,\theta) \end{bmatrix} = \Gamma(\theta) \begin{bmatrix} \hat{\phi}(t) \\ \tilde{\phi}(t) \\ \phi_r(t,1) \\ \phi_r(t,0) \\ \partial_\theta\phi_r(t,\theta) \end{bmatrix}, \qquad \forall (t,\theta) \in [0,+\infty) \times [0,1], \tag{5.15}$$

where $\Gamma : [0,1] \to \mathbb{R}^{n(p+2)\times n(p+p_e+3)}$ *is given by*

$$\Gamma(\theta) = \begin{bmatrix} \bar{F}^{-1}\bar{F}_\partial - \bar{F}^{-1}X^\top(D_{\bar{F}} - \bar{F}^\top) & -\bar{F}^{-1}X_e^\top \\ A_0F_0 + A_1F_1 - F_1\bar{F}^{-1}\bar{F}_\partial + F_1\bar{F}^{-1}X^\top(D_{\bar{F}} - \bar{F}^\top) & F_1\bar{F}^{-1}X_e^\top \\ F'(\theta) - F(\theta)\bar{F}^{-1}\bar{F}_\partial + F(\theta)\bar{F}^{-1}X^\top(D_{\bar{F}} - \bar{F}^\top) & F(\theta)\bar{F}^{-1}X_e^\top \end{bmatrix}$$
$$\begin{bmatrix} \bar{F}^{-1}F_1^\top & -\bar{F}^{-1}F_0^\top & 0_{np\times n} \\ A_1 - F_1\bar{F}^{-1}F_1^\top & A_0 + F_1\bar{F}^{-1}F_0^\top & 0_{n\times n} \\ -F(\theta)\bar{F}^{-1}F_1^\top & F(\theta)\bar{F}^{-1}F_0^\top & I_n \end{bmatrix},$$

ϕ_r *verifies* (5.12)*, for all* $t \geq 0$*, namely* $\int_0^1 F^\top(\theta)\phi_r(t,\theta)d\theta = (D_{\bar{F}} - \bar{F}^\top)\hat{\phi}(t)$*, and* $\tilde{\phi}$ *depends on* ϕ_r *as*

$$\tilde{\phi}(t) = \int_0^1 F_e^\top(\theta)\phi_r(t,\theta)d\theta, \qquad \forall t \geq 0, \tag{5.16}$$

where F_e *is obtained from an extension of the set of functions whenever* F' *is expressed as in* (5.2)*.*

The proof of the above proposition is given in Appendix B. In case the set $\{f_1, \cdots, f_p\}$ is closed under differentiation, we can express the dynamics (5.15) without the term $\tilde{\phi}$, as in (5.16),

$$\begin{bmatrix} \dot{\hat{\phi}}(t) \\ \dot{\phi}_r(t,1) \\ \partial_t\phi_r(t,\theta) \end{bmatrix} = \Gamma_s(\theta) \begin{bmatrix} \hat{\phi}(t) \\ \phi_r(t,1) \\ \phi_r(t,0) \\ \partial_\theta\phi_r(t,\theta) \end{bmatrix}, \qquad \forall (t,\theta) \in [0,+\infty) \times [0,1], \tag{5.17}$$

where $\Gamma_s : [0,1] \to \mathbb{R}^{n(p+2)\times n(p+3)}$ is given by

$$\Gamma_s(\theta) = \begin{bmatrix} \bar{F}^{-1}\bar{F}_\partial - \bar{F}^{-1}X^\top(D_{\bar{F}} - \bar{F}^\top) & \bar{F}^{-1}F_1^\top \\ A_0F_0 + A_1F_1 - F_1\bar{F}^{-1}\bar{F}_\partial + F_1\bar{F}^{-1}X^\top(D_{\bar{F}} - \bar{F}^\top) & A_1 - F_1\bar{F}^{-1}F_1^\top \\ F(\theta)X - F(\theta)\bar{F}^{-1}\bar{F}_\partial + F(\theta)\bar{F}^{-1}X^\top(D_{\bar{F}} - \bar{F}^\top) & -F(\theta)\bar{F}^{-1}F_1^\top \end{bmatrix}$$
$$\begin{bmatrix} -\bar{F}^{-1}F_0^\top & 0_{np\times n} \\ A_0 + F_1\bar{F}^{-1}F_0^\top & 0_{n\times n} \\ F(\theta)\bar{F}^{-1}F_0^\top & I_n \end{bmatrix}.$$

Therefore, for a set of functions $\{f_1, \cdots, f_p\}$ closed under differentiation, namely satisfying $F'(\theta) = F(\theta)X$, we obtain a simpler expression than (5.15). Note that both (5.15) and (5.17), depending on the choice of $F(\theta)$, are equivalent to (5.5) since no approximation is made and the dynamics of the residuals ϕ_r are kept.

5.2 SDP-based stability conditions using a separable parameter T

This section illustrates how the use of a separable T in the Lyapunov-Krasovskii functional given by (4.20) is suitable for SDP-based formulations to verify the conditions of Theorem 4.1. Whenever the set of functions parameterizing Q and a

separable T is the same as the set used to express the system in projected coordinates as in (5.15), the LKF is expressed as a quadratic form in the projected coordinates of the system. We also show that the parameterization of R is crucial for the formulation of SDP tests to verify the positivity of functionals as (4.20). Indeed, methods using integral inequalities impose this function to be affine, where SOS-based methods allow for polynomial parameterizations of this function.

5.2.1 General formulation

We have shown that the analytical solution detailed in Section 4.2 yields a matrix function T in the LKF that is not separable. However, to obtain a numerical formulation suitable for the verification of the Lyapunov inequalities, the usual approach is to impose a separable structure for T, as in [100, 90], without a direct relation to the solution of the equations (4.5)-(4.7). As a result, by imposing a separable T, we look for the LKF parameters satisfying inequalities instead. The key advantage, in comparison with the analytical method exposed in Section 4.2, is that we formulate the search for the parameters of V satisfying both the positivity conditions, as in (4.3), and the negativity of the time derivative along the solution of the time-delay system, as in (4.4).

This section presents methods to find the parameters of V satisfying (4.3)-(4.4) using semidefinite programming. The contribution is to present a unified method based on projections for a general set of linearly independent functions. Moreover, we relate two different approaches, namely the approach based on integral inequalities and the approach based on computing SOS decompositions. These approaches have emerged in recent years as systematic methods encompassing previous SDP-based results for the computation of LKFs. In particular, we point out the common features between SOS and Legendre polynomial projections (related to the integral inequality methods discussed in this section) showing that the main difference consists in the choice of the parameter R in (4.20) and how the conditions for its positivity are treated in the inequalities. Furthermore, we show that different polynomial bases are equivalent and that the general projection method allows to consider sets of functions that are not polynomials. For instance, we can handle projections on the set of functions in (4.13), appearing in the delay Lyapunov matrix.

In the rest of the chapter, we impose

(A) The parameter T in (4.20) is written as

$$T(\theta,\eta) = F(\theta)\bar{T}F^\top(\eta),$$

with $\bar{T} \in \mathbb{S}^{np}$.

(B) The parameter Q in (4.20) depends linearly on f_i, for $i = 1, \cdots, p$, as $Q(\theta) = \sum_{i=1}^{p} Q_i f_i(\theta) = \bar{Q}F^\top(\theta)$, where $Q_i \in \mathbb{R}^{n\times n}$ and $\bar{Q} = \begin{bmatrix} Q_1 & Q_2 & \cdots & Q_p \end{bmatrix}$.

Thus, using Lemma 5.2, we have

$$\int_0^1 \int_0^1 \rho^\top(\theta)T(\theta,\eta)\rho(\eta)d\eta d\theta = \hat{\rho}^\top \bar{F}^\top \bar{T}\bar{F}\hat{\rho} \tag{5.18}$$

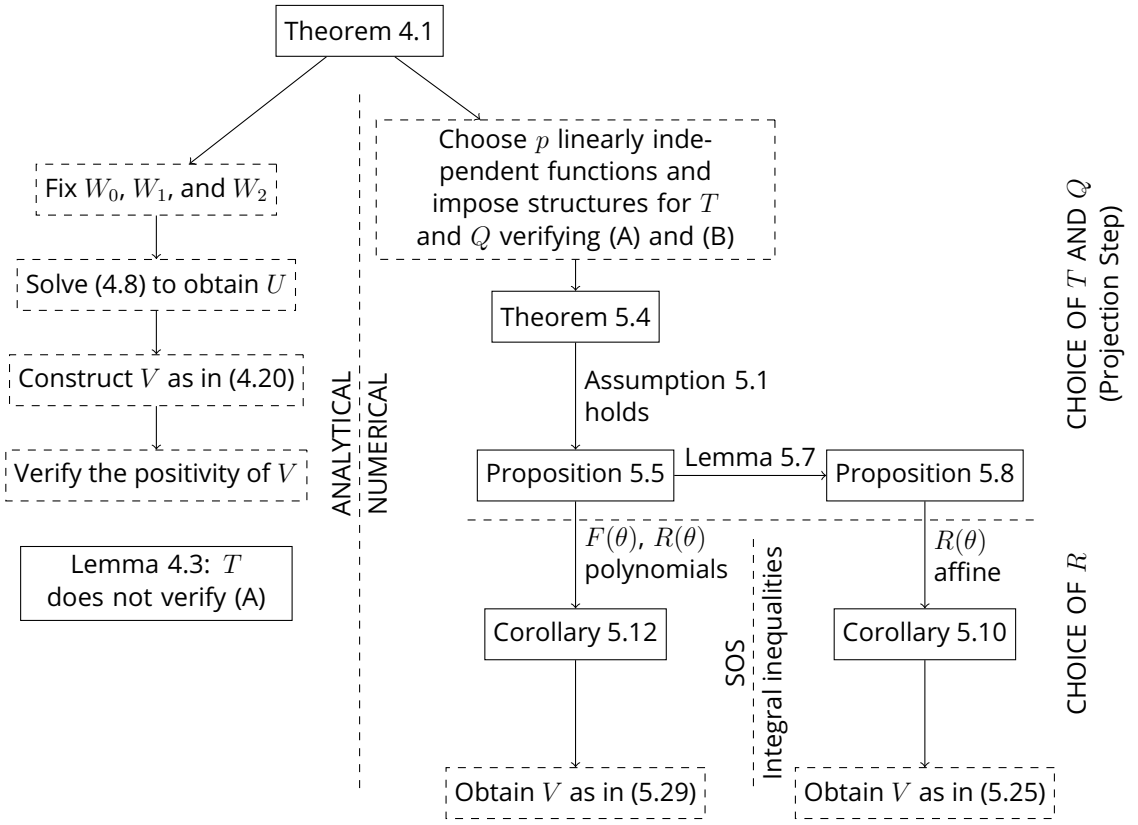

Figure 5.1: Flowchart of the structure of Part II.

and

$$\int_0^1 \bar{Q}F^\top(\theta)\rho(\theta)d\theta = \bar{Q}\bar{F}\hat{\rho}.$$

Figure 5.1 summarizes the steps to obtain an LKF, it also presents the relations between the stability analysis results presented in this chapter. Using (A) and (B) above and applying the results of Theorem 4.1 with the Lyapunov-Krasovskii functional in the projected coordinates, the stability conditions of a linear time-delay system can be expressed as matrix inequalities with an affine dependence on the parameters P, Q, R, and T as in the following theorem.

Theorem 5.4. *If* $\exists\ \alpha_1, \beta > 0$, $P \in \mathbb{S}^n$, $\bar{Q} \in \mathbb{R}^{n\times np}$, $R : [0,1] \to \mathbb{S}^n$, $\bar{T} \in \mathbb{S}^{np}$, $S_0 \in \mathbb{R}^{np\times np}$, $S_1 \in \mathbb{R}^{n\times np}$, $\bar{S}_0 \in \mathbb{R}^{np\times np}$, $\bar{S}_1 \in \mathbb{R}^{n(p_e+2)\times np}$, $\tilde{S}_0 \in \mathbb{R}^{np\times np_e}$, $\tilde{S}_1 \in \mathbb{R}^{np_e\times np_e}$, $\tilde{S}_2 \in \mathbb{R}^{2n\times np_e}$, *two differentiable functions* $C : [0,1] \to \mathbb{S}^{n(p+1)}$ *and* $\bar{C} : [0,1] \to \mathbb{S}^{n(p+p_e+2)}$, *and a set of linearly independent functions* $\{f_1, \ldots, f_p\}$ *such that*

$$\Omega(\theta) \geq 0_{n(p+2)\times n(p+2)}, \qquad \forall\theta \in [0,1],$$

and

$$\bar{\Omega}(\theta) \leq 0_{n(p+p_e+3)\times n(p+p_e+3)}, \qquad \forall\theta \in [0,1],$$

where

$$\Omega(\theta) = \left[\begin{array}{cc:c} \Omega_{11} & \bar{F}^\top\bar{Q}^\top + F_1^\top P & F^\top(\theta)R(\theta) \\ \bar{Q}\bar{F} + PF_1 & P & 0_{n\times n} \\ \hdashline R(\theta)F(\theta) & 0_{n\times n} & R(\theta) \end{array}\right] + \left[\begin{array}{cc:c} S_0(D_{\bar{F}} - \bar{F}^\top) + (D_{\bar{F}} - \bar{F})S_0^\top & (D_{\bar{F}} - \bar{F})S_1^\top & -S_0F^\top(\theta) \\ S_1(D_{\bar{F}} - \bar{F}^\top) & 0_{n\times n} & -S_1F^\top(\theta) \\ \hdashline -F(\theta)S_0^\top & -F(\theta)S_1^\top & 0_{n\times n} \end{array}\right] + \left[\begin{array}{c:c} C'(\theta) - C(1) + C(0) & 0_{n(p+1)\times n} \\ \hdashline 0_{n\times n(p+1)} & 0_{n\times n} \end{array}\right] - \alpha_1 \left[\begin{array}{cc:c} F_1^\top F_1 & F_1^\top & 0_{np\times n} \\ F_1 & I_n & 0_{n\times n} \\ \hdashline 0_{n\times np} & 0_{n\times n} & 0_{n\times n} \end{array}\right] \quad (5.19)$$

and

$$\bar{\Omega}(\theta) = \left[\begin{array}{cccc:c} \bar{\Omega}_{11}(\theta) + \bar{\Omega}_{11}^\top(\theta) & -\bar{F}^\top\bar{T}X_e^\top & \bar{\Omega}_{13} & \bar{\Omega}_{14} & -F^\top(\theta)R'(\theta) \\ -X_e\bar{T}\bar{F} & 0_{np_e\times np_e} & 0_{np_e\times n} & 0_{np_e\times n} & 0_{np_e\times n} \\ \bar{\Omega}_{13}^\top & 0_{n\times np_e} & \bar{\Omega}_{33} + \bar{\Omega}_{33}^\top & \bar{\Omega}_{34} & -\bar{Q}X_e^\top F_e^\top(\theta) \\ \bar{\Omega}_{14}^\top & 0_{n\times np_e} & \bar{\Omega}_{34}^\top & -R(0) & 0_{n\times n} \\ \hdashline -R'(\theta)F(\theta) & 0_{n\times np_e} & -F_e(\theta)X_e\bar{Q}^\top & 0_{n\times n} & -R'(\theta) \end{array}\right] + \left[\begin{array}{cc:c} \bar{S}_0(D_{\bar{F}} - \bar{F}^\top) + (D_{\bar{F}} - \bar{F})\bar{S}_0^\top & (D_{\bar{F}} - \bar{F})\bar{S}_1^\top & -\bar{S}_0F^\top(\theta) \\ \bar{S}_1(D_{\bar{F}} - \bar{F}^\top) & 0_{n(p_e+2)\times n(p_e+2)} & -\bar{S}_1F^\top(\theta) \\ \hdashline -F(\theta)\bar{S}_0^\top & -F(\theta)\bar{S}_1^\top & 0_{n\times n} \end{array}\right] + \left[\begin{array}{ccc:c} 0_{np\times np} & \tilde{S}_0 & 0_{np\times 2n} & -\tilde{S}_0F_e^\top(\theta) \\ \tilde{S}_0^\top & \tilde{S}_1 + \tilde{S}_1^\top & \tilde{S}_2^\top & -\tilde{S}_1F_e^\top(\theta) \\ 0_{2n\times np} & \tilde{S}_2 & 0_{2n\times 2n} & -\tilde{S}_2F_e^\top(\theta) \\ \hdashline -F_e(\theta)\bar{S}_0^\top & -F_e(\theta)\bar{S}_1^\top & -F_e(\theta)\bar{S}_2^\top & 0_{n\times n} \end{array}\right] + \left[\begin{array}{c:c} \bar{C}'(\theta) - \bar{C}(1) + \bar{C}(0) & 0_{n(p+p_e+2)\times n} \\ \hdashline 0_{n\times n(p+p_e+2)} & 0_{n\times n} \end{array}\right] + \beta \left[\begin{array}{ccccc:c} F_1^\top F_1 & 0_{np\times np_e} & F_1^\top & 0_{np\times n} & 0_{np\times n} \\ 0_{np_e\times np} & 0_{np_e\times np_e} & 0_{np_e\times n} & 0_{np_e\times n} & 0_{np_e\times n} \\ F_1 & 0_{n\times np_e} & I_n & 0_{n\times n} & 0_{n\times n} \\ 0_{n\times np} & 0_{n\times np_e} & 0_{n\times n} & 0_{n\times n} & 0_{n\times n} \\ \hdashline 0_{n\times np} & 0_{n\times np_e} & 0_{n\times n} & 0_{n\times n} & 0_{n\times n} \end{array}\right],$$

with

$$
\begin{aligned}
\Omega_{11} &= \bar{F}^\top \bar{T} \bar{F} + F_1^\top P F_1 + \bar{F}^\top \bar{Q}^\top F_1 + F_1^\top \bar{Q} \bar{F} + \int_0^1 F^\top(\theta) R(\theta) F(\theta) d\theta, \\
\bar{\Omega}_{11}(\theta) &= (\bar{F}^\top \bar{T} + F_1^\top \bar{Q})(\bar{F}_\partial - X^\top (D_{\bar{F}} - \bar{F}^\top)) + (\bar{F}^\top \bar{Q}^\top + F_1^\top P)(A_0 F_0 + A_1 F_1) \\
&\quad + F^\top(\theta) R(\theta) F'(\theta), \\
\bar{\Omega}_{13} &= (\bar{F}^\top \bar{T} + F_1^\top \bar{Q}) F_1^\top + (\bar{F}^\top \bar{Q}^\top + F_1^\top P) A_1 + F_1^\top R(1) + (F_0^\top A_0^\top + F_1^\top A_1^\top) P \\
&\quad + (\bar{F}_\partial^\top - (D_{\bar{F}} - \bar{F})) \bar{Q}^\top, \\
\bar{\Omega}_{14} &= -(\bar{F}^\top \bar{T} + F_1^\top \bar{Q}) F_0^\top + (\bar{F}^\top \bar{Q}^\top + F_1^\top P) A_0 - F_0^\top R(0), \\
\bar{\Omega}_{33} &= P A_1 + \bar{Q} F_1^\top + \frac{1}{2} R(1), \\
\bar{\Omega}_{34} &= P A_0 - \bar{Q} F_0^\top,
\end{aligned}
$$

where F_e is obtained from an extension of the set of functions whenever F' is expressed as in (5.14)*, then the origin of* (5.5) *is GES.*

The proof of the above theorem is given in Appendix B.

Remark 5.2. By convention [26, 76], we consider that the product of an empty matrix of dimension $m \times 0$ and an empty matrix of dimension $0 \times n$ is a matrix of dimension $m \times n$ with all elements equal to 0. Hence, if the set $\{f_1, \cdots, f_p\}$ is closed under differentiation, then $p_e = 0$ and the matrices $F_e(\theta)$, X_e, $\tilde{S}_0$, $\tilde{S}_1$, and $\tilde{S}_2$, that appear in Theorem 5.4, are empty matrices. Therefore, we have the products

$$
\begin{aligned}
\bar{Q} X_e^\top F_e^\top(\theta) &= 0_{n \times n}, \\
\tilde{S}_0 F_e^\top(\theta) &= 0_{np \times n}, \\
\tilde{S}_2 F_e^\top(\theta) &= 0_{2n \times n},
\end{aligned}
$$

and $X_e \bar{T} \bar{F}$ and $\tilde{S}_1 F_e^\top(\theta)$ are empty matrices.

To formulate an SDP test based on the use of integral inequalities and to simplify the SOS programming formulation, in addition to (A) and (B), we introduce the following assumption that simplifies the conditions in Theorem 5.4.

Assumption 5.1. The set of linearly independent functions is closed under differentiation, that is $F'(\theta) = F(\theta) X$, for some matrix $X \in \mathbb{R}^{np \times np}$.

Note that Assumption 5.1 holds for any set of p polynomial functions constructed using the terms of degree less than or equal to $p - 1$ in a polynomial basis. Under Assumption 5.1, we obtain the following proposition, using (5.17) instead of (5.15).

Proposition 5.5. *If $\exists\ \alpha_1, \beta > 0$, $P \in \mathbb{S}^n$, $\bar{Q} \in \mathbb{R}^{n \times np}$, $R : [0,1] \to \mathbb{S}^n$, $\bar{T} \in \mathbb{S}^{np}$, $S_0 \in \mathbb{R}^{np \times np}$, $S_1 \in \mathbb{R}^{n \times np}$, $\bar{S}_0 \in \mathbb{R}^{np \times np}$, $\bar{S}_1 \in \mathbb{R}^{2n \times np}$, two differentiable functions $C : [0,1] \to \mathbb{S}^{n(p+1)}$ and $\bar{C} : [0,1] \to \mathbb{S}^{n(p+2)}$, and a set of linearly independent functions $\{f_1, \ldots, f_p\}$ closed under differentiation such that*

$$
\Omega(\theta) \geq 0_{n(p+2) \times n(p+2)}, \qquad \forall \theta \in [0,1], \tag{5.20}
$$

where $\Omega(\theta)$ *as in* (5.19)*, and*

$$\bar{\Omega}_s(\theta) \leq 0_{n(p+3)\times n(p+3)}, \qquad \forall \theta \in [0,1], \tag{5.21}$$

where

$$\begin{aligned}
\bar{\Omega}_s(\theta) = &\left[\begin{array}{ccc:c} \bar{\Omega}_{s11}+\bar{\Omega}_{s11}^\top & \bar{\Omega}_{s12} & \bar{\Omega}_{s13} & -F^\top(\theta)R'(\theta) \\ \bar{\Omega}_{s12}^\top & \bar{\Omega}_{s22}+\bar{\Omega}_{22}^\top & \bar{\Omega}_{s23} & 0_{n\times n} \\ \bar{\Omega}_{s13}^\top & \bar{\Omega}_{s23}^\top & -R(0) & 0_{n\times n} \\ \hdashline -R'(\theta)F(\theta) & 0_{n\times n} & 0_{n\times n} & -R'(\theta) \end{array}\right] \\
&+ \left[\begin{array}{cc:c} \bar{S}_0(D_{\bar{F}}-\bar{F}^\top)+(D_{\bar{F}}-\bar{F})\bar{S}_0^\top & (D_{\bar{F}}-\bar{F})\bar{S}_1^\top & -\bar{S}_0F^\top(\theta) \\ \bar{S}_1(D_{\bar{F}}-\bar{F}^\top) & 0_{2n\times 2n} & -\bar{S}_1F^\top(\theta) \\ \hdashline -F(\theta)\bar{S}_0^\top & -F(\theta)\bar{S}_1^\top & 0_{n\times n} \end{array}\right] \\
&+ \left[\begin{array}{c:c} \bar{C}'(\theta)-\bar{C}(1)+\bar{C}(0) & 0_{n(p+2)\times n} \\ \hdashline 0_{n\times n(p+2)} & 0_{n\times n} \end{array}\right] + \beta \left[\begin{array}{ccc:c} F_1^\top F_1 & F_1^\top & 0_{np\times n} & 0_{np\times n} \\ F_1 & I_n & 0_{n\times n} & 0_{n\times n} \\ 0_{n\times np} & 0_{n\times n} & 0_{n\times n} & 0_{n\times n} \\ \hdashline 0_{n\times np} & 0_{n\times n} & 0_{n\times n} & 0_{n\times n} \end{array}\right],
\end{aligned} \tag{5.22}$$

with

$$\begin{aligned}
\bar{\Omega}_{s11} &= (\bar{F}^\top\bar{T}+F_1^\top\bar{Q})(\bar{F}_\partial - X^\top(D_{\bar{F}}-\bar{F}^\top)) + (\bar{F}^\top\bar{Q}^\top+F_1^\top P)(A_0F_0+A_1F_1) \\
&\quad + \int_0^1 F^\top(\theta)R(\theta)F(\theta)d\theta X, \\
\bar{\Omega}_{s12} &= (\bar{F}^\top\bar{T}+F_1^\top\bar{Q})F_1^\top + (\bar{F}^\top\bar{Q}^\top+F_1^\top P)A_1 + F_1^\top R(1) + (F_0^\top A_0^\top + F_1^\top A_1^\top)P \\
&\quad + (\bar{F}_\partial^\top - (D_{\bar{F}}-\bar{F})X)\bar{Q}^\top, \\
\bar{\Omega}_{s13} &= -(\bar{F}^\top\bar{T}+F_1^\top\bar{Q})F_0^\top + (\bar{F}^\top\bar{Q}^\top+F_1^\top P)A_0 - F_0^\top R(0), \\
\bar{\Omega}_{s22} &= PA_1 + \bar{Q}F_1^\top + \frac{1}{2}R(1), \\
\bar{\Omega}_{s23} &= PA_0 - \bar{Q}F_0^\top,
\end{aligned}$$

then the origin of (5.5) *is GES.*

Proof. The proof of the above proposition directly results from the proof of Theorem 5.4, where $p_e = 0$ and F' is expressed as in Assumption 5.1. □

Remark 5.3. The set of functions in (4.13), obtained from the delay Lyapunov matrix (4.14) verifies Assumption 5.1 and may be used to parameterize the LKF and to verify the conditions in Proposition 5.5. The difference in the parameterization we propose and the solution using the delay Lyapunov matrix remains the structure imposed for parameter T following item (A) above and on the choice of parameter R.

The proposition below states the equivalence of the conditions in Theorem 5.4 (or in Proposition 5.5) for two sets of functions defined on the interval $[0,1]$.

Proposition 5.6. *Let $\{f_1, \cdots, f_p\}$ and $\{g_1, \cdots, g_p\}$, where, for $i = 1, \cdots, p$, $f_i, g_i \in L_2([0,1], \mathbb{R})$ satisfying*

$$\begin{bmatrix} f_1(\theta) & \cdots & f_p(\theta) \end{bmatrix} = \begin{bmatrix} g_1(\theta) & \cdots & g_p(\theta) \end{bmatrix} B,$$

where $B \in \mathbb{R}^{p\times p}$ is a non-singular matrix. If Theorem 5.4 or Proposition 5.5 are feasible with the set $\{f_1, \cdots, f_p\}$, then they are also feasible with the set $\{g_1, \cdots, g_p\}$.

The proof of the above proposition is given in Appendix B. An implication of the above proposition is that given a polynomial set of functions satisfying Theorem 5.4, it is possible to find unknowns in the theorem for a different set of polynomials with the same degrees. On the other hand, the choice of orthogonal polynomials may be more suitable for the numerical solution, as detailed in Section 5.3 below. Proposition 5.5 requires the verification of (5.20)-(5.21) that is, two matrix inequalities on the interval $[0, 1]$. In the rest of the section, we present two approaches that allow to verify these inequalities.

5.2.2 Formulation based on integral inequalities

In this section, we present conditions to verify the inequalities (5.20)-(5.21) in Proposition 5.5 by using a general formulation for integral inequalities. We show how the proposed formulation encompasses the use of integral inequalities such as Jensen's inequality [98] and Bessel-Legendre inequality. Indeed, these are shown to correspond to particular choices of Legendre polynomials as the set of linearly independent functions in the projections. The key step in this formulation is to split the inequalities into a term containing the projected variables $\hat{\rho}$ and another term containing the residual ρ_r, which is the only term left within an integral. As a result, it allows us to formulate the stability conditions with constant matrix inequalities. Moreover, we show that with the proposed formulation it suffices to consider an affine parameter R. The results in this section are built upon the following lemma.

Lemma 5.7. *Let $S \in \mathbb{S}^n_{\geq 0}$, then for any function $\rho \in PC([0,1], \mathbb{R}^n)$ and any set of linearly independent functions $\{f_1, \cdots, f_p\}$, we have*

$$\int_0^1 \rho^\top(\theta) S \rho(\theta) d\theta \geq \hat{\rho}^\top (\tilde{D}_{\bar{F}} \otimes S)\hat{\rho}.$$

The proof of the above lemma is given in Appendix B.

The following proposition uses the integral inequality of Lemma 5.7 to obtain a set of conditions to verify the inequalities of Proposition 5.5. For this reason, we call it *formulation based on integral inequalities*.

Proposition 5.8. *If $\exists\, \alpha_1, \beta > 0$, $P \in \mathbb{S}^n$, $\bar{Q} \in \mathbb{R}^{n\times np}$, $R : [0,1] \to \mathbb{S}^n$, $\bar{T} \in \mathbb{S}^{np}$, $S \in \mathbb{S}^n$, $\bar{S} \in \mathbb{S}^n$, and a set of linearly independent functions $\{f_1, \ldots, f_p\}$ such that*

$$\begin{cases} \Omega_p \geq 0_{n(p+1)\times n(p+1)}, \\ R(\theta) \geq S, \qquad \forall \theta \in [0,1], \\ S \geq 0_{n\times n}, \end{cases} \tag{5.23}$$

and

$$\begin{cases} \bar{\Omega}_p \leq 0_{n(p+2)\times n(p+2)}, \\ R'(\theta) \geq \bar{S}, \qquad \forall \theta \in [0,1], \\ \bar{S} \geq 0_{n\times n}, \end{cases} \tag{5.24}$$

where

$$\Omega_p = \begin{bmatrix} \Omega_{p11} + (\tilde{D}_{\bar{F}} \otimes S) & F_1^\top P + \bar{F}^\top \bar{Q}^\top \\ PF_1 + \bar{Q}\bar{F} & P \end{bmatrix} - \alpha_1 \begin{bmatrix} F_1^\top F_1 & F_1^\top \\ F_1 & I_n \end{bmatrix}$$

and

$$\bar{\Omega}_p = \begin{bmatrix} \bar{\Omega}_{p11} + \bar{\Omega}_{p11}^\top - (\tilde{D}_{\bar{F}} \otimes \bar{S}) & \bar{\Omega}_{p12} & \bar{\Omega}_{p13} \\ \bar{\Omega}_{p12}^\top & \bar{\Omega}_{p22} + \bar{\Omega}_{p22}^\top & \bar{\Omega}_{p23} \\ \bar{\Omega}_{p13}^\top & \bar{\Omega}_{p23}^\top & -R(0) \end{bmatrix} + \beta \begin{bmatrix} F_1^\top F_1 & F_1^\top & 0_{np\times n} \\ F_1 & I_n & 0_{n\times n} \\ 0_{n\times np} & 0_{n\times n} & 0_{n\times n} \end{bmatrix},$$

with

$$\begin{aligned} \Omega_{p11} &= \bar{F}^\top \bar{T} \bar{F} + F_1^\top P F_1 + \bar{F}^\top \bar{Q}^\top F_1 + F_1^\top \bar{Q} \bar{F}, \\ \bar{\Omega}_{p11} &= (\bar{F}^\top \bar{T} + F_1^\top \bar{Q})(\bar{F}_\partial - X^\top (D_{\bar{F}} - \bar{F}^\top)) + (\bar{F}^\top \bar{Q}^\top + F_1^\top P)(A_0 F_0 + A_1 F_1) \\ &\quad + \frac{1}{2} F_1^\top R(1) F_1 - \frac{1}{2} F_0^\top R(0) F_0, \\ \bar{\Omega}_{p12} &= (\bar{F}^\top \bar{T} + F_1^\top \bar{Q}) F_1^\top + (\bar{F}^\top \bar{Q}^\top + F_1^\top P) A_1 + F_1^\top R(1) + (F_0^\top A_0^\top + F_1^\top A_1^\top) P \\ &\quad + (\bar{F}_\partial^\top - (D_{\bar{F}} - \bar{F}) X) \bar{Q}^\top, \\ \bar{\Omega}_{p13} &= -(\bar{F}^\top \bar{T} + F_1^\top \bar{Q}) F_0^\top + (\bar{F}^\top \bar{Q}^\top + F_1^\top P) A_0 - F_0^\top R(0), \\ \bar{\Omega}_{p22} &= \bar{Q} F_1^\top + P A_1 + \frac{1}{2} R(1), \\ \bar{\Omega}_{p23} &= -\bar{Q} F_0^\top + P A_0, \end{aligned}$$

then the origin of (5.5) *is GES.*

The proof of the above proposition is given in Appendix B.

Remark 5.4. Recall that, from Proposition 5.6, the conditions in Theorem 5.4 (also in Proposition 5.5) are equivalent for any linear combination of functions in a set of functions $\{f_1, \cdots, f_p\}$. The conditions in Proposition 5.8 instead, depend on the selected set of functions and may not hold for another set obtained from the linear combination of a set for which the conditions hold true. The reason for this is that the inequality from Lemma 5.7, used in the proposition, depends on the set of functions. The numerical examples in Section 5.3 will highlight this difference by applying the conditions to different sets of polynomials.

Following the conditions of Proposition 5.8, the proposition below shows that it is sufficient to consider R as an affine function.

Proposition 5.9. *If $\exists\ \alpha_1, \beta > 0$ and matrices $P \in \mathbb{S}^n$, $\bar{Q} \in \mathbb{R}^{n\times np}$, $\bar{T} \in \mathbb{S}^{np}$, $S \in \mathbb{S}^n$, $\bar{S} \in \mathbb{S}^n$, and $R : [0,1] \to \mathbb{S}^n$ such that the conditions of Proposition 5.8 hold. Then the conditions also hold with matrices $P^* = P$, $\bar{Q}^* = \bar{Q}$, $\bar{T}^* = \bar{T}$, and with $S^* = R(0)$, $\bar{S}^* = R(1) - R(0)$, and $R^*(\theta) = (1-\theta)R(0) + \theta R(1)$, for all $\theta \in [0,1]$.*

Proof. Let P, $\bar{Q}$, $\bar{T}$, S, $\bar{S}$, and $R(\theta)$ be such that the conditions of Proposition 5.8 are satisfied. By (5.23), we have $R(\theta) \geq S$, for all $\theta \in [0,1]$. Then, since $R(0) \geq S$ and $R(1) \geq S$, we obtain

$$R^*(\theta) \geq (1-\theta)S + \theta S = S, \qquad \forall \theta \in [0,1],$$

hence, $R^*(\theta) \geq S$, for all $\theta \in [0,1]$.

Moreover, by (5.24), we have $R'(\theta) \geq \bar{S}$, for all $\theta \in [0,1]$. Then, we have

$$R(1) - R(0) = \int_0^1 R'(\theta) d\theta \geq \int_0^1 \bar{S} d\theta = \bar{S}.$$

Therefore, since $R^{*\prime}(\theta) = R(1) - R(0)$, we also verify $R^{*\prime}(\theta) \geq \bar{S}$, for all $\theta \in [0,1]$. In addition, since S and $\bar{S}$ appear in the diagonal blocks of Ω_p and $\bar{\Omega}_p$, the inequalities (5.23) and (5.24) also hold if S and $\bar{S}$ are respectively replaced by the upper bounds $R(0)$ and $R(1) - R(0)$. □

Therefore, using integral inequalities, the conditions of Proposition 5.8 can be reduced to the verification of some constant linear matrix inequalities (matrices that do not depend on the parameter θ). Hence, an affine structure for R is not an assumption made to obtain Proposition 5.8 but rather it is a consequence of the use of the integral inequality of Lemma 5.7. From Proposition 5.8 and Proposition 5.9, we obtain the following corollary.

Corollary 5.10. *If* $\exists\, \alpha_1, \beta > 0$, $P \in \mathbb{S}^n$, $\bar{Q} \in \mathbb{R}^{n \times np}$, $R_0 \in \mathbb{S}^n$, $R_1 \in \mathbb{S}^n$, $\bar{T} \in \mathbb{S}^{np}$, *and a set of linearly independent functions* $\{f_1, \ldots, f_p\}$ *such that the inequalities* (5.23) *and* (5.24) *in Proposition 5.8 are satisfied with*

$$\begin{aligned} R(\theta) &= R_0 + \theta R_1, \\ S &= R_0, \\ \bar{S} &= R_1, \end{aligned}$$

then the origin of (5.5) *is GES.*

To the stability test in Corollary 5.10, obtained from the structures imposed for Q, T and R, we associate the following LKF candidate for system (5.17)

$$\begin{aligned} V(\hat{\rho}, \rho_r(1), \rho_r(\cdot)) = &\begin{bmatrix} \hat{\rho} \\ \rho_r(1) \end{bmatrix}^\top \begin{bmatrix} \Omega_{p11} & F_1^\top P + \bar{F}^\top \bar{Q}^\top \\ PF_1 + \bar{Q}\bar{F} & P \end{bmatrix} \begin{bmatrix} \hat{\rho} \\ \rho_r(1) \end{bmatrix} \\ &+ \int_0^1 \begin{bmatrix} \hat{\rho}^\top & \rho_r^\top(\theta) \end{bmatrix} \begin{bmatrix} F^\top(\theta) \\ I_n \end{bmatrix} (R_0 + \theta R_1) \begin{bmatrix} F(\theta) & I_n \end{bmatrix} \begin{bmatrix} \hat{\rho} \\ \rho_r(\theta) \end{bmatrix} d\theta, \end{aligned} \quad (5.25)$$

where $\Omega_{p11} = \bar{F}^\top \bar{T} \bar{F} + F_1^\top P F_1 + \bar{F}^\top \bar{Q}^\top F_1 + F_1^\top \bar{Q} \bar{F}$.

We end this section by showing that the integral inequality provided in Lemma 5.7 is a general formulation of some integral inequalities used in the literature. The expression for $\tilde{D}_{\bar{F}}$ used below is given in the Notation.

Integral inequalities as particular cases of Lemma 5.7

1. **Bessel-Legendre inequality.** Let $\{f_1, \cdots, f_p\}$ be the set of the first p shifted Legendre polynomial functions [93], then, for any matrix $S \in \mathbb{S}^n_{\geq 0}$, we obtain

$$\int_0^1 \rho^\top(\theta) S \rho(\theta) d\theta \geq \hat{\rho}^\top (\tilde{D}_{\bar{F}} \otimes S) \hat{\rho},$$

where, from the definition of $\tilde{D}_{\bar{F}}$, the above choice of the set $\{f_1, \cdots, f_p\}$ gives

$$\tilde{D}_{\bar{F}} = \begin{bmatrix} 1 & 0 & \cdots & 0 \\ 0 & \frac{1}{3} & \ddots & \vdots \\ \vdots & \ddots & \ddots & 0 \\ 0 & \cdots & 0 & \frac{1}{2p+1} \end{bmatrix}$$

and $\hat{\rho}$ is the projected term. The above integral inequality is equivalent to Bessel-Legendre integral inequality provided in [93, Lemma 2], where the projected term is not normalized there.

2. **Bessel-Legendre integral inequality.** Let $\{l_1, \cdots, l_{p-1}\}$ the set of the first $p-1$ shifted Legendre polynomial functions and define

$$L(\theta) = \begin{bmatrix} l_1(\theta) & \cdots & l_{p-1}(\theta) \end{bmatrix}.$$

Let $g \in C^0$, $g \in L_2([0,1], \mathbb{R})$, and introduce $g_r : [0,1] \to \mathbb{R}$ as

$$g_r(\theta) = g(\theta) - L(\theta)\hat{g},$$

where

$$\hat{g} = \bar{L}^{-1} \int_0^1 L^\top(\theta) g(\theta) d\theta,$$

and

$$\bar{L} = \begin{bmatrix} \langle l_1, l_1 \rangle & 0 & \dots & 0 \\ 0 & \langle l_2, l_2 \rangle & \ddots & \vdots \\ \vdots & \ddots & \ddots & 0 \\ 0 & \dots & 0 & \langle l_{p-1}, l_{p-1} \rangle \end{bmatrix}.$$

Consider the set of functions $\{l_1, \cdots, l_{p-1}, g_r\}$. Then, for any matrix $S \in \mathbb{S}^n_{\geq 0}$, we obtain

$$\int_0^1 \rho^\top(\theta) S \rho(\theta) d\theta \geq \hat{\rho}^\top (\tilde{D}_{\bar{F}} \otimes S) \hat{\rho},$$

where

$$\tilde{D}_{\bar{F}} = \begin{bmatrix} 1 & 0 & \cdots & 0 & 0 \\ 0 & \frac{1}{3} & \ddots & \vdots & \vdots \\ \vdots & \ddots & \ddots & 0 & \vdots \\ 0 & \cdots & 0 & \frac{1}{2(p-1)+1} & 0 \\ 0 & \cdots & \cdots & 0 & \langle g_r, g_r \rangle \end{bmatrix}$$

and $\hat{\rho}$ is the projected term. The above integral inequality is equivalent to Bessel-Legendre integral inequality presented in [100, Lemma 2].

3. **Jensen's inequality.** Consider the set of functions $\{1\}$, which gives $\tilde{D}_{\bar{F}} = 1$ and $\hat{\rho} = \int_0^1 \rho(\theta)d\theta$. Then, from Lemma 5.7, we obtain

$$\int_0^1 \rho^\top(\theta) S \rho(\theta) d\theta \geq \hat{\rho}^\top S \hat{\rho},$$

for any matrix $S \in \mathbb{S}^n_{\geq 0}$. The above integral inequality is equivalent to Jensen's inequality [98, Lemma 2].

5.2.3 Formulations based on polynomial SOS constraints

In this section, we consider $\{f_1, \cdots, f_p\}$ to be a set of polynomials verifying Assumption 5.1. We propose an SOS formulation as an SDP-based test to verify the conditions of Proposition 5.5. Thereby, we show that we can carry out a projection step to represent the system as in (5.17) and benefit from the SOS constraints to verify matrix inequalities on a bounded interval such as (5.20) and (5.21) in Proposition 5.5.

Before presenting the SOS constraints associated with the projections proposed in Proposition 5.5, we start by reformulating the SOS constraints for stability analysis of linear time-delay systems without projections, as presented in [90], in terms of the dynamics (5.5).

Consider the Lyapunov-Krasovskii functional in (4.20), then its time derivative along the solution of (5.5) is given by

$$\begin{aligned}\dot{V}(\phi(t,1),\phi(t,0),\phi(t,\cdot)) = \\ \int_0^1 \begin{bmatrix}\phi(t,1)\\ \phi(t,0)\\ \phi(t,\theta)\end{bmatrix}^\top \begin{bmatrix}\bar{\Upsilon}_{11} & PA_0 - Q(0) & \bar{\Upsilon}_{13}(\theta)\\ A_0^\top P - Q^\top(0) & -R(0) & \bar{\Upsilon}_{23}\\ \bar{\Upsilon}_{13}^\top(\theta) & \bar{\Upsilon}_{23}^\top & -R'(\theta)\end{bmatrix} \begin{bmatrix}\phi(t,1)\\ \phi(t,0)\\ \phi(t,\theta)\end{bmatrix} d\theta \\ - \int_0^1 \int_0^1 \phi^\top(t,\theta) \left[\frac{\partial T(\theta,\eta)}{\partial \theta} + \frac{\partial T(\theta,\eta)}{\partial \eta}\right] \phi(t,\eta) d\eta d\theta,\end{aligned}$$

where

$$\bar{\Upsilon}_{11} = PA_1 + A_1^\top P + Q(1) + Q^\top(1) + R(1), \tag{5.26}$$

$$\bar{\Upsilon}_{13}(\theta) = A_1^\top Q(\theta) - Q'(\theta) + T(1,\theta), \tag{5.27}$$

and

$$\bar{\Upsilon}_{23}(\theta) = A_0^\top Q(\theta) - T(0,\theta). \tag{5.28}$$

Let $T(\theta,\eta) = F(\theta)\bar{T}F^\top(\eta)$, for some $\bar{T} \in \mathbb{S}^{np}$, and Assumption 5.1 holds, then, from [90], we obtain the following proposition.

Proposition 5.11. *If $\exists\ \alpha_1, \beta > 0$, $P \in \mathbb{S}^n$, $\bar{Q} \in \mathbb{R}^{n\times np}$, polynomial $R : [0,1] \to \mathbb{S}^n$, $\bar{T} \in \mathbb{S}^{np}$, real polynomial matrices $C : [0,1] \to \mathbb{S}^n$ and $\bar{C} : [0,1] \to \mathbb{S}^{2n}$, and two real*

polynomial matrices $N_1 : [0,1] \to \mathbb{S}^n$ *and* $N_2 : [0,1] \to \mathbb{S}^{2n}$ *and an integer* m *such that*

$$\begin{aligned}
&\Upsilon(\theta) - N_1(\theta)\theta(1-\theta) \in \Sigma^{m,n}[\theta],\\
&N_1(\theta) \in \Sigma^{m,n}[\theta],\\
&\bar{T} \geq 0_{np\times np},\\
&-\bar{\Upsilon}(\theta) - N_2(\theta)\theta(1-\theta) \in \Sigma^{m,2n}[\theta],\\
&N_2(\theta) \in \Sigma^{m,2n}[\theta],\\
&X\bar{T} + \bar{T}X^\top \geq 0_{np\times np},
\end{aligned}$$

where

$$\Upsilon(\theta) = \begin{bmatrix} P + C'(\theta) - C(1) + C(0) - \alpha_1 I_n & Q(\theta) \\ Q^\top(\theta) & R(\theta) \end{bmatrix}$$

and

$$\bar{\Upsilon}(\theta) = \left[\begin{array}{cc:c} \bar{\Upsilon}_{11} + \beta I_n & PA_0 - Q(0) & \bar{\Upsilon}_{13}(\theta) \\ A_0^\top P - Q^\top(0) & -R(0) & \bar{\Upsilon}_{23} \\ \hdashline \bar{\Upsilon}_{13}^\top(\theta) & \bar{\Upsilon}_{23}^\top & -R'(\theta) \end{array}\right] + \left[\begin{array}{c:c} \bar{C}'(\theta) - \bar{C}(1) + \bar{C}(0) & 0_{2n\times n} \\ \hdashline 0_{n\times 2n} & 0_{n\times n} \end{array}\right],$$

where $\bar{\Upsilon}_{11}$, $\bar{\Upsilon}_{13}$, *and* $\bar{\Upsilon}_{23}$ *respectively as in* (5.26), (5.27), *and* (5.28), *then the origin of* (5.5) *is GES.*

In contrast to the above presented SOS formulation represented in the original coordinates of the time-delay system, using projections the SOS formulation associated with the conditions of Proposition 5.5 are formulated as below.

Corollary 5.12. *If* $\exists\, \alpha_1, \beta > 0$, $P \in \mathbb{S}^n$, $\bar{Q} \in \mathbb{R}^{n\times np}$, *polynomial* $R : [0,1] \to \mathbb{S}^n$, $\bar{T} \in \mathbb{S}^{np}$, $S_0 \in \mathbb{R}^{np\times np}$, $S_1 \in \mathbb{R}^{n\times np}$, $\bar{S}_0 \in \mathbb{R}^{np\times np}$, $\bar{S}_1 \in \mathbb{R}^{2n\times np}$, *real polynomial matrices* $C : [0,1] \to \mathbb{S}^{n(p+1)}$ *and* $\bar{C} : [0,1] \to \mathbb{S}^{n(p+2)}$, *and a set of polynomial functions* $\{f_1, \ldots, f_p\}$ *and two real polynomial matrices* $N_1 : [0,1] \to \mathbb{S}^{n(p+2)}$, $N_2 : [0,1] \to \mathbb{S}^{n(p+3)}$ *and an integer* m *such that*

$$\begin{aligned}
&\Omega(\theta) - N_1(\theta)\theta(1-\theta) \in \Sigma^{m,n(p+2)}[\theta],\\
&N_1(\theta) \in \Sigma^{m,n(p+2)}[\theta],\\
&-\bar{\Omega}_s(\theta) - N_2(\theta)\theta(1-\theta) \in \Sigma^{m,n(p+3)}[\theta],\\
&N_2(\theta) \in \Sigma^{m,n(p+3)}[\theta],
\end{aligned}$$

where Ω *and* $\bar{\Omega}_s$ *are respectively given by* (5.19) *and* (5.22), *then the origin of* (5.5) *is GES.*

To the stability test in Corollary 5.12, obtained from the structures imposed

for Q, T and R, we associate the following LKF candidate for system (5.5)

$$
\begin{aligned}
&V(\hat{\rho}, \rho_r(1), \rho_r(\cdot)) \\
&\quad = \int_0^1 \begin{bmatrix} \hat{\rho} \\ \rho_r(1) \\ \rho_r(\theta) \end{bmatrix}^\top \begin{bmatrix} \Omega_{11} & \bar{F}^\top \bar{Q}^\top + F_1^\top P & F^\top(\theta) R(\theta) \\ \bar{Q}\bar{F} + PF_1 & P & 0_{n\times n} \\ R(\theta)F(\theta) & 0_{n\times n} & R(\theta) \end{bmatrix} \begin{bmatrix} \hat{\rho} \\ \rho_r(1) \\ \rho_r(\theta) \end{bmatrix} d\theta \\
&\quad = \begin{bmatrix} \hat{\rho} \\ \rho_r(1) \end{bmatrix}^\top \begin{bmatrix} \Omega_{p11} & F_1^\top P + \bar{F}^\top \bar{Q}^\top \\ PF_1 + \bar{Q}\bar{F} & P \end{bmatrix} \begin{bmatrix} \hat{\rho} \\ \rho_r(1) \end{bmatrix} \\
&\qquad + \int_0^1 \begin{bmatrix} \hat{\rho}^\top & \rho_r^\top(\theta) \end{bmatrix} \begin{bmatrix} F^\top(\theta) \\ I_n \end{bmatrix} R(\theta) \begin{bmatrix} F(\theta) & I_n \end{bmatrix} \begin{bmatrix} \hat{\rho} \\ \rho_r(\theta) \end{bmatrix} d\theta,
\end{aligned}
\tag{5.29}
$$

where $\Omega_{11} = \bar{F}^\top \bar{T} \bar{F} + F_1^\top P F_1 + \bar{F}^\top \bar{Q}^\top F_1 + F_1^\top \bar{Q} \bar{F} + \int_0^1 F^\top(\theta) R(\theta) F(\theta) d\theta$ and $\Omega_{p11} = \bar{F}^\top \bar{T} \bar{F} + F_1^\top P F_1 + \bar{F}^\top \bar{Q}^\top F_1 + F_1^\top \bar{Q} \bar{F}$. Note that the only difference with respect to the LKF used in formulation based on integral inequalities as given in (5.25) is that the parameter R above can be a polynomial and not only an affine function.

The literature on the use of SOS methods to the stability analysis of time-delay systems can be traced back to [90]. Since significant progress was achieved [89, 87, 88], in particular, in [87] the assumption on the separability could be dropped.

Remark 5.5. Alternatively to the separable T in (A) above, a semi-separable kernel for the parameter T is studied in [89]. It is shown that semi-separable kernels, parameterized by positive semidefinite matrices, have advantage over separable kernels for the stability analysis of linear time-delay systems. However, to conclude on the positivity of the LKF, the positivity of the single integral term and the positivity of the double integral term in the LKF are treated separately. Hence, sufficient conditions for the positivity of the proposed LKF are provided. The way to handle the positivity of the LKF with a semi-separable kernel was later improved in [87], in which the LKF is constructed using a combined multiplier and integral operator parameterized using positive semidefinite matrices. These results were also applied to the study of partial differential equations in [31].

The numerical examples section below indicates that the conditions in Proposition 5.11 and Corollary 5.12 introduce more decision variables than Corollary 5.10, and the computation effort is more significant than Corollary 5.10. The main contrasts between the two tests are on the possible use of a polynomial function R instead of the simple affine structure in Corollary 5.10 and on the way (5.20) and (5.21) are checked on the interval [0,1]. Proposition 5.11 and Corollary 5.12 introduce variables N_1 and N_2, and need to enforce that these *multipliers* are non-negative by imposing them to be SOS.

5.3 Numerical validation on academic examples

In the following, we use the inequalities given in Corollary 5.10, Proposition 5.11, and Corollary 5.12 for the stability analysis of linear systems with a single delay. The integral inequality approach of Corollary 5.10 consider different sets of functions while the SOS approaches of Proposition 5.11 and corollary 5.12 can only

use polynomial parameterizations. In contrast, the approaches based on Corollary 5.10, where a lower bound of the integral of Lemma 5.7 is used, are limited to affine parameterizations of R, while Proposition 5.11 and Corollary 5.12 allow us to treat a polynomial R of any degree p_R. Moreover, we show the advantages of the projection methods by comparing the approaches based on projections (Corollary 5.10 and Corollary 5.12) to an SOS approach without projections (Proposition 5.11).

To illustrate the discussed methods, let us start with some benchmark examples from the literature. The first example is a classical scalar system studied in [91], where the analytical solution of the Lyapunov-Krasovskii functional associated with a prescribed time derivative is given.

5.3.1 Example 1

Consider the time-delay system

$$\begin{aligned} \dot{\phi}(t,1) &= -h\phi(t,0), \qquad \forall t \geq 0, \\ \partial_t \phi(t,\theta) &= \partial_\theta \phi(t,\theta), \qquad \forall (t,\theta) \in [0,+\infty) \times [0,1]. \end{aligned} \tag{5.30}$$

It can be represented as in (5.5), where $A_0 = -h$ and $A_1 = 0$. This system is stable for $h = 0$. Using a frequency-domain analysis, it can be shown that the maximum allowable delay is $h_{max} = \pi/2$—see, *e.g.*, [78, Proposition 3.15].

First, we start to compute the analytical solution of the LKF. Let impose the time derivative of the Lyapunov-Krasovskii functional as in (4.15)-(4.18) with $W_0 = W_1 = W_2 = 1$, that is

$$\dot{V}(\phi(t,1),\phi(t,0),\phi(t,\cdot)) = -\phi^2(t,1) - \phi^2(t,0) - \int_0^1 \phi^2(t,\theta)d\theta. \tag{5.31}$$

Thus $W = W_0 + W_1 + W_2 = 3$. By solving the boundary value problem (4.8) and boundary value conditions (4.9), we obtain the delay Lyapunov matrix associated with W, as in (4.14),

$$U(\theta) = \begin{cases} -\dfrac{3\sin(h\theta)}{2h} - \dfrac{3\cos(h)\cos(h\theta)}{2h(\sin(h)-1)}, & \forall \theta \in [0,1], \\ \dfrac{3\sin(h\theta)}{2h} - \dfrac{3\cos(h)\cos(h\theta)}{2h(\sin(h)-1)}, & \forall \theta \in [-1,0). \end{cases}$$

Therefore, from (4.20) and (4.21), we obtain

$$V(\rho(1),\rho(\cdot)) = \int_0^1 \begin{bmatrix} \rho^\top(1) & \rho^\top(\theta) \end{bmatrix} \begin{bmatrix} \dfrac{3\cos(h)}{2h(1-\sin(h))} & Q(\theta) \\ Q^\top(\theta) & 1+\theta \end{bmatrix} \begin{bmatrix} \rho(1) \\ \rho(\theta) \end{bmatrix} d\theta + \int_0^1 \int_0^1 \rho^\top(\theta) T(\theta,\eta)\rho(\eta) d\eta d\theta,$$

where

$$Q(\theta) = \frac{3\sin(h\theta)}{2} + \frac{3\cos(h)\cos(h\theta)}{2(\sin(h)-1)}$$

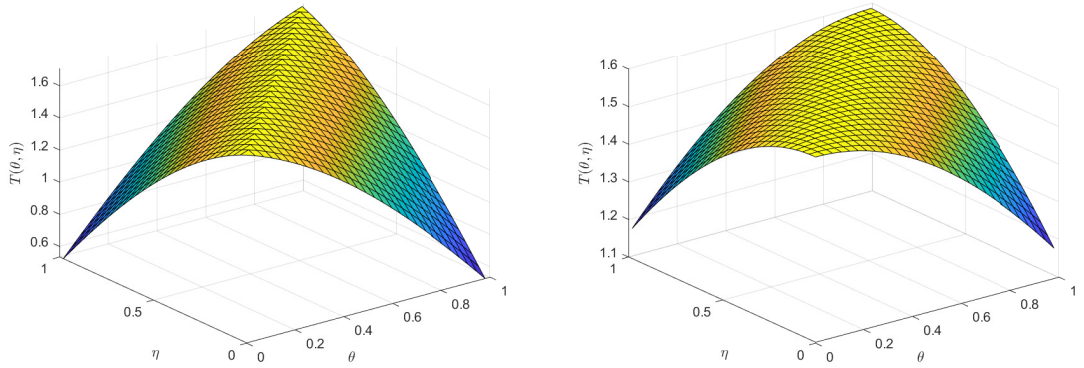

(a) (b)

Figure 5.2: (a) 3D plot for the analytical solution of T. (b) 3D plot for the solution obtained to the inequalities in Corollary 5.10 with the set $\{1, \cos(h\theta), \sin(h\theta)\}$.

and

$$T(\theta,\eta) = \begin{cases} -\dfrac{3\sin(h\theta - h\eta)}{2h} - \dfrac{3\cos(h)\cos(h\theta - h\eta)}{2h(\sin(h)-1)}, & \forall \theta - \eta \in [0,1], \\ \dfrac{3\sin(h\theta - h\eta)}{2h} - \dfrac{3\cos(h)\cos(h\theta - h\eta)}{2h(\sin(h)-1)}, & \forall \theta - \eta \in [-1,0). \end{cases} \tag{5.32}$$

As shown in Section 4.2.3, the parameter T is not separable, and it is difficult to show that the lower bound for V as in (4.3) holds. Then, to apply the results from Section 5.2, we consider a separable function T with respect to the set of functions in (4.13) as Section 5.2 as

$$T(\theta,\eta) = \tilde{F}(\theta)\bar{T}\tilde{F}^{\top}(\eta) = \begin{bmatrix} 1 & \cos(h\theta) & \sin(h\theta) \end{bmatrix} \bar{T} \begin{bmatrix} 1 \\ \cos(h\eta) \\ \sin(h\eta) \end{bmatrix}. \tag{5.33}$$

Using this separable form, Corollary 5.10 can be applied for the set of linearly independent functions $\{1, \cos(h\theta), \sin(h\theta)\}$. The obtained numerical results show that the system is stable for all $h \in [0, 1.5707963]$. Therefore, with only three functions $\{1, \cos(h\theta), \sin(h\theta)\}$, we obtain the delay margin of $\pi/2$ with 7-digit accuracy. Figure 5.2 compares the analytical expression of T given by (5.32) to the numerical approximation of T provided by (5.33), for $h = 1$. It is possible to notice in the figure on the left that the analytical expression of T is not differentiable in the set $\{(\theta,\eta) \mid \eta = \theta, \theta \in [0,1]\}$. The numerical results of Corollary 5.10, Proposition 5.11, and Corollary 5.12 are presented for two sets of polynomial functions in Table 5.1 (Canonical polynomials) and Table 5.2 (shifted Legendre polynomials). The exact value of the delay margin can be achieved for a large enough number p of linearly independent functions.

5.3.2 Example 2

Consider the linear time-delay system (5.5) with

$$A_1 = \begin{bmatrix} -2h & 0 \\ 0 & -0.9h \end{bmatrix} \quad \text{and} \quad A_0 = \begin{bmatrix} -h & 0 \\ -h & -h \end{bmatrix}, \tag{5.34}$$

taken from [99]. The origin is GES for $h = 0$. Using a frequency-domain analysis, the maximum allowable delay is $h_{max} = 6.1725$—see, *e.g.*, [78, Proposition 3.9]. The delay interval certified GES using the time-domain stability analysis results (Corollary 5.10, Proposition 5.11, and Corollary 5.12) are reported in Table 5.3, Table 5.4, Table 5.5, and Table 5.6.

In all the considered approaches, for large enough p, the stability analysis results are close to the exact value of the delay margin. Moreover, the use of higher degree polynomials to parameterize R may have an advantage when solving the SOS constraints, which is not possible with Corollary 5.10; see the columns of Table 5.3 and Table 5.4 for $p = 2$, 3, or 4.

Table 5.5 reports results obtained with Corollary 5.10 using different polynomial bases. Table 5.6 reports the results using sets of functions with 9 elements in Corollary 5.10, which can be polynomial, exponential, or trigonometric functions; or a combination of them. Only Legendre and Chebyshev polynomials achieved the stability limit with the accuracy of 4-digit. The results using exponential and trigonometric functions are reported in the last two rows of the table. For trigonometric functions, we used $k_0 = \sqrt{19}h/10$, the modulus of a pure imaginary eigenvalue of the matrix L in (4.10) for this example data. The last set of functions in Table 5.6 corresponds to the set (4.13) obtained with (5.34).

5.3.3 Example 3

Consider the linear time-delay system (5.5) with

$$A_1 = \begin{bmatrix} 0 & 0 & h & 0 \\ 0 & 0 & 0 & h \\ -4h & 0 & 0 & 0 \\ 0 & -16h & 0 & 0 \end{bmatrix} \quad \text{and} \quad A_0 = \begin{bmatrix} 0 & 0 & 0 & 0 \\ 0 & 0 & 0 & 0 \\ 0 & 0 & 0 & -h \\ 0 & 0 & h & 0 \end{bmatrix}, \tag{5.35}$$

taken from [100]. Based on a frequency-domain analysis, this system has three stable delay intervals $[0.4108, 0.7509]$, $[2.054, 2.252]$, and $[3.697, 3.754]$—see, *e.g.*, [27]. The time-domain stability analysis results obtained with Corollary 5.10 are reported in Figure 5.3. The SOS results from Corollary 5.12 provide approximately the same results as those provided by the constant LMI conditions from Corollary 5.10 with shifted Legendre polynomials. For the clarity of the figure illustrating the results, we have omitted the results obtained by the SOS constraints.

Table 5.1: Results for Example 1, using Canonical polynomials. The gray shaded cells highlight the combination of p_R and p showing the delay margin with 5-digit accuracy.

Method	p_R \ p	1	2	3	4	7	CPU time (secs)
Corollary 5.10	2	$[0, 1.29903]$	$[0, 1.40161]$	$[0, 1.43217]$	$[0, 1.47800]$	$[0, 1.56557]$	≈ 0.09 to 0.11
Proposition 5.11	2	$[0, 1.41340]$	$[0, 1.46562]$	$[0, 1.51544]$	$[0, 1.51607]$	$[0, 1.51611]$	≈ 0.20 to 0.23
	3	$[0, 1.41367]$	$[0, 1.48776]$	$[0, 1.51713]$	$[0, 1.51722]$	$[0, 1.51724]$	≈ 0.20 to 0.33
	4	$[0, 1.41371]$	$[0, 1.48895]$	$[0, 1.52522]$	$[0, 1.53323]$	$[0, 1.53597]$	≈ 0.20 to 0.33
	5	$[0, 1.41373]$	$[0, 1.48900]$	$[0, 1.52567]$	$[0, 1.53342]$	$[0, 1.54345]$	≈ 0.20 to 0.36
	6	$[0, 1.41373]$	$[0, 1.48900]$	$[0, 1.52574]$	$[0, 1.53344]$	$[0, 1.54907]$	≈ 0.20 to 0.52
Corollary 5.12	2	$[0, 1.41421]$	$[0, 1.56745]$	$[0, 1.57075]$	$[0, 1.57079]$	$[0, 1.57079]$	≈ 0.22 to 1.41
	3	$[0, 1.41421]$	$[0, 1.56745]$	$[0, 1.57075]$	$[0, 1.57079]$	$[0, 1.57079]$	≈ 0.22 to 1.41
	4	$[0, 1.41421]$	$[0, 1.57050]$	$[0, 1.57079]$	$[0, 1.57079]$	$[0, 1.57079]$	≈ 0.22 to 1.41
	5	$[0, 1.41421]$	$[0, 1.57054]$	$[0, 1.57079]$	$[0, 1.57079]$	$[0, 1.57079]$	≈ 0.23 to 1.42
	6	$[0, 1.41421]$	$[0, 1.57054]$	$[0, 1.57079]$	$[0, 1.57079]$	$[0, 1.57079]$	≈ 0.23 to 1.45

Table 5.2: Results for Example 1, using shifted Legendre polynomials. The gray shaded cells highlight the combination of p_R and p showing the delay margin with 5-digit accuracy.

Method	p_R \ p	1	2	3	4	7	CPU time (secs)
Corollary 5.10	2	$[0, 1.29903]$	$[0, 1.52268]$	$[0, 1.56844]$	$[0, 1.57074]$	$[0, 1.57079]$	≈ 0.09 to 0.11
Proposition 5.11	2	$[0, 1.41340]$	$[0, 1.46564]$	$[0, 1.51544]$	$[0, 1.51606]$	$[0, 1.51606]$	≈ 0.19 to 0.27
	3	$[0, 1.41367]$	$[0, 1.48775]$	$[0, 1.51714]$	$[0, 1.51720]$	$[0, 1.51720]$	≈ 0.19 to 0.27
	4	$[0, 1.41371]$	$[0, 1.48885]$	$[0, 1.52521]$	$[0, 1.53293]$	$[0, 1.53306]$	≈ 0.20 to 0.28
	5	$[0, 1.41373]$	$[0, 1.48893]$	$[0, 1.52574]$	$[0, 1.53325]$	$[0, 1.53904]$	≈ 0.20 to 0.28
	6	$[0, 1.41373]$	$[0, 1.48895]$	$[0, 1.52574]$	$[0, 1.53327]$	$[0, 1.54448]$	≈ 0.25 to 0.31
Corollary 5.12	2	$[0, 1.41421]$	$[0, 1.56745]$	$[0, 1.57075]$	$[0, 1.57079]$	$[0, 1.57079]$	≈ 0.20 to 2.02
	3	$[0, 1.41421]$	$[0, 1.56745]$	$[0, 1.57075]$	$[0, 1.57079]$	$[0, 1.57079]$	≈ 0.22 to 2.28
	4	$[0, 1.41421]$	$[0, 1.57050]$	$[0, 1.57079]$	$[0, 1.57079]$	$[0, 1.57079]$	≈ 0.22 to 2.33
	5	$[0, 1.41421]$	$[0, 1.57054]$	$[0, 1.57079]$	$[0, 1.57079]$	$[0, 1.57079]$	≈ 0.22 to 2.56
	6	$[0, 1.41421]$	$[0, 1.57054]$	$[0, 1.57079]$	$[0, 1.57079]$	$[0, 1.57079]$	≈ 0.22 to 2.61

Table 5.3: Results for Example 2, using Canonical polynomials. The gray shaded cells highlight the combination of p_R and p showing the delay margin with 5-digit accuracy.

Method	p_R \ p	1	2	3	4	7	CPU time (secs)
Corollary 5.10	2	$[0, 4.37741]$	$[0, 4.94654]$	$[0, 5.01296]$	$[0, 5.06399]$	$[0, 5.50656]$	≈ 0.11 to 0.13
Proposition 5.11	2	$[0, 4.46968]$	$[0, 4.65948]$	$[0, 5.40141]$	$[0, 5.41362]$	$[0, 5.41675]$	≈ 0.14 to 0.48
	3	$[0, 4.46968]$	$[0, 5.07221]$	$[0, 5.49235]$	$[0, 5.74018]$	$[0, 5.74806]$	≈ 0.14 to 0.48
	4	$[0, 4.46968]$	$[0, 5.08872]$	$[0, 5.80958]$	$[0, 5.90543]$	$[0, 6.04378]$	≈ 0.16 to 0.48
	5	$[0, 4.46968]$	$[0, 5.10230]$	$[0, 5.81837]$	$[0, 6.00625]$	$[0, 6.11751]$	≈ 0.16 to 0.64
	6	$[0, 4.46976]$	$[0, 5.10248]$	$[0, 5.81837]$	$[0, 6.00666]$	$[0, 6.14963]$	≈ 0.23 to 0.67
Corollary 5.12	2	$[0, 4.46800]$	$[0, 6.05921]$	$[0, 6.16894]$	$[0, 6.17250]$	$[0, 6.17258]$	≈ 0.55 to 33.88
	3	$[0, 4.46801]$	$[0, 6.05925]$	$[0, 6.16894]$	$[0, 6.17250]$	$[0, 6.17258]$	≈ 0.58 to 36.09
	4	$[0, 4.46801]$	$[0, 6.14077]$	$[0, 6.17225]$	$[0, 6.17257]$	$[0, 6.17258]$	≈ 0.61 to 36.31
	5	$[0, 4.46801]$	$[0, 6.14474]$	$[0, 6.17240]$	$[0, 6.17258]$	$[0, 6.17258]$	≈ 0.61 to 36.50
	6	$[0, 4.46801]$	$[0, 6.14560]$	$[0, 6.17253]$	$[0, 6.17258]$	$[0, 6.17258]$	≈ 0.61 to 36.58

Table 5.4: Results for Example 2, using shifted Legendre polynomials. The gray shaded cells highlight the combination of p_R and p showing the delay margin with 5-digit accuracy.

Method	p_R \ p	1	2	3	4	7	CPU time (secs)
Corollary 5.10	2	$[0, 4.37741]$	$[0, 5.67681]$	$[0, 6.04842]$	$[0, 6.16320]$	$[0, 6.17258]$	≈ 0.09 to 0.11
Proposition 5.11	2	$[0, 4.46968]$	$[0, 4.65949]$	$[0, 5.40169]$	$[0, 5.41346]$	$[0, 5.41783]$	≈ 0.20 to 0.41
	3	$[0, 4.46968]$	$[0, 5.07221]$	$[0, 5.49230]$	$[0, 5.73882]$	$[0, 5.75000]$	≈ 0.22 to 0.41
	4	$[0, 4.46968]$	$[0, 5.08839]$	$[0, 5.80922]$	$[0, 5.90389]$	$[0, 6.02524]$	≈ 0.22 to 0.41
	5	$[0, 4.46968]$	$[0, 5.10199]$	$[0, 5.81604]$	$[0, 6.00388]$	$[0, 6.06249]$	≈ 0.22 to 0.44
	6	$[0, 4.46976]$	$[0, 5.10287]$	$[0, 5.81604]$	$[0, 6.00413]$	$[0, 6.09404]$	≈ 0.23 to 0.55
Corollary 5.12	2	$[0, 4.46800]$	$[0, 6.05921]$	$[0, 6.16894]$	$[0, 6.17250]$	$[0, 6.17258]$	≈ 0.55 to 44.52
	3	$[0, 4.46801]$	$[0, 6.05925]$	$[0, 6.16894]$	$[0, 6.17250]$	$[0, 6.17258]$	≈ 0.56 to 45.11
	4	$[0, 4.46801]$	$[0, 6.14077]$	$[0, 6.17225]$	$[0, 6.17257]$	$[0, 6.17258]$	≈ 0.59 to 49.36
	5	$[0, 4.46801]$	$[0, 6.14474]$	$[0, 6.17240]$	$[0, 6.17258]$	$[0, 6.17258]$	≈ 0.61 to 52.02
	6	$[0, 4.46801]$	$[0, 6.14560]$	$[0, 6.17253]$	$[0, 6.17258]$	$[0, 6.17258]$	≈ 0.61 to 82.09

Table 5.5: Results for Example 2, using Corollary 5.10. The gray shaded cells highlight the combination of p and the set of linearly independent functions showing the delay margin with 4-digit accuracy.

p	1	2	3	4	5	6	7	CPU time (secs)
Canonical	$[0, 4.3773]$	$[0, 4.9465]$	$[0, 5.0129]$	$[0, 5.0640]$	$[0, 5.1631]$	$[0, 5.3135]$	$[0, 5.5068]$	≈ 0.11 to 0.13
shifted Legendre	$[0, 4.3773]$	$[0, 5.6772]$	$[0, 6.0484]$	$[0, 6.1631]$	$[0, 6.1722]$	$[0, 6.1725]$	$[0, 6.1725]$	≈ 0.09 to 0.11
Bernstein	$[0, 4.3773]$	$[0, 5.5273]$	$[0, 5.7997]$	$[0, 5.9270]$	$[0, 6.0586]$	$[0, 6.1370]$	$[0, 6.1638]$	≈ 0.09 to 0.14
Chebyshev	$[0, 4.3773]$	$[0, 5.6771]$	$[0, 6.0125]$	$[0, 6.1463]$	$[0, 6.1669]$	$[0, 6.1714]$	$[0, 6.1724]$	≈ 0.09 to 0.11
Hermite	$[0, 4.3773]$	$[0, 5.6771]$	$[0, 6.0125]$	$[0, 6.0855]$	$[0, 6.138]$	$[0, 6.1599]$	$[0, 6.1659]$	≈ 0.09 to 0.11

Table 5.6: Results for Example 2, using Corollary 5.10 for seven different sets of linearly independent functions. The sets of polynomial functions contain polynomials up to degree 8. The gray shaded cells highlight the two sets of functions achieving the delay margin with 4-digit accuracy.

Set of linearly independent functions	p	h_{max}	CPU time (secs)
Canonical polynomials	9	5.9101	≈ 0.13
shifted Legendre polynomials	9	6.1725	≈ 0.09
Bernstein polynomials	9	6.1722	≈ 0.13
Chebyshev polynomials	9	6.1725	≈ 0.09
Hermite polynomials	9	6.1714	≈ 0.16
$\{1, \cos(k_0\theta), \sin(k_0\theta), \cos(2k_0\theta), \sin(2k_0\theta), \cos(3k_0\theta), \sin(3k_0\theta), \cos(4k_0\theta), \sin(4k_0\theta)\}$	9	6.0502	≈ 0.13
$\{1, e^{\sqrt{3}h\theta}, e^{-\sqrt{3}h\theta}, e^{h\theta/2}, e^{-h\theta/2}, e^{8h\theta/5}, e^{-8h\theta/5}, \cos(\sqrt{19}h\theta/10), \sin(\sqrt{19}h\theta/10)\}$	9	6.0411	≈ 0.09

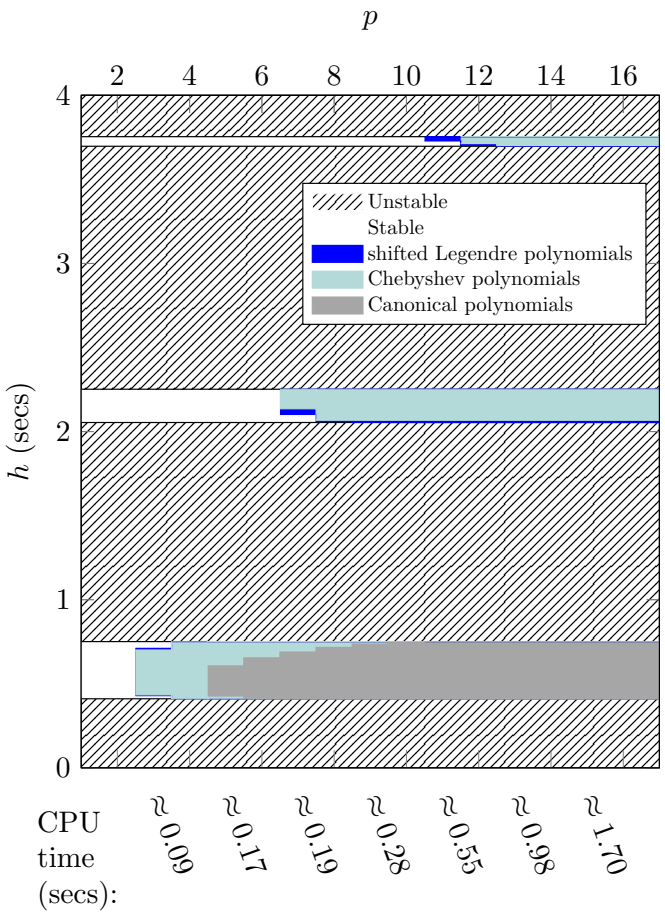

Figure 5.3: Results for Example 3, using Corollary 5.10.

5.3.4 Notes on the numerical implementation

The numerical tests presented in this section were obtained using MOSEK [75] and YALMIP [61]. We reported the computational time for the solution of the associated SDPs to Corollary 5.10, Proposition 5.11, and Corollary 5.12 without including the parsing time. The main difference in computation time is related to the number of variables in the SDPs. We compare the number of variables in Corollary 5.10 and Corollary 5.12, the two results using projections.

The inequalities in Corollary 5.10 contain

$$\frac{5(n^2+n)}{2} + n^2 p + \frac{n^2 p^2}{2} + \frac{np}{2}$$

scalar unknowns.

In Corollary 5.12, denote by m_C and $\bar{m}_C$, respectively, the degrees of the polynomials appearing in $C(\theta)$ and $\bar{C}(\theta)$. Denote, moreover, by m_1 and m_2, respectively, the degrees of the polynomials in the multipliers $N_1(\theta)$ and $N_2(\theta)$, and by p_R the degree of the polynomials in $R(\theta)$. Then, the SOS constraints in Corollary 5.12

contain

$$\frac{n^2}{2}+\frac{n}{2}+4n^2p+(p_R+1)n^2+(p_R+1)n+\frac{5n^2p^2}{2}+\frac{np}{2}$$
$$+\frac{m_C(n^2(p+1)^2+np+n)}{2}+\frac{\bar{m}_C(n^2(p+2)^2+np+2n)}{2}$$
$$+\frac{m_1(n^2(p+2)^2+np+2n)}{2}+\frac{m_2(n^2(p+3)^2+np+3n)}{2}$$

scalar unknowns.

To solve the SOS programs related to Proposition 5.11 and Corollary 5.12, we used

$$m_C=\bar{m}_C=2p+p_R,\qquad \text{and}\qquad m_1=m_2=8.$$

5.4 Applications to steering systems

In this section, we illustrate how the results obtained in this chapter can be used for applications to the Electric Power Steering (EPS) and Steer-by-Wire (SBW) systems. First, we use the stability conditions formulated in Corollary 5.10 to retrieve the delay margin of the steering systems and we compare the results to those obtained in chapters 2 and 3 where a frequency domain approach was adopted. We also show that the Lyapunov-Krasovskii functionals can be used to estimate the *decay rate* of the steering systems defined as below.

Definition 5.1 ([73])**.** Consider the solutions s of the equation $\det(sI_n-A_1-e^{-s}A_0)=0$, where A_1, A_0 are the matrices that appear in the dynamics equation of the time-delay system (5.5). For $\beta>0$, system (5.5) is said to be β-stable if $Re(s)+\beta<0$. Or, equivalently, the system

$$\begin{aligned}\dot{\xi}(t,1)&=(A_1+\beta I_n)\xi(t,1)+e^{\beta h}A_0\xi(t,0),\qquad \forall t\geq 0,\\ \partial_t\xi(t,\theta)&=\partial_\theta\xi(t,\theta),\qquad \forall(t,\theta)\in[0,+\infty)\times[0,1],\end{aligned}\tag{5.36}$$

is GES. In other words, system (5.5) is GES with the decay rate β.

We can then use the above definition to estimate the decay rate of a delay system as (5.5). To evaluate the decay rate we carry out a line search on the parameter β by evaluating whether system (5.36) is GES, namely, whether the global exponential stability conditions of Theorem 4.1 hold for (5.36).

5.4.1 Applications to the EPS

Consider the electric power steering system studied in Chapter 2 with filter C_2. As explained in Section 4.1, the dynamics of the pinon subsystem depicted in Figure 2.3 can be written in the state-space representation as in (5.5), where $x(t)=\begin{bmatrix}\theta_p(t) & \dot{\theta}_p(t)\end{bmatrix}^\top$,

$$A_1=\begin{bmatrix}0 & h\\ -\dfrac{k_sh}{J_p} & -\dfrac{\sigma_ph}{J_p}\end{bmatrix},\quad \text{and}\quad A_0=\begin{bmatrix}0 & 0\\ -\dfrac{Kk_sh}{J_p} & -\dfrac{Kk_sh}{J_p\omega_a}\end{bmatrix}.$$

As in the numerical examples of Chapter 2, we consider $J_p = 0.11\,\mathrm{Kg.m^2}$, $k_s = 143.24\,\mathrm{Nm/rad}$, $\sigma_p = 16.79\,\mathrm{Nm.s/rad}$, and we set $K = 35$ and $\omega_a = 39.15\,\mathrm{Hz}$.

The origin is GES for $h = 0$. From Proposition 2.3, the maximum allowable delay is $h_{max} = 5.8673\,\mathrm{ms}$. Table 5.7 reports the stability analysis results obtained with Corollary 5.10 using different polynomial bases. The Legendre and Chebyshev polynomials achieved the stability limit with the accuracy of 4-digit.

The eigenvalues of matrix L in (4.10) associated with the above dynamics of the electric power steering system are given by

$$\lambda_1 = \frac{\sigma_p h}{J_p},$$

$$\lambda_2 = \frac{h\sqrt{-K^2 k_s^2 + \sigma_p^2 \omega_a^2}}{J_p \omega_a},$$

and $\lambda_3 = \lambda_4 = 0$. Therefore, the last two rows of Table 5.8 reported the stability results using exponential and trigonometric functions.

In the numerical results of Table 5.9, we use the Lyapunov-Krasovskii functional inequalities provided in this chapter to obtain a lower bound to the decay rate of the electric power steering system following Definition 5.1. Namely, the stability conditions of Corollary 5.10 are used to provide a lower bound on the value of the parameter β in Definition 5.1, with matrices A_0 and A_1 as above.

Table 5.7: Results for Example EPS, using Corollary 5.10. The gray shaded cells highlight the combination of p and the set of linearly independent functions showing the delay margin with 4-digit accuracy.

p	1	2	3	4	5	6	7	CPU time (secs)
Canonical	$[0, 5.4322]$	$[0, 5.6119]$	$[0, 5.6545]$	$[0, 5.7123]$	$[0, 5.7974]$	$[0, 5.8461]$	$[0, 5.8617]$	≈ 0.14 to 0.33
shifted Legendre	$[0, 5.4322]$	$[0, 5.8605]$	$[0, 5.8672]$	$[0, 5.8673]$	$[0, 5.8673]$	$[0, 5.8673]$	$[0, 5.8673]$	≈ 0.13 to 0.19
Bernstein	$[0, 5.4322]$	$[0, 5.7291]$	$[0, 5.7402]$	$[0, 5.8294]$	$[0, 5.8613]$	$[0, 5.8665]$	$[0, 5.8672]$	≈ 0.16 to 0.36
Chebyshev	$[0, 5.4322]$	$[0, 5.8605]$	$[0, 5.8661]$	$[0, 5.8666]$	$[0, 5.8672]$	$[0, 5.8673]$	$[0, 5.8673]$	≈ 0.14 to 0.25
Hermite	$[0, 5.4322]$	$[0, 5.8605]$	$[0, 5.8661]$	$[0, 5.8662]$	$[0, 5.8670]$	$[0, 5.8672]$	$[0, 5.8672]$	≈ 0.14 to 0.20

Table 5.8: Results for Example EPS, using Corollary 5.10. The gray shaded cells highlight the combination of p and the set of linearly independent functions showing the delay margin with 4-digit accuracy.

Set of linearly independent functions	p	h_{max} (ms)	CPU time (secs)
Canonical polynomials	5	5.7974	≈ 0.23
shifted Legendre polynomials	5	5.8673	≈ 0.13
Bernstein polynomials	5	5.8613	≈ 0.16
Chebyshev polynomials	5	5.8672	≈ 0.14
Hermite polynomials	5	5.8670	≈ 0.14
$\{1, \cos(\lambda_2\theta), \sin(\lambda_2\theta), \cos(2\lambda_2\theta), \sin(2\lambda_2\theta)\}$	5	5.4322	≈ 0.16
$\{1, e^{\lambda_1(\theta-1)}, e^{-\lambda_1\theta}, \cos(\lambda_2\theta), \sin(\lambda_2\theta)\}$	5	5.4379	≈ 0.16

Table 5.9: Results for Example EPS and for $h = 4\,\mathrm{ms}$, using 5.10. The gray shaded cells highlight the combination of p and the set of linearly independent functions showing the highest obtained value of the decay rate with 5-digit accuracy.

Set of linearly independent functions	p	decay rate	CPU time (secs)
Canonical polynomials	5	59.98851	≈ 0.23
shifted Legendre polynomials	5	60.77182	≈ 0.22
Bernstein polynomials	5	60.69816	≈ 0.25
Chebyshev polynomials	5	60.77114	≈ 0.28
Hermite polynomials	5	60.76898	≈ 0.23
$\{1, \cos(\lambda_2\theta), \sin(\lambda_2\theta), \cos(2\lambda_2\theta), \sin(2\lambda_2\theta)\}$	5	51.59984	≈ 0.23
$\{1, e^{\lambda_1(\theta-1)}, e^{-\lambda_1\theta}, \cos(\lambda_2\theta), \sin(\lambda_2\theta)\}$	5	51.77843	≈ 0.20

5.4.2 Applications to the SBW

Consider the SBW system (3.1)-(3.2) with $\tau_w = \tau_p = 0$ and $\tau_1 = \tau_2 = h$, for some $h > 0$, that is

$$J_w\ddot{\theta}_w(t) + \sigma_w\dot{\theta}_w(t) = T_w(t) + T_d(t),$$
$$J_p\ddot{\theta}_p(t) + \sigma_p\dot{\theta}_p(t) = T_p(t) + T_r(t),$$

with the control law

$$T_w(t) = k_w(\theta_p(t-h) - \theta_w(t)) + \rho_w(\dot{\theta}_p(t-h) - \dot{\theta}_w(t)),$$
$$T_p(t) = k_p(\theta_w(t-h) - \theta_p(t)) + \rho_p(\dot{\theta}_w(t-h) - \dot{\theta}_p(t)).$$

As in the numerical example in Chapter 3, we consider $J_p = 0.11\,\mathrm{Kg.m^2}$ and we set $k_p = 5013.4\,\mathrm{Nm/rad}$, and $\sigma_p = 1.35\,\mathrm{Nm.s/rad}$.

We assume that the road torque T_r is given by

$$T_r(t) = -k_r\theta_p(t) - \rho_r\dot{\theta}_p(t),$$

where $k_r = 300\,\mathrm{Nm/rad}$ and $\rho_r = 25\,\mathrm{Nm.s/rad}$.

Then, for $T_d(t) = 0$, the above system can be written as in (5.5), where

$$A_1 = \begin{bmatrix} 0 & h & 0 & 0 \\ -\dfrac{k_w h}{J_w} & -\dfrac{(\sigma_w+\rho_w)h}{J_w} & 0 & 0 \\ 0 & 0 & 0 & h \\ 0 & 0 & -\dfrac{(k_p+k_r)h}{J_p} & -\dfrac{(\sigma_p+\rho_p+\rho_r)h}{J_p} \end{bmatrix}$$

and

$$A_0 = \begin{bmatrix} 0 & 0 & 0 & 0 \\ 0 & 0 & \dfrac{k_w h}{J_w} & \dfrac{\rho_w h}{J_w} \\ 0 & 0 & 0 & 0 \\ \dfrac{k_p h}{J_p} & \dfrac{\rho_p h}{J_p} & 0 & 0 \end{bmatrix}.$$

The origin is GES for $h = 0$. Using the results of Section 3.2, the maximum allowable delay is $h_{max} = 20.0996\,\mathrm{ms}$. Table 5.10 reports results obtained with Corollary 5.10 using different polynomial bases. The Legendre and Chebyshev polynomials achieved the stability limit with the accuracy of 4-digit. Table 5.11 reports the decay rate estimates obtained with different polynomial sets, where all considered sets reached the same estimate for only two functions. Increasing the number of functions did not improve the estimate.

Table 5.10: Results for SBW, using Corollary 5.10. The gray shaded cells highlight the combination of p and the set of linearly independent functions showing the delay margin with 4-digit accuracy.

p	1	2	3	4	5	6	7	CPU time (secs)
Canonical	$[0, 3.3501]$	$[0, 18.8960]$	$[0, 19.0793]$	$[0, 19.2847]$	$[0, 19.6538]$	$[0, 19.9421]$	$[0, 20.0578]$	≈ 0.20 to 0.91
shifted Legendre	$[0, 3.3501]$	$[0, 20.0549]$	$[0, 20.0990]$	$[0, 20.0996]$	$[0, 20.0966]$	$[0, 20.0966]$	$[0, 20.0966]$	≈ 0.20 to 0.33
Bernstein	$[0, 3.3501]$	$[0, 19.5589]$	$[0, 19.5885]$	$[0, 19.9005]$	$[0, 20.0615]$	$[0, 20.0939]$	$[0, 20.0988]$	≈ 0.20 to 0.64
Chebyshev	$[0, 3.3501]$	$[0, 20.0549]$	$[0, 20.0918]$	$[0, 20.0947]$	$[0, 20.0988]$	$[0, 20.0995]$	$[0, 20.0996]$	≈ 0.20 to 0.44
Hermite	$[0, 3.3501]$	$[0, 20.0549]$	$[0, 20.0918]$	$[0, 20.0923]$	$[0, 20.0970]$	$[0, 20.0985]$	$[0, 20.0993]$	≈ 0.20 to 0.89

Table 5.11: Results for SBW and for $h = 4\,\mathrm{ms}$, using Corollary 5.10. The gray shaded cells highlight the combination of p and the set of linearly independent functions showing the highest obtained value of the decay rate with 5-digit accuracy.

Set of linearly independent functions	p	decay rate	CPU time (secs)
Canonical polynomials	2	4.29512	≈ 0.23
shifted Legendre polynomials	2	4.29512	≈ 0.20
Bernstein polynomials	2	4.29512	≈ 0.38
Chebyshev polynomials	2	4.29512	≈ 0.19
Hermite polynomials	2	4.29512	≈ 0.17

5.5 Conclusions

We studied the problem of stability analysis of time-delay systems with a single delay. By recalling the results on the analytical construction of LKF by assigning derivatives, in Chapter 4, we point out the difficulties in assessing the positivity of the functional obtained from the delay Lyapunov matrix. Moreover, we highlight the advantages and drawbacks of the two main trends in SDP approaches that emerged in the last decade for the analysis of time-delay systems, namely the SOS approaches and the approaches based on projections. Importantly, here we show that SOS methods can also be formulated using projections. For this reason, we use instead of projections the term integral inequalities to describe these approaches.

A limiting assumption in both approaches is the hypothesis on the separability of the double integral term in the LKF. Such an assumption is not always considered in SOS methods [87]. It allows, however, to show the connections between SOS and integral inequalities methods. Moreover, the general formulation presented here allows to consider projections on functions other than polynomials. We also show that the technique to test the positivity of integral forms with projections encompasses the set of Bessel-Legendre integral inequalities and is applicable to general functions [100]. The results can readily be extended (as sufficient stability conditions) to systems with distributed delays and systems with multiple delays, which were not introduced here to simplify the exposition of the results. Finally, the need for more general projection functions than polynomials can also appear in other contexts such as the stability analysis of nonlinear partial differential equations [33, 105].

Conclusions and perspectives

Motivated by control problems in steering systems, we have developed methods for control design and stability analysis of systems with delays. We have shown that taking into account the presence of delays in a steering system is essential since they can degrade vibration attenuation and reduce stability margins. In particular, the delays limit the admissible values of the assist gain and thus reduce the level of driver comfort. We introduced a generic model for steering systems with delays encompassing several examples of steering systems and, in particular, electric power steering and steer-by-wire systems. We described a list of performance requirements and associated them with metrics that allow us to assess and compare the proposed controllers.

Our study started with the electric power steering system, which has a single delay in its main feedback loop, consisting of a second-order transfer function in feedback with different filter structures. An analytical expression for a tight lower bound on the delay margin was proposed as a function of the filter and system parameters. Thanks to the fixed structure of the filter, we were able to select the system and control parameters that affect the stability and performance degradation of the steering system.

We then addressed a more complex case, the steer-by-wire system, which has multiple delays. We considered proportional-derivative control architectures and, to remove the internal delays, we proposed a modified Smith predictor adapted to steering systems. This modification to the proportional-derivative control architecture overcame the lack of robustness with respect to the internal and transmission delays, especially for high gains of the steering system. Thanks to this modification, the closed-loop stability is only a function of the round-trip delays and does not depend separately on each feedback loop delay. In addition, to assess the stability of the steer-by-wire systems, we provided a method to approximate the delay margin based on the Padé approximation of the open-loop transfer function.

To overcome the restrictions associated with the frequency-domain approach, which prevents the study of nonlinear torque maps, we have also explored a time-domain approach. We first revised the problem of constructing Lyapunov-Krasovskii functionals for linear time-delay systems using the delay Lyapunov matrix. We discussed the properties of these functionals and highlighted the main assumptions needed to compute the Lyapunov-Krasovskii functionals using semidefinite programming and how they differ from the Lyapunov-Krasovskii functionals constructed using the delay Lyapunov matrix. In particular, we showed that the kernel of a double integral term in the Lyapunov-Krasovskii functional could not be written as a separable function.

Table 5.12: Summary of the contributions of the thesis. Contributions (C) in red, Bibliographical studies (B) in green, and Didactic illustrations (I) in blue.

I	**Steering systems**	
1	Preliminaries on steering systems	
	1.1 A model for steering systems	I & B
	1.2 Control objectives and performance criteria	I & B
	1.3 Literature review on steering systems	B
2	Increasing the delay margin of electric power steering systems	
	2.1 EPS model and problem statement	I
	2.2 Robustness with respect to delays	C
	2.3 Simulations	C & I
3	Increasing the delay margin of steer-by-wire systems	
	3.1 A modified Smith predictor	C
	3.2 Stability analysis	C
	3.3 Simulations	C & I
II	**Lyapunov-Krasovskii functional computation approaches**	
4	Preliminaries on time-domain stability analysis	
	4.1 Stability of time-delay systems	I
	4.2 Construction of Lyapunov-Krasovskii functionals using the delay Lyapunov matrix	B & C
	4.3 Literature review on LKF	B
5	Verification methods for the Lyapunov-Krasovskii functional inequalities	
	5.1 Delay systems with projections	C
	5.2 SDP-based stability conditions using a separable parameter T	C
	5.3 Numerical validation on academic examples	C & I
	5.4 Applications to steering systems	C & I

Then, we presented the two numerical approaches that are used to check bounds on the Lyapunov-Krasovskii functionals, namely the method based on the use of integral inequalities and the method based on sum-of-squares decompositions, highlighting the advantages of each method. Moreover, we showed how the method based on integral inequalities allows to recover known integral inequalities used in the literature. We have also shown that the projection-based method leads either to a sum-of-squares representation or to a formulation with constant linear matrix inequalities (for the approach based on integral inequalities).

Importantly, the general formulation presented in Chapter 5 allows considering projections on functions other than polynomials. Moreover, the proposed approach can be useful in providing solutions to several problems associated with Lyapunov-Krasovskii functionals. The obtained results are applied to the steering systems in Section 5.4, where the Lyapunov-Krasovskii functional is used to compute the delay margin and determine the decay rate of the steering system.

Finally, these results can be extended to systems with distributed delays and systems with multiple delays. In addition, the choice of more general projection functions than polynomials will have advantages in studying nonlinear partial differential equation systems [33, 105].

Summary of the contributions

In what follows, we highlight the main results and contributions of each chapter. Importantly, we believe that the results of Chapters 2, 3, and 5 are new. Chapter 2 is now accepted, up to a minor revision, in *International Journal of Control*; Chapter 3 has been published in the *Proceedings of the International Symposium on Advanced Vehicle Control*; and Chapter 5 has been submitted to *SIAM Journal on Control and Optimization*.

These contributions propose two distinct approaches for stability analysis and control design of linear time-delay systems, the approach using Laplace transform and the approach using Lyapunov-Krasovskii functional. For this reason, the manuscript is composed of two parts, in which these two approaches are developed.

In addition, to emphasize the contributions of our work, preliminary results are presented and discussed in the first chapter of each part. Chapter 1 gave a generic model for steering systems, where we highlighted the presence of delays in the system. Thanks to this generic model, we could define the required performance criteria of a steering system and introduce some metrics to evaluate the performance of a controller in this system. Chapter 4 gave an overview of a method to construct Lyapunov-Krasovskii functionals from a solution to the delay Lyapunov matrix. We describe there the set of functions that constitute this matrix. In addition, we prove that the parameter in the double integral term of this Lyapunov-Krasovskii functional is not separable. The main points addressed in Chapters 1 and 4:

- Description of a generic model for steering systems;
- Presentation of an existing method for constructing Lyapunov-Krasovskii functions using the delay Lyapunov matrix and proof that the parameter in the double integral term of this functional is not separable.

Chapter 2 provides a delay margin analysis of electric power steering systems using lead-lag filter structures. The delay margin was lower-bounded as explicit functions of the filter parameters. We focused on filters with a limited order to allow an analytical computation of the delay margin as a function of the filter parameters. We also gave guidelines on adjusting the different filter parameters to ensure system stability. In this chapter, to motivate the assumption of constant delays, we presented the sources of delays in an electric power steering system and discussed why these delays could be considered constant. In addition, simulation tests considering time-varying delays are also discussed to assess the impact

of such perturbations by means of an example. We compared our results with recent results in the literature. Main contributions of Chapter 2:

- Presentation of the impact of delays on an EPS system.
- A lower bound of the delay margin by analytical expressions.
- Guidelines to adjust the different parameters of the filter.

Chapter 3 proposed a modified Smith predictor adapted to steer-by-wire systems. The proposed controller removes the internal delays from the feedback loops of the steering system and showed an advantage in increasing the delay margin of the steering systems. In addition, this proposed control architecture is associated with a stability analysis approach which provides an approximation of the delay margin of the steering system using a Padé approximation. Main contributions of Chapter 3:

- A modified Smith predictor for SBW systems.
- A simple stability analysis approach that gives an analytical lower bound of the delay margin.

Chapter 5 rewrote the dynamics of a time-delay system by projecting the state into a set of linearly independent functions. Based on this representation of the time-delay system, two formulations for the stability conditions of a time-delay system were formulated there (Corollary 5.10 and Corollary 5.10). They generalize existing approaches in the literature for stability analysis using semidefinite programming and make connections between them. Moreover, the proposed approach allows parameterizing Lyapunov-Krasovskii functional using any set of linearly independent functions. The main tool to obtain the formulation proposed in Corollary 5.10 is the use of an integral inequality. The generalized formulation proposed in this chapter leads to a general form of integral inequalities allowing us to retrieve some integral inequalities used in the literature. Main contributions of Chapter 5:

- A projection method to represent the dynamics of a time-delay system in projected coordinates.
- Formulation of the stability conditions of the time-delay system using two numerical approaches: method based on the use of integral inequalities and method based on the sum-of-squares programming.
- Comparison of the two numerical approaches mentioned above for stability analysis and discussion of the main assumptions used to obtain them.
- A general form of integral inequalities based on projections and formulation of some integral inequalities used in the literature.

Perspectives

Some comments and perspectives for future research on the topics described in this manuscript are given below.

In Chapter 2, to provide an explicit expression of the delay margin allowing to adjust the different filter parameters, we consider the delay margin as the only variable of the objective function associated with the optimization problem. This choice was made because increasing the delay margin of the system usually has a positive impact on most performance criteria considered for the steering system. Nevertheless, thanks to the metrics introduced in Chapter 1 to assess the performance of steering systems (the hysteresis, the bandwidth of the system, or induced norms of the transfer functions presented there), more complex objective functions can be considered. However, the analytical bounds proposed in Chapter 2, which are also used to provide filter design guidelines, could be difficult to obtain with these more sophisticated objective functions. In this case, instead of analytical expressions, we would rely on numerical methods to compute the filter parameters and use delay margins as constraints. Another direction of research is to analyze the modified Smith predictor approach described in Chapter 3 for the case of electric power steering systems. Moreover, the analytical results to estimate the delay margin for electric power steering systems, presented in Chapter 2 of this manuscript, assume that the delay is constant. Even though the simulations in this chapter show a high degree of robustness to some time-varying delay signals, it is unclear whether or not these analytical results (obtained from a frequency-domain analysis of the system) can ensure the stability of the system in the case of a time-varying delay. Finally, even though the linearized system remains insightful to design control laws, it yields local stability conditions. The stability analysis of the nonlinear system (including a nonlinear torque map) is needed to assess global stability and the region of attraction.

In Chapter 3, similarly to Chapter 2, the internal delays and the transmission delays for steer-by-wire systems are also considered constant. In addition, estimates of the internal delays and the dynamics equations of the steering wheel and the pinion subsystems are used in the inner feedback loops around the controllers. It is therefore crucial to find the admissible uncertainty margin on the estimated internal delays as well as on the parameters of the steering system. In contrast, in a scenario where the steer-by-wire system is teleoperated, the assumption of constant delays becomes too restrictive and has to be dropped. Finally, we must mention that the proposed controllers for steering systems were only verified with simulations. Simulations are very restricted environments and do not reflect all characteristics of an actual vehicle and neglect some dynamics of the system. A first critical modeling to be introduced is the model of the forces in different simulation conditions [81].

Concerning the second part of the manuscript, we parameterized a Lyapunov-Krasovskii functional for continuous time-delay systems with a finite number of linearly independent functions. The results can be extended for discrete-time systems [101, 22, 12]. For these systems, the matrix that describes the dynamics of this discrete-time system has large dimensions, especially if the values of the

delays are large compared to the discretization time. Consequently, to construct a Lyapunov-Krasovskii functional, many scalar unknowns are required within a convex optimization problem, requiring high computation time to solve the associated semidefinite programming problem. Furthermore, *Lyapunov matrix* can also be defined for the discrete-time systems as shown in [56] for some particular systems.

Moreover, we mainly focus on the use of the Lyapunov-Krasovskii functional for stability analysis of linear time-delay systems. This functional can also be used to compute upper exponential estimates (decay rate) of the solutions of time-delay systems, as shown in Section 5.4 for application to steering systems. We would also like to establish input-output performance indices, for delay systems with disturbance inputs, using Lyapunov-Krasovskii functionals, and relate these performance indicators to the performance metrics defined in Chapter 1. Moreover, we would like to assess the advantage of using a polynomial $R(\theta)$ in the sum-of-squares methods to obtain tighter estimates of the convergence rates. In addition, the projection methods introduced in Section 5.1 to represent the dynamics equation of linear time-delay systems could be equivalently used to obtain sufficient stability conditions for nonlinear systems with time-delays.

Finally, one challenging problem is the design of feedback control laws for time-delay systems. The resulting stability conditions obtained with Lyapunov-Krasovskii inequalities yield constraints of a nonconvex optimization problem. In [17], the dynamics equation of a linear time-delay system is restated as $\dot{x} = \mathcal{A}x(t)$, where $\mathcal{A}$ is an unbounded operator. It is shown that the stability conditions of the system are equivalent to the existence of a positive operator $\mathcal{P}$ satisfying some conditions [17, Theorem 5.1.3]. In [88], a dual version of these results is introduced, and the stabilizability conditions are formulated as a convex optimization problem. These dual stability conditions are then formulated as positivity of a dual form of a Lyapunov-Krasovskii functional. A second potential approach is to define dual and adjoint systems [6, Chapter 1] for a linear time-delay system. However, the relationship between the stability of the dual system and the stability of the original time-delay system has to be established.

Appendix A

Technical proofs of Chapter 2

Lemma A.1 and proof of Proposition 2.3

The following lemma, see [9] and [66], will be used to prove Proposition 2.3 and at several other places of Chapter 2.

Lemma A.1. *Suppose that $\xi \geq 0$, $\eta \geq 0$. Then,*

(i) $\tan^{-1}\xi + \tan^{-1}\eta = \begin{cases} \tan^{-1}\dfrac{\xi+\eta}{1-\xi\eta}, & \xi\eta < 1, \\ \dfrac{\pi}{2}, & \xi\eta = 1, \\ \tan^{-1}\dfrac{\xi+\eta}{1-\xi\eta} + \pi, & \xi\eta > 1; \end{cases}$

(ii) $\tan^{-1}\xi - \tan^{-1}\eta = \tan^{-1}\dfrac{\xi-\eta}{1+\xi\eta}$;

(iii) $\dfrac{\xi}{1+\xi^2} \leq \tan^{-1}\xi \leq \xi$;

(iv) $0 \leq \tan^{-1}\xi < \dfrac{\pi}{2}$.

Proof of Proposition 2.3. *Item (i).* Let $\tilde{\omega}_c(\omega_a)$ be the unity-gain crossover frequency of the open-loop transfer function $P(s)C_2(s)$. If it exists, the frequency $\tilde{\omega}_c(\omega_a)$ is necessarily a positive real root of the polynomial equation

$$\tilde{\omega}_c^4(\omega_a) - \left(\frac{K^2}{\omega_a^2} + 2 - 4\zeta^2\right)\tilde{\omega}_c^2(\omega_a) + 1 - K^2 = 0. \tag{A.1}$$

Observe that the closed-loop delay margin is infinite if and only if the Nyquist diagram of the open-loop transfer function does not intersect the unity gain circle (at a strictly positive frequency). Hence, to have infinite delay margin, the above polynomial should not have any strictly positive real root. By Routh's criterion, this is equivalent to condition (2.10) of the Proposition's first item.

Item (ii). The open-loop transfer function is given by

$$P(s)C_2(s) = \frac{K\left(\dfrac{s}{\omega_a}+1\right)}{s^2+2\zeta s+1}. \tag{A.2}$$

Denote by p_1 and p_2 the two poles of the system. Since the system is stable, there exist two real numbers $\alpha > 0$ and $\beta \geq 0$ such that $p_1 = -\alpha + j\beta$ and $p_2 = -\alpha - j\beta$. From (A.2), we have $\alpha = \zeta$ and $\alpha^2 + \beta^2 = 1$.

Define $s = j\omega$. The phase of the open-loop transfer function is given by

$$\phi(\omega) = \tan^{-1}\frac{\omega}{\omega_a} - \tan^{-1}\frac{\omega+\beta}{\alpha} - \tan^{-1}\frac{\omega-\beta}{\alpha} - \pi.$$

The delay margin is given by

$$\Delta\bar{\tau}(\omega_a) = \frac{\phi(\tilde{\omega}_c(\omega_a)) + \pi}{\tilde{\omega}_c(\omega_a)},$$

where

$$\tilde{\omega}_c(\omega_a) = \sqrt{\frac{\dfrac{K^2}{\omega_a^2}+2-4\zeta^2+\sqrt{\left(\dfrac{K^2}{\omega_a^2}+2-4\zeta^2\right)^2-4+4K^2}}{2}}$$

is the largest root of equation (A.1). Indeed, $\dfrac{d}{d\omega}\left(\dfrac{\phi(\omega)+\pi}{\omega}\right)$ is a strictly decreasing function of ω. Using Lemma A.1.(i), we obtain the solutions of the delay margin $\Delta\bar{\tau}(\omega_a)$ stated in the proposition. □

Proof of Theorem 2.4

At the optimal value ω_a^* we have that $\dfrac{d\Delta\bar{\tau}}{d\omega_a}(\omega_a^*) = 0$. Based on this observation, we have that any interval $I = [\bar{\omega}_a^*, \infty)$ satisfying $\dfrac{d\Delta\bar{\tau}(\omega_a)}{d\omega_a} \leq 0$, $\forall \omega_a \in I$, yields an upper bound $\bar{\omega}_a^*$ for ω_a^*. The goal in the steps detailed below is to obtain small values for $\bar{\omega}_a^*$.

First step. Consider the derivative of $\tilde{\omega}_c(\omega_a)$ in (2.12) with respect to ω_a,

$$\frac{d\tilde{\omega}_c(\omega_a)}{d\omega_a} = -\frac{K^2 X(\omega_a)}{\omega_a^3\tilde{\omega}_c(\omega_a)}, \tag{A.3}$$

where

$$X(\omega_a) = \frac{\tilde{\omega}_c^2(\omega_a)}{\sqrt{\left(\dfrac{K^2}{\omega_a^2}+2-4\zeta^2\right)^2-4+4K^2}}. \tag{A.4}$$

Since we assume that (2.6) does not hold, following Proposition 2.3.(i), condition (2.10) does not hold. Therefore $\tilde{\omega}_c(\omega_a)$ is well defined and $\tilde{\omega}_c(\omega_a)$ is well defined and verifies $\tilde{\omega}_c(\omega_a) > 0, \forall \omega_a > 0$. Moreover,

$$\sqrt{\left(\frac{K^2}{\omega_a^2} + 2 - 4\zeta^2\right)^2 - 4 + 4K^2} > 0, \quad \forall \omega_a > 0,$$

therefore $X(\omega_a) > 0$, hence (A.3) is negative. It follows that $\tilde{\omega}_c(\omega_a)$ is a strictly decreasing function of ω_a. In addition, from (2.12) we have

$$\lim_{\omega_a \to +\infty} \tilde{\omega}_c(\omega_a) = \hat{\omega}_c,$$

with $\hat{\omega}_c$ as in (2.7). Since $\tilde{\omega}_c$ is strictly decreasing on ω_a, the above limit implies

$$\tilde{\omega}_c(\omega_a) > \hat{\omega}_c, \qquad \forall \omega_a > 0. \tag{A.5}$$

In (A.4), replacing the expression of $\tilde{\omega}_c(\omega_a)$ given by (2.12) leads to

$$X(\omega_a) = \frac{\dfrac{K^2}{\omega_a^2} + 2 - 4\zeta^2 + \sqrt{\left(\dfrac{K^2}{\omega_a^2} + 2 - 4\zeta^2\right)^2 - 4 + 4K^2}}{2\sqrt{\left(\dfrac{K^2}{\omega_a^2} + 2 - 4\zeta^2\right)^2 - 4 + 4K^2}}. \tag{A.6}$$

We can show that

$$X(\omega_a) \leq \begin{cases} 1, & \text{if } K > 1, \\ c_0, & \text{if } K \leq 1 \text{ and } 2\zeta\sqrt{1-\zeta^2} < K. \end{cases} \tag{A.7}$$

Indeed, since we assume that (2.6) does not hold let us consider the two cases below:

- For $K > 1$, (cases I and III)

  $$\frac{K^2}{\omega_a^2} + 2 - 4\zeta^2 < \sqrt{\left(\frac{K^2}{\omega_a^2} + 2 - 4\zeta^2\right)^2 - 4 + 4K^2}, \qquad \omega_a > 0.$$

  This implies that, from (A.6), $X(\omega_a) \leq 1$;

- For $K \leq 1$ and $2\zeta\sqrt{1-\zeta^2} < K$, (cases II and IV)

  $$\frac{K^2}{\omega_a^2} + 2 - 4\zeta^2 \geq \sqrt{\left(\frac{K^2}{\omega_a^2} + 2 - 4\zeta^2\right)^2 - 4 + 4K^2}, \qquad \omega_a > 0.$$

  In this case, from (A.6), we have

  $$X(\omega_a) \leq \frac{\dfrac{K^2}{\omega_a^2} + 2 - 4\zeta^2}{\sqrt{\left(\dfrac{K^2}{\omega_a^2} + 2 - 4\zeta^2\right)^2 - 4 + 4K^2}} < c_0,$$

  where the second inequality is obtained by observing that, in this case, the function $X(\omega_a)$ is strictly increasing, and by letting $\omega_a \to \infty$.

Second step. For $K \geq 2\zeta$ (cases I and II), from (2.7) we obtain $\hat{\omega}_c(K,\zeta) \geq 1$. Indeed, the function $\hat{\omega}_c$ is strictly increasing with respect to K and $\hat{\omega}_c(K,\zeta) = 1$ when $K = 2\zeta$. Moreover, from (A.5), we have $\tilde{\omega}_c(\omega_a) > \hat{\omega}_c$, $\forall \omega_a > 0$ which gives $\tilde{\omega}_c(\omega_a) > 1$, $\forall \omega_a > 0$. In this case, using Item (ii) of Proposition 2.3, we have

$$\Delta\bar{\tau}(\omega_a) = \frac{\tan^{-1}\dfrac{\tilde{\omega}_c(\omega_a)}{\omega_a} + \tan^{-1}\dfrac{2\zeta\tilde{\omega}_c(\omega_a)}{\tilde{\omega}_c^2(\omega_a)-1}}{\tilde{\omega}_c(\omega_a)}, \tag{A.8}$$

of which the derivative with respect to ω_a gives

$$\frac{d\Delta\bar{\tau}(\omega_a)}{d\omega_a} = \frac{d}{d\omega_a}\left(\frac{\tan^{-1}\dfrac{\tilde{\omega}_c(\omega_a)}{\omega_a} + \tan^{-1}\dfrac{2\zeta\tilde{\omega}_c(\omega_a)}{\tilde{\omega}_c^2(\omega_a)-1}}{\tilde{\omega}_c(\omega_a)}\right).$$

Multiplying the above expression by $\tilde{\omega}_c^2(\omega_a)$, we obtain

$$\begin{aligned}\tilde{\omega}_c^2(\omega_a)\frac{d\Delta\bar{\tau}(\omega_a)}{d\omega_a} = {} & \frac{\tilde{\omega}_c(\omega_a)\dfrac{d}{d\omega_a}\left(\dfrac{\tilde{\omega}_c(\omega_a)}{\omega_a}\right)}{1+\dfrac{\tilde{\omega}_c^2(\omega_a)}{\omega_a^2}} - \frac{d\tilde{\omega}_c(\omega_a)}{d\omega_a}\tan^{-1}\frac{\tilde{\omega}_c(\omega_a)}{\omega_a} \\ & + \frac{\tilde{\omega}_c(\omega_a)\dfrac{d}{d\omega_a}\left(\dfrac{2\zeta\tilde{\omega}_c(\omega_a)}{\tilde{\omega}_c^2(\omega_a)-1}\right)}{1+\left(\dfrac{2\zeta\tilde{\omega}_c(\omega_a)}{\tilde{\omega}_c^2(\omega_a)-1}\right)^2} - \frac{d\tilde{\omega}_c(\omega_a)}{d\omega_a}\tan^{-1}\frac{2\zeta\tilde{\omega}_c(\omega_a)}{\tilde{\omega}_c^2(\omega_a)-1}.\end{aligned} \tag{A.9}$$

From (2.12), we have the following derivatives

$$\frac{d}{d\omega_a}\left(\frac{\tilde{\omega}_c(\omega_a)}{\omega_a}\right) = -\frac{\tilde{\omega}_c(\omega_a)}{\omega_a^2} - \frac{K^2X(\omega_a)}{\omega_a^4\tilde{\omega}_c(\omega_a)} \tag{A.10}$$

and

$$\begin{aligned}\frac{d}{d\omega_a}\left(\frac{2\zeta\tilde{\omega}_c(\omega_a)}{\tilde{\omega}_c^2(\omega_a)-1}\right) &= \frac{2\zeta K^2(\tilde{\omega}_c^2(\omega_a)+1)X(\omega_a)}{\omega_a^3\tilde{\omega}_c(\omega_a)(\tilde{\omega}_c^2(\omega_a)-1)^2} \\ &= -\frac{2\zeta(\tilde{\omega}_c^2(\omega_a)+1)}{(\tilde{\omega}_c^2(\omega_a)-1)^2}\left(\frac{d\tilde{\omega}_c(\omega_a)}{d\omega_a}\right).\end{aligned} \tag{A.11}$$

Replacing (A.3), (A.10), and (A.11) in (A.9) and using Item (iii) of Lemma A.1, in the Appendix, we have

$$\tilde{\omega}_c^2(\omega_a)\frac{d\Delta\bar{\tau}(\omega_a)}{d\omega_a} \leq \frac{-\frac{\tilde{\omega}_c^2(\omega_a)}{\omega_a^2} - \frac{K^2X(\omega_a)}{\omega_a^4}}{1+\frac{\tilde{\omega}_c^2(\omega_a)}{\omega_a^2}} + \frac{K^2X(\omega_a)}{\omega_a^4}\left(1+\frac{4\zeta\omega_a\tilde{\omega}_c^2(\omega_a)}{(\tilde{\omega}_c^2(\omega_a)-1)^2}\right)$$
$$= \frac{-\frac{\tilde{\omega}_c^2(\omega_a)}{\omega_a^2} + \frac{K^2X(\omega_a)}{\omega_a^4}\left(\frac{\tilde{\omega}_c^2(\omega_a)}{\omega_a^2} + \frac{4\zeta\omega_a^2\tilde{\omega}_c^2(\omega_a)+4\zeta\tilde{\omega}_c^4(\omega_a)}{\omega_a(\tilde{\omega}_c^2(\omega_a)-1)^2}\right)}{1+\frac{\tilde{\omega}_c^2(\omega_a)}{\omega_a^2}}$$
$$= \frac{\frac{\tilde{\omega}_c^2(\omega_a)}{\omega_a^2}\left(-1+\frac{K^2X(\omega_a)}{\omega_a^4}\left(1+\frac{4\zeta\omega_a^3+4\zeta\omega_a\tilde{\omega}_c^2(\omega_a)}{(\tilde{\omega}_c^2(\omega_a)-1)^2}\right)\right)}{1+\frac{\tilde{\omega}_c^2(\omega_a)}{\omega_a^2}}.$$

Now consider the term $\frac{\tilde{\omega}_c^2(\omega_a)}{(\tilde{\omega}_c^2(\omega_a)-1)^2}$ in the above expression, we have

$$\frac{d}{d\tilde{\omega}_c^2(\omega_a)}\left(\frac{\tilde{\omega}_c^2(\omega_a)}{(\tilde{\omega}_c^2(\omega_a)-1)^2}\right) = \frac{1-\tilde{\omega}_c^4(\omega_a)}{(\tilde{\omega}_c^2(\omega_a)-1)^4},$$

and since $1 \leq \hat{\omega}_c < \tilde{\omega}_c(\omega_a)$, we can conclude that $\frac{\tilde{\omega}_c^2(\omega_a)}{(\tilde{\omega}_c^2(\omega_a)-1)^2}$ is a strictly decreasing function of $\tilde{\omega}_c(\omega_a)$. Thus $\frac{\tilde{\omega}_c^2(\omega_a)}{(\tilde{\omega}_c^2(\omega_a)-1)^2} < \frac{\hat{\omega}_c^2}{(\hat{\omega}_c^2-1)^2}$, and we obtain

$$\tilde{\omega}_c^2(\omega_a)\frac{d\Delta\bar{\tau}(\omega_a)}{d\omega_a} < \left(\frac{\frac{\tilde{\omega}_c^2(\omega_a)}{\omega_a^2}}{1+\frac{\tilde{\omega}_c^2(\omega_a)}{\omega_a^2}}\right)\left(\frac{K^2X(\omega_a)}{\omega_a^4}\left(1+\frac{4\zeta\omega_a(\hat{\omega}_c^2+\omega_a^2)}{(\hat{\omega}_c^2-1)^2}\right)-1\right).$$

Using $\frac{\frac{\tilde{\omega}_c^2(\omega_a)}{\omega_a^2}}{1+\frac{\tilde{\omega}_c^2(\omega_a)}{\omega_a^2}} < 1$ gives

$$\tilde{\omega}_c^2(\omega_a)\frac{d\Delta\bar{\tau}(\omega_a)}{d\omega_a} < \frac{K^2X(\omega_a)}{\omega_a^4}\left(1+\frac{4\zeta\omega_a(\hat{\omega}_c^2+\omega_a^2)}{(\hat{\omega}_c^2-1)^2}\right)-1.$$

With the upper bounds of $X(\omega_a)$ in (A.7), the above inequality yields

- For $K > 1$, (case I)

$$\tilde{\omega}_c^2(\omega_a)\frac{d\Delta\bar{\tau}(\omega_a)}{d\omega_a} < \frac{K^2+c_1\omega_a+c_2\omega_a^3-\omega_a^4}{\omega_a^4};$$

- For $K \leq 1$, (case II)

$$\tilde{\omega}_c^2(\omega_a)\frac{d\Delta\bar{\tau}(\omega_a)}{d\omega_a} < \frac{K^2c_0+c_1c_0\omega_a+c_2c_0\omega_a^3-\omega_a^4}{\omega_a^4}.$$

The above expressions can be used to obtain values of $\bar{\omega}_a^*$, from which we have $\dfrac{d\Delta\bar{\tau}(\omega_a)}{d\omega_a} < 0$, $\forall \omega_a > \bar{\omega}_a^*$. Note, however, to obtain values bounding the set where $\dfrac{d\Delta\bar{\tau}(\omega_a)}{d\omega_a} < 0$, we must find roots of the polynomials $K^2 + c_1\omega_a + c_2\omega_a^3 - \omega_a^4$ and $K^2c_0 + c_1c_0\omega_a + c_2c_0\omega_a^3 - \omega_a^4$. To obtain an explicit expression for $\bar{\omega}_a^*$, given by the explicit solution of a polynomial of degree 4, we introduce upper-bounds on the right hand side of the above inequalities by applying the Cauchy–Schwarz inequality either to the terms $c_1\omega_a$ and $c_2\omega_a^3$, or to the terms $c_1c_0\omega_a$ and $c_2c_0\omega_a^3$. The above inequality gives

- For $K > 1$, (case I)

$$\tilde{\omega}_c^2(\omega_a)\frac{d\Delta\bar{\tau}(\omega_a)}{d\omega_a} < \frac{K^2 + \dfrac{c_1^2}{2} + \dfrac{\omega_a^2}{2} + 2c_2^2\omega_a^2 + \dfrac{\omega_a^4}{8} - \omega_a^4}{\omega_a^4};$$

- For $K \leq 1$, (case II)

$$\tilde{\omega}_c^2(\omega_a)\frac{d\Delta\bar{\tau}(\omega_a)}{d\omega_a} < \frac{K^2c_0 + \dfrac{c_1^2c_0^2}{2} + \dfrac{\omega_a^2}{2} + 2c_2^2c_0^2\omega_a^2 + \dfrac{\omega_a^4}{8} - \omega_a^4}{\omega_a^4}.$$

Again, applying the Cauchy–Schwarz inequality to the term ω_a^2, $c_2^2\omega_a^2$, and $c_2^2c_0^2\omega_a^2$, we obtain

- For $K > 1$, (case I)

$$\tilde{\omega}_c^2(\omega_a)\frac{d\Delta\bar{\tau}(\omega_a)}{d\omega_a} < \frac{K^2 + \dfrac{c_1^2}{2} + \dfrac{1}{2} + \dfrac{\omega_a^4}{8} + 8c_2^4 + \dfrac{\omega_a^4}{8} + \dfrac{\omega_a^4}{8} - \omega_a^4}{\omega_a^4};$$

- For $K \leq 1$, (case II)

$$\tilde{\omega}_c^2(\omega_a)\frac{d\Delta\bar{\tau}(\omega_a)}{d\omega_a} < \frac{K^2c_0 + \dfrac{c_1^2c_0^2}{2} + \dfrac{1}{2} + \dfrac{\omega_a^4}{8} + 8c_2^4c_0^4 + \dfrac{\omega_a^4}{8} + \dfrac{\omega_a^4}{8} - \omega_a^4}{\omega_a^4}.$$

Thus, from the roots to the right hand side of the above two inequalities, we get directly the explicit upper bound $\bar{\omega}_a^*$ stated in the theorem for which $\dfrac{d\Delta\bar{\tau}(\omega_a)}{d\omega_a}$ is negative for all $\omega_a \geq \bar{\omega}_a^*$.

Third step. The argument invoked at the beginning of the *Second step*, for $K < 2\zeta$ (cases III and IV), gives $\hat{\omega}_c < 1$. From (2.12), we can show that $\tilde{\omega}_c(\omega_a) < 1$ if and only if $\omega_a > \dfrac{K}{\sqrt{4\zeta^2 - K^2}}$. Then, in this case, the set $\{\omega_a \mid \tilde{\omega}_c(\omega_a) < 1\}$ is not empty. Therefore, given any pair (K, ζ) in the set III $\cup$ IV, from Item (iv) of Lemma A.1, we have, for all $\omega_a > 0$,

$$\max_{\tilde{\omega}_c(\omega_a)>1}\left\{\tan^{-1}\frac{2\zeta\tilde{\omega}_c(\omega_a)}{\tilde{\omega}_c^2(\omega_a) - 1}\right\} < \frac{\pi}{2} < \min_{\tilde{\omega}_c(\omega_a)<1}\left\{-\tan^{-1}\frac{2\zeta\tilde{\omega}_c(\omega_a)}{1 - \tilde{\omega}_c^2(\omega_a)} + \pi\right\}. \quad \text{(A.12)}$$

Moreover, since $\dfrac{\tan^{-1}\dfrac{\tilde{\omega}_c(\omega_a)}{\omega_a}}{\tilde{\omega}_c(\omega_a)}$ is a decreasing function with respect to $\tilde{\omega}_c(\omega_a)$, we also have, for all $\omega_a > 0$,

$$\max_{\tilde{\omega}_c(\omega_a)>1}\left\{\frac{\tan^{-1}\dfrac{\tilde{\omega}_c(\omega_a)}{\omega_a}}{\tilde{\omega}_c(\omega_a)}\right\} < \min_{\tilde{\omega}_c(\omega_a)<1}\left\{\frac{\tan^{-1}\dfrac{\tilde{\omega}_c(\omega_a)}{\omega_a}}{\tilde{\omega}_c(\omega_a)}\right\}. \tag{A.13}$$

Using (A.12), (A.13), and Proposition 2.3.(ii), we can show that, for all $\omega_a > 0$, the delay margin in the case where $\tilde{\omega}_c(\omega_a) < 1$ (which is only possible in the cases III and IV) is larger than the delay margin in the case where $\tilde{\omega}_c(\omega_a) \geq 1$. For this reason, and using the fact that the set $\{\omega_a \mid \tilde{\omega}_c(\omega_a) > 1\}$ is not empty, we consider the case where $\tilde{\omega}_c(\omega_a) < 1$ to maximize the delay margin. In this case, from (2.11), we have

$$\Delta\bar{\tau}(\omega_a) = \frac{\tan^{-1}\dfrac{\tilde{\omega}_c(\omega_a)}{\omega_a} - \tan^{-1}\dfrac{2\zeta\tilde{\omega}_c(\omega_a)}{1-\tilde{\omega}_c^2(\omega_a)} + \pi}{\tilde{\omega}_c(\omega_a)}.$$

From the above expression, we then follow closely the developments starting from (A.8) in the above *Second step*, which we omit for brevity, to arrive at the following expressions

- For $K > 1$, (case III)

$$\tilde{\omega}_c^2(\omega_a)\frac{d\Delta\bar{\tau}(\omega_a)}{d\omega_a} < \frac{4 + 4K^2 + 2(c_1^2 + c_3^2) + 32(c_2^4 + c_4^4) - \omega_a^4}{4\omega_a^4};$$

- For $K \leq 1$ and $2\zeta\sqrt{1-\zeta^2} < K$, (case IV)

$$\tilde{\omega}_c^2(\omega_a)\frac{d\Delta\bar{\tau}(\omega_a)}{d\omega_a} < \frac{4 + 4K^2c_0 + 2(c_1^2 + c_3^2)c_0^2 + 32(c_2^4 + c_4^4)c_0^4 - \omega_a^4}{4\omega_a^4}.$$

Finally, from the right hand side of the last inequality, we get directly the explicit upper bound $\bar{\omega}_a^*$ stated in the theorem. □

Lemma A.2 and proof of Theorem 2.5

We provide here the following lemma, which is used in the proof, given below, of Theorem 2.5.

Lemma A.2. *For any scalar $K > 0$, let the function $Z : \mathbb{R}_{>0} \times \mathbb{R}_{>0} \to \mathbb{R}_{>0}$ be defined as*

$$Z(\omega_a, K) = Y(\omega_a, K)\tan^{-1}\frac{\bar{\omega}_c(\omega_a, K)}{\omega_a} - \frac{\bar{\omega}_c^2(\omega_a, K) + \dfrac{\bar{\omega}_c(\omega_a, K)}{\omega_a}Y(\omega_a, K)}{1 + \dfrac{\bar{\omega}_c^2(\omega_a, K)}{\omega_a^2}}, \tag{A.14}$$

where

$$\bar{\omega}_c(\omega_a, K) = \sqrt{\frac{K^2}{\omega_a^2} + \sqrt{\frac{K^4}{\omega_a^4} + 4K^2}}{2} \quad \textit{and} \quad Y(\omega_a, K) = \frac{K^2 \bar{\omega}_c(\omega_a, K)}{\omega_a \sqrt{\frac{K^4}{\omega_a^4} + 4K^2}}. \tag{A.15}$$

Moreover, let the function $\psi : \mathbb{R}_{>0} \to \mathbb{R}_{>0}$ *be defined as*

$$\psi(\vartheta) = \frac{\beta(\vartheta)}{\vartheta\gamma(\vartheta)} \tan^{-1} \frac{\beta(\vartheta)}{\vartheta} - \frac{\beta^2(\vartheta) + \frac{\beta^2(\vartheta)}{\vartheta^2\gamma(\vartheta)}}{1 + \frac{\beta^2(\vartheta)}{\vartheta^2}}, \tag{A.16}$$

where

$$\beta(\vartheta) = \sqrt{\frac{\frac{1}{\vartheta^2} + \sqrt{\frac{1}{\vartheta^4} + 4}}{2}} \quad \textit{and} \quad \gamma(\vartheta) = \sqrt{\frac{1}{\vartheta^4} + 4}. \tag{A.17}$$

The functions Z *and* ψ *have the following properties:*

(i) There exists a unique solution $\alpha > 0$ *of the implicit equation* $\psi(\vartheta) = 0$*.*

(ii) For any $\eta \in \mathbb{R}_{>0}$ *and* $K \in \mathbb{R}_{>0}$*, we have* $Z(\alpha\sqrt{K}\eta, K) = \psi(\alpha\eta)$*.*

(iii) For any fixed value of $K > 0$*, the equation* $Z(\omega_a, K) = 0$ *admits a unique solution* $\omega_a = \alpha\sqrt{K}$*.*

Proof of Lemma A.2. *Item (i).* Let us first show that $\frac{d\psi(\vartheta)}{d\vartheta} < 0$. The derivative of ψ with respect to ϑ is given by

$$\begin{aligned}\frac{d\psi(\vartheta)}{d\vartheta} = \frac{d}{d\omega_a}\left(\frac{\beta(\vartheta)}{\vartheta\gamma(\vartheta)}\right) \tan^{-1}\frac{\beta(\vartheta)}{\vartheta} - \frac{\frac{\beta(\vartheta)}{\vartheta}\frac{d}{d\vartheta}\left(\frac{\beta(\vartheta)}{\vartheta\gamma(\vartheta)}\right)}{1 + \frac{\beta^2(\vartheta)}{\vartheta^2}} \\ - \frac{2\beta(\vartheta)\frac{d\beta(\vartheta)}{d\vartheta}}{1 + \frac{\beta^2(\vartheta)}{\vartheta^2}} + \frac{\beta^2(\vartheta)\frac{d}{d\vartheta}\left(\frac{\beta^2(\vartheta)}{\vartheta^2}\right)}{\left(1 + \frac{\beta^2(\vartheta)}{\vartheta^2}\right)^2} + \frac{\frac{\beta^2(\vartheta)}{\vartheta^2\gamma(\vartheta)}\frac{d}{d\vartheta}\left(\frac{\beta^2(\vartheta)}{\vartheta^2}\right)}{\left(1 + \frac{\beta^2(\vartheta)}{\vartheta^2}\right)^2}.\end{aligned}$$

From (A.17), we have $\frac{d}{d\vartheta}\left(\frac{\beta(\vartheta)}{\vartheta\gamma(\vartheta)}\right) < 0$ for all $\vartheta > 0$. Using Lemma A.1.(iii), the above expression is upper-bounded by

$$\frac{d\psi(\vartheta)}{d\vartheta} \leq -\frac{2\beta(\vartheta)\frac{d\beta(\vartheta)}{d\vartheta}}{1 + \frac{\beta^2(\vartheta)}{\vartheta^2}} + \frac{\beta^2(\vartheta)\frac{d}{d\vartheta}\left(\frac{\beta^2(\vartheta)}{\vartheta^2}\right)}{\left(1 + \frac{\beta^2(\vartheta)}{\vartheta^2}\right)^2} + \frac{\frac{\beta^2(\vartheta)}{\vartheta^2\gamma(\vartheta)}\frac{d}{d\vartheta}\left(\frac{\beta^2(\vartheta)}{\vartheta^2}\right)}{\left(1 + \frac{\beta^2(\vartheta)}{\vartheta^2}\right)^2}. \tag{A.18}$$

From (A.17), we have

$$\frac{d\beta(\vartheta)}{d\vartheta} = -\frac{1}{\vartheta^3\beta(\vartheta)}\left(\frac{\frac{1}{\vartheta^2}+\sqrt{\frac{1}{\vartheta^4}+4}}{2\sqrt{\frac{1}{\vartheta^4}+4}}\right).$$

Using the fact that $0 < \dfrac{\frac{1}{\vartheta^2}+\sqrt{\frac{1}{\vartheta^4}+4}}{2\sqrt{\frac{1}{\vartheta^4}+4}} \leq 1$ and since $\dfrac{1}{\vartheta^3\beta(\vartheta)} > 0$, the above equation gives

$$-\frac{1}{\vartheta^3\beta(\vartheta)} \leq \frac{d\beta(\vartheta)}{d\vartheta} < 0. \tag{A.19}$$

Using (A.19), we have

$$\frac{d}{d\vartheta}\left(\frac{\beta^2(\vartheta)}{\vartheta^2}\right) = \frac{2\beta(\vartheta)}{\vartheta^2}\left(\frac{d\beta(\vartheta)}{d\vartheta}-\frac{\beta(\vartheta)}{\vartheta}\right) < 0. \tag{A.20}$$

Then, since the last term in (A.18) is negative, it gives

$$\begin{aligned}
\frac{d\psi(\vartheta)}{d\vartheta} &< \frac{-2\beta(\vartheta)\left(1+\frac{\beta^2(\vartheta)}{\vartheta^2}\right)\frac{d\beta(\vartheta)}{d\vartheta}+\beta^2(\vartheta)\frac{d}{d\vartheta}\left(\frac{\beta^2(\vartheta)}{\vartheta^2}\right)}{\left(1+\frac{\beta^2(\vartheta)}{\vartheta^2}\right)^2} \\
&\overset{\text{(A.20)}}{=} \frac{-2\beta(\vartheta)\frac{d\beta(\vartheta)}{d\vartheta}-\frac{2\beta^3(\vartheta)}{\vartheta^2}\frac{d\beta(\vartheta)}{d\vartheta}+\frac{2\beta^3(\vartheta)}{\vartheta^2}\left(\frac{d\beta(\vartheta)}{d\vartheta}-\frac{\beta(\vartheta)}{\vartheta}\right)}{\left(1+\frac{\beta^2(\vartheta)}{\vartheta^2}\right)^2} \\
&= \frac{-2\beta(\vartheta)\frac{d\beta(\vartheta)}{d\vartheta}-\frac{2\beta^4(\vartheta)}{\vartheta^3}}{\left(1+\frac{\beta^2(\vartheta)}{\vartheta^2}\right)^2} \\
&\overset{\text{(A.19)}}{<} \frac{\frac{2}{\vartheta^3}-\frac{2\beta^4(\vartheta)}{\vartheta^3}}{\left(1+\frac{\beta^2(\vartheta)}{\vartheta^2}\right)^2}.
\end{aligned}$$

Using the fact that, from (A.17), we have $\beta(\vartheta) > 1$, the above inequality gives

$$\frac{d\psi(\vartheta)}{d\vartheta} < 0.$$

Therefore, the function $\psi(\vartheta)$ is a strictly decreasing function with respect to ϑ.

To obtain existence and uniqueness of a solution to $\psi(\vartheta) = 0$, we show that $\lim_{\vartheta \to 0} \psi(\vartheta) > 0$ and $\lim_{\vartheta \to +\infty} \psi(\vartheta) < 0$. From (A.17), we have

$$\lim_{\vartheta \to 0} \frac{\beta(\vartheta)}{\frac{1}{\vartheta}} = 1 \tag{A.21}$$

and

$$\lim_{\vartheta \to 0} \frac{\gamma(\vartheta)}{\frac{1}{\vartheta^2}} = 1. \tag{A.22}$$

We also have

$$\lim_{\vartheta \to +\infty} \beta(\vartheta) = 1 \tag{A.23}$$

and

$$\lim_{\vartheta \to +\infty} \gamma(\vartheta) = 2. \tag{A.24}$$

Then, let us consider the expression of $\psi(\vartheta)$ in (A.16). Using (A.21) and (A.22), namely by replacing $\beta(\vartheta)$ by $\frac{1}{\vartheta}$ and replacing $\gamma(\vartheta)$ by $\frac{1}{\vartheta^2}$, we obtain

$$\lim_{\vartheta \to 0} \psi(\vartheta) = \frac{\pi}{2} - \lim_{\vartheta \to 0} \frac{\beta^2(\vartheta) + \frac{\beta^2(\vartheta)}{\vartheta^2 \gamma(\vartheta)}}{1 + \frac{\beta^2(\vartheta)}{\vartheta^2}} = \frac{\pi}{2}.$$

And, using (A.23) and (A.24), namely by setting $\beta(\vartheta) = 1$ and $\gamma(\vartheta) = 2$, we obtain

$$\lim_{\vartheta \to +\infty} \psi(\vartheta) = 0 - \lim_{\vartheta \to +\infty} \frac{\beta^2(\vartheta) + \frac{\beta^2(\vartheta)}{\vartheta^2 \gamma(\vartheta)}}{1 + \frac{\beta^2(\vartheta)}{\vartheta^2}} = -1.$$

Therefore, since $\psi(\vartheta)$ is positive near zero, negative at $+\infty$, and it is continuous and a strictly decreasing function with respect to ϑ, then, the solution of $\psi(\vartheta) = 0$ exists and is unique.

Item (ii). To show that, for any $\eta \in \mathbb{R}_{>0}$ and $K \in \mathbb{R}_{>0}$, we have $Z(\alpha\sqrt{K}\eta, K) = \psi(\alpha\eta)$, consider (A.14) and (A.15) to obtain

$$\begin{aligned} Z(\alpha\sqrt{K}\eta, K) = Y(\alpha\sqrt{K}\eta, K) \tan^{-1} \frac{\bar{\omega}_c(\alpha\sqrt{K}\eta, K)}{\alpha\sqrt{K}\eta} \\ - \frac{\bar{\omega}_c^2(\alpha\sqrt{K}\eta, K) + \frac{\bar{\omega}_c(\alpha\sqrt{K}\eta, K)}{\alpha\sqrt{K}\eta} Y(\alpha\sqrt{K}\eta, K)}{1 + \frac{\bar{\omega}_c^2(\alpha\sqrt{K}\eta, K)}{\alpha^2 K \eta^2}}, \end{aligned}$$

$$\bar{\omega}_c(\alpha\sqrt{K}\eta, K) = \sqrt{\frac{K^2}{\alpha^2 K\eta^2} + \sqrt{\frac{K^4}{\alpha^4 K^2\eta^4} + 4K^2}\over 2}$$
$$= \sqrt{K}\beta(\alpha\eta),$$

and

$$Y(\alpha\sqrt{K}\eta, K) = \frac{K^2\bar{\omega}_c(\alpha\sqrt{K}\eta)}{\alpha\sqrt{K}\eta\sqrt{\frac{K^4}{\alpha^4 K^2\eta^4} + 4K^2}}$$
$$= \frac{K^2\sqrt{K}\beta(\alpha\eta)}{\alpha\sqrt{K}\eta K\sqrt{\frac{1}{\alpha^4\eta^4} + 4}}$$
$$= \frac{K\beta(\alpha\eta)}{\alpha\eta\gamma(\alpha\eta)}.$$

Replacing the expression of $\bar{\omega}_c(\alpha\sqrt{K}\eta, K)$ and $Y(\alpha\sqrt{K}\eta, K)$ in the expression of $Z(\alpha\sqrt{K}\eta, K)$ and simplifying with K, we thus have, for any $\eta \in \mathbb{R}_{>0}$ and $K \in \mathbb{R}_{>0}$, $Z(\alpha\sqrt{K}\eta, K) = \psi(\alpha\eta)$, where ψ is given by (A.16).

Item (iii). For a fixed value of K, suppose that $\omega_a = x^*$ is a solution to $Z(\omega_a, K) = 0$. From *Item* (ii), we have $Z(\alpha\sqrt{K}\eta, K) = \psi(\alpha\eta)$.
Take $\eta = \dfrac{x^*}{\alpha\sqrt{K}}$, we obtain

$$\psi\left(\frac{x^*}{\sqrt{K}}\right) = 0$$

since by assumption $Z(x^*, K) = 0$. Then, from *Item* (i), we must have

$$\frac{x^*}{\sqrt{K}} = \alpha.$$

Therefore, $\omega_a = x^* = \alpha\sqrt{K}$ is the unique solution of $Z(\omega_a, K) = 0$. □

Proof of Theorem 2.5. The goal in the steps detailed below is to obtain the asymptote of ω_a^*, the value of ω_a yielding the optimal delay margin $\Delta\bar{\tau}(\omega_a)$, as K tends to $+\infty$.

First step. For any fixed value of $\zeta > 0$, using the results of Theorem 2.4 (case I), there exist a scalar $\delta > 0$, where $\omega_a^*(K, \zeta) < \delta\sqrt{K}$ as K tends to $+\infty$. Then, from (2.12), for any $\omega_a < \delta\sqrt{K}$ we have

$$\lim_{K\to+\infty} \frac{\tilde{\omega}_c(\omega_a, K, \zeta)}{\sqrt{\frac{K^2}{\omega_a^2} + \sqrt{\frac{K^4}{\omega_a^4} + 4K^2}\over 2}} = 1. \tag{A.25}$$

We thus have that $\lim_{K\to+\infty} \tilde{\omega}_c(\omega_a) = +\infty$. Using the argument invoked at the beginning of *Second step* in the proof of Theorem 2.4, for $K \geq 2\zeta$, we have $\tilde{\omega}_c(\omega_a) > 1$. In this case, from (2.11), we have

$$\Delta\bar{\tau}(\omega_a) = \frac{\tan^{-1}\dfrac{\tilde{\omega}_c(\omega_a)}{\omega_a} + \tan^{-1}\dfrac{2\zeta\tilde{\omega}_c(\omega_a)}{\tilde{\omega}_c^2(\omega_a)-1}}{\tilde{\omega}_c(\omega_a)}.$$

of which the derivative with respect to ω_a gives

$$\frac{d\Delta\bar{\tau}(\omega_a)}{d\omega_a} = \frac{d}{d\omega_a}\left(\frac{\tan^{-1}\dfrac{\tilde{\omega}_c(\omega_a)}{\omega_a} + \tan^{-1}\dfrac{2\zeta\tilde{\omega}_c(\omega_a)}{\tilde{\omega}_c^2(\omega_a)-1}}{\tilde{\omega}_c(\omega_a)}\right).$$

Multiplying the above expression by $\tilde{\omega}_c^2(\omega_a)$, we obtain

$$\begin{aligned}\tilde{\omega}_c^2(\omega_a)\frac{d\Delta\bar{\tau}(\omega_a)}{d\omega_a} &= \frac{\tilde{\omega}_c(\omega_a)\dfrac{d}{d\omega_a}\left(\dfrac{\tilde{\omega}_c(\omega_a)}{\omega_a}\right)}{1+\dfrac{\tilde{\omega}_c^2(\omega_a)}{\omega_a^2}} - \frac{d\tilde{\omega}_c(\omega_a)}{d\omega_a}\tan^{-1}\frac{\tilde{\omega}_c(\omega_a)}{\omega_a} \\ &\quad + \frac{\tilde{\omega}_c(\omega_a)\dfrac{d}{d\omega_a}\left(\dfrac{2\zeta\tilde{\omega}_c(\omega_a)}{\tilde{\omega}_c^2(\omega_a)-1}\right)}{1+\left(\dfrac{2\zeta\tilde{\omega}_c(\omega_a)}{\tilde{\omega}_c^2(\omega_a)-1}\right)^2} - \frac{d\tilde{\omega}_c(\omega_a)}{d\omega_a}\tan^{-1}\frac{2\zeta\tilde{\omega}_c(\omega_a)}{\tilde{\omega}_c^2(\omega_a)-1}. \quad \text{(A.26)}\end{aligned}$$

From (A.3), (A.4), (A.10), and (A.11), we can obtain

$$\lim_{K\to+\infty} \frac{\dfrac{d}{d\omega_a}\left(\dfrac{\tilde{\omega}_c(\omega_a)}{\omega_a}\right)}{-\dfrac{\tilde{\omega}_c(\omega_a)}{\omega_a^2} - \dfrac{K^2\tilde{\omega}_c(\omega_a)}{\omega_a^4\sqrt{\dfrac{K^4}{\omega_a^4}+4K^2}}} = 1, \quad \text{(A.27)}$$

$$\lim_{K\to+\infty} \frac{\dfrac{d\tilde{\omega}_c(\omega_a)}{d\omega_a}}{-\dfrac{K^2\tilde{\omega}_c(\omega_a)}{\omega_a^3\sqrt{\dfrac{K^4}{\omega_a^4}+4K^2}}} = 1, \quad \text{(A.28)}$$

and

$$\lim_{K\to+\infty} \frac{\dfrac{d}{d\omega_a}\left(\dfrac{2\zeta\tilde{\omega}_c(\omega_a)}{\tilde{\omega}_c^2(\omega_a)-1}\right)}{\dfrac{2\zeta K^2}{\omega_a^3\tilde{\omega}_c(\omega_a)\sqrt{\dfrac{K^4}{\omega_a^4}+4K^2}}} = 1.$$

Now, using the above three limits and since $\lim_{K\to+\infty} \frac{2\zeta\tilde{\omega}_c(\omega_a)}{\tilde{\omega}_c^2(\omega_a)-1} = 0$, we have

$$\lim_{K\to+\infty} \frac{\frac{\tilde{\omega}_c(\omega_a)\frac{d}{d\omega_a}\left(\frac{2\zeta\tilde{\omega}_c(\omega_a)}{\tilde{\omega}_c^2(\omega_a)-1}\right)}{1+\left(\frac{2\zeta\tilde{\omega}_c(\omega_a)}{\tilde{\omega}_c^2(\omega_a)-1}\right)^2} - \frac{d\tilde{\omega}_c(\omega_a)}{d\omega_a}\tan^{-1}\frac{2\zeta\tilde{\omega}_c(\omega_a)}{\tilde{\omega}_c^2(\omega_a)-1}}{\frac{\tilde{\omega}_c(\omega_a)\frac{d}{d\omega_a}\left(\frac{\tilde{\omega}_c(\omega_a)}{\omega_a}\right)}{1+\frac{\tilde{\omega}_c^2(\omega_a)}{\omega_a^2}} - \frac{d\tilde{\omega}_c(\omega_a)}{d\omega_a}\tan^{-1}\frac{\tilde{\omega}_c(\omega_a)}{\omega_a}} = 0.$$

Therefore, from (A.26), we obtain the following expression:

$$\lim_{K\to+\infty} \frac{\tilde{\omega}_c^2(\omega_a)\frac{d\Delta\bar{\tau}(\omega_a)}{d\omega_a}}{\frac{\tilde{\omega}_c(\omega_a)\frac{d}{d\omega_a}\left(\frac{\tilde{\omega}_c(\omega_a)}{\omega_a}\right)}{1+\frac{\tilde{\omega}_c^2(\omega_a)}{\omega_a^2}} - \frac{d\tilde{\omega}_c(\omega_a)}{d\omega_a}\tan^{-1}\frac{\tilde{\omega}_c(\omega_a)}{\omega_a}} = 1.$$

Using (A.27) and (A.28), namely, replacing $\frac{d}{d\omega_a}\left(\frac{\tilde{\omega}_c(\omega_a)}{\omega_a}\right)$ by $-\frac{\tilde{\omega}_c(\omega_a)}{\omega_a^2} - \frac{K^2\tilde{\omega}_c(\omega_a)}{\omega_a^4\sqrt{\frac{K^4}{\omega_a^4}+4K^2}}$ and replacing $\frac{d\tilde{\omega}_c(\omega_a)}{d\omega_a}$ by $-\frac{K^2\tilde{\omega}_c(\omega_a)}{\omega_a^3\sqrt{\frac{K^4}{\omega_a^4}+4K^2}}$ in the above equation and multiplying by ω_a^2, we obtain

$$\lim_{K\to+\infty} \frac{\omega_a^2\tilde{\omega}_c^2(\omega_a)\frac{d\Delta\bar{\tau}(\omega_a)}{d\omega_a}}{Z(\omega_a,K)} = 1, \qquad \forall\omega_a > 0, \tag{A.29}$$

where, using (A.25), $Z(\omega_a, K)$ is given by (A.14) in Lemma A.2.

Second step. Using Lemma A.2, the optimal solution $\omega_a^*(K,\zeta)$ exists and is unique. Now, consider a function $\varphi : \mathbb{R}_{>0} \to \mathbb{R}_{>0}$, such that $\varphi(K) < \delta\sqrt{K}$ satisfying

$$\lim_{K\to+\infty} \frac{\omega_a^*(K,\zeta)}{\varphi(K)} = 1. \tag{A.30}$$

Setting $\omega_a = \varphi(K)$, and from the fact that ω_a^* yields the maximum delay margin, namely, for all K, $\frac{d\Delta\bar{\tau}}{d\omega_a}(\omega_a^*(K,\zeta)) = 0$, thus $(\omega_a^*(K,\zeta)\tilde{\omega}_c(\omega_a^*(K,\zeta)))^2\frac{d\Delta\bar{\tau}}{d\omega_a}(\omega_a^*(K,\zeta)) = 0$. Hence, using the above equivalence between $\omega_a^*(K,\zeta)$ and $\varphi(K)$, we have

$$\lim_{K\to+\infty} \varphi^2(K)\tilde{\omega}_c^2(\varphi(K))\frac{d\Delta\bar{\tau}}{d\omega_a}(\varphi(K)) = 0.$$

Therefore, from (A.29), we must have

$$\lim_{K\to+\infty} Z(\varphi(K), K) = 0. \tag{A.31}$$

Third step. Consider the unique solution $\alpha > 0$ of (A.16) and let us rewrite $\varphi(K)$ as

$$\varphi(K) = \alpha\sqrt{K}\eta(K),$$

where $\eta : \mathbb{R}_{>0} \to \mathbb{R}_{>0}$. Let us suppose that (A.31) holds and that $\lim_{K\to+\infty} \frac{\alpha\sqrt{K}}{\varphi(K)} \neq 1$, which from the above equation is equivalent to $\lim_{K\to+\infty} \eta(K) \neq 1$. Using Lemma A.2, we have $Z(\alpha\sqrt{K}\eta(K), K) = \psi(\alpha\eta(K))$. Since the unique solution of equation $\psi(\vartheta) = 0$ is $\vartheta = \alpha$ we have that

$$\psi\left(\alpha \lim_{K\to+\infty} \eta(K)\right) \neq 0.$$

The continuity of ψ thus implies that

$$\lim_{K\to+\infty} \psi(\alpha\eta(K)) \neq 0,$$

which from Lemma A.2.(ii) implies

$$\lim_{K\to+\infty} Z(\varphi(K), K) \neq 0,$$

that is, (A.31) can not hold, leading to a contradiction. We thus conclude that

$$\lim_{K\to+\infty} \frac{\alpha\sqrt{K}}{\varphi(K)} = 1$$

and, from (A.30), we have

$$\lim_{K\to+\infty} \frac{\omega_a^*(K,\zeta)}{\alpha\sqrt{K}} = 1.$$

□

Appendix B

Technical proofs of Chapter 5

Proof of Lemma 5.1

From (5.7), we have

$$\rho_r(\theta) = \rho_{r(j-1)}(\theta) - \sum_{i=j}^{p} \hat{\rho}_i f_i(\theta).$$

Multiplying the above equation by $f_j(\theta)$, for $j = 1, \cdots, p$, and integrating from 0 to 1 with respect to θ, we obtain, using (5.8),

$$\begin{aligned}
\int_0^1 \rho_r(\theta) f_j(\theta) d\theta &= \int_0^1 \rho_{r(j-1)}(\theta) f_j(\theta) d\theta - \sum_{i=j}^{p} \hat{\rho}_i \int_0^1 f_i(\theta) f_j(\theta) d\theta \\
&= \begin{bmatrix} \langle \rho^{(1)}_{r(j-1)}, f_j \rangle \\ \vdots \\ \langle \rho^{(n)}_{r(j-1)}, f_j \rangle \end{bmatrix} - \sum_{i=j}^{p} \hat{\rho}_i \int_0^1 f_i(\theta) f_j(\theta) d\theta \\
&= \hat{\rho}_j \int_0^1 f_j(\theta) f_j(\theta) d\theta - \sum_{i=j}^{p} \hat{\rho}_i \int_0^1 f_i(\theta) f_j(\theta) d\theta.
\end{aligned}$$

Evaluating the above equation for $j = 1, \cdots, p$, we obtain Lemma 5.1. □

Proof of Lemma 5.2

Since, from (5.7),

$$\rho_{r(i-1)}(\theta) = \rho_{r(i-2)}(\theta) - \hat{\rho}_{i-1} f_{i-1}(\theta)$$

and $\rho_{r0}(\theta) = \rho(\theta)$, we obtain

$$\begin{aligned}
\|f_i(\theta)\|^2_{[0,1]} \hat{\rho}_i &= \int_0^1 \left(\rho(\theta) - \sum_{j=1}^{i-1} \hat{\rho}_j f_j(\theta) \right) f_i(\theta) d\theta \\
&= \int_0^1 \rho(\theta) f_i(\theta) d\theta - \bar{F}_{i-1} \hat{\rho}.
\end{aligned}$$

This is equivalent to

$$\bar{F}_i \hat{\rho} = \int_0^1 \rho(\theta) f_i(\theta) d\theta.$$

Therefore, considering the above equation, for $i = 1, \ldots, p$, we obtain

$$\bar{F}\hat{\rho} = \int_0^1 F^\top(\theta)\rho(\theta)d\theta,$$

which is equivalent to (5.13). □

Proof of Proposition 5.3

From (5.11), we have that the derivative of ϕ with respect to t gives

$$\partial_t\phi(t,\theta) = \partial_t\phi_r(t,\theta) + F(\theta)\dot{\hat{\phi}}(t),$$

and its derivative with respect to θ gives

$$\partial_\theta\phi(t,\theta) = \partial_\theta\phi_r(t,\theta) + F'(\theta)\hat{\phi}(t). \tag{B.1}$$

Thus, using (5.5b), we obtain the following identity

$$\partial_t\phi_r(t,\theta) = \begin{bmatrix} F'(\theta) & I_n & -F(\theta) \end{bmatrix} \begin{bmatrix} \hat{\phi}(t) \\ \partial_\theta\phi_r(t,\theta) \\ \dot{\hat{\phi}}(t) \end{bmatrix}. \tag{B.2}$$

From (5.5a), we have $\dot{\phi}(t,1) = A_0\phi(t,0) + A_1\phi(t,1)$, which using (5.11), gives

$$\dot{\phi}_r(t,1) + F_1\dot{\hat{\phi}}(t) = A_0\left(\phi_r(t,0) + F_0\hat{\phi}(t)\right) + A_1\left(\phi_r(t,1) + F_1\hat{\phi}(t)\right),$$

or, equivalently

$$\dot{\phi}_r(t,1) = \begin{bmatrix} A_0F_0 + A_1F_1 & A_1 & A_0 & -F_1 \end{bmatrix} \begin{bmatrix} \hat{\phi}(t) \\ \phi_r(t,1) \\ \phi_r(t,0) \\ \dot{\hat{\phi}}(t) \end{bmatrix}. \tag{B.3}$$

From (5.8), we also have

$$\dot{\hat{\phi}}_i(t) = \frac{1}{\|f_i(\theta)\|^2_{[0,1]}} \int_0^1 \partial_t\phi_{r(i-1)}(t,\theta)f_i(\theta)d\theta.$$

Since, from (5.7),

$$\partial_t\phi_{r(i-1)}(t,\theta) = \partial_t\phi_{r(i-2)}(t,\theta) - \dot{\hat{\phi}}_{i-1}(t)f_{i-1}(\theta),$$

and $\phi_{r0}(t,\theta) = \phi(t,\theta)$, we obtain

$$\begin{aligned}\|f_i(\theta)\|^2_{[0,1]}\dot{\hat{\phi}}_i(t) &= \int_0^1 \left(\partial_t\phi(t,\theta) - \sum_{j=1}^{i-1}\dot{\hat{\phi}}_j(t)f_j(\theta)\right) f_i(\theta)d\theta \\ &= \int_0^1 \partial_\theta\phi(t,\theta)f_i(\theta)d\theta - \bar{F}_{i-1}\dot{\hat{\phi}}(t).\end{aligned}$$

The last expression is equivalent to

$$\bar{F}_i\dot{\hat{\phi}}(t) = \int_0^1 \partial_\theta\phi(t,\theta)f_i(\theta)d\theta. \tag{B.4}$$

Moreover, using (B.1), we have

$$\begin{aligned}\int_0^1 \partial_\theta\phi(t,\theta)f_i(\theta)d\theta &= \int_0^1 \left(\partial_\theta\phi_r(t,\theta) + \sum_{j=1}^{p}\hat{\phi}_j(t)f_j'(\theta)\right) f_i(\theta)d\theta \\ &= \int_0^1 \partial_\theta\phi_r(t,\theta)f_i(\theta)d\theta + F_{\partial i}\hat{\phi}(t).\end{aligned}$$

Therefore, considering (B.4), and $i = 1,\ldots,p$, we obtain

$$\bar{F}\dot{\hat{\phi}}(t) = \int_0^1 F^\top(\theta)\partial_\theta\phi_r(\theta,t)d\theta + \bar{F}_\partial\hat{\phi}(t). \tag{B.5}$$

By applying integration by parts, we obtain

$$\begin{aligned}\int_0^1 F^\top(\theta)\partial_\theta\phi_r(t,\theta)d\theta &= -\int_0^1 F'^\top(\theta)\phi_r(t,\theta)d\theta + F_1^\top\phi_r(t,1) - F_0^\top\phi_r(t,0) \\ &= -X^\top(D_{\bar{F}} - \bar{F}^\top)\hat{\phi}(t) - X_e^\top\tilde{\phi}(t) + F_1^\top\phi_r(t,1) - F_0^\top\phi_r(t,0),\end{aligned}$$

where $\tilde{\phi}(t)$ satisfies (5.16).

Finally, from (B.5), we have

$$\begin{aligned}\dot{\hat{\phi}}(t) = (\bar{F}^{-1}\bar{F}_\partial - \bar{F}^{-1}X^\top(D_{\bar{F}} - \bar{F}^\top))\hat{\phi}(t) - \bar{F}^{-1}X_e^\top\tilde{\phi}(t) \\ + \bar{F}^{-1}F_1^\top\phi_r(t,1) - \bar{F}^{-1}F_0^\top\phi_r(t,0).\end{aligned} \tag{B.6}$$

Therefore, from (B.6), and by replacing the expression of (B.6) into (B.2) and (B.3), we obtain (5.15). □

Proof of Theorem 5.4

First step. For any piecewise continuous function $\rho : [0,1] \to \mathbb{R}^n$, from (5.11), we have, for the terms with P in (4.20)

$$\rho^\top(1)P\rho(1) = \begin{bmatrix}\hat{\rho}^\top & \rho_r^\top(1)\end{bmatrix}\begin{bmatrix}F_1^\top PF_1 & F_1^\top P \\ PF_1 & P\end{bmatrix}\begin{bmatrix}\hat{\rho} \\ \rho_r(1)\end{bmatrix}. \tag{B.7}$$

For the terms with $Q(\theta)$, since $Q(\theta) = \bar{Q}F^\top(\theta)$ and from (5.12),

$$\begin{aligned}\rho^\top(1)\int_0^1 Q(\theta)\rho(\cdot,\theta)d\theta &= \begin{bmatrix}\hat{\rho}^\top & \rho_r^\top(1)\end{bmatrix}\int_0^1\begin{bmatrix}F_1^\top Q_f & F_1^\top Q(\theta) \\ Q_fF_1 & Q(\theta)\end{bmatrix}\begin{bmatrix}\hat{\rho}^\top \\ \rho_r^\top(\theta)\end{bmatrix}d\theta \\ &= \begin{bmatrix}\hat{\rho}^\top & \rho_r^\top(1)\end{bmatrix}\int_0^1\begin{bmatrix}F_1^\top\bar{Q}\bar{F} & 0_{np\times n} \\ \bar{Q}\bar{F} & 0_{n\times n}\end{bmatrix}\begin{bmatrix}\hat{\rho}^\top \\ \rho_r^\top(\theta)\end{bmatrix}d\theta.\end{aligned} \tag{B.8}$$

For the term with $R(\theta)$,

$$\int_0^1 \rho^\top(\theta)R(\theta)\rho(\theta)d\theta = \int_0^1 \begin{bmatrix}\hat{\rho}^\top & \rho_r^\top(\theta)\end{bmatrix} \begin{bmatrix} R_f & F^\top(\theta)R(\theta) \\ R(\theta)F(\theta) & R(\theta)\end{bmatrix} \begin{bmatrix}\hat{\rho} \\ \rho_r(\theta)\end{bmatrix} d\theta, \quad \text{(B.9)}$$

where $R_f = \int_0^1 F^\top(\theta)R(\theta)F(\theta)d\theta$.

From (5.18), (B.7), (B.8), and (B.9), we obtain

$$V(\hat{\rho}, \rho_r(1), \rho_r(\cdot)) = \int_0^1 \begin{bmatrix}\hat{\rho} \\ \rho_r(1) \\ \rho_r(\theta)\end{bmatrix}^\top \Omega_V(\theta) \begin{bmatrix}\hat{\rho} \\ \rho_r(1) \\ \rho_r(\theta)\end{bmatrix} d\theta, \quad \text{(B.10)}$$

where

$$\Omega_V(\theta) = \begin{bmatrix} \Omega_{11} & \bar{F}^\top\bar{Q}^\top + F_1^\top P & F^\top(\theta)R(\theta) \\ \bar{Q}\bar{F} + PF_1 & P & 0_{n\times n} \\ R(\theta)F(\theta) & 0_{n\times n} & R(\theta)\end{bmatrix}.$$

Second step. Since, by Lemma 5.1, $\int_0^1 F^\top(\theta)\rho_r(\theta)d\theta = (D_{\bar{F}} - \bar{F}^\top)\hat{\rho}$, we have

$$\int_0^1 \begin{bmatrix} D_{\bar{F}} - \bar{F}^\top & 0_{np\times n} & -F^\top(\theta)\end{bmatrix} \begin{bmatrix}\hat{\rho} \\ \rho_r(1) \\ \rho_r(\theta)\end{bmatrix} d\theta = 0_{np\times 1}.$$

Then, for any $S_0 \in \mathbb{R}^{np\times np}$ and $S_1 \in \mathbb{R}^{n\times np}$, we define

$$\begin{aligned} &W_0(\hat{\rho},\rho_r(1), \rho_r(\cdot)) \\ &\quad = 2\int_0^1 \begin{bmatrix}\hat{\rho} \\ \rho_r(1) \\ \rho_r(\theta)\end{bmatrix}^\top \begin{bmatrix} S_0 \\ S_1 \\ 0_{n\times np}\end{bmatrix} \begin{bmatrix} D_{\bar{F}} - \bar{F}^\top & 0_{np\times n} & -F^\top(\theta)\end{bmatrix} \begin{bmatrix}\hat{\rho} \\ \rho_r(1) \\ \rho_r(\theta)\end{bmatrix} d\theta \\ &\quad = 0. \end{aligned}$$

Applying the fundamental theorem of calculus, for any differential matrix functions $C : [0, 1] \to \mathbb{S}^{n(p+1)\times n(p+1)}$, we define

$$\begin{aligned} W_1(\hat{\rho}, \rho_r(1)) &= \int_0^1 \begin{bmatrix}\hat{\rho} \\ \rho_r(1)\end{bmatrix}^\top \left[\frac{d}{d\theta}C(\theta) - C(1) + C(0)\right] \begin{bmatrix}\hat{\rho} \\ \rho_r(1)\end{bmatrix} d\theta \\ &= 0. \end{aligned}$$

Thus,

$$\begin{aligned} V(\rho) - \alpha_1\|\rho(1)\|^2 &= V(\hat{\rho}, \rho_r(1), \rho_r(\cdot)) + W_0(\hat{\rho}, \rho_r(1), \rho_r(\cdot)) + W_1(\hat{\rho}, \rho_r(1)) \\ &\qquad - \alpha_1 \left[\begin{array}{cc:c} F_1^\top F_1 & F_1^\top & 0_{np\times n} \\ F_1 & I_n & 0_{n\times n} \\ \hdashline 0_{n\times np} & 0_{n\times n} & 0_{n\times n}\end{array}\right] \\ &= \int_0^1 \begin{bmatrix}\hat{\rho} \\ \rho_r(1) \\ \rho_r(\theta)\end{bmatrix}^\top \Omega(\theta) \begin{bmatrix}\hat{\rho} \\ \rho_r(1) \\ \rho_r(\theta)\end{bmatrix} d\theta. \end{aligned}$$

Third step. The time derivative of (B.10) along the solution of (5.5), is given by

$$\frac{d}{dt}V(\hat{\phi}(t),\phi_r(t,1),\phi_r(t,\cdot)) = 2\int_0^1 \begin{bmatrix}\hat{\phi}(t)\\ \phi_r(t,1)\\ \phi_r(t,\theta)\end{bmatrix}^\top \Omega_V(\theta) \begin{bmatrix}\dot{\hat{\phi}}(t)\\ \partial_t\phi_r(t,1)\\ \partial_t\phi_r(t,\theta)\end{bmatrix} d\theta,$$

and, from (5.15), we obtain

$$\dot{V}(\hat{\phi}(t),\tilde{\phi}(t),\phi_r(t,1),\phi_r(t,0),\phi_r(t,\cdot)) = 2\int_0^1 \begin{bmatrix}\hat{\phi}(t)\\ \phi_r(t,1)\\ \phi_r(t,\theta)\end{bmatrix}^\top \Omega_V(\theta)\Gamma(\theta) \begin{bmatrix}\hat{\phi}(t)\\ \tilde{\phi}(t)\\ \phi_r(t,1)\\ \phi_r(t,0)\\ \partial_\theta\phi_r(t,\theta)\end{bmatrix} d\theta.$$

Since

$$\int_0^1 \phi_r^\top(t,\theta)R(\theta)\partial_\theta\phi_r(t,\theta)d\theta = \frac{1}{2}\int_0^1 \begin{bmatrix}\phi_r(t,1)\\ \phi_r(t,0)\\ \phi_r(t,\theta)\end{bmatrix}^\top \begin{bmatrix}R(1) & 0_{n\times n} & 0_{n\times n}\\ 0_{n\times n} & -R(0) & 0_{n\times n}\\ 0_{n\times n} & 0_{n\times n} & -R'(\theta)\end{bmatrix} \begin{bmatrix}\phi_r(t,1)\\ \phi_r(t,0)\\ \phi_r(t,\theta)\end{bmatrix} d\theta,$$

$$\phi_r^\top(t,1)\int_0^1 Q(\theta)\partial_\theta\phi_r(t,\theta)d\theta = \phi_r^\top(t,1)\int_0^1 \begin{bmatrix}Q(1) & -Q(0) & -Q'(\theta)\end{bmatrix} \begin{bmatrix}\phi_r(t,1)\\ \phi_r(t,0)\\ \phi_r(t,\theta)\end{bmatrix} d\theta,$$

and

$$\hat{\phi}^\top(t)\int_0^1 (F^\top(\theta)R(\theta)+F_1^\top Q(\theta))\partial_\theta\phi_r(t,\theta)d\theta = \hat{\phi}^\top(t)\int_0^1 \begin{bmatrix}R(1)F_1+Q^\top(1)F_1\\ -R(0)F_0-Q^\top(0)F_1\\ -R(\theta)F'(\theta)+R'(\theta)F(\theta)+Q'^\top(\theta)F_1\end{bmatrix}^\top \begin{bmatrix}\phi_r(t,1)\\ \phi_r(t,0)\\ \phi_r(t,\theta)\end{bmatrix} d\theta,$$

then, $\dot{V}$ is given by

$$\dot{V}(\eta(t,\cdot)) = \int_0^1 \eta^\top(t,\theta)\bar{\Omega}_V(\theta)\eta(t,\theta)d\theta,$$

where

$$\eta(t,\theta) = \begin{bmatrix}\hat{\phi}(t)\\ \tilde{\phi}(t)\\ \phi_r(t,1)\\ \phi_r(t,0)\\ \phi_r(t,\theta)\end{bmatrix}$$

and

$$\bar{\Omega}_V = \begin{bmatrix}\Omega_{11}(\theta)+\Omega_{11}^\top(\theta) & -\bar{F}^\top\bar{T}X_e^\top & \Omega_{13} & \Omega_{14} & -F^\top(\theta)R'(\theta)\\ -X_e\bar{T}\bar{F} & 0_{np_e\times np_e} & 0_{np_e\times n} & 0_{np_e\times n} & 0_{np_e\times n}\\ \Omega_{13}^\top & 0_{n\times np_e} & \Omega_{33}+\Omega_{33}^\top & \Omega_{34} & -\bar{Q}X_e^\top F_e^\top(\theta)\\ \Omega_{14}^\top & 0_{n\times np_e} & \Omega_{34}^\top & -R(0) & 0_{n\times n}\\ -R'(\theta)F(\theta) & 0_{n\times np_e} & -F_e(\theta)X_e\bar{Q}^\top & 0_{n\times n} & -R'(\theta)\end{bmatrix}.$$

Since $\int_0^1 F^\top(\theta)\phi_r(t,\theta)d\theta = (D_{\bar{F}} - \bar{F}^\top)\hat{\phi}(t)$, we have

$$\int_0^1 \begin{bmatrix} D_{\bar{F}} - \bar{F}^\top & 0_{np\times n(p_e+2)} & -F^\top(\theta) \end{bmatrix} \eta(t,\theta)d\theta = 0_{np\times 1},$$

then, for any $\bar{S}_0 \in \mathbb{R}^{np\times np}$ and $\bar{S}_1 \in \mathbb{R}^{n(p_e+2)\times np}$, we have

$$\begin{aligned}\bar{W}_0(\eta(t,\cdot)) &= 2\int_0^1 \eta^\top(t,\theta) \begin{bmatrix} \bar{S}_0 \\ \bar{S}_1 \\ 0_{n\times np} \end{bmatrix} \begin{bmatrix} D_{\bar{F}} - \bar{F}^\top & 0_{np\times n(p_e+2)} & -F^\top(\theta) \end{bmatrix} \eta(t,\theta)d\theta \\ &= 0.\end{aligned}$$

Similarly, since $\int_0^1 F_e^\top(\theta)\phi_r(t,\theta)d\theta = \tilde{\phi}(t)$, we have

$$\int_0^1 \begin{bmatrix} 0_{np_e\times np} & I_{p_e} & 0_{np_e\times 2n} & -F_e^\top(\theta) \end{bmatrix} \eta(t,\theta)d\theta = 0_{np_e\times 1},$$

then, for any $\tilde{S}_0 \in \mathbb{R}^{np\times np_e}$, $\tilde{S}_1 \in \mathbb{R}^{np_e\times np_e}$, and $\tilde{S}_2 \in \mathbb{R}^{2n\times np_e}$, we have

$$\begin{aligned}\bar{W}_1(\eta(t,\cdot)) &= 2\int_0^1 \eta^\top(t,\theta) \begin{bmatrix} \tilde{S}_0 \\ \tilde{S}_1 \\ \tilde{S}_2 \\ 0_{n\times np_e} \end{bmatrix} \begin{bmatrix} 0_{np_e\times np} & I_{p_e} & 0_{np_e\times 2n} & -F_e^\top(\theta) \end{bmatrix} \eta(t,\theta)d\theta \\ &= 0.\end{aligned}$$

Applying the fundamental theorem of calculus, for any differential matrix functions $\bar{C}(\theta) : [0,1] \to \mathbb{S}^{n(p+p_e+2)\times n(p+p_e+2)}$, we define

$$\begin{aligned}&\bar{W}_2(\hat{\phi}(t),\tilde{\phi}(t),\phi_r(t,1),\phi_r(t,0)) \\ &\qquad = \int_0^1 \begin{bmatrix} \hat{\phi}(t) \\ \tilde{\phi}(t) \\ \phi_r(t,1) \\ \phi_r(t,0) \end{bmatrix}^\top \left[\frac{d}{d\theta}\bar{C}(\theta) - \bar{C}(1) + \bar{C}(0)\right] \begin{bmatrix} \hat{\phi}(t) \\ \tilde{\phi}(t) \\ \phi_r(t,1) \\ \phi_r(t,0) \end{bmatrix} d\theta \\ &\qquad = 0.\end{aligned}$$

Thus, by adding $\dot{V}$, $\bar{W}_0$, $\bar{W}_1$, and $\bar{W}_2$, we obtain

$$\begin{aligned}\dot{V}(\phi) + \beta\|\phi(t,1)\|^2 &= \dot{V}(\eta(t,\cdot)) + \bar{W}_0(\eta(t,\cdot)) + \bar{W}_1(\eta(t,\cdot)) + \bar{W}_2(\eta(t,\cdot)) \\ &\qquad + \beta \left[\begin{array}{ccccc} F_1^\top F_1 & 0_{np\times np_e} & F_1^\top & 0_{np\times n} & 0_{np\times n} \\ 0_{np_e\times np} & 0_{np_e\times np_e} & 0_{np_e\times n} & 0_{np_e\times n} & 0_{np_e\times n} \\ F_1 & 0_{n\times np_e} & I_n & 0_{n\times n} & 0_{n\times n} \\ 0_{n\times np} & 0_{n\times np_e} & 0_{n\times n} & 0_{n\times n} & 0_{n\times n} \\ \hdashline 0_{n\times np} & 0_{n\times np_e} & 0_{n\times n} & 0_{n\times n} & 0_{n\times n} \end{array}\right] \\ &= \int_0^1 \eta^\top(t,\theta)\bar{\Omega}(\theta)\eta(t,\theta)d\theta.\end{aligned}$$

Fourth step. By Theorem 4.1, the origin is GES. □

Proof of Proposition 5.6

By projecting the function ρ respectively on the set $\{f_1, \cdots, f_p\}$ and $\{g_1, \cdots, g_p\}$ as in (5.11), we obtain

$$\rho(\theta) = F(\theta)\hat{\rho}^f + \rho_r^f(\theta)$$

and

$$\rho(\theta) = G(\theta)\hat{\rho}^g + \rho_r^g(\theta),$$

where

$$F(\theta) = \begin{bmatrix} f_1(\theta) & \cdots & f_p(\theta) \end{bmatrix} \otimes I_n$$

and

$$G(\theta) = \begin{bmatrix} g_1(\theta) & \cdots & g_p(\theta) \end{bmatrix} \otimes I_n.$$

Using Lemma 5.2 and since $F(\theta) = G(\theta)(B \otimes I_n)$, we have

$$\begin{aligned} \hat{\rho}^f &= \bar{F}^{-1} \int_0^1 F^\top(\theta)\rho(\theta)d\theta \\ &= \bar{F}^{-1}(B^\top \otimes I_n) \int_0^1 G^\top(\theta)\rho(\theta)d\theta \end{aligned}$$

and

$$\hat{\rho}^g = \bar{G}^{-1} \int_0^1 G^\top(\theta)\rho(\theta)d\theta,$$

where $\bar{F}$ and $\bar{G}$ are structured as in (5.3).

Then, we obtain

$$\hat{\rho}^f = \bar{F}^{-1}(B^\top \otimes I_n)\bar{G}\hat{\rho}^g$$

and

$$\rho_r^f(\theta) = (G(\theta) - F(\theta)\bar{F}^{-1}(B^\top \otimes I_n)\bar{G})\hat{\rho}^g + \rho_r^g(\theta).$$

Therefore, we have

$$\begin{aligned} V(\rho) - \alpha_1\|\rho(1)\|^2 &= \int_0^1 \begin{bmatrix} \hat{\rho}^f \\ \rho_r^f(1) \\ \rho_r^f(\theta) \end{bmatrix}^\top \Omega(\theta) \begin{bmatrix} \hat{\rho}^f \\ \rho_r^f(1) \\ \rho_r^f(\theta) \end{bmatrix} d\theta \\ &= \int_0^1 \begin{bmatrix} \hat{\rho}^g \\ \rho_r^g(1) \\ \rho_r^g(\theta) \end{bmatrix}^\top K^\top \Omega(\theta) K \begin{bmatrix} \hat{\rho}^g \\ \rho_r^g(1) \\ \rho_r^g(\theta) \end{bmatrix} d\theta, \end{aligned}$$

where

$$K = \begin{bmatrix} \bar{F}^{-1}(B^\top \otimes I_n)\bar{G} & 0_{np\times n} & 0_{np\times n} \\ G(1) - F(1)\bar{F}^{-1}(B^\top \otimes I_n)\bar{G} & I_n & 0_{n\times n} \\ G(\theta) - F(\theta)\bar{F}^{-1}(B^\top \otimes I_n)\bar{G} & 0_{n\times n} & I_n \end{bmatrix}.$$

And

$$\dot{V}(\phi) + \beta\|\phi(t,1)\|^2 = \int_0^1 \begin{bmatrix} \hat{\phi}^f(t) \\ \tilde{\phi}^f(t) \\ \phi_r^f(t,1) \\ \phi_r^f(t,0) \\ \phi_r^f(t,\theta) \end{bmatrix}^\top \bar{\Omega}(\theta) \begin{bmatrix} \hat{\phi}^f(t) \\ \tilde{\phi}^f(t) \\ \phi_r^f(t,1) \\ \phi_r^f(t,0) \\ \phi_r^f(t,\theta) \end{bmatrix} d\theta$$

$$= \int_0^1 \begin{bmatrix} \hat{\phi}^g(t) \\ \tilde{\phi}^g(t) \\ \phi_r^g(t,1) \\ \phi_r^g(t,0) \\ \phi_r^g(t,\theta) \end{bmatrix}^\top \bar{K}^\top \bar{\Omega}(\theta) \bar{K} \begin{bmatrix} \hat{\phi}^g(t) \\ \tilde{\phi}^g(t) \\ \phi_r^g(t,1) \\ \phi_r^g(t,0) \\ \phi_r^g(t,\theta) \end{bmatrix} d\theta,$$

where

$$\bar{K} = \begin{bmatrix} \bar{F}^{-1}(B^\top \otimes I_n)\bar{G} & 0_{np\times np_e} & 0_{np\times n} & 0_{np\times n} & 0_{np\times n} \\ 0_{np_e\times np} & (B^{-1}\otimes I_n) & 0_{np_e\times np_e} & 0_{np_e\times n} & 0_{np_e\times n} \\ G(1) - F(1)\bar{F}^{-1}(B^\top \otimes I_n)\bar{G} & 0_{n\times np_e} & I_n & 0_{n\times n} & 0_{n\times n} \\ G(0) - F(0)\bar{F}^{-1}(B^\top \otimes I_n)\bar{G} & 0_{n\times np_e} & 0_{n\times n} & I_n & 0_{n\times n} \\ G(\theta) - F(\theta)\bar{F}^{-1}(B^\top \otimes I_n)\bar{G} & 0_{n\times np_e} & 0_{n\times n} & 0_{n\times n} & I_n \end{bmatrix}.$$

Since $\bar{F}$, B, and $\bar{G}$ are full rank matrices, K is also a full rank matrix. Therefore, the matrix $\bar{\Omega}$ in Theorem 5.4 is a positive definite matrix, if and only if the matrix $K^\top MK$ is positive definite. Note that the above statements stay valid for the matrix $\bar{\Omega}_s$ in Proposition 5.5, where $p_e = 0$. □

Proof of Lemma 5.7

We have

$$\int_0^1 \rho^\top(\theta) S \rho(\theta) d\theta = \int_0^1 \begin{bmatrix} \hat{\rho} \\ \rho_r(\theta) \end{bmatrix}^\top \begin{bmatrix} F^\top(\theta)SF(\theta) & F^\top(\theta)S \\ SF(\theta) & S \end{bmatrix} \begin{bmatrix} \hat{\rho} \\ \rho_r(\theta) \end{bmatrix} d\theta. \tag{B.11}$$

Since S is a symmetric matrix, we have

$$\int_0^1 F^\top(\theta) S \rho_r(\theta) d\theta = (I_p \otimes S) \int_0^1 F^\top(\theta)\rho_r(\theta) d\theta \tag{B.12}$$

and, from Lemma 5.1, we have

$$(I_p \otimes S) \int_0^1 F^\top(\theta)\rho_r(\theta) d\theta = (I_p \otimes S)(D_{\bar{F}} - \bar{F}^\top)\hat{\rho}. \tag{B.13}$$

Again, since S is a symmetric matrix, we have

$$\begin{aligned} \int_0^1 F^\top(\theta) S F(\theta) d\theta &= (I_p \otimes S) \int_0^1 F^\top(\theta) F(\theta) d\theta \\ &= (I_p \otimes S)(\bar{F} + \bar{F}^\top - D_{\bar{F}}). \end{aligned} \tag{B.14}$$

Therefore, using (B.12)-(B.13) in (B.11), we obtain

$$\begin{aligned}\int_0^1 \rho^\top(\theta) S \rho(\theta) d\theta &= \int_0^1 \begin{bmatrix} \hat{\rho} \\ \rho_r(\theta) \end{bmatrix}^\top \begin{bmatrix} F^\top(\theta) S F(\theta) & F^\top(\theta) S \\ S F(\theta) & S \end{bmatrix} \begin{bmatrix} \hat{\rho} \\ \rho_r(\theta) \end{bmatrix} d\theta \\ &= \int_0^1 \begin{bmatrix} \hat{\rho} \\ \rho_r(\theta) \end{bmatrix}^\top \begin{bmatrix} (I_p \otimes S) D_{\bar{F}} & 0_{np \times n} \\ 0_{n \times np} & S \end{bmatrix} \begin{bmatrix} \hat{\rho} \\ \rho_r(\theta) \end{bmatrix} d\theta \\ &\geq \hat{\rho}^\top (\tilde{D}_{\bar{F}} \otimes S) \hat{\rho},\end{aligned}$$

since $(I_p \otimes S) D_{\bar{F}} = \tilde{D}_{\bar{F}} \otimes S$ and S is positive semidefinite. □

Proof of Proposition 5.8

Consider V in the proof of Theorem 5.4 and Proposition 5.5, for $p_e = 0$, and setting $S_0 = 0_{np \times np}$, $S_1 = 0_{n \times np}$, and $C(\theta) = 0_{n(p+1) \times n(p+1)}$, for all $\theta \in [0, 1]$, we obtain

$$\begin{aligned}&V(\hat{\rho}, \rho_r(1), \rho_r(\cdot)) = \\ &\int_0^1 \begin{bmatrix} \hat{\rho} \\ \rho_r(1) \\ \rho_r(\theta) \end{bmatrix}^\top \begin{bmatrix} \Omega_{p11} + F^\top(\theta) R(\theta) F(\theta) & \bar{F}^\top \bar{Q}^\top + F_1^\top P & F^\top(\theta) R(\theta) \\ \bar{Q}\bar{F} + P F_1 & P & 0_{n \times n} \\ R(\theta) F(\theta) & 0_{n \times n} & R(\theta) \end{bmatrix} \begin{bmatrix} \hat{\rho} \\ \rho_r(1) \\ \rho_r(\theta) \end{bmatrix} d\theta.\end{aligned}$$

Since, from Lemma 5.7, we have $\int_0^1 \rho^\top(\theta) S \rho(\theta) d\theta \geq \hat{\rho}^\top (\tilde{D}_{\bar{F}} \otimes S) \hat{\rho}$, for any positive semidefinite matrix S, we obtain

$$V(\rho) \geq V(\rho) - \int_0^1 \rho^\top(\theta) S \rho(\theta) d\theta + \hat{\rho}^\top (\tilde{D}_{\bar{F}} \otimes S) \hat{\rho}.$$

That is equivalent to

$$\begin{aligned}V(\rho) - \alpha_1 \|\rho(1)\|^2 \geq &\begin{bmatrix} \hat{\rho} \\ \rho_r(1) \end{bmatrix}^\top \begin{bmatrix} \Omega_{p11} + (\tilde{D}_{\bar{F}} \otimes S) & \bar{F}^\top \bar{Q}^\top + F_1^\top P \\ \bar{Q}\bar{F} + P F_1 & P \end{bmatrix} \begin{bmatrix} \hat{\rho} \\ \rho_r(1) \end{bmatrix} \\ &- \alpha_1 \begin{bmatrix} \hat{\rho} \\ \rho_r(1) \end{bmatrix}^\top \begin{bmatrix} F_1^\top F_1 & F_1^\top \\ F_1 & I_n \end{bmatrix} \begin{bmatrix} \hat{\rho} \\ \rho_r(1) \end{bmatrix} \\ &+ \int_0^1 \begin{bmatrix} \hat{\rho} \\ \rho_r(1) \\ \rho_r(\theta) \end{bmatrix}^\top \begin{bmatrix} F^\top(\theta) \\ 0_{n \times n} \\ I_n \end{bmatrix} (R(\theta) - S) \begin{bmatrix} F^\top(\theta) \\ 0_{n \times n} \\ I_n \end{bmatrix}^\top \begin{bmatrix} \hat{\rho} \\ \rho_r(1) \\ \rho_r(\theta) \end{bmatrix} d\theta.\end{aligned}$$

From the above expression, we conclude that the LKF is positive definite if the inequalities in (5.23) hold.

Similarly, from the expression of the time derivative of the LKF given in the proof of Theorem 5.4 and Proposition 5.5, for $p_e = 0$, and setting $\bar{S}_0 = 0_{np \times np}$,

$\bar{S}_1 = 0_{n\times np}$, and $\bar{C}(\theta) = 0_{n(p+2)\times n(p+2)}$, we obtain

$$\dot{V}(\hat{\phi}(t), \tilde{\phi}(t), \phi_r(t,1), \phi_r(t,0), \phi_r(t,\cdot)) =$$
$$\begin{bmatrix} \hat{\phi}(t) \\ \tilde{\phi}(t) \\ \phi_r(t,1) \\ \phi_r(t,0) \end{bmatrix}^\top \begin{bmatrix} \bar{\Omega}_{p11} + \bar{\Omega}_{p11}^\top & \bar{\Omega}_{p12} & \bar{\Omega}_{p13} \\ \bar{\Omega}_{p12}^\top & \bar{\Omega}_{p22} + \bar{\Omega}_{p22}^\top & \bar{\Omega}_{p23} \\ \bar{\Omega}_{p13}^\top & \bar{\Omega}_{p23}^\top & -R(0) \end{bmatrix} \begin{bmatrix} \hat{\phi}(t) \\ \tilde{\phi}(t) \\ \phi_r(t,1) \\ \phi_r(t,0) \end{bmatrix}$$
$$- \int_0^1 \begin{bmatrix} \hat{\phi}(t) \\ \tilde{\phi}(t) \\ \phi_r(t,1) \\ \phi_r(t,0) \\ \phi_r(t,\theta) \end{bmatrix}^\top \begin{bmatrix} F^\top(\theta) \\ 0_{n(p_e+2)\times n} \\ I_n \end{bmatrix} R'(\theta) \begin{bmatrix} F^\top(\theta) \\ 0_{n(p_e+2)\times n} \\ I_n \end{bmatrix}^\top \begin{bmatrix} \hat{\phi}(t) \\ \tilde{\phi}(t) \\ \phi_r(t,1) \\ \phi_r(t,0) \\ \phi_r(t,\theta) \end{bmatrix} d\theta.$$

Since, from Lemma 5.7, we have $\int_0^1 \phi^\top(\theta)\bar{S}\phi(\theta)d\theta \geq \hat{\phi}^\top(\tilde{D}_{\bar{F}} \otimes \bar{S})\hat{\phi}$, for any positive semidefinite matrix S, we obtain

$$\dot{V}(\phi) \leq \dot{V}(\phi) + \int_0^1 \phi^\top(\theta)\bar{S}\phi(\theta)d\theta - \hat{\phi}^\top(\tilde{D}_{\bar{F}} \otimes \bar{S})\hat{\phi}.$$

That is equivalent to

$$\dot{V}(\phi) + \beta\|\phi(t,1)\|^2 \leq$$
$$\begin{bmatrix} \hat{\phi}(t) \\ \tilde{\phi}(t) \\ \phi_r(t,1) \\ \phi_r(t,0) \end{bmatrix}^\top \begin{bmatrix} \bar{\Omega}_{p11} + \bar{\Omega}_{p11}^\top - (\tilde{D}_{\bar{F}} \otimes \bar{S}) & \bar{\Omega}_{p12} & \bar{\Omega}_{p13} \\ \bar{\Omega}_{p12}^\top & \bar{\Omega}_{p22} + \bar{\Omega}_{p22}^\top & \bar{\Omega}_{p23} \\ \bar{\Omega}_{p13}^\top & \bar{\Omega}_{p23}^\top & -R(0) \end{bmatrix} \begin{bmatrix} \hat{\phi}(t) \\ \tilde{\phi}(t) \\ \phi_r(t,1) \\ \phi_r(t,0) \end{bmatrix}$$
$$+ \beta \begin{bmatrix} \hat{\phi}(t) \\ \tilde{\phi}(t) \\ \phi_r(t,1) \\ \phi_r(t,0) \end{bmatrix}^\top \begin{bmatrix} F_1^\top F_1 & F_1^\top & 0_{np\times n} \\ F_1 & I_n & 0_{n\times n} \\ 0_{n\times np} & 0_{n\times n} & 0_{n\times n} \end{bmatrix} \begin{bmatrix} \hat{\phi}(t) \\ \tilde{\phi}(t) \\ \phi_r(t,1) \\ \phi_r(t,0) \end{bmatrix}$$
$$- \int_0^1 \begin{bmatrix} \hat{\phi}(t) \\ \tilde{\phi}(t) \\ \phi_r(t,1) \\ \phi_r(t,0) \\ \phi_r(t,\theta) \end{bmatrix}^\top \begin{bmatrix} F^\top(\theta) \\ 0_{n(p_e+2)\times n} \\ I_n \end{bmatrix} (R'(\theta) - \bar{S}) \begin{bmatrix} F^\top(\theta) \\ 0_{n(p_e+2)\times n} \\ I_n \end{bmatrix}^\top \begin{bmatrix} \hat{\phi}(t) \\ \tilde{\phi}(t) \\ \phi_r(t,1) \\ \phi_r(t,0) \\ \phi_r(t,\theta) \end{bmatrix} d\theta.$$

From the above expression, we conclude that the time derivative of the LKF along the solution of the time-delay system is negative if the inequalities in (5.24) hold. □

Appendix C

Adopted methods to reduce the conservatism of stability criteria

We give an overview of the stability criteria using Lyapunov-Krasovskii functionals. The following list summarizes some of the widely used techniques to verify Lyapunov-Krasovskii functionals.

- Integral inequalities [84, 85]: Jensen's inequality [98, 72], Wirtinger-based integral inequality [97], Wirtinger-based double integral inequality [83].
- Double integral forms of Lyapunov-Krasovskii functional [84, 85, 72].
- Triple integral forms of Lyapunov-Krasovskii functional [104, 83].
- Cross terms [46].
- Free-weighting matrices [37, 38].
- Reciprocally convex approach [86].
- Descriptor model transform [29].
- Delay decomposition [36, 120].

Mainly, based on the above results, modifying the original Lyapunov-Krasovskii functional with additional terms as the term $\dot{x}$ adopted in [29], cross terms of variables [46], and multiple integral terms [104] can reduce the conservatism of stability criteria. Below, we show that some of these additional terms adopted in the literature yield particular parameterizations of the complete Lyapunov-Krasovskii functional introduced in [44], given by

$$V(\bar{\rho}) = \bar{\rho}^\top(0)\bar{P}\bar{\rho}(0) + 2\bar{\rho}^\top(0)\int_{-h}^{0}\bar{Q}(\theta)\bar{\rho}(\theta)d\theta + \int_{-h}^{0}\bar{\rho}^\top(\theta)\bar{R}(\theta)\bar{\rho}(\theta)d\theta + \int_{-h}^{0}\int_{-h}^{0}\bar{\rho}^\top(\theta)\bar{T}(\theta,\eta)\bar{\rho}(\eta)d\eta d\theta, \quad \text{(C.1)}$$

where $\bar{\rho} \in PC([-h,0],\mathbb{R}^{\bar{n}})$, $\bar{P} \in \mathbb{S}^{\bar{n}}$, $\bar{Q} : [-h,0] \to \mathbb{R}^{\bar{n}\times\bar{n}}$, $\bar{R} : [-h,0] \to \mathbb{S}^{\bar{n}}$, and $\bar{T} : [-h,0]\times[-h,0] \to \mathbb{R}^{\bar{n}\times\bar{n}}$.

For the sake of simplicity, we focus on the linear time-delay system of the form

$$\begin{aligned} &\frac{d}{dt}x(t) = Ax(t) + A_d x(t-h), \qquad \forall t \geq 0, \\ &x(t) = \varphi_0(t), \qquad \forall t \in [-h, 0], \end{aligned} \tag{C.2}$$

where $A \in \mathbb{R}^{n\times n}$, $A_d \in \mathbb{R}^{n\times n}$, h is a positive scalar, and $\varphi_0 \in PC([-h, 0], \mathbb{R}^n)$ is the initial function of (C.2).

Let us start with the terms with multiple integral forms. We state the following lemma.

Lemma C.1. *For any continuous function $f : [-h, 0] \to \mathbb{R}$, we have*

$$\int_{t-h}^{t}\int_{s}^{t} f(u)duds = \int_{t-h}^{t}(s-t+h)f(s)ds \tag{C.3}$$

and

$$\int_{t-h}^{t}\int_{s}^{t}\int_{u}^{t} f(v)dvduds = \frac{1}{2}\int_{t-h}^{t}(s-t+h)^2 f(s)ds.$$

Proof. Consider the double integral term. By switching the order of integration, we obtain

$$\begin{aligned} \int_{t-h}^{t}\int_{s}^{t} f(u)duds &= \int_{t-h}^{t}\int_{t-h}^{u} f(u)dsdu \\ &= \int_{t-h}^{t}(u-t+h)f(u)du. \end{aligned}$$

Consider the triple integral term. Define $\bar{f}(u) = \int_u^t f(v)dv$, we have

$$\int_{t-h}^{t}\int_{s}^{t}\int_{u}^{t} f(v)dvduds = \int_{t-h}^{t}\int_{s}^{t}\bar{f}(u)duds.$$

From (C.3), we have $\int_{t-h}^{t}\int_{s}^{t}\bar{f}(u)duds = \int_{t-h}^{t}(s-t+h)\bar{f}(s)ds$, then we obtain

$$\begin{aligned} \int_{t-h}^{t}\int_{s}^{t}\int_{u}^{t} f(v)dvduds &= \int_{t-h}^{t}\int_{s}^{t}\bar{f}(u)duds \\ &= \int_{t-h}^{t}(s-t+h)\bar{f}(s)ds. \end{aligned}$$

Since $\bar{f}(s) = \int_s^t f(u)du$, we have

$$\begin{aligned} \int_{t-h}^{t}\int_{s}^{t}\int_{u}^{t} f(v)dvduds &= \int_{t-h}^{t}(s-t+h)\bar{f}(s)ds \\ &= \int_{t-h}^{t}(s-t+h)\int_{s}^{t} f(u)duds \\ &= \int_{t-h}^{t}\int_{s}^{t}(s-t+h)f(u)duds. \end{aligned}$$

Finally, by switching the order of integration, we obtain

$$\begin{aligned}\int_{t-h}^{t}\int_{s}^{t}\int_{u}^{t} f(v)dvduds &= \int_{t-h}^{t}\int_{s}^{t}(s-t+h)f(u)duds \\ &= \int_{t-h}^{t}\int_{t-h}^{u}(s-t+h)f(u)dsdu \\ &= \frac{1}{2}\int_{t-h}^{t}(u-t+h)^2 f(u)du.\end{aligned}$$

□

As a first example, for any $\rho \in H^1([-h,0],\mathbb{R}^n)$, let us consider the functional proposed in [84], given by

$$V_{Park}(\rho,\dot{\rho}) = \rho^\top(0)P\rho(0) + \int_{-h}^{0}\rho^\top(\theta)Q\rho(\theta)d\theta + \int_{-h}^{0}\int_{\theta}^{0}\dot{\rho}^\top(\eta)A_d^\top X A_d\dot{\rho}(\eta)d\eta d\theta, \tag{C.4}$$

where P, Q, $X \in \mathbb{S}^n$, and A_d as in (C.2).

Using Lemma C.1, this functional can be written as

$$V_{Park}(\rho,\dot{\rho}) = \rho^\top(0)P\rho(0) + \int_{-h}^{0}\rho^\top(\theta)Q\rho(\theta)d\theta + \int_{-h}^{0}(\theta+h)\dot{\rho}^\top(\theta)A_d^\top X A_d\dot{\rho}(\theta)d\theta. \tag{C.5}$$

The time derivative of the above Lyapunov-Krasovskii functional along the solution of the time-delay system (C.2) is given by

$$\begin{aligned}\dot{V}_{Park}(x,\dot{x}) = 2x^\top(t)P\dot{x}(t) + x^\top(t)Qx(t) - x^\top(t-h)Qx(t-h) \\ + h\dot{x}^\top(t)A_d^\top X A_d\dot{x}(t) - \int_{t-h}^{t}\dot{x}^\top(\theta)A_d^\top X A_d\dot{x}(\theta)d\theta.\end{aligned}$$

Now, we will try to find another Lyapunov-Krasovskii functional $\tilde{V}_{Park}$ of the complete type given in (C.1) and such that its time derivative along the solution of the system (C.2) is equal to that of V_{Park}, that is $\dot{\tilde{V}}_{Park} = \dot{V}_{Park}$. To that aim, for any $\rho \in H^1([-h,0],\mathbb{R}^n)$, let us define a function $\tilde{\rho} : [-2h,0] \to \mathbb{R}^n$, such that, for all $\theta \in [-h,0]$,

$$\tilde{\rho}(\theta) = \rho(\theta) \qquad \text{and} \qquad A_d\tilde{\rho}(\theta-h) = -A\tilde{\rho}(\theta) + \dot{\rho}(\theta).$$

Then, consider the functional in (C.5) and replacing ρ by $\tilde{\rho}$, we obtain

$$\begin{aligned}\tilde{V}_{Park}(\tilde{\rho}) = \tilde{\rho}^\top(0)P\tilde{\rho}(0) + \int_{-h}^{0}\tilde{\rho}^\top(\theta)Q\tilde{\rho}(\theta)d\theta \\ + \int_{-h}^{0}(\theta+h)\begin{bmatrix}\tilde{\rho}^\top(\theta) & \tilde{\rho}^\top(\theta-h)\end{bmatrix}\begin{bmatrix}A^\top \\ A_d^\top\end{bmatrix}A_d^\top X A_d\begin{bmatrix}A & A_d\end{bmatrix}\begin{bmatrix}\tilde{\rho}(\theta) \\ \tilde{\rho}(\theta-h)\end{bmatrix}d\theta.\end{aligned}$$

The time derivative of the above considered Lyapunov-Krasovskii functional along

the solution of the time delay system (C.2) is given by

$$\begin{aligned}\dot{\tilde{V}}_{Park}(x) = {} & 2x^\top(t)P\dot{x}(t) + x^\top(t)Qx(t) - x^\top(t-h)Qx(t-h) \\ & + h\begin{bmatrix}x^\top(t) & x^\top(t-h)\end{bmatrix}\begin{bmatrix}A^\top \\ A_d^\top\end{bmatrix}A_d^\top X A_d\begin{bmatrix}A & A_d\end{bmatrix}\begin{bmatrix}x(t) \\ x(t-h)\end{bmatrix} \\ & - \int_{t-h}^{t}\begin{bmatrix}x^\top(\theta) & x^\top(\theta-h)\end{bmatrix}\begin{bmatrix}A^\top \\ A_d^\top\end{bmatrix}A_d^\top X A_d\begin{bmatrix}A & A_d\end{bmatrix}\begin{bmatrix}x(\theta) \\ x(\theta-h)\end{bmatrix}d\theta.\end{aligned}$$

Since we evaluate the dynamics (C.2) with the initial condition $\varphi_0(\theta) = \tilde{\rho}(\theta)$, for all $\theta \in [-2h, 0]$, we have

$$\dot{x}(t+\theta) = Ax(t+\theta) + A_d x(t+\theta-h), \qquad \forall t \geq 0 \text{ and } \theta \in [-h, 0].$$

Therefore, we obtain

$$\dot{\tilde{V}}_{Park}(x) = \dot{V}_{Park}(x, \dot{x}).$$

Note that the Lyapunov-Krasovskii functional $\tilde{V}_{Park}$ is written in the form of a complete Lyapunov-Krasovskii functional in (C.1) with $\bar{n} = 2n$,

$$\begin{aligned}\bar{P} &= \begin{bmatrix}P & 0_{n\times n} \\ 0_{n\times n} & 0_{n\times n}\end{bmatrix}, \\ \bar{Q}(\theta) &= 0_{2n\times 2n}, \\ \bar{R}(\theta) &= \begin{bmatrix}Q + (\theta+h)A^\top A_d^\top X A_d A & (\theta+h)A^\top A_d^\top X A_d A_d \\ (\theta+h)A_d^\top A_d^\top X A_d A & (\theta+h)A_d^\top A_d^\top X A_d A_d\end{bmatrix}, \\ \bar{T}(\theta,\eta) &= 0_{2n\times 2n},\end{aligned}$$

and

$$\bar{\rho}(\theta) = \begin{bmatrix}\tilde{\rho}(\theta) \\ \tilde{\rho}(\theta-h)\end{bmatrix}.$$

As a second example, consider the functional proposed in [46], given by

$$\begin{aligned}V_{Kim}(\rho, \dot{\rho}) = {} & \begin{bmatrix}\rho^\top(0) & \int_{-h}^{0}\rho^\top(\theta)d\theta\end{bmatrix}\begin{bmatrix}P_{11} & P_{12} \\ P_{12}^\top & P_{22}\end{bmatrix}\begin{bmatrix}\rho(0) \\ \int_{-h}^{0}\rho(\theta)d\theta\end{bmatrix} \\ & + \int_{-h}^{0}\begin{bmatrix}\rho(0) \\ \rho(\theta) \\ \dot{\rho}(\theta)\end{bmatrix}^\top\begin{bmatrix}Q_{11}(\theta) & Q_{12}(\theta) & Q_{13}(\theta) \\ Q_{12}^\top(\theta) & Q_{22}(\theta) & Q_{23}(\theta) \\ Q_{13}^\top(\theta) & Q_{23}^\top(\theta) & Q_{33}(\theta)\end{bmatrix}\begin{bmatrix}\rho(0) \\ \rho(\theta) \\ \dot{\rho}(\theta)\end{bmatrix}d\theta, \quad \text{(C.6)}\end{aligned}$$

where, for $i \neq j$ in the set $i, j \in \{1, 2, 3\}$, $P_{ii}, Q_{ii} \in \mathbb{S}^n$ and $P_{ij}, Q_{ij} \in \mathbb{R}^{n\times n}$. Its time

derivative along the solution of the time-delay system (C.2) is given by

$$\begin{aligned}\dot{V}_{Kim}(x,\dot{x}) = 2\begin{bmatrix}x^\top(t) & \int_{t-h}^{t} x^\top(\theta)d\theta\end{bmatrix}\begin{bmatrix}P_{11}+\int_{-h}^{0}Q_{11}(\theta)d\theta & P_{12}\\ P_{12}^\top & P_{22}\end{bmatrix}\begin{bmatrix}\dot{x}(t)\\ \int_{t-h}^{t}\dot{x}(\theta)d\theta\end{bmatrix}\\ +2\dot{x}^\top(t)\int_{-h}^{0}\begin{bmatrix}Q_{12}(\theta) & Q_{13}(\theta)\end{bmatrix}\begin{bmatrix}x(t+\theta)\\ \dot{x}(t+\theta)\end{bmatrix}d\theta\\ +2x^\top(t)\begin{bmatrix}Q_{12}(0) & Q_{13}(0)\end{bmatrix}\begin{bmatrix}x(t)\\ \dot{x}(t)\end{bmatrix}\\ -2\dot{x}^\top(t)\begin{bmatrix}Q_{12}(-h) & Q_{13}(-h)\end{bmatrix}\begin{bmatrix}x(t-h)\\ \dot{x}(t-h)\end{bmatrix}\\ -2\dot{x}^\top(t)\int_{-h}^{0}\begin{bmatrix}Q'_{12}(\theta) & Q_{13}\prime(\theta)\end{bmatrix}\begin{bmatrix}x(t+\theta)\\ \dot{x}(t+\theta)\end{bmatrix}d\theta\\ +\begin{bmatrix}x^\top(t) & \dot{x}^\top(t)\end{bmatrix}\begin{bmatrix}Q_{22}(0) & Q_{23}(0)\\ Q_{23}^\top(0) & Q_{33}(0)\end{bmatrix}\begin{bmatrix}x(t)\\ \dot{x}(t)\end{bmatrix}\\ -\begin{bmatrix}x^\top(t-h) & \dot{x}^\top(t-h)\end{bmatrix}\begin{bmatrix}Q_{22}(-h) & Q_{23}(-h)\\ Q_{23}^\top(-h) & Q_{33}(-h)\end{bmatrix}\begin{bmatrix}x(t-h)\\ \dot{x}(t-h)\end{bmatrix}\\ -\int_{-h}^{0}\begin{bmatrix}x^\top(t+\theta) & \dot{x}^\top(t+\theta)\end{bmatrix}\begin{bmatrix}Q'_{22}(\theta) & Q'_{23}(\theta)\\ Q'_{23}{}^\top(\theta) & Q'_{33}(\theta)\end{bmatrix}\begin{bmatrix}x(t+\theta)\\ \dot{x}(t+\theta)\end{bmatrix}d\theta.\end{aligned}$$

Now, we will try to find another Lyapunov-Krasovskii functional $\tilde{V}_{Kim}$ of the complete type given in (C.1) and such that its time derivative along the solution of the system (C.2) is equal to that of V_{Kim}, that is $\dot{\tilde{V}}_{Kim} = \dot{V}_{Kim}$. To that aim, for any $\rho \in H^1([-h,0],\mathbb{R}^n)$, let us define a function $\tilde{\rho} : [-2h,0] \to \mathbb{R}^n$, such that, for all $\theta \in [-h,0]$,

$$\tilde{\rho}(\theta) = \rho(\theta) \qquad \text{and} \qquad A_d\tilde{\rho}(\theta-h) = -A\tilde{\rho}(\theta) + \dot{\rho}(\theta).$$

Then, consider the functional in (C.6) and replacing ρ by $\tilde{\rho}$, we obtain

$$\begin{aligned}\tilde{V}_{Kim}(\tilde{\rho}) = \tilde{\rho}^\top(0)\left(P_{11}+\int_{-h}^{0}Q_{11}(\theta)d\theta\right)\tilde{\rho}(0)\\ +2\begin{bmatrix}\tilde{\rho}^\top(0) & \tilde{\rho}^\top(-h)\end{bmatrix}\int_{-h}^{0}\begin{bmatrix}\tilde{Q}_{11}(\theta) & \tilde{Q}_{12}(\theta)\\ \tilde{Q}_{12}^\top(\theta) & \tilde{Q}_{22}(\theta)\end{bmatrix}\begin{bmatrix}\tilde{\rho}(\theta)\\ \tilde{\rho}(\theta-h)\end{bmatrix}d\theta\\ +\int_{-h}^{0}\begin{bmatrix}\tilde{\rho}^\top(\theta) & \tilde{\rho}^\top(\theta-h)\end{bmatrix}\begin{bmatrix}Q_{22}(\theta)+Q_{23}(\theta)A+A^\top Q_{23}^\top(\theta) & A_d^\top Q_{23}^\top(\theta)\\ Q_{23}(\theta)A_d & 0_{n\times n}\end{bmatrix}\begin{bmatrix}\tilde{\rho}(\theta)\\ \tilde{\rho}(\theta-h)\end{bmatrix}d\theta\\ +\int_{-h}^{0}\int_{-h}^{0}\begin{bmatrix}\tilde{\rho}^\top(\theta) & \tilde{\rho}^\top(\theta-h)\end{bmatrix}\begin{bmatrix}P_{22} & 0_{n\times n}\\ 0_{n\times n} & 0_{n\times n}\end{bmatrix}\begin{bmatrix}\tilde{\rho}(\eta)\\ \tilde{\rho}(\eta-h)\end{bmatrix}d\eta d\theta, \quad \text{(C.7)}\end{aligned}$$

where

$$\begin{aligned}\tilde{Q}_{11}(\theta) &= P_{12}+Q_{12}(\theta)+Q_{13}(\theta)A+A^\top Q_{33}(\theta)A,\\ \tilde{Q}_{12}(\theta) &= A_d^\top Q_{13}^\top(\theta)+A_d^\top Q_{33}(\theta)A,\end{aligned}$$

and

$$\tilde{Q}_{22}(\theta) = A_d^\top Q_{33}(\theta) A_d.$$

The time derivative of the above considered Lyapunov-Krasovskii functional along the solution of the time delay system (C.2) is given by

$$\begin{aligned}
\dot{\tilde{V}}_{Kim}(x) = {} & 2x^\top(t)\left(P_{11} + \int_{-h}^{0} Q_{11}(\theta)d\theta\right)\dot{x}(t) \\
& + 2\begin{bmatrix} x^\top(t) & x^\top(t-h)\end{bmatrix}\begin{bmatrix}\tilde{Q}_{11}(0) & \tilde{Q}_{12}(0)\\ \tilde{Q}_{12}(0) & \tilde{Q}_{22}(0)\end{bmatrix}\begin{bmatrix} x(t)\\ x(t-h)\end{bmatrix} \\
& - 2\begin{bmatrix} x^\top(t) & x^\top(t-h)\end{bmatrix}\begin{bmatrix}\tilde{Q}_{11}(-h) & \tilde{Q}_{12}(-h)\\ \tilde{Q}_{12}^\top(-h) & \tilde{Q}_{22}(-h)\end{bmatrix}\begin{bmatrix} x(t-h)\\ x(t-2h)\end{bmatrix} \\
& - 2\begin{bmatrix} x^\top(t) & x^\top(t-h)\end{bmatrix}\int_{-h}^{0}\begin{bmatrix}\tilde{Q}'_{11}(\theta) & \tilde{Q}'_{12}(\theta)\\ \tilde{Q}'_{12}{}^\top(\theta) & \tilde{Q}'_{22}(\theta)\end{bmatrix}\begin{bmatrix} x(t+\theta)\\ x(t+\theta-h)\end{bmatrix}d\theta \\
& + 2\begin{bmatrix} x(t)A + x(t-h)A_d\\ x(t-h)A + x(t-2h)A_d\end{bmatrix}^\top\int_{-h}^{0}\begin{bmatrix}\tilde{Q}_{11}(\theta) & \tilde{Q}_{12}(\theta)\\ \tilde{Q}_{12}^\top(\theta) & \tilde{Q}_{22}(\theta)\end{bmatrix}\begin{bmatrix} x(t+\theta)\\ x(t+\theta-h)\end{bmatrix}d\theta \\
& + \begin{bmatrix} x^\top(t) & x^\top(t-h)\end{bmatrix}\begin{bmatrix} Q_{22}(0) + Q_{23}(0)A + A^\top Q_{23}^\top(0) & A_d^\top Q_{23}^\top(0)\\ Q_{23}(0)A_d & 0_{n\times n}\end{bmatrix}\begin{bmatrix} x(t)\\ x(t-h)\end{bmatrix} \\
& - \begin{bmatrix} x(t-h)\\ x(t-2h)\end{bmatrix}^\top\begin{bmatrix} Q_{22}(-h) + Q_{23}(-h)A + A^\top Q_{23}^\top(-h) & A_d^\top Q_{23}^\top(-h)\\ Q_{23}(-h)A_d & 0_{n\times n}\end{bmatrix}\begin{bmatrix} x(t-h)\\ x(t-2h)\end{bmatrix} \\
& - \int_{-h}^{0}\begin{bmatrix} x(t+\theta)\\ x(t+\theta-h)\end{bmatrix}^\top\begin{bmatrix} Q'_{22}(\theta) + Q'_{23}(\theta)A + A^\top Q'_{23}{}^\top(\theta) & A_d^\top Q'_{23}{}^\top(\theta)\\ Q'_{23}(\theta)A_d & 0_{n\times n}\end{bmatrix}\begin{bmatrix} x(t+\theta)\\ x(t+\theta-h)\end{bmatrix}d\theta \\
& + 2\begin{bmatrix} x^\top(t) & x^\top(t-h)\end{bmatrix}\int_{-h}^{0}\begin{bmatrix} P_{22} & 0_{n\times n}\\ 0_{n\times n} & 0_{n\times n}\end{bmatrix}\begin{bmatrix} x(t+\theta)\\ x(t+\theta-h)\end{bmatrix}d\theta \\
& - 2\begin{bmatrix} x^\top(t-h) & x^\top(t-2h)\end{bmatrix}\int_{-h}^{0}\begin{bmatrix} P_{22} & 0_{n\times n}\\ 0_{n\times n} & 0_{n\times n}\end{bmatrix}\begin{bmatrix}\tilde{\rho}(t+\theta)\\ \tilde{\rho}(t+\theta-h)\end{bmatrix}d\theta.
\end{aligned}$$

Since we evaluate the dynamics (C.2) with the initial condition $\varphi_0(\theta) = \tilde{\rho}(\theta)$, for all $\theta \in [-2h, 0]$, we have

$$\dot{x}(t+\theta) = Ax(t+\theta) + A_d x(t+\theta-h), \qquad \forall t \geq 0 \text{ and } \theta \in [-h, 0].$$

Therefore, we obtain

$$\dot{\tilde{V}}_{Kim}(x) = \dot{V}_{Kim}(x, \dot{x}).$$

Note that the Lyapunov-Krasovskii functional $\tilde{V}_{Kim}$ is written in the form of a complete Lyapunov-Krasovskii functional in (C.1) with $\bar{n} = 2n$,

$$\begin{aligned}
\bar{P} &= \begin{bmatrix} P + \int_{-h}^{0} Q_{11}(\theta)d\theta & 0_{n\times n}\\ 0_{n\times n} & 0_{n\times n}\end{bmatrix}, \\
\bar{Q}(\theta) &= \begin{bmatrix}\tilde{Q}_{11} & \tilde{Q}_{12}\\ \tilde{Q}_{12}^\top & \tilde{Q}_{22}\end{bmatrix}, \\
\bar{R}(\theta) &= \begin{bmatrix} Q_{22}(\theta) + Q_{23}(\theta)A + A^\top Q_{23}^\top(\theta) & A_d^\top Q_{23}^\top(\theta)\\ Q_{23}(\theta)A_d & 0_{n\times n}\end{bmatrix}, \\
\bar{T}(\theta, \eta) &= \begin{bmatrix} P_{22} & 0_{n\times n}\\ 0_{n\times n} & 0_{n\times n}\end{bmatrix},
\end{aligned}$$

and

$$\bar{\rho}(\theta) = \begin{bmatrix} \tilde{\rho}(\theta) \\ \tilde{\rho}(\theta - h) \end{bmatrix}.$$

As a third example, consider the functional presented in [83], given by

$$\begin{aligned} V_{Pm}(\rho, \dot{\rho}) = & \begin{bmatrix} \rho(0) \\ \rho(-h) \\ \int_{-h}^{0} \rho(\theta) d\theta \\ \int_{-h}^{0} \int_{\theta}^{0} \rho(\eta) d\eta d\theta \end{bmatrix}^{\top} \begin{bmatrix} P_{11} & P_{12} & P_{13} & P_{14} \\ P_{12}^{\top} & P_{22} & P_{23} & P_{24} \\ P_{13}^{\top} & P_{23}^{\top} & P_{33} & P_{34} \\ P_{14}^{\top} & P_{24}^{\top} & P_{34}^{\top} & P_{44} \end{bmatrix} \begin{bmatrix} \rho(0) \\ \rho(-h) \\ \int_{-h}^{0} \rho(\theta) d\theta \\ \int_{-h}^{0} \int_{\theta}^{0} \rho(\eta) d\eta d\theta \end{bmatrix} \\ & + \int_{-h}^{0} \begin{bmatrix} \rho^{\top}(\theta) & \dot{\rho}^{\top}(\theta) \end{bmatrix} \begin{bmatrix} S_{11} & S_{12} \\ S_{12}^{\top} & S_{22} \end{bmatrix} \begin{bmatrix} \rho(\theta) \\ \dot{\rho}(\theta) \end{bmatrix} d\theta \\ & + h \int_{-h}^{0} \int_{\theta}^{0} \begin{bmatrix} \rho^{\top}(\eta) & \dot{\rho}^{\top}(\eta) \end{bmatrix} \begin{bmatrix} D_{11} & D_{12} \\ D_{12}^{\top} & D_{22} \end{bmatrix} \begin{bmatrix} \rho(\eta) \\ \dot{\rho}(\eta) \end{bmatrix} d\eta d\theta \\ & + \frac{h^2}{2} \int_{-h}^{0} \int_{\theta}^{0} \int_{\eta}^{0} \dot{\rho}^{\top}(\zeta) T \dot{\rho}(\zeta) d\zeta d\eta d\theta, \end{aligned} \tag{C.8}$$

where $T \in \mathbb{S}^n$ and, for $i \neq j$ in the set $i, j \in \{1, 2, 3, 4\}$, P_{ii}, S_{ii}, $D_{ii} \in \mathbb{S}^n$ and P_{ij}, S_{ij}, $D_{ij} \in \mathbb{R}^{n \times n}$.

Using Lemma C.1, this functional can be written as

$$\begin{aligned} V_{Pm}(\rho, \dot{\rho}) = & \begin{bmatrix} \rho(0) \\ \rho(-h) \\ \int_{-h}^{0} \rho(\theta) d\theta \\ \int_{-h}^{0} \int_{\theta}^{0} \rho(\eta) d\eta d\theta \end{bmatrix}^{\top} \begin{bmatrix} P_{11} & P_{12} & P_{13} & P_{14} \\ P_{12}^{\top} & P_{22} & P_{23} & P_{24} \\ P_{13}^{\top} & P_{23}^{\top} & P_{33} & P_{34} \\ P_{14}^{\top} & P_{24}^{\top} & P_{34}^{\top} & P_{44} \end{bmatrix} \begin{bmatrix} \rho(0) \\ \rho(-h) \\ \int_{-h}^{0} \rho(\theta) d\theta \\ \int_{-h}^{0} \int_{\theta}^{0} \rho(\eta) d\eta d\theta \end{bmatrix} \\ & + \int_{-h}^{0} \begin{bmatrix} \rho(\theta) \\ \dot{\rho}(\theta) \end{bmatrix}^{\top} \begin{bmatrix} S_{11} + h(\theta + h) D_{11} & S_{12} + h(\theta + h) D_{12} \\ S_{12}^{\top} + h(\theta + h) D_{12}^{\top} & S_{22} + h(\theta + h) D_{22} + \frac{h^2}{2} (\theta + h)^2 T \end{bmatrix} \begin{bmatrix} \rho(\theta) \\ \dot{\rho}(\theta) \end{bmatrix} d\theta. \end{aligned} \tag{C.9}$$

The time derivative of the above Lyapunov-Krasovskii functional along the solution of the time-delay system (C.2) is given by

$$\begin{aligned} \dot{V}_{Pm}(x, \dot{x}) = & \begin{bmatrix} x(t) \\ x(t-h) \\ \int_{t-h}^{t} x(\theta) d\theta \\ \int_{t-h}^{t} \int_{\theta}^{t} x(\eta) d\eta d\theta \end{bmatrix}^{\top} \begin{bmatrix} P_{11} & P_{12} & P_{13} & P_{14} \\ P_{12}^{\top} & P_{22} & P_{23} & P_{24} \\ P_{13}^{\top} & P_{23}^{\top} & P_{33} & P_{34} \\ P_{14}^{\top} & P_{24}^{\top} & P_{34}^{\top} & P_{44} \end{bmatrix} \begin{bmatrix} \dot{x}(t) \\ \dot{x}(t-h) \\ \int_{t-h}^{t} \dot{x}(\theta) d\theta \\ \int_{t-h}^{t} \int_{\theta}^{t} \dot{x}(\eta) d\eta d\theta \end{bmatrix} \\ & + \begin{bmatrix} x(0) \\ \dot{x}(0) \end{bmatrix}^{\top} \begin{bmatrix} S_{11} + h^2 D_{11} & S_{12} + h^2 D_{12} \\ S_{12}^{\top} + h^2 D_{12}^{\top} & S_{22} + h^2 D_{22} + \frac{h^4}{2} T \end{bmatrix} \begin{bmatrix} x(0) \\ \dot{x}(0) \end{bmatrix} \\ & - \begin{bmatrix} x(-h) \\ \dot{x}(-h) \end{bmatrix}^{\top} \begin{bmatrix} S_{11} & S_{12} \\ S_{12}^{\top} & S_{22} \end{bmatrix} \begin{bmatrix} x(-h) \\ \dot{x}(-h) \end{bmatrix} \\ & + \int_{-h}^{0} \begin{bmatrix} x(t+\theta) \\ \dot{x}(t+\theta) \end{bmatrix}^{\top} \begin{bmatrix} hD_{11} & hD_{12} \\ hD_{12}^{\top} & hD_{22} + h^2 (\theta + h) T \end{bmatrix} \begin{bmatrix} x(t+\theta) \\ \dot{x}(t+\theta) \end{bmatrix} d\theta. \end{aligned}$$

Now, we will try to find another Lyapunov-Krasovskii functional $\tilde{V}_{Pm}$ such that its time derivative along the solution of the system (C.2) is equal to that of V_{Pm}, that is $\dot{\tilde{V}}_{Pm} = \dot{V}_{Pm}$. To that aim, for any $\rho \in H^1([-h, 0], \mathbb{R}^n)$, let us define a function $\tilde{\rho} : [-2h, 0] \to \mathbb{R}^n$, such that, for all $\theta \in [-h, 0]$,

$$\tilde{\rho}(\theta) = \rho(\theta) \qquad \text{and} \qquad A_d\tilde{\rho}(\theta - h) = -A\tilde{\rho}(\theta) + \dot{\rho}(\theta).$$

Then, consider the functional in (C.5) and replacing ρ by $\tilde{\rho}$, we obtain

$$\begin{aligned}
\tilde{V}_{Pm}(\tilde{\rho}) = {} & \begin{bmatrix}\tilde{\rho}^\top(0) & \tilde{\rho}^\top(-h)\end{bmatrix} \begin{bmatrix}P_{11} & P_{12}\\ P_{12}^\top & P_{22}\end{bmatrix} \begin{bmatrix}\tilde{\rho}(0)\\ \tilde{\rho}(-h)\end{bmatrix} \\
& + 2\begin{bmatrix}\tilde{\rho}^\top(0) & \tilde{\rho}^\top(-h)\end{bmatrix} \int_{-h}^{0} \begin{bmatrix}P_{13} + (\theta + h)P_{14} & 0_{n\times n}\\ P_{23} + (\theta + h)P_{24} & 0_{n\times n}\end{bmatrix} \begin{bmatrix}\tilde{\rho}(\theta)\\ \tilde{\rho}(\theta - h)\end{bmatrix} d\theta \\
& + \int_{-h}^{0} \begin{bmatrix}\tilde{\rho}(\theta)\\ \tilde{\rho}(\theta - h)\end{bmatrix}^\top \begin{bmatrix}S_{11} + A^\top S_{12}^\top + S_{12}A + A^\top S_{22}A & S_{12}A_d + A^\top S_{22}A_d\\ A_d^\top S_{12}^\top + A_d^\top S_{12}A & A_d^\top S_{22}A_d\end{bmatrix} \begin{bmatrix}\tilde{\rho}(\theta)\\ \tilde{\rho}(\theta - h)\end{bmatrix} d\theta \\
& + \int_{-h}^{0} \begin{bmatrix}\tilde{\rho}(\theta)\\ \tilde{\rho}(\theta - h)\end{bmatrix}^\top h(\theta + h) \begin{bmatrix}D_1 + A^\top D_3^\top + D_3A + A^\top D_2A & D_3A_d + A^\top D_2A_d\\ A_d^\top D_3^\top + A_d^\top D_2A & A_d^\top D_2A_d\end{bmatrix} \begin{bmatrix}\tilde{\rho}(\theta)\\ \tilde{\rho}(\theta - h)\end{bmatrix} d\theta \\
& + \int_{-h}^{0} \begin{bmatrix}\tilde{\rho}^\top(\theta) & \tilde{\rho}^\top(\theta - h)\end{bmatrix} \frac{h^2}{2}(\theta + h)^2 \begin{bmatrix}A^\top TA & A^\top TA_d\\ A_d^\top TA & A_d^\top TA_d\end{bmatrix} \begin{bmatrix}\tilde{\rho}(\theta)\\ \tilde{\rho}(\theta - h)\end{bmatrix} d\theta \\
& + \int_{-h}^{0}\int_{-h}^{0} \begin{bmatrix}\tilde{\rho}(\theta)\\ \tilde{\rho}(\theta - h)\end{bmatrix}^\top \begin{bmatrix}P_{33} + 2(\eta + h)P_{34} + (\theta + h)(\eta + h)P_{44} & 0_{n\times n}\\ 0_{n\times n} & 0_{n\times n}\end{bmatrix} \begin{bmatrix}\tilde{\rho}(\eta)\\ \tilde{\rho}(\eta - h)\end{bmatrix} d\eta d\theta.
\end{aligned}$$

The time derivative of the above considered Lyapunov-Krasovskii functional along

the solution of the time delay system (C.2) is given by

$$
\begin{aligned}
\dot{\tilde{V}}_{Pm}(x) = {} & 2\begin{bmatrix} x^\top(t) & x^\top(t-h)\end{bmatrix}\begin{bmatrix} P_{11} & P_{12} \\ P_{12}^\top & P_{22}\end{bmatrix}\begin{bmatrix} Ax(t)+A_dx(t-h) \\ Ax(t-h)+A_dx(t-2h)\end{bmatrix} \\
& + 2\begin{bmatrix} x^\top(t) & x^\top(t-h)\end{bmatrix}\begin{bmatrix} P_{13}+hP_{14} & 0_{n\times n} \\ P_{23}+hP_{24} & 0_{n\times n}\end{bmatrix}\begin{bmatrix} x(t) \\ x(t-h)\end{bmatrix} \\
& + 2\begin{bmatrix} x^\top(t) & x^\top(t-h)\end{bmatrix}\begin{bmatrix} P_{13} & 0_{n\times n} \\ P_{23} & 0_{n\times n}\end{bmatrix}\begin{bmatrix} x(t-h) \\ x(t-2h)\end{bmatrix} \\
& + 2\begin{bmatrix} x^\top(t) & x^\top(t-h)\end{bmatrix}\int_{-h}^{0}\begin{bmatrix} P_{14} & 0_{n\times n} \\ P_{24} & 0_{n\times n}\end{bmatrix}\begin{bmatrix} x(t+\theta) \\ x(t+\theta-h)\end{bmatrix}d\theta \\
& + \begin{bmatrix} x^\top(t) & x^\top(t-h)\end{bmatrix}\begin{bmatrix} S_{11}+A^\top S_{12}^\top+S_{12}A+A^\top S_{22}A & S_{12}A_d+A^\top S_{22}A_d \\ A_d^\top S_{12}^\top+A_d^\top S_{12}A & A_d^\top S_{22}A_d\end{bmatrix}\begin{bmatrix} x(t) \\ x(t-h)\end{bmatrix} \\
& - \begin{bmatrix} x(t-h) \\ x(t-2h)\end{bmatrix}^\top\begin{bmatrix} S_{11}+A^\top S_{12}^\top+S_{12}A+A^\top S_{22}A & S_{12}A_d+A^\top S_{22}A_d \\ A_d^\top S_{12}^\top+A_d^\top S_{12}A & A_d^\top S_{22}A_d\end{bmatrix}\begin{bmatrix} x(t-h) \\ x(t-2h)\end{bmatrix} \\
& + \begin{bmatrix} x^\top(t) & x^\top(t-h)\end{bmatrix}h^2\begin{bmatrix} D_1+A^\top D_3^\top+D_3A+A^\top D_2A & D_3A_d+A^\top D_2A_d \\ A_d^\top D_3^\top+A_d^\top D_2A & A_d^\top D_2A_d\end{bmatrix}\begin{bmatrix} x(t) \\ x(t-h)\end{bmatrix} \\
& + \int_{-h}^{0}\begin{bmatrix} x(t+\theta) \\ x(t+\theta-h)\end{bmatrix}^\top h\begin{bmatrix} D_1+A^\top D_3^\top+D_3A+A^\top D_2A & D_3A_d+A^\top D_2A_d \\ A_d^\top D_3^\top+A_d^\top D_2A & A_d^\top D_2A_d\end{bmatrix}\begin{bmatrix} x(t+\theta) \\ x(t+\theta-h)\end{bmatrix}d\theta \\
& + \begin{bmatrix} x^\top(t) & x^\top(t-h)\end{bmatrix}\frac{h^4}{2}\begin{bmatrix} A^\top TA & A^\top TA_d \\ A_d^\top TA & A_d^\top TA_d\end{bmatrix}\begin{bmatrix} x(t) \\ x(t+-h)\end{bmatrix} \\
& + \int_{-h}^{0}\begin{bmatrix} x^\top(t+\theta) & x^\top(t+\theta-h)\end{bmatrix}h^2(\theta+h)\begin{bmatrix} A^\top TA & A^\top TA_d \\ A_d^\top TA & A_d^\top TA_d\end{bmatrix}\begin{bmatrix} x(t+\theta) \\ x(t+\theta-h)\end{bmatrix}d\theta \\
& - \int_{-h}^{0}\int_{-h}^{0}\begin{bmatrix} x^\top(t+\theta) & x^\top(t+\theta-h)\end{bmatrix}\begin{bmatrix} (\eta+h)P_{44} & 0_{n\times n} \\ 0_{n\times n} & 0_{n\times n}\end{bmatrix}\begin{bmatrix} x(t+\eta) \\ x(t+\eta-h)\end{bmatrix}d\eta d\theta \\
& - \int_{-h}^{0}\int_{-h}^{0}\begin{bmatrix} x^\top(t+\theta) & x^\top(t+\theta-h)\end{bmatrix}\begin{bmatrix} 2P_{34}+(\theta+h)P_{44} & 0_{n\times n} \\ 0_{n\times n} & 0_{n\times n}\end{bmatrix}\begin{bmatrix} x(t+\eta) \\ x(t+\eta-h)\end{bmatrix}d\eta d\theta \\
& + 2\begin{bmatrix} x^\top(t) & x^\top(t-h)\end{bmatrix}\int_{-h}^{0}\begin{bmatrix} P_{33}+2(\theta+h)P_{34}+h(\theta+h)P_{44} & 0_{n\times n} \\ 0_{n\times n} & 0_{n\times n}\end{bmatrix}\begin{bmatrix} x(t+\theta) \\ x(t+\theta-h)\end{bmatrix}d\theta \\
& - \begin{bmatrix} x^\top(t-h) & x^\top(t-2h)\end{bmatrix}\int_{-h}^{0}\begin{bmatrix} P_{33}+2(\theta+h)P_{34} & 0_{n\times n} \\ 0_{n\times n} & 0_{n\times n}\end{bmatrix}\begin{bmatrix} \tilde{\rho}(\theta) \\ \tilde{\rho}(\theta-h)\end{bmatrix}d\theta.
\end{aligned}
$$

Since we evaluate the dynamics (C.2) with the initial condition $\varphi_0(\theta) = \tilde{\rho}(\theta)$, for all $\theta \in [-2h, 0]$, we have

$$\dot{x}(t+\theta) = Ax(t+\theta) + A_dx(t+\theta-h), \qquad \forall t \geq 0 \text{ and } \theta \in [-h, 0].$$

Therefore, we obtain

$$\dot{\tilde{V}}_{Pm}(x) = \dot{V}_{Pm}(x, \dot{x}).$$

Note that the Lyapunov-Krasovskii functional $\tilde{V}_{Pm}$ is written in the form of a complete Lyapunov-Krasovskii functional.

As a conclusion, a general approach to construct Lyapunov-Krasovskii functionals is to represent the original time-delay system in projected coordinates (augmented dynamics) and to parameterize the complete Lyapunov-Krasovskii functional given in (C.1).

Bibliography

[1] F. J. Adams. Power steering 'road feel'. *SAE Transactions*, 92:326–334, 1983.

[2] K. J. Astrom, C. C. Hang, and B. C. Lim. A new Smith predictor for controlling a process with an integrator and long dead-time. *IEEE Transactions on Automatic Control*, 39(2):343–345, 1994.

[3] J. Baek and C. Kang. Time-delayed control for automated steering wheel tracking of electric power steering systems. *IEEE Access*, 8:95457–95464, 2020.

[4] A. Bahill. A simple adaptive Smith-predictor for controlling time-delay systems: A tutorial. *IEEE Control Systems Magazine*, 3(2):16–22, 1983.

[5] A. Benine-Neto, S. Scalzi, M. Netto, S. Mammar, and W. Pasillas-Lepine. Vehicle yaw rate control based on piecewise affine regions. In *Proceedings of the IEEE Intelligent Vehicles Symposium*, pages 20–25, 2010.

[6] A. Bensoussan, G. Da Prato, M. C. Delfour, and S. K. Mitter. *Representation and control of infinite dimensional systems*. Springer, 2007.

[7] M. Berriri, P. Chevrel, and D. Lefebvre. Active damping of automotive powertrain oscillations by a partial torque compensator. *Control Engineering Practice*, 16(7):874–883, 2008.

[8] P. Boehm, A. H. Ghasemi, S. O'Modhrain, P. Jayakumar, and R. B. Gillespie. Architectures for shared control of vehicle steering. *Proceedings of the IFAC Symposium on Analysis, Design, and Evaluation of Human-Machine Systems*, 49 (19):639–644, 2016.

[9] G. Boros and V. H. Moll. Sums of arctangents and some formulas of Ramanujan. *Scientia*, 11(540623):13–24, 2005.

[10] M. Bröcker. New control algorithms for steering feel improvements of an electric powered steering system with belt drive. *Vehicle System Dynamics*, 44(sup1):759–769, 2006.

[11] W. B. Castelan and E. F. Infante. On a functional equation arising in the stability theory of difference-differential equations. *Quarterly of Applied Mathematics*, 35(3):311–319, 1977.

[12] M. F. F. Castro, A. Seuret, V. J. S. Leite, and L. F. P. Silva. Robust local stabilization of discrete time-varying delayed state systems under saturating actuators. *Automatica*, 122:109266, 2020.

[13] R. C. Chabaan and L. Y. Wang. Control of electrical power assist systems: H_∞ design, torque estimation and structural stability. *JSAE Review*, 22(4): 435–444, 2001.

[14] X. Chen, T. Yang, X. Chen, and K. Zhou. A generic model-based advanced control of electric power-assisted steering systems. *IEEE Transactions on Control Systems Technology*, 16(6):1289–1300, 2008.

[15] J. Cheong, S.-I. Niculescu, A. Annaswamy, and M. Srinivasan. Motion synchronization in virtual environments with shared haptics and large time delays. In *Proceedings of the IEEE Eurohaptics Conference and Symposium on Haptic Interfaces for Virtual Environment and Teleoperator Systems.*, pages 277–282, 2005.

[16] V. Ciarla, V. Cahouet, C. Canudas de Wit, and F. Quaine. Genesis of booster curves in electric power assistance steering systems. In *Proceedings of the IEEE International Conference on Intelligent Transportation Systems*, pages 1345–1350, 2012.

[17] R. F. Curtain and H. Zwart. *An introduction to infinite-dimensional linear systems theory*, volume 21. Springer Science & Business Media, 2012.

[18] Q. V. Dang, A. Dequidt, L. Vermeiren, and M. Dambrine. Design and control of force feedback haptic systems with time delay. In T. Vyhlídal, J.-F. Lafay, and R. Sipahi, editors, *Delay Systems: From Theory to Numerics and Applications*, pages 373–387. Springer International Publishing, Cham, 2014.

[19] Q. V. Dang, L. Vermeiren, A. Dequidt, and M. Dambrine. Experimental study on the stability of an impedance-type force-feedback architecture based on an augmented-state observer for a haptic system under time delay using a LMI approach. *Proceedings of the Institution of Mechanical Engineers. Part I: Journal of Systems and Control Engineering*, 230(1):58–71, 2016.

[20] R. Datko. An algorithm for computing Liapunov functionals for some differential-difference equations. In L. Weiss, editor, *Ordinary Differential Equations*, pages 387–398. Academic Press, 1972.

[21] R. Datko. Lyapunov functionals for certain linear delay differential equations in a Hilbert space. *Journal of Mathematical Analysis and Applications*, 76 (1):37–57, 1980.

[22] C. de Souza, V. J. S. Leite, L. F. P. Silva, and E. B. Castelan. ISS robust stabilization of state-delayed discrete-time systems with bounded delay variation and saturating actuators. *IEEE Transactions on Automatic Control*, 64(9): 3913–3919, 2019.

[23] A. V. Egorov. A finite necessary and sufficient stability condition for linear retarded type systems. In *Proceedings of the IEEE Conference on Decision and Control*, pages 3155–3160, Las Vegas (Nevada), 2016.

[24] A. V. Egorov and S. Mondié. Necessary stability conditions for linear delay systems. *Automatica*, 50(12):3204–3208, 2014.

[25] A. V. Egorov, C. Cuvas, and S. Mondié. Necessary and sufficient stability conditions for linear systems with pointwise and distributed delays. *Automatica*, 80:218–224, 2017.

[26] Y. Eidelman, I. Gohberg, and V. Olshevsky. The QR iteration method for Hermitian quasiseparable matrices of an arbitrary order. *Linear Algebra and its Applications*, 404:305–324, 2005.

[27] P. Freitas. Delay-induced instabilities in gyroscopic systems. *SIAM Journal on Control and Optimization*, 39(1):196–207, 2000.

[28] E. Fridman. Tutorial on Lyapunov-based methods for time-delay systems. *European Journal of Control*, 20(6):271–283, 2014.

[29] E. Fridman and U. Shaked. A descriptor system approach to H_∞ control of linear time-delay systems. *IEEE Transactions on Automatic Control*, 47(2): 253–270, 2002.

[30] A. Gahlawat and M. M. Peet. A convex sum-of-squares approach to analysis, state feedback and output feedback control of parabolic PDEs. *IEEE Transactions on Automatic Control*, 62(4):1636–1651, 2017.

[31] A. Gahlawat and G. Valmorbida. Stability analysis of linear partial differential equations with generalized energy functions. *IEEE Transactions on Automatic Control*, 65(5):1924–1939, 2020.

[32] M. A. Gomez, A. V. Egorov, and S. Mondié. Lyapunov matrix based necessary and sufficient stability condition by finite number of mathematical operations for retarded type systems. *Automatica*, 108:108475, 2019.

[33] P. J. Goulart and S. Chernyshenko. Global stability analysis of fluid flows using sum-of-squares. *Physica D: Nonlinear Phenomena*, 241(6):692–704, 2012.

[34] K. Gu. A further refinement of discretized Lyapunov functional method for the stability of time-delay systems. *International Journal of Control*, 74(10): 967–976, 2001.

[35] D. Gualino and I.-J. Adounkpe. Force-feedback system design for the steer-by-wire: Optimisation and performance evaluation. In *Proceedings of the IEEE International Conference on Intelligent Transportation Systems*, pages 181–187, 2006.

[36] Q.-L. Han. A discrete delay decomposition approach to stability of linear retarded and neutral systems. *Automatica*, 45(2):517–524, 2009.

[37] Y. He, Q.-G. Wang, C. Lin, and M. Wu. Augmented Lyapunov functional and delay-dependent stability criteria for neutral systems. *International Journal of Robust and Nonlinear Control*, 15(18):923–933, 2005.

[38] Y. He, Q.-G. Wang, C. Lin, and M. Wu. Delay-range-dependent stability for systems with time-varying delay. *Automatica*, 43(2):371–376, 2007.

[39] Y.-H. J. Hsu, S. M. Laws, and J. C. Gerdes. Estimation of tire slip angle and friction limits using steering torque. *IEEE Transactions on Control Systems Technology*, 18(4):896–907, 2010.

[40] E. F. Infante and W. B. Castelan. A Liapunov functional for a matrix difference-differential equation. *Journal of Differential Equations*, 29(3):439–451, 1978.

[41] JTEKT. Steering systems. https://www.jtekt.eu/innovation-produit/automotive-industry/steerings-systems. Accessed: 2022-09-30.

[42] V. L. Kharitonov. Lyapunov functionals and matrices. *Annual Reviews in Control*, 34(1):13–20, 2010.

[43] V. L. Kharitonov. *Time-delay systems: Lyapunov functionals and matrices*. Birkhäuser, New York, 2012.

[44] V. L. Kharitonov and E. Plischke. Lyapunov matrices for time-delay systems. *Systems & Control Letters*, 55(9):697–706, 2006.

[45] V. L. Kharitonov and A. P. Zhabko. Lyapunov–Krasovskii approach to the robust stability analysis of time-delay systems. *Automatica*, 39(1):15–20, 2003.

[46] J.-H. Kim. Note on stability of linear systems with time-varying delay. *Automatica*, 47(9):2118–2121, 2011.

[47] J.-H. Kim and J.-B. Song. Control logic for an electric power steering system using assist motor. *Mechatronics*, 12(3):447–459, 2002.

[48] M. Kissai, A.-L. Do, B. Monsuez, X. Mouton, and A. Tapus. Optimal coordination of adas and chassis systems with different time-delays. In *Proceedings of the IEEE Intelligent Vehicles Symposium*, pages 253–258, 2020.

[49] N. N. Krasovskii. Stability of motion. *Stanford University Press*, 1963.

[50] M. Krstic. *Delay compensation for nonlinear, adaptive, and PDE systems*. Birkhäuser, Boston, 2009.

[51] D. Lee and M. Spong. Passive bilateral teleoperation with constant time delay. *IEEE Transactions on Robotics*, 22(2):269–281, 2006.

[52] D. Lee, K. Kim, and S. Kim. Controller design of an electric power steering system. *IEEE Transactions on Control Systems Technology*, 26(2):748–755, 2018.

[53] D. Lee, K. Yi, S. Chang, B. Lee, and B. Jang. Robust steering-assist torque control of electric-power-assisted-steering systems for target steering wheel torque tracking. *Mechatronics*, 49:157–167, 2018.

[54] D. Lee, B. Jang, M. Han, and K.-S. Kim. A new controller design method for an electric power steering system based on a target steering torque feedback controller. *Control Engineering Practice*, 106:104658, 2021.

[55] M. H. Lee, K. H. Seung, J. Y. Choi, and K. S. Yoon. Improvement of the steering feel of an electric power steering system by torque map modification. *Journal of Mechanical Science and Technology*, 19(3):792–801, 2005.

[56] H. Li, N. Zhao, X. Wang, X. Zhang, and P. Shi. Necessary and sufficient conditions of exponential stability for delayed linear discrete-time systems. *IEEE Transactions on Automatic Control*, 64(2):712–719, 2019.

[57] X. Li, X.-P. Zhao, and J. Chen. Controller design for electric power steering system using TS fuzzy model approach. *International Journal of Automation and Computing*, 6(2):198–203, 2009.

[58] Y. Li, T. Shim, D. Wang, and T. Offerle. Study on parameters affecting steering feel of column assist electric power steering. *International Journal of Vehicle Design*, 77(3):153–179, 2018.

[59] F.-J. Lin, Y.-C. Hung, and K.-C. Ruan. An intelligent second-order sliding-mode control for an electric power steering system using a wavelet fuzzy neural network. *IEEE Transactions on Fuzzy Systems*, 22(6):1598–1611, 2014.

[60] Y. H. Liu and X. W. Ji. Matching strategy of electric power steering assistant characters based on the vehicle inherent road feel. *Proceedings of the Institution of Mechanical Engineers. Part D: Journal of Automobile Engineering*, 225 (11):1481–1491, 2011.

[61] J. Lofberg. Yalmip: A toolbox for modeling and optimization in Matlab. In *Proceedings of the IEEE International Conference on Robotics and Automation*, pages 284–289, Taipei (Taiwan), 2004.

[62] J. Loof, I. Besselink, and H. Nijmeijer. Implementation and validation of a three degrees of freedom steering-system model in a full vehicle model. *Vehicle System Dynamics*, 57(1):86–107, 2019.

[63] J. Louisell. Numerics of the stability exponent and eigenvalue abscissas of a matrix delay system. In L. Dugard and E. I. Verriest, editors, *Stability and Control of Time-delay Systems*, pages 140–157. Springer, Berlin, 1998.

[64] J. Louisell. A matrix method for determining the imaginary axis eigenvalues of a delay system. *IEEE Transactions on Automatic Control*, 46(12):2008–2012, 2001.

[65] W. Lu, K. Zhou, and J. Doyle. Stabilization of LFT systems. In *Proceedings of the IEEE Conference on Decision and Control*, volume 2, pages 1239–1244, 1991.

[66] D. Ma, J. Chen, A. Liu, J. Chen, and S.-I. Niculescu. Explicit bounds for guaranteed stabilization by PID control of second-order unstable delay systems. *Automatica*, 100:407–411, 2019.

[67] X. Ma, Y. Guo, and L. Chen. Active disturbance rejection control for electric power steering system with assist motor variable mode. *Journal of the Franklin Institute*, 355(3):1139–1155, 2018.

[68] A. Marouf, M. Djemai, C. Sentouh, and P. Pudlo. A new control strategy of an electric-power-assisted steering system. *IEEE Transactions on Vehicular Technology*, 61(8):3574–3589, 2012.

[69] M. Matausek and A. Micic. A modified smith predictor for controlling a process with an integrator and long dead-time. *IEEE Transactions on Automatic Control*, 41(8):1199–1203, 1996.

[70] R. H. Middleton and D. E. Miller. On the achievable delay margin using LTI control for unstable plants. *IEEE Transactions on Automatic Control*, 52(7): 1194–1207, 2007.

[71] S. Mondié. Assessing the exact stability region of the single-delay scalar equation via its Lyapunov function. *IMA Journal of Mathematical Control and Information*, 29(4):459–470, 12 2012.

[72] Y. S. Moon, P. Park, and W. H. Kwon. Robust stabilization of uncertain input-delayed systems using reduction method. *Automatica*, 37(2):307–312, 2001.

[73] T. Mori, N. Fukuma, and M. Kuwahara. On an estimate of the decay rate for stable linear delay systems. *International Journal of Control*, 36(1):95–97, 1982.

[74] C. Mortici and H. M. Srivastava. Estimates for the arctangent function related to Shafer's inequality. *Colloquium Mathematicum*, 136(2):263–270, 2014.

[75] Mosek ApS. *Mosek optimization toolbox for Matlab*, 2019.

[76] C. N. Nett and W. M. Haddad. A system-theoretic appropriate realization of the empty matrix concept. *IEEE Transactions on Automatic Control*, 38(5): 771–775, 1993.

[77] A.-T. Nguyen, M. Sugeno, V. Campos, and M. Dambrine. LMI-based stability analysis for piecewise multi-affine systems. *IEEE Transactions on Fuzzy Systems*, 25(3):707–714, 2017.

[78] S.-I. Niculescu. *Delay Effects on Stability: A Robust Control Approach*, volume 269. Springer Science & Business Media, 2001.

[79] E. Nuño, I. Sarras, A. Loría, M. Maghenem, E. Cruz-Zavala, and E. Panteley. Strict Lyapunov-Krasovskiĭ functionals for undirected networks of Euler-Lagrange systems with time-varying delays. *Systems & Control Letters*, 135: 104579, 2020.

[80] M. Nybacka, X. He, G. Gómez, E. Bakker, and L. Drugge. Links between subjective assessments and objective metrics for steering. *International Journal of Automotive Technology*, 15(6):893–907, 2014.

[81] H. Pacejka. *Tire and vehicle dynamics*. Elsevier, 2005.

[82] A. Papachristodoulou, M. Peet, and S. Lall. Constructing Lyapunov-Krasovskii functionals for linear time delay systems. In *Proceedings of the IEEE American Control Conference*, volume 4, pages 2845–2850, Portland (Oregon), 2005.

[83] M. Park, O. Kwon, J. H. Park, S. Lee, and E. Cha. Stability of time-delay systems via Wirtinger-based double integral inequality. *Automatica*, 55:204–208, 2015.

[84] P. Park. A delay-dependent stability criterion for systems with uncertain time-invariant delays. *IEEE Transactions on Automatic Control*, 44(4):876–877, 1999.

[85] P. Park and J. Wan Ko. Stability and robust stability for systems with a time-varying delay. *Automatica*, 43(10):1855–1858, 2007.

[86] P. Park, J. W. Ko, and C. Jeong. Reciprocally convex approach to stability of systems with time-varying delays. *Automatica*, 47(1):235–238, 2011.

[87] M. M. Peet. LMI parametrization of Lyapunov functions for infinite-dimensional systems: A framework. In *Proceedings of the IEEE American Control Conference*, pages 359–366, Portland (Oregon), 2014.

[88] M. M. Peet. A dual to Lyapunov's second method for linear systems with multiple delays and implementation using SOS. *IEEE Transactions on Automatic Control*, 64(3):944–959, 2019.

[89] M. M. Peet and A. Papachristodoulou. Using polynomial semi-separable kernels to construct infinite-dimensional Lyapunov functions. In *Proceedings of the IEEE Conference on Decision and Control*, pages 847–852, Cancun (Mexico), 2008.

[90] M. M. Peet, A. Papachristodoulou, and S. Lall. Positive forms and stability of linear time-delay systems. *SIAM Journal on Control and Optimization*, 47(6): 3237–3258, 2009.

[91] I. Repin. Quadratic Liapunov functionals for systems with delay. *Journal of Applied Mathematics and Mechanics*, 29(3):669–672, 1965.

[92] H. E. B. Russell and J. C. Gerdes. Design of variable vehicle handling characteristics using four-wheel steer-by-wire. *IEEE Transactions on Control Systems Technology*, 24(5):1529–1540, 2016.

[93] M. Safi, L. Baudouin, and A. Seuret. Tractable sufficient stability conditions for a system coupling linear transport and differential equations. *Systems & Control Letters*, 110:1–8, 2017.

[94] D. Saifia, M. Chadli, H. Karimi, and S. Labiod. Fuzzy control for electric power steering system with assist motor current input constraints. *Journal of the Franklin Institute*, 352(2):562–576, 2015.

[95] L. Saleh, P. Chevrel, F. Claveau, J.-F. Lafay, and F. Mars. Shared steering control between a driver and an automation: Stability in the presence of driver behavior uncertainty. *IEEE Transactions on Intelligent Transportation Systems*, 14(2):974–983, 2013.

[96] D. Scott. When is an ordinary differential equation separable? *The American Mathematical Monthly*, 92(6):422–423, 1985.

[97] A. Seuret and F. Gouaisbaut. Wirtinger-based integral inequality: Application to time-delay systems. *Automatica*, 49(9):2860–2866, 2013.

[98] A. Seuret and F. Gouaisbaut. Jensen's and Wirtinger's inequalities for time-delay systems. *Proceedings of the IFAC Workshop on Time-Delay Systems*, 46 (3):343–348, 2013.

[99] A. Seuret and F. Gouaisbaut. Hierarchy of LMI conditions for the stability analysis of time-delay systems. *Systems & Control Letters*, 81:1–7, 2015.

[100] A. Seuret, F. Gouaisbaut, and Y. Ariba. Complete quadratic Lyapunov functionals for distributed delay systems. *Automatica*, 62:168–176, 2015.

[101] A. Seuret, F. Gouaisbaut, and E. Fridman. Stability of discrete-time systems with time-varying delays via a novel summation inequality. *IEEE Transactions on Automatic Control*, 60(10):2740–2745, 2015.

[102] R. Sipahi, S.-I. Niculescu, C. T. Abdallah, W. Michiels, and K. Gu. Stability and stabilization of systems with time delay. *IEEE Control Systems Magazine*, 31 (1):38–65, 2011.

[103] N. Sugitani, Y. Fujuwara, K. Uchida, and M. Fujita. Electric power steering with H-infinity control designed to obtain road information. In *Proceedings of the IEEE American Control Conference*, volume 5, pages 2935–2939. IEEE, 1997.

[104] J. Sun, G. Liu, J. Chen, and D. Rees. Improved delay-range-dependent stability criteria for linear systems with time-varying delays. *Automatica*, 46(2): 466–470, 2010.

[105] G. Valmorbida, M. Ahmadi, and A. Papachristodoulou. Stability analysis for a class of partial differential equations via semidefinite programming. *IEEE Transactions on Automatic Control*, 61(6):1649–1654, 2015.

[106] T. Van der Sande, P. Zegelaar, I. Besselink, and H. Nijmeijer. A robust control analysis for a steer-by-wire vehicle with uncertainty on the tyre forces. *Vehicle System Dynamics*, 54(9):1247–1268, 2016.

[107] K. Walton and J. Marshall. Direct method for TDS stability analysis. *IEE Proceedings D-Control Theory and Applications*, 2(134):101–107, 1987.

[108] H. Wang, Z. Man, H. Kong, Y. Zhao, M. Yu, Z. Cao, J. Zheng, and M. T. Do. Design and implementation of adaptive terminal sliding-mode control on a steer-by-wire equipped road vehicle. *IEEE Transactions on Industrial Electronics*, 63(9):5774–5785, 2016.

[109] Z. Wang. Adaptive fuzzy system compensation based model-free control for steer-by-wire systems with uncertainty. *International Journal of Innovative Computing, Information and Control*, 17(1):141–152, 2021.

[110] K. Watanabe and M. Ito. A process-model control for linear systems with delay. *IEEE Transactions on Automatic control*, 26(6):1261–1269, 1981.

[111] H. Wenzhang. Generalization of Liapunov's theorem in a linear delay system. *Journal of Mathematical Analysis and Applications*, 142(1):83–94, 1989.

[112] H. Xing, J. Ploeg, and H. Nijmeijer. Smith predictor compensating for vehicle actuator delays in cooperative ACC systems. *IEEE Transactions on Vehicular Technology*, 68(2):1106–1115, 2019.

[113] S. Yang, X. Guo, B. Yang, and G. Tan. Return-to-center control of electric power steering. In *Proceedings of the IEEE International Conference on Electronic Measurement & Instruments*, pages 435–439, 2009.

[114] T. Yang. A new control framework of electric power steering system based on admittance control. *IEEE Transactions on Control Systems Technology*, 23 (2):762–769, 2015.

[115] P. Yih and J. Gerdes. Modification of vehicle handling characteristics via steer-by-wire. *IEEE Transactions on Control Systems Technology*, 13(6):965–976, 2005.

[116] J. Zabczyk. Classical control theory. Technical report, 2002.

[117] M. I. Zakaria, A. R. Husain, Z. Mohamed, N. El Fezazi, and M. B. N. Shah. Lyapunov-Krasovskii stability condition for system with bounded delay - An application to steer-by-wire system. In *Proceedings of the IEEE International Conference on Control System, Computing and Engineering*, pages 543–547, 2015.

[118] A. T. Zaremba, M. K. Liubakka, and R. M. Stuntz. Vibration control based on dynamic compensation in an electric power steering system. In *Proceedings of the IEEE International Conference on Control of Oscillations and Chaos*, volume 3, pages 453–456, 1997.

[119] A. T. Zaremba, M. K. Liubakka, and R. M. Stuntz. Control and steering feel issues in the design of an electric power steering system. In *Proceedings of the IEEE American Control Conference*, volume 1, pages 36–40, 1998.

[120] X.-L. Zhu and G.-H. Yang. New results of stability analysis for systems with time-varying delay. *International Journal of Robust and Nonlinear Control*, 20 (5):596–606.

[121] J. Ángel Cid. A simple method to find out when an ordinary differential equation is separable. *International Journal of Mathematical Education in Science and Technology*, 40(5):659–662, 2009.

université PARIS-SACLAY

ÉCOLE DOCTORALE
Sciences et technologies de l'information et de la communication (STIC)

Titre : Analyse de stabilité et conception de lois de commande pour des systèmes à retards avec applications aux systèmes de direction automobiles

Mots clés : automatique et automobile, commande des systèmes de direction, fonctionnelles de Lyapunov-Krasovskii, inégalités matricielles linéaires, programmation semi-définie, systèmes avec retards

Résumé : L'assistance de direction aide le conducteur à manoeuvrer son véhicule en diminuant le couple exercé sur le volant. Dans le cas de la « *direction assistée électrique* » et du « *steer-by-wire* », le système d'assistance est composé de moteurs électriques placés au niveau de la crémaillère (pour déplacer les roues) et au niveau du volant (pour fournir au conducteur un retour des forces agissant sur les roues). Cependant, ces architectures introduisent des retards dans les boucles de rétroaction du système. Pour assurer la stabilité en présence de retards, on peut réduire le gain d'assistance ou augmenter l'amortissement du volant, mais cela a un impact négatif sur les performances du système et détériore le retour d'effort renvoyé au conducteur. Afin de surmonter cette limitation, nous concevons et analysons des lois de commande pour les systèmes de direction qui augmentent (par rapport aux stratégies actuelles) la marge de retard du système. Nous utilisons une approche fréquentielle pour analyser les contraintes imposées par la stabilité du système de rétroaction générant le couple volant. Nos algorithmes s'appuient sur des architectures de commande proportionnelles-dérivées classiques, comprenant des lois d'assistance et des filtres. La simplicité des méthodes proposées permet un calcul analytique de la marge de retard. De plus, pour rendre nos résultats plus généraux (par exemple, pour des lois d'assistance non linéaires), nous développons des techniques dans le domaine temporel pour analyser la stabilité des systèmes linéaires à retards en utilisant des fonctionnelles de Lyapunov-Krasovskii. Nous formulons une méthode basée sur des projections permettant à des ensembles généraux de fonctions de paramétrer les fonctionnelles de Lyapunov-Krasovskii. Nous discutons des principales hypothèses considérées dans notre formulation et établissons des connexions entre les approches existantes pour l'analyse de la stabilité des systèmes à retard basées sur la programmation semi-définie, à savoir la méthode basée sur l'utilisation d'inégalités intégrales et la méthode basée sur la programmation par somme de carrés. Enfin, les résultats obtenus sont également appliqués au cas test des systèmes de direction.

Title: Stability analysis and control design for time-delay systems with applications to automotive steering systems

Keywords: automotive control, control of steering systems, Lyapunov-Krasovskii functionals, linear matrix inequalities (LMI), semidefinite programming, time-delay systems

Abstract: Steering assistance helps the driver to maneuver the vehicle by reducing the steering effort. In the case of electric power steering and steer-by-wire, the assistance system is composed of electrical drives placed at the rack pinion (allowing the wheels to move) and at the steering wheel (providing the driver a feeling of the forces acting on the wheels). These architectures introduce, however, delays in the feedback loops of the system. To ensure its stability in the presence of delays, one can reduce the assist gain or increase the damping of the steering wheel, but this negatively impacts the system's performance and degrades the force feedback returned to the driver. In order to counter this limitation, we design and analyze control laws for steering systems that increase (compared to current strategies) the delay margin of the system. We use a frequency-domain approach to analyze the constraints imposed by the stability of the feedback system generating the steering wheel torque. Our algorithms rely on classical proportional-derivative control architectures, including torque maps and filters. The simplicity of the proposed methods allows an analytical computation of the delay margin. In addition, to make our results more general (for example, for nonlinear torque maps), we develop time-domain techniques to analyze the stability of linear time-delay systems using Lyapunov-Krasovskii functionals. We formulate a projection-based method allowing general sets of functions to parameterize Lyapunov-Krasovskii functionals. We discuss the main assumptions considered in our formulation and establish connections between the existing approaches for the stability analysis of time-delay systems based on semidefinite programming, namely the method based on the use of integral inequalities and the method based on sum-of-squares programming. Finally, the obtained results are also applied to the test case of steering systems.